

A BIOASSAY-GUIDED INVESTIGATION INTO THE CANCER
CHEMOPREVENTIVE POTENTIAL OF SELECTED NON-
DIETARY PLANTS AND SELECTED FLAVONOIDS

ALEXANDRA-GEORGIANA ZAVOIANU

A thesis submitted in partial fulfilment of the requirements of Liverpool John Moores
University for the degree of PhD/ Master of Philosophy

March 2020

Table of Contents

<i>Abstract</i>	6
<i>Declaration</i>	7
<i>List of Abbreviations</i>	8
<i>List of Tables</i>	10
<i>List of Figures</i>	12
CHAPTER 1 General Introduction	25
1.1 Cancer Outlines	25
1.1.1 Statistics.....	25
1.1.2 Cancer biology and lifestyle	26
1.1.3 Oxidative stress	29
1.1.4 Cancer Chemoprevention	32
1.1.5 Targets and Mechanisms of Chemopreventive Agents.....	36
1.2.1 Phytochemicals As Bioactive Compounds	41
1.2.1 Sources, classes and functions of phytochemicals	41
1.2.2 Polyphenols	45
1.2.3 Terpenoids.....	50
1.2.4 Organosulfur compounds.....	55
1.2.5 Phytochemicals as chemopreventive agents	55
1.3 Selected Non-Dietary Plants	58
1.3.1 <i>Centaurea asiatica, Centaurea dichroa, Centaurea kirdigensis, Centaurea pamphylica, Arctium lappa</i> (Asteraceae).....	58
1.3.2 <i>Equisetum arvense</i> (Equisetaceae)	61
1.3.3 <i>Gardenia ternifolia</i> (Rubiaceae).....	62
1.3.4 <i>Gypsophila pilulifera</i> (Caryophyllaceae)	63
1.3.5 <i>Hyssopus officinalis</i> (Lamiaceae).....	64
1.3.6 <i>Kitaibelia balansae</i> (Malvaceae)	65
1.3.7 <i>Solanum anguivi</i> (Solanaceae)	66
1.3.8 <i>Ziziphus mucronata</i> (Rhamnaceae).....	67
1.4 Aims and research outlines	69

CHAPTER 2 Materials and Methods	71
2.1 <i>Phytochemical Methods</i>	71
2.1.1 Plant materials	71
2.1.2 Soxhlet extraction	71
2.1.3 Sample cleaning and separation	73
2.1.4 Analytical TLC and free-radical scavenging assay (DPPH qualitative and quantitative assay)	74
2.1.5 Isolation and identification of phytochemicals	76
2.1.6 Selected phytochemical compounds (flavonoids) used for bioassays	77
2.1.6 Sample naming convention	79
2.2 <i>Cell Biology And Biochemical Methods</i>	81
2.2.1 Cell culture	81
2.2.2 Cytotoxicity Assay	81
2.2.3 Cell treatment schedules for the MTT assay	82
2.2.4 Luciferase Assay for measuring Nrf2/ARE induction	82
2.2.5 Western Blotting	82
2.2.6 Cytotoxicity profile (LD ₅₀) of ethacrynic acid following pretreatment with bioactive compounds ..	85
CHAPTER 3 Results and Discussion	86
3.1 <i>Study 1: Sample preparation and Soxhlet extraction of plant materials followed by screening of phytochemical composition (TLC) and free-radical scavenging activity of crude extracts (DPPH assay).....</i>	<i>87</i>
3.2 <i>Study 2: Cytotoxicity assay and luciferase reporter assay of methanol and n-hexane extracts of selected plants and precipitated compounds.....</i>	<i>94</i>
3.2.1 Cytotoxicity (MTT assay) of tBHQ and luciferase activity induction in AREc32 cells	94
3.2.2 Cytotoxicity (MTT assay) and Nrf2 induction results (luciferase assay) of crude methanol extracts	96
3.2.3 Results of luciferase assays of crude methanol extracts in AREc32 cells	105
3.2.3 Cytotoxicity (MTT assay) and Nrf2 induction (luciferase assay) of crude n-hexane extracts	107
3.2.4 Cytotoxicity and luciferase assay results for compounds precipitated during the Soxhlet extraction of <i>Gypsophila pilulifera</i> , <i>Gardenia ternifolia</i> and <i>Ziziphus mucronata</i>	116
3.3 <i>Study 3: Chromatographic fractionation of bioactive crude methanol extracts of Centaurea dichroa (CD), Centaurea pamphylica (CP), Gardenia ternifolia (GT) and Ziziphus mucronata (ZM), followed by cytotoxicity assay and luciferase assay using AREc32 cells and DPPH assay of fractions.....</i>	<i>117</i>
3.3.1 Cytotoxicity results for methanol fractions of <i>Centaurea dichroa</i> (CD-Me), <i>Centaurea pamphylica</i> (CP-Me), <i>Gardenia ternifolia</i> (GT-Me) and <i>Ziziphus mucronata</i> (ZM-Me) in AREc32 cells...	117

3.3.2	Luciferase assay results for methanol fractions of <i>Centaurea dichroa</i> (CD-Me), <i>Centaurea pamphylica</i> (CP-Me), <i>Gardenia ternifolia</i> (GT-Me) and <i>Ziziphus mucronata</i> (ZM-Me)	121
3.3.3	DPPH assay results for bioactive methanol fractions of <i>Centaurea dichroa</i> (CD-Me), <i>Centaurea pamphylica</i> (CP-Me), <i>Gardenia ternifolia</i> (GT-Me) and <i>Ziziphus mucronata</i> (ZM-Me)	124
3.4	<i>Study 4: Identification of compounds from bioactive fractions of methanol extracts by means of UV-Vis, nuclear magnetic resonance (NMR) and mass spectrometry (MS) analysis</i>	127
3.4.1	Structural characterisation of compounds precipitated during Soxhlet extraction	127
3.4.2	Structural characterisation of compounds isolated from bioactive methanol fractions	134
3.5	<i>Study 5: Cytotoxicity assay and luciferase assay in AREc32 cells of selected polyphenolic compounds: apigenin, genkwanin, hesperetin, hispidulin, kaempferol, luteolin, naringenin, quercetin, sakuranetin and velutin</i>	145
3.5.1	Cytotoxicity assay results for selected polyphenolic compounds: apigenin, genkwanin, hesperetin, hispidulin, kaempferol, luteolin, naringenin, quercetin, sakuranetin and velutin	145
3.5.2	Luciferase assay results on AREc32 cells for selected polyphenolic compounds: apigenin, genkwanin, hesperetin, hispidulin, kaempferol, luteolin, naringenin, quercetin, sakuranetin and velutin	150
3.6	<i>Study 6: Determination of NQO1 gene expression induced by selected phytochemical compounds</i>	153
3.6.1	Cytotoxicity assay of bioactive compounds on MCF-7 cells	153
3.6.2	Western Blotting results for induction of NQO1 by sakuranetin and naringenin	159
3.7	<i>Study 7: Effect of selected flavonoids on ethacrynic acid-induced oxidative stress in MCF-7 cells.</i>	161
CHAPTER 4 Conclusions and recommendations for future work		172
4.1	<i>Conclusions of Study 1</i>	172
4.2	<i>Conclusions of Study 2</i>	172
4.3	<i>Conclusions of Study 3 and recommendations for future work</i>	173
4.4	<i>Conclusions of Study 4 and recommendations for future work</i>	173
4.5	<i>Conclusions of Study 5 and recommendations for future work</i>	174
4.6	<i>Conclusions of Study 6 and recommendations for future work</i>	175
4.7	<i>Conclusions of Study 7 and recommendations for future work</i>	175
4.8	<i>Final conclusions and recommendations for future work</i>	176

References	178
Appendices.....	196
<i>Appendix A</i> <i>NMR and MS spectra of precipitated compounds</i>	<i>196</i>
Appendix A.1 NMR and MS data for precipitate GPS1 as stachyose	196
Appendix A.2 NMR and MS data for precipitate GTS1/GTS2.....	199
Appendix A.3 NMR and MS data for precipitate ZMPH1	200
<i>Appendix B</i> <i>NMR and MS data for isolated compounds from Gardenia ternifolia Schumach.& Thonn.</i>	
<i>(GT-Me)</i> <i>203</i>	
Appendix B.1 NMR and MS data for compound F3-GT-Me-PA (aka F3GTME-PA/F3GTME-P4)	203

Abstract

A selection of twelve non-dietary plants were subjected to Soxhlet extraction with *n*-hexane and methanol and the crude extracts were screened for Nrf2 induction potential using a AREc32 cell-based luciferase gene reporter assay. Screening for free-radical scavenging activity using the DPPH assay was also performed. The highest increase in Nrf2 induction was achieved by the methanol extract of *Centaurea dichroa* Boiss.& Heldr. (CD-Me, 250 µg/ml), with a 22.7-fold to control induction, followed by the *n*-hexane extract of *Solanum anguivi* Lam. (SA-He, 100 µg/ml), with 20.2-fold to control induction. The Nrf2/ARE signaling pathway was also up-regulated by two other methanol extracts, of *Centaurea pamphylica* Boiss. & Heldr. (CP-Me, 100 µg/ml) and *Gardenia ternifolia* Schumach. & Thonn. (GT-Me, 750 µg/ml), with 11.22-fold and 8.94-fold to control luciferase induction, respectively. The bioassay guided investigation led to further fractionation of the bioactive methanol extracts so that the less polar methanolic fractions F3 and F4 of CP-Me and GT-Me increased Nrf2 activity more than their respective crude extracts; up to 12.6 - 13.4-fold for CP-Me fractions, and up to 11.6 – 12.6-fold for GT-Me fractions. Moreover, compounds isolated from the bioactive fractions indicated flavonoid type structures, identifying sakuranetin for the first time in *Gardenia ternifolia* Schumach.& Thonn. Stachyose, mannitol and betulinic acid were also identified as precipitates from solvent extraction. Because of limited amount of material, various types of flavonoids such as flavones, flavanones and flavonols were purchased with the purpose of screening them for Nrf2 activity in AREc32 cells. The flavonoids alone increased the luciferase activity to no more than 3.1-fold (hesperetin, 40 µM), with most reaching slightly above 2-fold induction, indicating a possible synergy in the way of action of the natural products since mixtures of compounds showed higher bioactivity in the same assay. Fractions F3 of CP-Me and GT-Me showed the highest free radical-scavenging potential in the DPPH assay, with IC₅₀ values of 0.072 mg/ml and 0.132 mg/ml respectively (IC₅₀ exerted by positive control quercetin was 0.005 mg/ml). Finally, all flavonoids tested offered protection against oxidative stress induced by ethacrynic acid (ETA) in MCF-7 cells (LD₅₀=68.5 µM), with the flavone velutin (2.5 µM) and flavanone sakuranetin (20 µM) increasing the LD₅₀ of ETA more than 200 times, while all flavonoid pretreatment conditions generally increased the LD₅₀ of ETA more than 9 times.

Declaration

I declare that no portion of the work referred to in the thesis has been submitted in support of an application for another degree or qualification of this or any other university or other institute of learning.

Alexandra-Georgiana Zavoianu

List of Abbreviations

ACF	aberrant crypt foci
AOM	azoxymethane
ARE/EpRE	antioxidant-responsive element/electrophile-responsive element
tBHQ	<i>tert</i> -butylhydroquinone
CAN	acetonitrile
COX1	cyclooxygenase-1
COX-2	cyclooxygenase-2
DCM	dichloromethane
DPPH	2,2-diphenyl-1-picrylhydrazyl
ETA	ethacrynic acid
EtOAc	ethyl acetate
EtOH	ethanol
GCL	glutamate-cysteine ligase
GPx	glutathione peroxidase
GSH	glutathione
GST	glutathione S-transferase
HMOX-1/HO-1	heme oxygenase 1
Keap 1	Kelch-like ECH-associated protein 1
MAPK	mitogen-activated protein kinase
MeOH	methanol
MMP-9	matrix metalloproteinase-1
MS	Mass Spectrometry
MTT	3-(4,5-dimethylthiazol-2-yl)-2,5-diphenyltetrazolium bromide
NAD(P)H	nicotine adenine dinucleotide phosphate

NMR	Nuclear Magnetic Resonance
NQO1	NAD(P)H dehydrogenase (quinone 1)
Nrf2	nuclear factor erythroid 2-related factor 2
PG	prostaglandins
PKC	protein kinase C
RhoA	Ras homolog family member A
RT	room temperature
SFN	sulforaphane

List of Tables

Table 1 Fruits and vegetables intake associated with a decreased risk of various types of cancer. Adapted from Turati <i>et al.</i> 2015	28
Table 2 Chemical structures of some dietary flavonoids with cancer chemoprevention properties.....	43
Table 3 Subclasses of terpenoids and their chemopreventive properties (Source: Huang <i>et al.</i> 2012).....	52
Table 4 Amounts of plant materials used for Soxhlet extraction	72
Table 5 SPE solvent gradient steps.....	74
Table 6 Preparative HPLC gradient method.....	76
Table 7 Polyphenolic phytochemicals used in bioassays and their chemical structure. Structures generated in ChemDraw	77
Table 8 Code names of plant extracts and fractions.....	79
Table 9 Concentrations (μM) of bioactive compounds used, with tBHQ as positive control	83
Table 10 Summary of crude extracts resulted after Soxhlet extraction. Note that as different sample materials have different densities, the masses contained in the same thimble vary.	87
Table 11 TLC retention factors (R_f) of compounds observed at 254 nm and 366 nm for <i>n</i> -hexane and methanol extracts. A 1:4 ethyl acetate: <i>n-n-hexane</i> solvent system was used for non-polar extracts and a 2:3 ethyl acetate: <i>n-hexane</i> for methanol extracts. For non-polar extracts extra spots were observed after spraying with anisaldehyde reagent.....	89
Table 12 TLC retention factors (R_f) of compounds observed at 254 nm and 366 nm for <i>n</i> -hexane and methanol extracts. A 1:4 ethyl acetate: <i>n-hexane</i> solvent system was used for non-polar extracts and a 2:3 ethyl acetate: <i>n-n-hexane</i> for methanol extracts. For non-polar extracts extra spots were observed after spraying with anisaldehyde reagent.....	89
Table 13 The DPPH IC_{50} values (mg/ml) of methanol extracts of <i>Arctium lappa</i> , <i>Ziziphus mucronata</i> , <i>Gardenia ternifolia</i> , <i>Equisetum arvense</i> , <i>Centaurea pamphylica</i> , <i>Solanum anguivi</i> and <i>Hyssopus officinalis</i> , and positive control quercetin.....	93

Table 14 Overview of LD₅₀ of ethacrynic acid after pre-treatment with various flavonoids and without pretreatment 169

List of Figures

Figure 1 Oxidative stress: causes and consequences (Adapted from Sharma, 2014)	30
Figure 2 Chemical formation of reactive oxygen and nitrogen species (Source: Ríos-Arrabal <i>et al.</i> 2013).....	31
Figure 3 Main reaction steps for antioxidant defense, where SOD = superoxide dismutase, CAT = catalase, GPx = glutathione peroxidase and GR = glutathione reductase	32
Figure 4 Classification of cancer chemoprevention agents (Adapted from Surh, 2003)	34
Figure 5 The Nrf2/Keap1 regulatory pathway. Under homeostatic conditions, Nrf2 is localised in the cytoplasm, bound to a Keap1 homodimer, which forms a complex with Cullin3-Rbx1 E3 ubiquitin ligase. This facilitates the ubiquitination and proteolysis of Nrf2 via the 26S proteasome. Under electrophilic/oxidative stress, the Keap1-Cul3-E3 ubiquitin complex is disrupted and Nrf2 can translocate to the nucleus where it forms a heterodimer with small Maf proteins and binds to the ARE, promoting the transcription of cytoprotective genes. (Source: Sznarkowska <i>et al.</i> 2017).....	39
Figure 6 Example of primary metabolites (Sources: https://pubchem.ncbi.nlm.nih.gov/ ; Xu, 2002).....	41
Figure 7 Examples of secondary metabolites (source: PubChem).....	42
Figure 8 Structural backbone of flavonoids (C6-C3-C6) showing a chromane ring (A and C) attaching a second aromatic ring (B) in position 2, 3 or 4. Source: Balentine <i>et al.</i> 2015... 48	48
Figure 11 Mechanisms of chemoprevention exhibited by phytochemicals (Source: Iqbal <i>et al.</i> 2018).....	57
Figure 10 Photo of <i>Centaurea</i> sp. Source: Jouko Lehmuskallio at http://www.luontoportti.com	59
Figure 13 Photo of <i>Arctium lappa</i> . Source: http://www.herbgarden.co.za/mountainherb/seedinfo.php?id=201	60
Figure 14 Photo of <i>Equisetum arvense</i> . Source: Bobby Hattaway at https://www.discoverlife.org/mp/20p?see=I_TQBH11687&res=640	61
Figure 13 Chemical structure of N,N-dimethyltryptamine from the Rubiaceae (Source: https://pubchem.ncbi.nlm.nih.gov/compound/6089#section=2D-Structure)	62

Figure 16 Photo of <i>Gardenia ternifolia</i> Schumach.& Thonn. Source: D.C.H. Plowes at www.zambiaflora.com	63
Figure 17 Photo of <i>Gypsophila fastigiata</i> . Source: Jouko Lehmuskallio at http://www.luontoportti.com	64
Figure 16 Photo of <i>Hyssopus officinalis</i> . Source: Jouko Lehmuskallio at http://www.luontoportti.com	65
Figure 17 Photo of <i>Kitaibelia balansae</i> . Source: Prof. Avinoam Danin at https://flora.org.il/en/plants/KITBAL/	66
Figure 18 Photo of <i>Solanum anguivi</i> . Source: Robert v. Blittersdorff at http://www.africanplants.senckenberg.de	67
Figure 19 Photo of mature <i>Ziziphus mucronata</i> . Source: Michael Briza at http://www.krugerpark.co.za/africa_buffalothorn.html	68
Figure 20 Flow diagram of the bioassay-guided investigation.....	70
Figure 21 Soxhlet apparatus at the end of a reflux cycle (500 ml)	72
Figure 22 Evaporation of methanol from an extract fraction using a rotary evaporator	73
Figure 23 %Inhibition of DPPH by methanol extracts of CP, GT, SA, ZM and quercetin at 10-fold dilutions between 0.0001 and 1 mg/ml. Graph shows the average values of triplicate experiments.	90
Figure 24 %Inhibition of DPPH by methanol extracts of <i>Equisetum arvense</i> , <i>Arctium Lappa</i> , <i>Hyssopus officinalis</i> , <i>Centaurea dichroa</i> and the positive control quercetin at concentrations between 0.0001 and 1 mg/ml. Graph shows the average values of triplicate experiments.	91
Figure 25 %Inhibition of DPPH by quercetin at 1-fold dilutions between 0.001 and 0.01 mg/ml. Graph shows the average values of duplicate experiments.....	92
Figure 26 %Inhibition of DPPH by CP-ME, GTME, SAME, EAME and HOME at concentrations of 1-fold dilutions between 0.1 and 1 mg/ml. Graph shows the average values of duplicate experiments.	92
Figure 27 Graph showing the %inhibition of DPPH by ZM-Me and AL-Me at 1-fold dilutions between 0.01 and 0.1 mg/ml. Graph shows the average values of duplicate experiments	93

Figure 28 Cell viability as percentage to control (0 mg/ml) observed after treatment of AREc32 cells for 24 h with tBHQ (10-100 μ M). DMSO represents the vehicle control and its concentration is expressed as v/v%. Results show the mean +/- SEM (n=12)..... 95

Figure 29 Effect of tBHQ on the induction of luciferase activity. AREc32 cells were incubated for 24 h with non-cytotoxic concentrations of tBHQ (10-50 μ M). DMSO represents the vehicle control and its concentration is expressed as v/v%. Values show the average of n=3. 95

Figure 32 Cell viability as percentage to control (0 mg/ml) observed after treatment of AREc32 cells for 24 h with AL-Me (0.01-1 mg/ml). DMSO represents the vehicle control and its concentration is expressed as v/v%. Results show the mean +/- SEM (n=3, 3 replicates). 96

Figure 33 Cell viability as percentage to control (0 mg/ml) observed after treatment of AREc32 cells for 24 h with CA-Me (0.01-1 mg/ml). DMSO represents the vehicle control and its concentration is expressed as v/v%. Results show the mean +/- SEM (n=3, 3 replicates). 97

Figure 32 Cell viability as percentage to control (0 mg/ml) observed after treatment of AREc32 cells for 24 h with CD-Me (0.01-1 mg/ml). DMSO represents the vehicle control and its concentration is expressed as v/v%. Results show the mean +/- SEM (n=3, 3 replicates). 98

Figure 35 Cell viability as percentage to control (0 mg/ml) observed after treatment of AREc32 cells for 24 h with CK-Me (0.01-1 mg/ml). DMSO represents the vehicle control and its concentration is expressed as v/v%. Results show the mean +/- SEM (n=3, 3 replicates). 98

Figure 36 Cell viability percentage of control (0 mg/ml) observed after treatment of AREc32 cells for 24 h with CP-Me (0.025-1 mg/ml). DMSO represents the vehicle control and its concentration is expressed as v/v%. Results show the mean +/- SEM (n=3, 3 replicates). 99

Figure 37 Cell viability percentage of control (0 mg/ml) observed after treatment of AREc32 cells for 24 h with EA-Me (0.01-1 mg/ml). DMSO represents the vehicle control and its concentration is expressed as v/v%. Results show the mean +/- SEM (n=3, 3 replicates). 99

Figure 38 Cell viability percentage to control (0 mg/ml) observed after treatment of AREc32 cells for 24 h with GP-Me (0.025-1 mg/ml). DMSO represents the vehicle control and its concentration is expressed as v/v%. Results show the mean +/- SEM (n=3, 3 replicates)100

Figure 39 Cell viability percentage to control (0 mg/ml) observed after treatment of AREc32 cells for 24 h with GT-Me (0.025-1 mg/ml). DMSO represents the vehicle control and its concentration is expressed as v/v%. Results show the mean +/- SEM (n=3, 3 replicates)101

Figure 40 Cell viability percentage to control (0 mg/ml) observed after treatment of AREc32 cells for 24 h with HO-Me (0.01-1 mg/ml). DMSO represents the vehicle control and its concentration is expressed as v/v%. Results show the mean +/- SEM (n=3, 3 replicates)101

Figure 41 Cell viability percentage to control (0 mg/ml) observed after treatment of AREc32 cells for 24 h with KB-Me (0.005-1 mg/ml). DMSO represents the vehicle control and its concentration is expressed as v/v%. Results show the mean +/- SEM (n=3, 3 replicates)102

Figure 42 Cell viability as percentage to control (0 mg/ml) observed after treatment of AREc32 cells for 24 h with SA-Me (0.005-1 mg/ml). DMSO represents the vehicle control and its concentration is expressed as v/v%. Results show the mean +/- SEM (n=3, 3 replicates)102

Figure 43 Cell viability as percentage to control (0 mg/ml) observed after treatment of AREc32 cells for 24 h with ZA-Me (0.025-1 mg/ml). DMSO represents the vehicle control and its concentration is expressed as v/v%. Results show the mean +/- SEM (n=3, 3 replicates)103

Figure 42 Simulation of MTT assay on ZMME extract (0.025-1 mg/ml) without seeded cells. The methanol extract reacts with the MTT in the culture medium in a concentration-dependent manner. 104

Figure 45 Cell viability percentage to control (0 mg/ml) observed after treatment of AREc32 cells for 24 h with ZM-Me (0.025-1 mg/ml). DMSO represents the vehicle control and its concentration is expressed as v/v%. Results show the mean +/- SEM (n=3, 3 replicates). 104

Figure 46 Effect of methanol extracts on the induction of luciferase activity and tBHQ as postive control. AREc32 cells were incubated for 24 h with non-cytotoxic concentrations of methanol extracts of AL, CA, CD, CK, CP, EA, GP, GT, HO, KB, SA and ZM. DMSO represents the vehicle control and its concentration is expressed as v/v%. Values show mean +/- SEM (n=3, 3 replicates), control=1. 106

Figure 47 Cell viability as percentage to control (0 µg/ml) observed after treatment of AREc32 cells for 24 h with AL-He (5-1000 µg/ml). DMSO represents the vehicle control and its concentration is expressed as v/v%. Results show the mean +/- SEM (n=3, 3 replicates)107

Figure 48 Cell viability as percentage to control (0 µg/ml) observed after treatment of AREc32 cells for 24 h with CA-He (10-1000 µg/ml). DMSO represents the vehicle control and its concentration is expressed as v/v%. Results show the mean +/- SEM (n=3, 3 replicates)108

Figure 49 Cell viability as percentage to control (0 µg/ml) observed after treatment of AREc32 cells for 24 h with CK-He (10-1000 µg/ml). DMSO represents the vehicle control and its concentration is expressed as v/v%. Results show the mean +/- SEM (n=3, 3 replicates)108

Figure 50 Cell viability percentage to control (0 µg/ml) observed after treatment of AREc32 cells for 24 h with CP-He (10 - 1000 µg/ml). DMSO represents the vehicle control and its concentration is expressed as v/v%. Results show the mean +/- SEM (n=3, 3 replicates)109

Figure 49 Cell viability percentage to control (0 µg/ml) observed after treatment of AREc32 cells for 24 h with EA-He (5-1000 µg/ml). DMSO represents the vehicle control and its concentration is expressed as v/v%. Results show the mean +/- SEM (n=3, 3 replicates)109

Figure 52 Cell viability percentage to control (0 µg/ml) observed after treatment of AREc32 cells for 24 h with GP-He (10-1000 µg/ml). DMSO represents the vehicle control and its concentration is expressed as v/v%. Results show the mean +/- SEM (n=3, 3 replicates).

..... 110

Figure 53 Cell viability percentage to control (0 µg/ml) observed after treatment of AREc32 cells for 24 h with GT-He (5-1000 µg/ml). DMSO represents the vehicle control and its concentration is expressed as v/v%. Results show the mean +/- SEM (n=3, 3 replicates).

..... 111

Figure 54 Cell viability percentage to control (0 µg/ml) observed after treatment of AREc32 cells for 24 h with HO-He (5-1000 µg/ml). DMSO represents the vehicle control and its concentration is expressed as v/v%. Results show the mean +/- SEM (n=3, 3 replicates)111

Figure 55 Cell viability percentage to control (0 µg/ml) observed after treatment of AREc32 cells for 24 h with HO-He (5-1000 µg/ml). DMSO represents the vehicle control and its concentration is expressed as v/v%. Results show the mean +/- SEM (n=3, 3 replicates)112

Figure 56 Cell viability percentage of control (0 µg/ml) observed after treatment of AREc32 cells for 24 h with SA-He (5-1000 µg/ml). DMSO represents the vehicle control and its concentration is expressed as v/v%. Results show the mean +/- SEM (n=3, 3 replicates).

..... 113

Figure 57 Cell viability percentage of control (0 µg/ml) observed after treatment of AREc32 cells for 24 h with ZM-He (5-1000 µg/ml). DMSO represents the vehicle control and its concentration is expressed as v/v%. Results show the mean +/- SEM (n=3, 3 replicates).

..... 113

Figure 58 Cell viability as percentage to control (0 µg/ml) observed after treatment of AREc32 cells for 24 h with CD-He (1-500 µg/ml). DMSO represents the vehicle control and its concentration is expressed as v/v%. Results show the mean +/- SEM (n=3, 3 replicates) 114

Figure 59 Effect of *n*-hexane extracts on the induction of luciferase activity and tBHQ as positive control. AREc32 cells were incubated for 24 h with non-cytotoxic concentrations of AL-He, CA-He, CD-He, CK-He, CP-He, EA-He, GP-He, GT-He, HO-He, KB-He, SA-He and ZM-He. DMSO represents the vehicle control and its concentration is expressed as v/v%. Values show mean +/- SEM (n=3, 3 replicates), control=1. 115

Figure 60 Cell viability as percentage of control (0 mg/ml) observed after treatment of AREc32 cells for 24 h with betulinic acid (0.625-40 µM). DMSO represents the vehicle control and its concentration is expressed as v/v%. Results show the mean +/- SEM (n=3, 4 replicates) 116

Figure 59 Cell viability as percentage to control (0 µg/ml) observed after treatment of AREc32 cells for 24 h with CD-Me fractions (1-500 µg/ml). Results show the mean +/- SEM (n=3, 3 replicates). 118

Figure 62 Cell viability as percentage to control (0 µg/ml) observed after treatment of AREc32 cells for 24 h with CP-Me fractions (20-1000 µg/ml). Results show the mean +/- SEM (n=3, 3 replicates). 119

Figure 63 Cell viability as percentage to control (0 µg/ml) observed after treatment of AREc32 cells for 24 h with fractions of GT-Me (20-1000 µg/ml). Results show the mean +/- SEM (n=3, 3 replicates). 120

Figure 64 Cell viability as percentage to control (0 µg/ml) observed after treatment of AREc32 cells for 24 h with ZM-Me fractions (20-1000 µg/ml). Results show the mean +/- SEM (n=3, 3 replicates). 121

Figure 63 Effect of fractions of *Centaurea dichroa* methanol extract on the induction of luciferase activity and of tBHQ as positive control. AREc32 cells were incubated for 24 h with non-cytotoxic concentrations of CD-Me. Values show mean +/- SEM (n=3, 3 replicates), control=1. 122

Figure 66 Effect of fractions of *Centaurea pamphilica* methanol extract on the induction of luciferase activity and of tBHQ as positive control. AREc32 cells were incubated for 24 h with non-cytotoxic concentrations of CP-Me. Values show mean +/- SEM (n=3, 3 replicates), control=1. 122

Figure 65 Effect of fractions of <i>Gardenia ternifolia</i> methanol extract on the induction of luciferase activity and tBHQ as positive control. AREc32 cells were incubated for 24 h with non-cytotoxic concentrations of GT-Me. Values show mean +/- SEM (n=3, 3 replicates), control=1.	123
Figure 66 Effect of fractions of <i>Ziziphus mucronata</i> methanol extract on the induction of luciferase activity and tBHQ as positive control. AREc32 cells were incubated for 24 h with non-cytotoxic concentrations of ZM-Me. Values show mean +/- SEM (n=3, 3 replicates), control=1.	123
Figure 69 %Inhibition of DPPH by fractions F3 of methanol extracts of <i>Centaurea dichroa</i> , <i>Centaurea pamphylica</i> , <i>Gardenia ternifolia</i> and the positive control quercetin at concentrations between 0.0001 and 1 mg/ml. Graph shows the average values of triplicate experiments.	124
Figure 70 Graph showing the %inhibition of DPPH by CD-Me and GT-Me at 1-fold dilutions between 0.1 and 0.01 mg/ml. Graph shows the average values of duplicate experiments	125
Figure 71 Graph showing the %inhibition of DPPH by CP-Me at 1-fold dilutions between 0.1 and 0.01 mg/ml. Graph shows the average values of duplicate experiments.....	126
Figure 70 Graph showing the %inhibition of DPPH by quercetin at 1-fold dilutions between 0.001 and 0.01 mg/ml. Graph shows the average values of duplicate experiments.	126
Figure 73 Chemical structure of stachyose C ₂₄ H ₄₂ O ₂₁ , 666 g/mol.....	127
Figure 74 GPS1 experimental NMR assignments (in black) compared to those for stachiose in literature (blue and magenta in the image)	129
Figure 75 Chemical structure of mannitol	130
Figure 74 ¹ H and ¹³ C assignments for mannitol (upper left) based on NMR spectra presented in Appendix A.2; ¹ H and ¹³ C assignments for mannitol (lower right) based on NMR spectra from literature	131
Figure 77 ¹ H and ¹³ C assignments for mannitol from online catalogues.	131
Figure 78 Chemical structure of betulinic acid	132
Figure 77 ¹ H and ¹³ C assignments for betulinic acid based on NMR data recorded for ZMPH1 (in black) and on NMR data from literature (blue and magenta; Berger and Sicker, 2009)	133

Figure 80 Preparative HPLC chromatogram of F3 CD-Me (30% to 90% MeOH in H ₂ O gradient solvent system, 200 µL injection).....	134
Figure 81 UV spectrum of Peak 1 of F3 CD-Me	135
Figure 80 UV spectrum of Peak 2 of F3 CD-Me	135
Figure 83 UV spectrum of Peak 3 of F3 CD-Me	136
Figure 82 Analytical chromatogram of isolated compound F3CD-Me-P2, with the UV spectrum recorded on Agilent 1260 in methanol:water gradient solvent system.....	136
Figure 83 MS spectrum of F3CD-Me-P2	137
Figure 84 Analytical HPLC chromatogram of isolated compound F3CDMe-P3 in methanol/water solvent system with gradient; 10 mg/ml.....	137
Figure 87 MS spectrum of F3CD-Me-P3	138
Figure 86 Preparative HPLC chromatogram for F3 CP-Me	139
Figure 89 Analytical HPLC chromatogram of F3CPME-P5, 1 mg/ml	139
Figure 90 Analytical chromatogram of apigenin, 10 mg/ml	140
Figure 91 Analytical HPLC chromatogram of F3CP-Me-P7(IV) and recorded UV spectrum	140
Figure 92 Preparative HPLC chromatogram for F3 GT-Me	141
Figure 91 Analytical HPLC chromatogram for F3 GT-Me-P4/PA, 1 mg/ml.....	141
Figure 94 Chemical structure of sakuranetin C ₁₆ H ₁₄ O ₅ , 286 g/mol.....	142
Figure 95 Experimental NMR assignments for F3GT-Me-P4/PA as sakuranetin	143
Figure 96 NMR assignments presented in literature for sakuranetin (in blue or magenta depending on source; references in text)	143
Figure 97 Analytical HPLC chromatogram for F3 GT-Me-PB/P6, 1 mg/ml.....	144
Figure 98 UV spectrum of Peak 2 as F3 GT-Me-PB/P6.....	144
Figure 99 Cell viability as percentage to control (0 mg/ml) observed after treatment of AREc32 cells for 24 h with apigenin (1-50 µM). DMSO represents the vehicle control and its concentration is expressed as v/v%. Results show the mean +/- SEM (n=3, 3 replicates).....	145

Figure 100 Cell viability as percentage to control (0 mg/ml) observed after treatment of AREc32 cells for 24 h with genkwanin (1-50 μ M). DMSO represents the vehicle control and its concentration is expressed as v/v%. Results show the mean +/- SEM (n=3, 3 replicates) 146

Figure 99 Cell viability as percentage to control (0 mg/ml) observed after treatment of AREc32 cells for 24 h with hesperetin (1-50 μ M). DMSO represents the vehicle control and its concentration is expressed as v/v%. Results show the mean +/- SEM (n=3, 3 replicates)146

Figure 102 Cell viability as percentage to control (0 mg/ml) observed after treatment of AREc32 cells for 24 h with hispidulin (1-50 μ M). DMSO represents the vehicle control and its concentration is expressed as v/v%. Results show the mean +/- SEM (n=3, 3 replicates)147

Figure 101 Cell viability as percentage to control (0 mg/ml) observed after treatment of AREc32 cells for 24 h with kaempferol (1-50 μ M). DMSO represents the vehicle control and its concentration is expressed as v/v%. Results show the mean +/- SEM (n=3, 3 replicates) 147

Figure 104 Cell viability as percentage to control (0 mg/ml) observed after treatment of AREc32 cells for 24 h with luteolin (1-50 μ M). DMSO represents the vehicle control and its concentration is expressed as v/v%. Results show the mean +/- SEM (n=3, 3 replicates)148

Figure 103 Cell viability as percentage to control (0 mg/ml) observed after treatment of AREc32 cells for 24 h with naringenin (1-50 μ M). DMSO represents the vehicle control and its concentration is expressed as v/v%. Results show the mean +/- SEM (n=3, 3 replicates) 148

Figure 104 Cell viability as percentage to control (0 mg/ml) observed after treatment of AREc32 cells for 24 h with quercetin (1-50 μ M). DMSO represents the vehicle control and its concentration is expressed as v/v%. Results show the mean +/- SEM (n=3, 3 replicates)149

Figure 105 Cell viability as percentage to control (0 mg/ml) observed after treatment of AREc32 cells for 24 h with sakuranetin (1-50 μ M). DMSO represents the vehicle control and its concentration is expressed as v/v%. Results show the mean +/- SEM (n=3, 3 replicates) 149

Figure 108 Cell viability as percentage to control (0 mg/ml) observed after treatment of AREc32 cells for 24 h with velutin (1-50 μ M). DMSO represents the vehicle control and its concentration is expressed as v/v%. Results show the mean +/- SEM (n=3, 3 replicates)150

Figure 107 Effect of various flavonoids on the induction of luciferase activity and tBHQ as positive control. AREc32 cells were incubated for 24 h with non-cytotoxic concentrations of apigenin, genkwanin, hesperetin, hispidulin, kaempferol, luteolin, naringenin, quercetin, sakuranetin and velutin. DMSO represents the vehicle control and its concentration is expressed as v/v%. Values show mean +/- SEM (n=3, 3 replicates), control=1..... 151

Figure 108 Cell viability as percentage to control (0 mg/ml) observed after treatment of MCF-7 cells for 24 h with quercetin (2.5 µM). DMSO represents the vehicle control and its concentration is expressed as v/v%. Results show the mean +/- SEM (n=3, 3 replicates)154

Figure 111 Cell viability as percentage to control (0 mg/ml) observed after treatment of MCF-7 cells for 24 h with apigenin (5 µM). DMSO represents the vehicle control and its concentration is expressed as v/v%. Results show the mean +/- SEM (n=3, 3 replicates)154

Figure 112 Cell viability as percentage to control (0 mg/ml) observed after treatment of MCF-7 cells for 24 h with genkwanin (2.50 µM). DMSO represents the vehicle control and its concentration is expressed as v/v%. Results show the mean +/- SEM (n=3, 3 replicates)155

Figure 113 Cell viability as percentage to control (0 mg/ml) observed after treatment of MCF-7 cells for 24 h with hesperetin (1 µM). DMSO represents the vehicle control and its concentration is expressed as v/v%. Results show the mean +/- SEM (n=3, 3 replicates)155

Figure 114 Cell viability as percentage to control (0 mg/ml) observed after treatment of MCF-7 cells for 24 h with hispidulin (2.5 µM). DMSO represents the vehicle control and its concentration is expressed as v/v%. Results show the mean +/- SEM (n=3, 3 replicates)156

Figure 115 Cell viability as percentage to control (0 mg/ml) observed after treatment of MCF-7 cells for 24 h with kaempferol (2.5 µM). DMSO represents the vehicle control and its concentration is expressed as v/v%. Results show the mean +/- SEM (n=3, 3 replicates)156

Figure 116 Cell viability as percentage to control (0 mg/ml) observed after treatment of MCF-7 cells for 24 h with luteolin (2.5 µM). DMSO represents the vehicle control and its concentration is expressed as v/v%. Results show the mean +/- SEM (n=3, 3 replicates)157

Figure 117 Cell viability as percentage to control (0 mg/ml) observed after treatment of MCF-7 cells for 24 h with naringenin (2.5 µM). DMSO represents the vehicle control and its concentration is expressed as v/v%. Results show the mean +/- SEM (n=3, 3 replicates)157

Figure 118 Cell viability as percentage to control (0 mg/ml) observed after treatment of MCF-7 cells for 24 h with sakuranetin (20 μ M). DMSO represents the vehicle control and its concentration is expressed as v/v%. Results show the mean \pm SEM (n=3, 3 replicates) 158

Figure 117 Cell viability as percentage to control (0 mg/ml) observed after treatment of MCF-7 cells for 24 h with velutin (1-50 μ M). DMSO represents the vehicle control and its concentration is expressed as v/v%. Results show the mean \pm SEM (n=3, 3 replicates) 158

Figure 118 Effect of 24 h treatment of MCF-7 cells with (a) sakuranetin and (b) naringenin on NQO1 protein expression..... 160

Figure 119 Cell viability as percentage to control (no treatment) observed after treatment of MCF-7 cells for 24 h with ethacrynic acid (3.125-1000 μ M). Results of the MTT assay show the mean of 3 experiments (n=3, 2 replicates)..... 161

Figure 122 Cell viability as percentage to control (no treatment) observed after pre-treatment of MCF-7 cells for 24 h with tBHQ (10 μ M) and ethacrynic acid (3.125-1000 μ M). Results of the MTT assay show the mean of 2 experiments (total n=6). $P < .0001$, significant difference between the cytotoxicity of ETA in pretreated cells and the cytotoxicity of ETA alone. 162

Figure 123 Cell viability as percentage to control (no treatment) observed after pre-treatment of MCF-7 cells for 24 h with apigenin (5 μ M) and ethacrynic acid (3.125-1000 μ M). Results of the MTT assay show the mean of 2 experiments (total n=6). $P < .0001$, significant difference between the cytotoxicity of ETA in pretreated cells and the cytotoxicity of ETA alone. 163

Figure 124 Cell viability as percentage to control (no treatment) observed after pre-treatment of MCF-7 cells for 24 h with genkwanin (2.5 μ M) and ethacrynic acid (3.125-1000 μ M). Results of the MTT assay show the mean of 2 experiments (total n=6). $P < .0001$, significant difference between the cytotoxicity of ETA in pretreated cells and the cytotoxicity of ETA alone. 163

Figure 125 Cell viability as percentage to control (no treatment) observed after pre-treatment of MCF-7 cells for 24 h with hesperetin (1 μ M). and ethacrynic acid (3.125-1000 μ M). Results of the MTT assay show the mean of 2 experiments (total n=6). $P < .0001$, significant difference between the cytotoxicity of ETA in pretreated cells and the cytotoxicity of ETA alone. 164

Figure 124 Cell viability as percentage to control (no treatment) observed after pre-treatment of MCF-7 cells for 24 h with hispidulin (2.5 μ M) and ethacrynic acid (3.125-1000 μ M). Results

of the MTT assay show the mean of 2 experiments (total n=6). $P < .0001$, significant difference between the cytotoxicity of ETA in pretreated cells and the cytotoxicity of ETA alone.	165
Figure 125 Cell viability as percentage to control (no treatment) observed after pre-treatment of MCF-7 cells for 24 h with kaempferol (2.5 μM) and ethacrynic acid (3.125-1000 μM). Results of the MTT assay show the mean of 2 experiments (total n=6). $P < .0001$, significant difference between the cytotoxicity of ETA in pretreated cells and the cytotoxicity of ETA alone.	166
Figure 128 Cell viability as percentage to control (no treatment) observed after pre-treatment of MCF-7 cells for 24 h with luteolin (2.5 μM) and ethacrynic acid (3.125-1000 μM). Results of the MTT assay show the mean of 2 experiments (total n=6). $P < .0001$, significant difference between the cytotoxicity of ETA in pretreated cells and the cytotoxicity of ETA alone.	166
Figure 127 Cell viability as percentage to control (no treatment) observed after pre-treatment of MCF-7 cells for 24 h with naringenin (2.5 μM) and ethacrynic acid (3.125-1000 μM). Results of the MTT assay show the mean of 2 experiments (total n=6). $P < .0001$, significant difference between the cytotoxicity of ETA in pretreated cells and the cytotoxicity of ETA alone.	167
Figure 128 Cell viability as percentage to control (no treatment) observed after pre-treatment of MCF-7 cells for 24 h with sakuranetin (20 μM) and ethacrynic acid (3.125-1000 μM). Results of the MTT assay show the mean of 2 experiments (total n=6). $P < .0001$, significant difference between the cytotoxicity of ETA in pretreated cells and the cytotoxicity of ETA alone.	168
Figure 129 Cell viability as percentage to control (no treatment) observed after pre-treatment of MCF-7 cells for 24 h with velutin (2.5 μM) and ethacrynic acid (3.125-1000 μM). Results of the MTT assay show the mean of 2 experiments (total n=6). $P < .0001$, significant difference between the cytotoxicity of ETA in pretreated cells and the cytotoxicity of ETA alone.	168
Figure 132 ^1H NMR spectrum of GPS1	196
Figure 133 DEPTQ experiment spectrum of GPS1	197
Figure 134 COSY experiment spectrum of stachyose	197
Figure 135 HSQC experiment spectrum of stachyose	198
Figure 136 HMBC experiment spectrum of stachyose	198
Figure 137 ^1H NMR spectrum of mannitol isolated after filtration of GT methanol extract	199

Figure 138 ¹ H NMR spectrum of mannitol isolated after evaporation of GT methanol extract	199
Figure 139 ¹ H NMR spectrum of betulinic acid	200
Figure 140 Expansion of ¹ H NMR spectrum of betulinic acid.....	200
Figure 141 DEPTQ experiment spectrum of betulinic acid	201
Figure 142 HSQC experiment spectrum of betulinic acid	201
Figure 143 HMBC experiment spectrum of betulinic acid	202
Figure 144 Proton NMR spectrum of F3GT-Me-P4/PA.....	203
Figure 145 Proton NMR spectrum of F3GT-Me-P4/PA.....	204
Figure 146 ¹ H NMR spectrum of F3 GT-Me-P4	205
Figure 147 COSY experiment spectrum for F3GT-Me-P4/PA.....	205
Figure 148 ¹³ C NMR spectrum of F3 GT-Me-P4/PA	206
Figure 149 HSQC experiment spectrum of F3 GT-Me-P4/PA.....	207
Figure 150 MS spectrum for F3 GT-Me-P4/PA (data entry error for sample name displayed at the top of spectrum)	208
Figure 151 MS spectrum for F3 GT-Me-P4/PA (data entry error for sample name displayed at the top of spectrum)	209

CHAPTER 1 General Introduction

1.1 Cancer Outlines

1.1.1 Statistics

Cancer represents a major public health problem worldwide. According to The Global Cancer Observatory (GLOBOCAN), there will be an estimated 18.1 million new cancer cases and 9.6 million cancer deaths globally in 2018 (Bray *et al.* 2018). These data indicate an increase compared to the 2015 world estimates: a rise of about 0.6 million cancer cases and 0.9 million cancer deaths (Fitzmaurice *et al.* 2017). It is estimated that about 1 in 5 men and 1 in 6 women will develop cancer during their lifetime, with 1 in 8 men and 1 in 10 women dying of this cause (Bray *et al.* 2018). Globally, about 1 in 6 deaths is due to cancer (World Health Organization, 2018). Worldwide, the estimated 5-year cancer prevalence is 43.8 million, while cancer is the second leading cause of death, showing a need for an effective reduction of the global cancer burden, especially through prevention and early diagnosis (Bray *et al.* 2018; World Health Organization, 2018).

Globally, the latest GLOBOCAN estimates show that the highest number of new cancer cases was noted for lung and breast cancer equally (approximately 2.1 million), while the highest number of cancer deaths was recorded for lung cancer (approximately 1.8 million), followed by stomach and liver cancer (Bray *et al.* 2018). Incidence rates per 100,000 persons vary substantially across the world; in men, incidence rates vary from 571.2 in Australia/New Zealand to 95.6 in Western Africa, and in women from 362 in Australia/ New Zealand to 96.2 in South-Central Asia. Similarly, death rates varied from 171 per 100,000 in Eastern Europe to 67.4 per 100,000 in Central America in men and from 120.7 per 100,000 in Melanesia to 64.2 per 100,000 in Central America and Eastern Asia in women (Bray *et al.* 2018).

The differences in cancer incidence and mortality can be attributed to differences in the prevalence of risk factors and the availability of preventive, diagnostic and treatment services in different countries. The major risk factors identified globally are tobacco use, unhealthy diet, insufficient physical activity, being overweight and obese, exposure to ionizing and ultraviolet (UV) radiation, certain hormones, alcohol use, infection by some viruses and bacteria (Human papillomavirus (HPV), Hepatitis B virus, Hepatitis C virus, Epstein-Barr virus, *Helicobacter pylori*), and certain chemicals (urban air pollution) (Sauer *et al.* 2017; World

Health Organization, 2018). Also, the differences and rise in cancer incidence and mortality can partly be attributed to population growth, varying socio-economic factors, and aging of the population. The latter indicates a need for a lifetime approach to cancer prevention (Shoemaker *et al.* 2015).

1.1.2 Cancer biology and lifestyle

Cancer is characterized by abnormal cell growth. Carcinogenesis is a complex multi-stage process in which normal cells alter their behaviour and metabolism. As a result, they start unregulated and uncontrolled proliferation in any part of the body (site of origin), with the potential of subsequent invasion of surrounding tissues and spreading to other locations in the body, i.e., metastasis (Hesketh, 2013; Timofte, 2017).

The cause of cancer is attributed to a mix of altering genetic and non-genetic factors (Toyokuni, 2016). The non-genetic factors, also called external, can be of physical (UV and ionising radiation), chemical (asbestos, carcinogenic substances from tobacco smoke) or biological in nature (infections with certain viruses and bacteria e.g. HPV, *Helicobacter pylori*) (World Health Organization, 2018). Some of the factors linked to cancer occurrence are modifiable (binge drinking, tobacco smoking, diet which includes frequent consumption of red and processed meat, obesity, recreational sunlight exposure and indoor tanning, environmental and work exposure to carcinogenic substances, etc.) while others are not (genetics, age) (White *et al.* 2017; World Health Organization, 2018). Prevention strategies and efforts are aimed at modifiable risk factors (White *et al.* 2017).

The above mentioned factors can initiate or contribute to carcinogenesis by causing mutations in healthy cells. Mutations which affect genes involved in the process of apoptosis (programmed cell death) can lead to uncontrolled proliferation. The programmed cell death response is still being investigated, as it involves a complex interplay of signaling pathways and is dependent on cell type, as well as the extent and type of DNA damage. To promote the malignant cellular phenotype, apoptotic pathways are usually impaired in cells undergoing neoplastic transformation, so that cells with irreparable DNA damage e.g. double strand DNA breaks or incomplete DNA repairs can continue proliferating. This process is important for both the initiation and progression phases of tumorigenesis, where uncontrolled proliferation supports the continued expansion of premalignant cells with high potential of continued proliferation and invasiveness. (Sun, Hail and Lotan, 2004; Hesketh, 2013; Surova and Zhivotovsky, 2013). Tissue homeostasis is maintained through a delicate balance

between cell proliferation and senescence/apoptosis. In non-cancer cells, apoptosis is activated, when DNA is damaged and helps remove damaged cells. However, cells which suffer mutations in segments of DNA responsible for growth control, such as mutations in the regions coding transforming growth factor beta (TGF- β) and tumour suppressor gene p53, which controls both senescence and apoptosis, eventually avoid regulation and become cancer cells. Mutations of positive cell-cycle regulators (proto-oncogenes) lead to formation of oncogenes, which can cause growth of cancer cells, and mutations of negative cell-cycle regulators (tumour suppressor genes) can lead to unregulated cell division. All of these changes occur in carcinogenesis as consequences of a complex interaction between the genetic and non-genetic cancer risk factors and cells (Hesketh, 2013).

The length of the carcinogenesis can take anywhere between a few years and a few decades (Toyokuni, 2016), during which time mutations are being accumulated until cells' regulators of growth and division become uncontrolled. This loss of regulation manifests itself in altered response to positive and negative external growth signals leading to indefinite growth and proliferation. Still, the accumulation of mutations can happen over a lifetime and WHO estimates that currently between 30% and 50% of cancer cases can be prevented by altering diet and lifestyle habits (World Health Organization, 2018).

Several case-control and cohort studies showed that an intake of at least five fruits and vegetables a day can decrease the risk of developing cancer by almost 50% (Surh, 2003). Notably, the European Prospective Investigation into Cancer and Nutrition (EPIC prospective cohort study) showed that intake of fruit, vegetables and fibre (plant-based complex carbohydrates) reduced the risk for colorectal cancer. The intake of fibre, usually found in cereal, as well as fruits, also correlated with a reduced the risk of liver and breast cancer, while the risk of both the upper gastrointestinal tract cancer and lung cancer (only in smokers) was inversely associated with fruit intake (Bradbury *et al.* 2014).

Table 1 below shows a list of fruits and vegetables that have been implicated in cancer risk reduction and quantities associated with this decrease (Turati *et al.* 2015). As a result, several initiatives have been promoted in Europe and the United States with the purpose of encouraging people to include more fruits and vegetables in their diet as an incentive for cancer prevention. Examples are the 'Five-A-Day for Better Health' and 'Savor the spectrum' in the US and '5 A DAY' in the United Kingdom (Surh, 2003).

Table 1 Fruits and vegetables intake associated with a decreased risk of various types of cancer. Adapted from Turati *et al.* 2015

Fruit/ vegetable	Cancer localisation	Quantity
Cabbages	Oral cavity	
Cauliflowers	Pharynx	
Broccoli	Oesophagus	≥1 portion/week
Brussels sprouts	Colorectum	
	Breast	
Turnip greens	Kidney	
Onion	Oral cavity	
Garlic	Pharynx	
	Oesophagus	
	Colorectum	≥7 portions/week
	Larynx	High use
	Endometrium	
	Ovary	
	Kidney (garlic only)	
Citrus fruit	Oral cavity	
	Pharynx	≥4 portions/week
	Oesophagus	
Apple	Oral cavity	
	Pharynx	
	Colorectum	
	Larynx	
	Breast	At least one/day

	Ovary	
	Oesophagus (risk reduction did not reach statistical significance)	
	Prostate (risk reduction did not reach statistical significance)	

Tomatoes	Colorectum	
	Oral cavity	
	Pharynx	Highest vs. lowest intake (no quantity specified, higher intake favourable)
	Oesophagus	
	Stomach (highest reduction)	

1.1.3 Oxidative stress

Oxidative stress relates to an imbalance between reactive oxygen/nitrogen species (ROS/RNS) and the counter acting activity of antioxidant defence mechanisms (enzymatic or non-enzymatic) (Su *et al.* 2013; Kaur *et al.* 2014). On a daily basis, we are persistently exposed to external factors such as air pollutants, heavy metals, industrial emissions of organic compounds or nuclear emissions. These factors, together with our diets and compounded by smoking, alcohol intake and sun exposure, cause oxidative stress.

Oxidative stress is responsible for the development of a series of pathologies, among which cancer represents one of the most dangerous risks, as the oxidative stress ultimately threatens the integrity of the genome (Kaur *et al.* 2014). Other pathologies include neurodegenerative diseases such as Alzheimer's and Parkinson disease, cardiovascular diseases and diabetes (Lee *et al.* 2013, Lichtenberg and Pinchuk, 2015).

Reactive oxygen species (ROS) are a class of highly reactive molecules, which result from the metabolism of oxygen (Subhasree, 2008). This leads to the conclusion that all aerobic organisms produce ROS as a by-product of biochemical utilisation of oxygen and are prone to oxidative stress (Liu *et al.* 2007), as an excess of ROS can cause a redox imbalance and lead to important pathological states by means of lipid, protein and DNA damage (Cho and

Kleeberger, 2007). These effects are shown in Figure 1; membrane lipids undergo lipid peroxidation with production of toxic products, changes to proteins affect their function (enzymes, structural proteins) and lead to further production of free radicals through synthesis of protein hydroperoxides, while DNA undergoes mutations and fragmentation (Sharma, 2014). These alterations are also responsible for ageing (Liu *et al.* 2007). Other reactive species that require oxygen for their production are reactive nitrogen species (RNS) – nitric oxide and nitrogen dioxide, and reactive chlorine species (Fang *et al.* 2002).

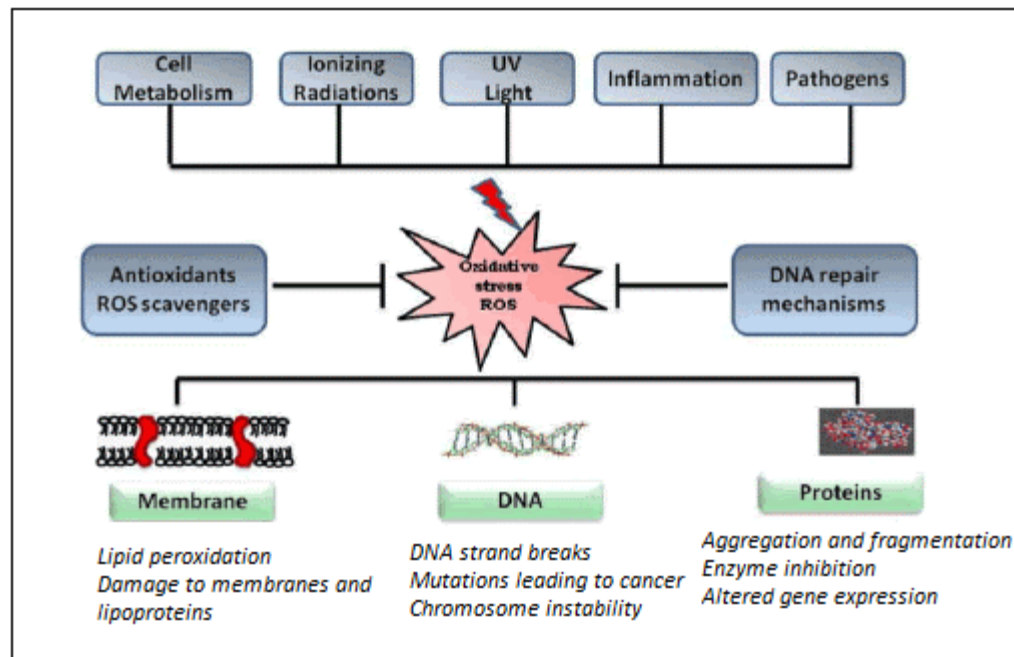


Figure 1 Oxidative stress: causes and consequences (Adapted from Sharma, 2014)

Important examples of ROS are superoxide (O_2^-), hydroxyl (OH^\cdot), peroxy (RO_2^\cdot), alkoxy (RO^\cdot) and hydroperoxy (HO_2^\cdot) radicals (Figure 2). The extent of damage produced by ROS is amplified because they cause a series of reactions of lipid oxidation (Fang *et al.* 2002).

REACTIVE OXYGEN SPECIES		REACTIVE NITROGEN SPECIES	
Superoxide anion	$O_2 \xrightarrow[\text{oxidase}]{\text{NADPH}} O_2^{\bullet -}$	Nitric oxide	$L\text{-Arginina} \xrightarrow[\text{NOS}]{L\text{-Citruilina}} NO^{\bullet}$
Hydrogen peroxide	$O_2^{\bullet -} \xrightarrow[\text{SOD}]{O_2} H_2O_2$	Peroxynitrite	$NO^{\bullet} \xrightarrow[\text{O}_2]{O_2^{\bullet -}} ONOO^-$
Hydroxyl radical	$H_2O_2 \xrightarrow{\text{Fenton reaction}} \bullet OH$	Dioxide of nitrogen	$ONOO^- \rightarrow NO^{\bullet}_2$
Hydroperoxyl radical	$O_2 \xrightarrow{H^{\bullet}} HO_2^{\bullet}$	Anhydride nitrous	$NO^{\bullet} \xrightarrow{NO^{\bullet}_2} N_2O_3$

Figure 2 Chemical formation of reactive oxygen and nitrogen species (Source: Ríos-Arrabal *et al.* 2013)

ROS are produced by mitochondria, phagocytes, peroxisomes and cytochrome P450s (Gordon, 2012). Enzymes, which participate in their production, are NADPH oxidase, xanthine oxidase, lipoxygenase, cyclooxygenase and uncoupled endothelial nitric oxide synthase, while the non-enzymatic reactions that lead to ROS production involve the mitochondrial respiratory chain (Gorrini *et al.* 2013). The latter source of ROS is mainly responsible for the formation of superoxide anions and hydrogen peroxide, as a result of regular oxidative metabolism. This is possible in a non-enzymatic manner because it is caused by an electron leakage that happens during the synthesis of ATP facilitated by the oxidative phosphorylation process. Oxidative phosphorylation is a process that depends on proton gradients (electron transfer reactions) in order to convert molecular oxygen to water and takes place in the electron-transport chain. When partial reduction of molecular oxygen happens, it leads to the formation of unstable intermediates (ROS); more specifically, during recycling of coenzyme Q (ubiquinone), an unstable intermediate is formed (free radical semiquinone anion) that can readily transfer electrons to molecular oxygen, resulting in a one-electron reduction of molecular oxygen to the superoxide ion, instead of the four-electron reduction catalysed by complex IV (cytochrome c oxidase) (Finkel and Holbrook, 2000). Thus, the electron leakage that happens during oxidative phosphorylation is responsible for the non-enzymatic production of ROS such as superoxide anions (one-electron reduction) and hydrogen peroxide (two-electron reduction) (Berg, 2002; Gogvadze *et al.* 2008).

The endogenous defence against ROS is represented by glutathione, ubiquinol, uric acid and bilirubin, and enzymes, such as superoxide dismutase (converts $O_2^{\bullet -}$ into $O_2 + H_2O_2$),

glutathione peroxidase (reduces H_2O_2 to H_2O), catalase (dismutes H_2O_2 into $\text{O}_2 + \text{H}_2\text{O}$) (Fridovich, 1999; Gordon, 2012). Figure 3 illustrates the enzyme-catalysed reactions that take place. On the other hand, the exogenous system of defense includes dietary antioxidants such as vitamin C, vitamin E, selenium and β -carotene (Turati *et al.* 2015).

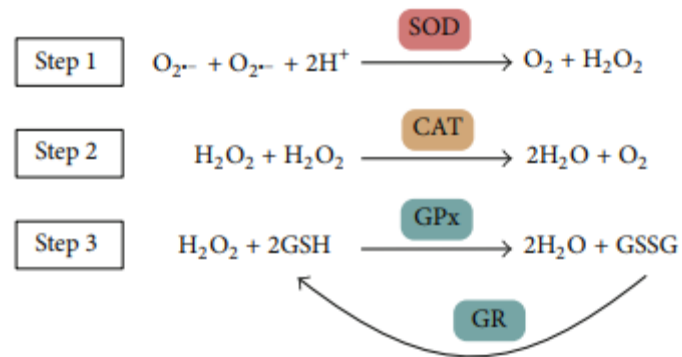


Figure 3 Main reaction steps for antioxidant defense, where SOD = superoxide dismutase, CAT = catalase, GPx = glutathione peroxidase and GR = glutathione reductase

The homeostasis of free radicals is important for many processes in our bodies, such as muscle contraction, immune responses, food to energy conversion (Lichtenberg and Pinchuk, 2015). However, increased ROS and oxidative stress can occur as a result of cigarette smoking, unhealthy diet and chronic inflammation due to chronic infection – all of which are known risk factors for cancer, as well as obesity and diabetes. ROS stimulate metabolic pathways, which are associated with tumour cell growth and survival, and they block the function of tumour suppressing molecules (Gorrini *et al.* 2013).

1.1.4 Cancer Chemoprevention

Cancer chemoprevention represents the use of synthetic or natural agents, including drugs and vitamins, with the aim of reducing the risk of cancer, delaying carcinogenesis or preventing recurrence of cancer (Steward and Brown, 2013; Meyskens *et al.* 2015). The goal is to prevent occurrence of cancer, and in the case of metastasis, to prevent breach through the basement membrane (Wu *et al.* 2011). The term “cancer chemoprevention” was first introduced by Michael Sporn, who defined it as “the use of specific agents to reverse, suppress or prevent the carcinogenic process to invasive cancer” (Mukhtar, 2012). Lee Wattenberg used the term “chemoprophylaxis” to refer to cancer prevention with the use of chemical agents (Mukhtar, 2012).

The definition and understanding of cancer chemoprevention have evolved over time since the term first appeared in medical literature more than 40 years ago, and it is currently considered a method of active preventive intervention, which is aimed at stopping, slowing down or reversing carcinogenesis (Meyskens *et al.* 2015). Because of the multiple factors and development stages of this disease, from the epigenetic to the cellular level, chemoprevention could prove more efficient than cancer treatment and it is also more cost-effective (Amin *et al.* 2009). However, there has been much debate over the success of chemoprevention and its efficiency.

Agents involved in cancer chemoprevention include natural agents, dietary compounds and drugs, many of which originally had different indications (Meyskens *et al.* 2015). The latter is the case with aspirin: its capacity to irreversibly inhibit enzymes that elicit pro-inflammatory responses, support cell proliferation, angiogenesis and apoptotic resistance, has made aspirin a promising cancer chemopreventive agent. The enzymes acetylated by aspirin are prostaglandin-endoperoxide synthase 1 (PTGS1 or COX1) and prostaglandin-endoperoxide synthase 2 (PTGS2 or COX2) (Drew, Cao and Chan, 2016). Moreover, because elevated levels of prostaglandins are found in colon cancer, this led to its use in chemoprevention of this malignant disease (Mukhtar, 2012). The Breast Cancer Prevention Trial was one of the first, which examined a chemopreventive agent – tamoxifen, and it showed a significant reduction in breast cancer occurrence in women with an increased risk of the disease. However, tamoxifen's serious side effects have limited its use for this indication (Wu *et al.* 2011).

There are three stages of chemoprevention: primary – aimed at high-risk individuals, secondary – aimed at individuals with pre-malignant lesions, and tertiary – aimed at patients treated for a primary cancer to prevent secondary forms and reoccurrence (Rashid, 2017). Moreover, chemopreventive agents are classified (Figure 4) into inhibitors (prevent formation of carcinogens from precursors), blocking agents (prevent mutations caused by carcinogens, enhance detoxification pathways and trap ROS) and suppressing agents (intervene in cell proliferation, differentiation, senescence and apoptosis) (Priyadarsini and Nagini, 2012). Blocking agents are most effective if they are used prior to exposure to carcinogens. However, if the cell suffers damage from carcinogens, then suppressing agents take effect in the promotion and progression stages of carcinogenesis, with the aim of suppressing the development of cancer. Some chemopreventive agents can show both blocking and suppressing means of action (e.g. curcumin and indole-3-carbinol) (Rashid, 2017).

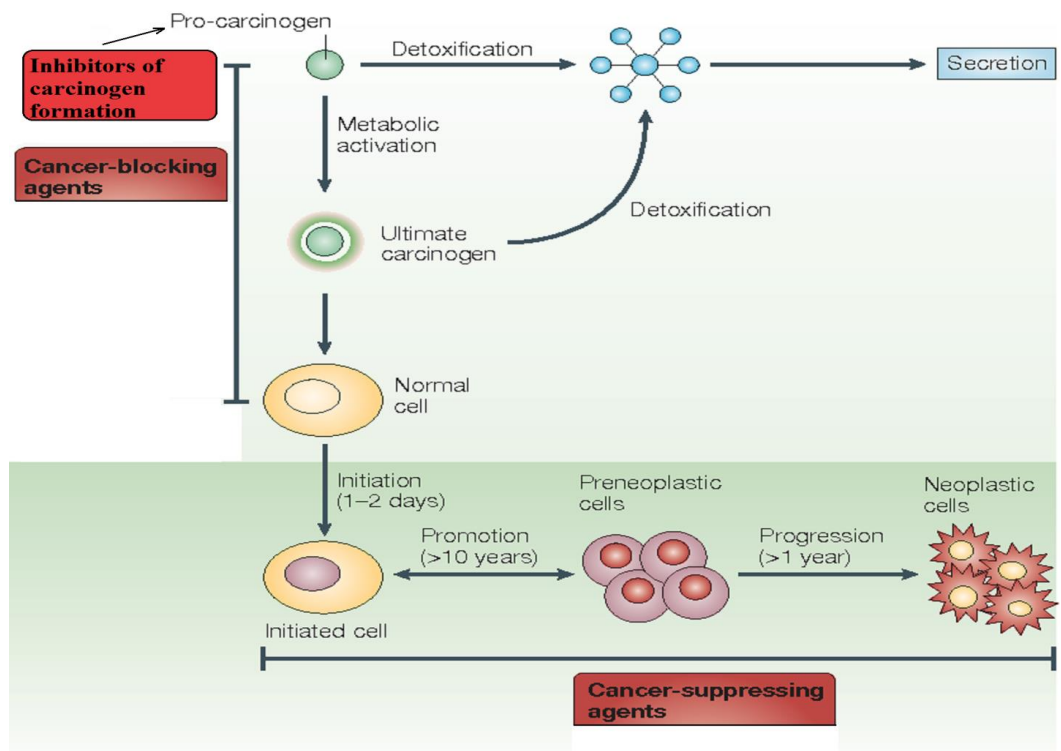


Figure 4 Classification of cancer chemoprevention agents (Adapted from Surh, 2003)

Compounds that inhibit metabolic transformation of carcinogens and block their damaging effects on DNA are referred to as “blocking agents”, because they “block” mutagenic interactions of carcinogens with DNA. They do so by helping prevent the irreparable DNA damage that occurs during initiation in the following ways: by inactivating or metabolizing carcinogens directly, acting as free-radical scavengers, or inducing antioxidative enzyme activity and activating mechanisms of DNA repair. Furthermore, blocking agents can also exert epigenetic modifications (Priyadarsini and Nagini, 2012; Rashid, 2017).

In contrast to blocking agents, “suppressing agents” are compounds that affect the later stages of carcinogenesis and they can interfere with cancer cell proliferation by down-regulating signal transduction pathways such as the NF- κ B (see 1.1.5.1), mTOR (mammalian target of rapamycin) and STAT3 (part of STAT family of transcription factors: signal transducer and activator of transcription). mTOR has been shown to regulate cell differentiation in both murine and human cells through a signaling cascade that includes

STAT3. Disregulation of mTOR contributes to poor cell differentiation, which is commonly associated with uncontrolled cell proliferation and tumorigenesis (Ma *et al.* 2010). STAT3 activity is relevant to cancer inflammation and immunity and as such, this transcription factor is observed in cancer cells and immune cells. Its activation is markedly increased in tumour cells and also in conditions of high inflammation, strongly indicating that STAT3 could play an important role in carcinogenesis. Furthermore, inhibition of the mTOR pathway in various cancer cell lines using rapamycin showed a decrease in the STAT3 activity, while hyperactivation of mTOR resulted in increased STAT3 activity (He *et al.* 2014).

Suppressing agents also work by inhibiting cytochrome P450 enzymes that modulate signal transduction to hormone responsive elements. They induce terminal cell differentiation and restore immune response (Rashid, 2017).

Additionally, suppressing agents are likely to reduce or delay metastasis by inducing apoptosis, promoting intercellular communication and inhibiting angiogenesis, basement membrane degradation, epithelial-mesenchymal transition (EMT), cell invasion and dissemination. All these processes lead to the onset of metastasis, a stage that is linked to poor clinical outcomes. Cells usually undergo transformations during embryonic development, regeneration of tissues or wound healing and this is a process where epithelial cells transition to a mesenchymal phenotype. This process is also observed in tumour progression; cancer cells exist in various transitional states with mixed epithelial and mesenchymal gene expression and this contributes to their ability to circulate in clusters (Roche, 2018). Increased N-cadherin expression in pancreatic cancer cells was linked to the acquisition of the mesenchymal phenotype (Nakajima *et al.* 2004) and phytochemicals such as silibinin, curcumin and resveratrol showed to modulate EMT pathways to increase expression of E-cadherin instead, which is associated with the epithelial phenotype (Landis-Piwowar and Iyer, 2014). By acquiring the mesenchymal phenotype, cancer cells acquire motility properties and their invasiveness potential increases, largely dependent on remodelling of the extracellular matrix. Inhibiting expression of matrix metalloproteinases (MMPs), for example, enables cancer cells to disseminate to other locations less hindered, thus advancing metastasis (Landis-Piwowar and Iyer, 2014).

Still, the role of cancer chemoprevention agents as suppressors is not limited only to delaying the promotion and progression stages of carcinogenesis, as they also inhibit metabolism of polyamines providing protection from heterocyclic amines, which are known carcinogens

found particularly in well cooked meats (Zheng and Lee, 2009). Once a cell undergoes initiation, suppressive agents help by enhancing the apoptosis rate of such cells and reducing their proliferation (Priyadarsini and Nagini, 2012; Rashid, 2017).

1.1.5 Targets and Mechanisms of Chemopreventive Agents

Chemopreventive agents can have various targets, depending on the level of chemoprevention. Many molecules involved in cell cycle regulation, inflammation, metabolism of carcinogens, inter-cell communication and cell adhesion can be deregulated in carcinogenesis. All of these represent potential targets for cancer prevention.

1.1.5.1 Modulation of signal transduction pathways

Nuclear factor kappa-light-chain-enhancer of activated B cells (NF- κ B) is involved in cancer progression through its role in regulation of cell cycle progression, apoptosis, proliferation and cell differentiation. This family of transcription factors is redox sensitive. Pro-inflammatory cytokines interact with the I κ B family of proteins, which are bound to members of NF- κ B family (Landis-Piowar and Iyer, 2014). This results in activation of NF- κ B target genes. The NF- κ B is activated in most tumours (DiDonato *et al.* 2012). Chemopreventive agents that inhibit the NF- κ B signaling pathway are involved in tertiary chemoprevention due to NF- κ B's involvement in inflammation, which plays a significant role in carcinogenesis (e.g. colitis-associated colon cancer, hepatitis-associated liver cancer) (Di Donato *et al.* 2012; Landis-Piowar and Iyer, 2014). Reduced NF- κ B activity correlates with an increase in apoptosis rate. Also, it is important to note that inhibition of NF- κ B can also make cancers more susceptible to treatment (Kuno *et al.* 2012).

Pro-inflammatory mediators can bind to cytokine receptor tyrosine kinases, activate Janus Kinase-3 (Jak3) and finally activate the mitogen activated protein kinase and extracellular receptor kinase (MAPK/Erk) pathway. The MAPK/Erk pathway regulates cell growth, proliferation, survival and invasion via the phosphatidylinositol-3 kinase (PI3K) pathway. The RAS-Erk and PI3K pathways are activated in inflammation-mediated carcinogenesis and their suppression represents a possible target for cancer chemoprevention. Research shows that the effects of the activation of these pathways can be reduced significantly with the use of celecoxib, an NSAID (non-steroidal anti-inflammatory drug) (Setia *et al.* 2014).

Toll-like receptors (TLRs) are specific transmembrane pattern recognition receptors (PRP) expressed on various cells, including immune cells. Cells of immune system respond to

various pathogens following their interaction with TLRs, which leads to production of pro-inflammatory mediators. Recent research indicated a possible role of TLRs in cancer development, both as antitumour and pro-tumour promoters. TLR4 is found on membrane of immune cells and it shows antitumour effects in skin cancer, pro-tumour effects in prostate and head and neck cancer, and both in breast and lung cancer. Activation of TLR4 leads to production of IL-6 and IL-8 in breast cancer, as well as increased expression of VEGF and TGF- β 1 in prostate cancer. It also increases production of NF- κ B. The TLR4 MyD88 pathway promotes carcinogenesis and curcumin, resveratrol, caffeic acid phenethyl ester and 6-gingerol, among other phytochemicals, can inhibit the TLR4 signalling pathway (Chen *et al.* 2018).

1.1.5.2 Detoxification through cytochrome P450 enzymes

Cytochrome P450 enzymes represent a superfamily of proteins involved in many significant biochemical processes, which involve biotransformation of various endogenous (hormones) and exogenous molecules, including carcinogenic substances (Landis-Piwowar and Iyer, 2014; Rashid, 2017).

It is known that human CYP1A1, 1A2, 2A6, 2A13, 2E1 and 3A4 enzymes have a major role in transformation of carcinogens to their active metabolites, which then cause DNA damage. Examples of carcinogenic compounds that can be metabolically activated by the P450 enzymes are polycyclic aromatic hydrocarbons (PAH), arylamines and heterocyclic amines, but also estrogens and mycotoxins such as aflatoxins (Shimada, 2017). Increased expression of these proteins is noticed in tumours (Landis-Piwowar and Iyer, 2014). Inhibition of CYP-450 is the mechanism of action for certain blocking chemopreventive agents such as curcumin. These agents prevent formation of highly electrophilic products by inhibiting the CYP450. Diallyl-sulfide, present in allium vegetables, has the same mechanism of action (Rashid, 2017). Aromatase inhibitors block activity of CYP19, resulting in blocked transformation of androgens to estrogens (Landis-Piwowar and Iyer, 2014).

Phase 2 enzymes conjugate the hydrophobic metabolic products of carcinogens to make them water-soluble, neutralising their reactivity and promoting their excretion from the body (Yu and Kensler, 2005). Induction of the Phase II detoxification enzymes such as glutathione S-transferase, UDP glucuronosyltransferase and quinone reductase can help inhibit development of cancer. Resveratrol increases detoxification of carcinogens by inducing the

activity of these enzymes, apart from also inhibiting activities of some CYP-450 enzymes (Chow *et al.* 2010).

1.1.5.3 Detoxification through modulation of Keap1-Nrf2-ARE signaling pathway

Nuclear factor-erythroid 2 related factor 2 (Nrf2) is a transcription factor, which interferes with the function of cytoprotective enzymes. These enzymes reduce the damage caused by carcinogens, electrophiles and free radicals and are involved in antioxidative and detoxifying processes. The transcription factor Nrf2 binds to the antioxidant responsive elements (ARE) of cytoprotective genes (Zhao, Gao and Qu, 2010), which represent parts of genes whose main products are detoxifying enzymes such as NAD(P)H:quinone oxidoreductase 1 (NQO1) and glutathione S-transferases (GST), antioxidant proteins such as glutamate-cysteine ligase (GCL), glutathione reductase-1 (GR-1), glutathione peroxidase (GPx), thioredoxin reductase-1 (TrxR1) and haem-oxigenase-1 (HMOX-1/HO-1) and drug transport proteins (Higgins *et al.* 2009).

As Figure 5 below explains, Keap1-Nrf2-ARE pathway inducers, such as ROS producing oxidative stress, act by releasing Nrf2 from the acting binding Kelch-like ECH associating protein 1 (Keap1), leading to the accumulation of Nrf2 in the cytoplasm and its translocation to the nucleus, where it forms a heterodimer with small Maf proteins. This heterodimer binds specifically to the AREs of genes promoting the induction of cytoprotective enzymes (Zhao *et al.* 2010). Target genes of Nrf2 are involved in a plethora of processes: glutathione synthesis and conjugation, metabolism and transport of xenobiotics through efflux pumps, activity of antioxidant enzymes, metabolic genes and transcription factors (Lu *et al.* 2016).

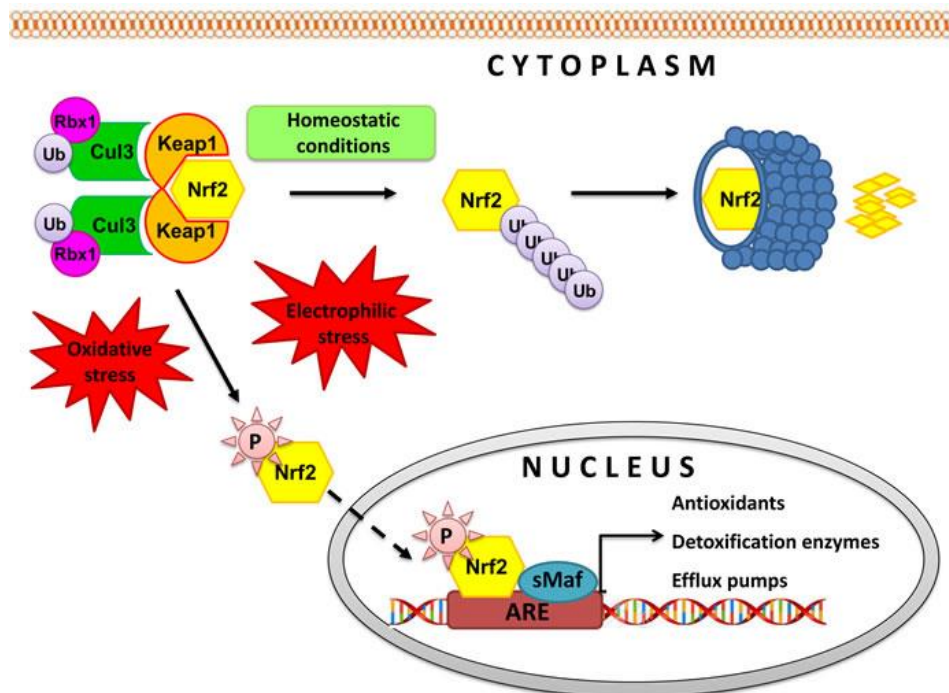


Figure 5 The Nrf2/Keap1 regulatory pathway. Under homeostatic conditions, Nrf2 is localised in the cytoplasm, bound to a Keap1 homodimer, which forms a complex with Cullin3-Rbx1 E3 ubiquitin ligase. This facilitates the ubiquitination and proteolysis of Nrf2 via the 26S proteasome. Under electrophilic/oxidative stress, the Keap1-Cul3-E3 ubiquitin complex is disrupted and Nrf2 can translocate to the nucleus where it forms a heterodimer with small Maf proteins and binds to the ARE, promoting the transcription of cytoprotective genes. (Source: Sznarkowska *et al.* 2017)

The ARE element has been accepted as the consensus enhancer element for phase 2 metabolic enzymes (Rashid, 2017), whilst the transcription factor Nrf2 up-regulates transcription of cytoprotective genes in response to chemopreventive inducers (e.g. isothiocyanates, allyl-sulfides, coumarins, flavonoids and triterpenoids) or oxidative stress (e.g. heavy metals, mercaptans, oxidisable polycyclic aromatic hydrocarbons, peroxides) (Dinkova-Kostova *et al.* 2004 and Yu and Kensler, 2005). What these xenobiotics have in common is their thiol-reactive structure that helps them bind to or oxidise cysteine residues in Keap1, leading to the stabilisation/activation of Nrf2 (Higgins *et al.* 2009).

Yet, a continuous activation of the Nrf2 pathway is considered to favour carcinogenesis and proliferation of cancer cells, as many tumours, especially lung, pancreatic and cervical, show high expression of Nrf2. This situation also correlates with anticancer drugs resistance and it is still a complex process not well understood. Still, a down regulation of the Keap1-Nrf2 pathway can happen because of genetic and epigenetic alterations, cooperation with diverse oncogenic pathways or from over-exposure of epithelial cells to oxidative stress, resulting in chronic inflammation (Schafer *et al.* 2014).

For example, overexpression of Nrf2 in human breast cancer cells has been linked to increased proliferation and migration of these cells and one of the causes for subsequent metastasis might be that Nrf2 promotes expression of RhoA, which correlates strongly with poor prognosis of breast cancer patients (Zhang *et al.* 2016; Zhang *et al.* 2019). RhoA (Ras homolog family member A) is a key regulatory enzyme for promotion of motility of cells and supports progression of breast cancer (Zhang *et al.* 2016).

Therefore, Nrf2 is thought to have a dual role in the development of cancer, so that Nrf2 inducers play an important role in cancer prevention in healthy subjects (as long as it does not disrupt the homeostatic control), whereas Nrf2 inhibitors could contribute to preventing cancer progression (Schafer *et al.* 2014).

Moreover, newest research suggests a promising role of Nrf1 in prevention of cancer (triple-negative breast cancer and multiple myeloma) and other diseases (e.g. neurodegenerative, hepatotoxic, mitochondrial injury), as it has a critical role in embryonic development, organ differentiation and neuronal protection (Yuan *et al.* 2018).

1.1.5.4 Reduced expression of enzymes involved in cancer cell invasion

Metastasis is the main cause of cancer-related death. Extracellular matrix can be remodelled by matrix metalloproteinase (MMP) enzymes. In tumours, these enzymes can lead to spreading of cancer cells and have a role in neo-vascularization. Therefore, reducing the expression of MMP-9 is one of the chemopreventive mechanisms (e.g. curcumin) (Landis-Piwowar and Iyer, 2014).

1.1.5.5 Down-Regulation of Cox-2 Pathway

Prostaglandins (PGs) are molecules which are found in excess in colorectal cancer as well as in its precursors, benign polyps. Cyclooxygenases (COX) are enzymes involved in the metabolism of arachidonic acid. The COX-2 is the isoenzyme mostly induced by cytokines, growth factors and tumour promoters, which leads to increased expression of PGs. This causes induction of various growth factors, which promote angiogenesis, and it promotes division and spreading of cancer cells. At the same time levels of arachidonic acid are reduced which can reduce the rate of apoptosis. Studies have shown that the use of aspirin, non-steroidal anti-inflammatory drugs and COX-2 inhibitors leads to colorectal cancer prevention and risk reduction in patients with adenomas (Ranger, 2014).

1.2.1 Phytochemicals As Bioactive Compounds

1.2.1 Sources, classes and functions of phytochemicals

Plant natural products, commonly known as phytochemicals, are broadly classified into primary and secondary metabolites.

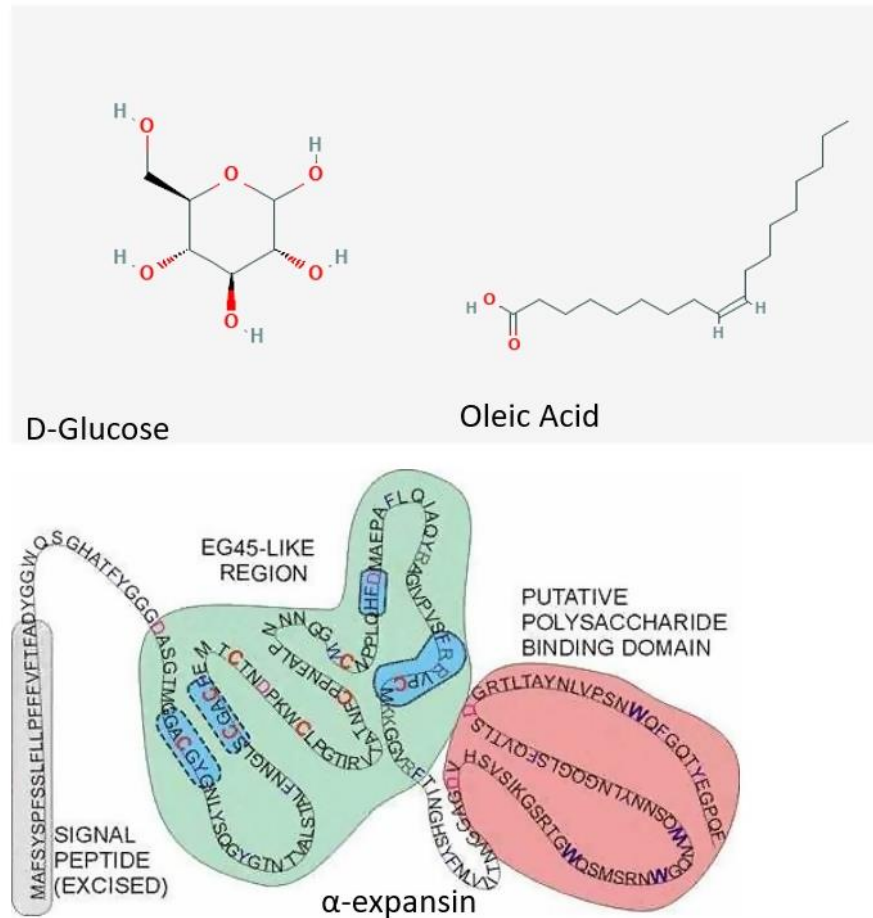


Figure 6 Example of primary metabolites (Sources: <https://pubchem.ncbi.nlm.nih.gov/>; Xu, 2002)

Primary metabolites (sugars, fats, amino-acids, starch etc.) are essential to plant life and they occur in all plants, as they are associated with vital processes such as photosynthesis, respiration and growth (Sato and Matsui, 2012). Examples of primary metabolites are in Figure 6 above.

Secondary metabolites, although maybe not essential for the plants, do have a role in plant defence, allelopathy, pollination and UV protection (Fulda and Efferth, 2015). Therefore, they enable a plant's survival as well as evolution.

Plant secondary metabolites have been proven useful for humans not only for their use as fibres, dyes, waxes, oils, flavouring and aromatic agents etc., but also for their pharmacological activity (Huang *et al.* 2012; Fulda and Efferth, 2015). Examples of secondary metabolites are in Figure 7.

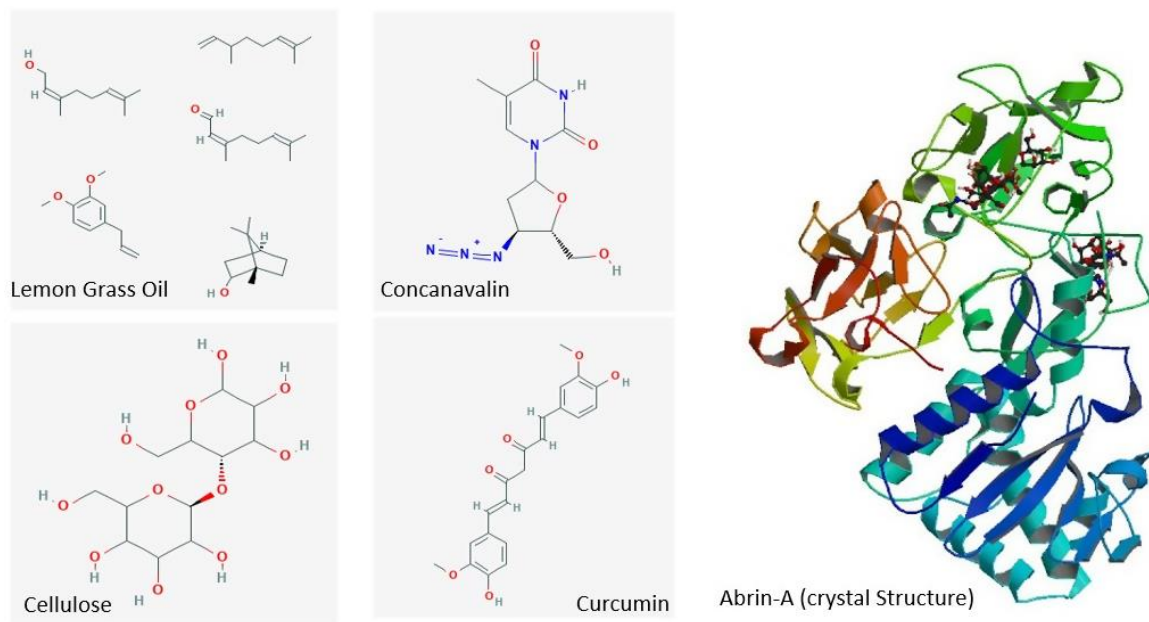
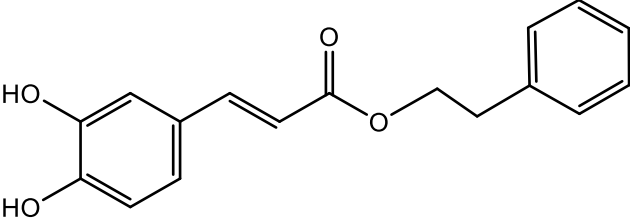
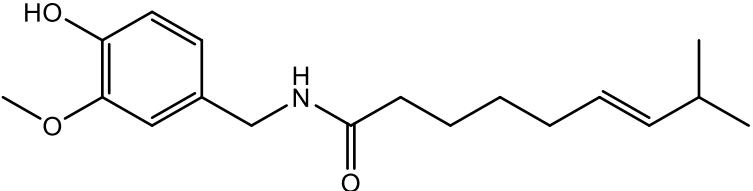
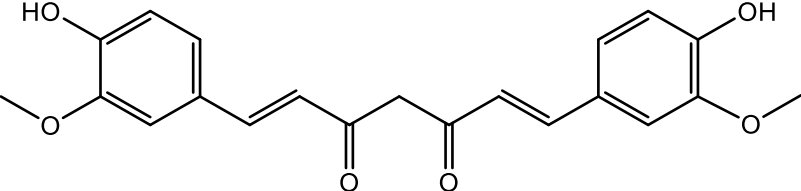
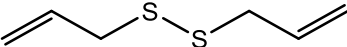
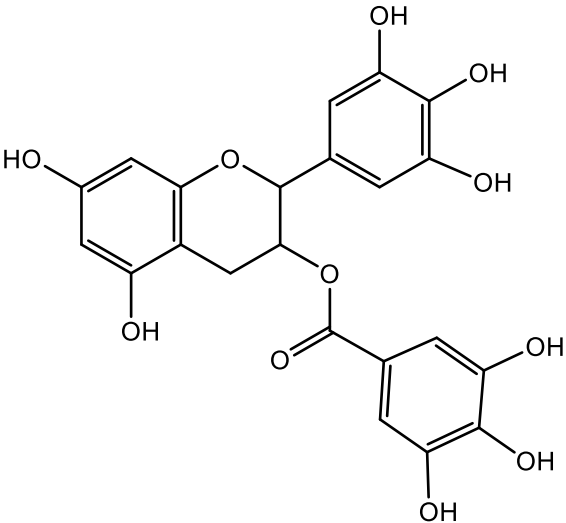


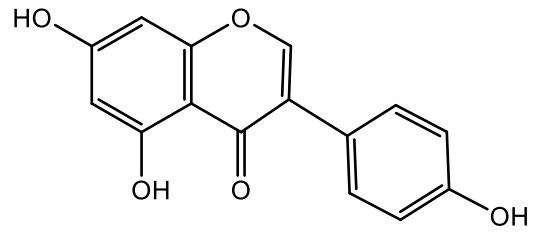
Figure 7 Examples of secondary metabolites (source: PubChem)

Dietary phytochemicals are found in plants used as food – vegetables, fruits, grains and tea. Anticancer properties have been shown both for phytochemicals from dietary plants (see Table 2) such as garlic – selenium, soy – genistein, crucifers - phenethyl isothiocyanate, green tea - epigallocatechin-3-gallate) and non-dietary plants (Pacific yew tree – paclitaxel, Camptotheca – camptothecin, Evodia fruits - evodiamine, Madagascar periwinkle – vincristine and vinblastine (Oh *et al.* 2016).

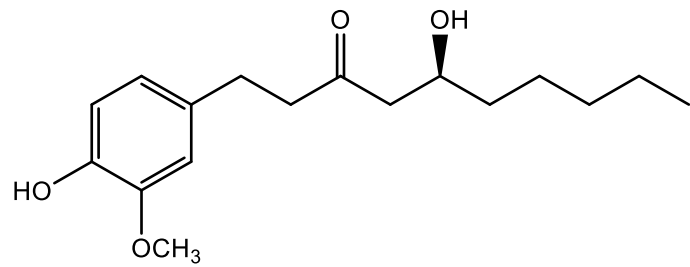
Table 2 Chemical structures of some dietary flavonoids with cancer chemoprevention properties

Dietary phytochemical	Chemical structure
Caffeic acid phenethyl ester	 <p>The structure shows a benzene ring with two hydroxyl groups at the 3 and 4 positions. This ring is connected via a trans-vinyl bridge to a propenoic acid chain, which is esterified to a phenethyl group (a benzene ring attached to a two-carbon ethyl chain).</p>
Capsaicin	 <p>The structure features a benzene ring with a methoxy group at the 3-position and a hydroxyl group at the 4-position. A methylene group at the 1-position is connected to the nitrogen of an amide bond. The amide is linked to a long, branched aliphatic chain that includes a trans-double bond and a methyl group.</p>
Curcumin	 <p>The structure consists of two 3,4-dimethoxyphenyl rings connected to a central heptane-1,6-dione chain via trans-vinyl bridges. The central chain contains two ketone groups and a methylene group.</p>
Diallylsulfide	 <p>The structure shows two allyl groups (CH₂=CH-CH₂-) connected to each other through a disulfide bridge (-S-S-).</p>
Epigallocatechin-3-galate	 <p>The structure is a complex polyphenol consisting of a flavan-3-ol core (epigallocatechin) esterified to a gallic acid moiety. It features multiple hydroxyl groups on the aromatic rings.</p>

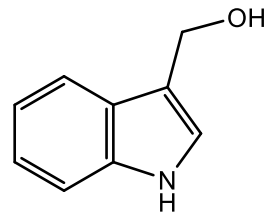
Genistein



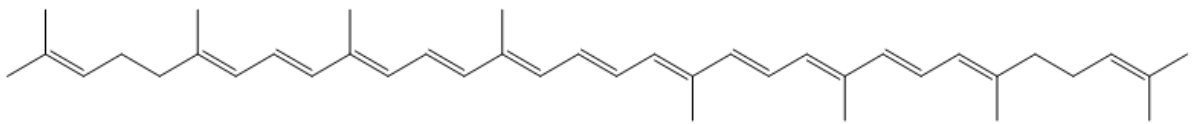
Gingerol



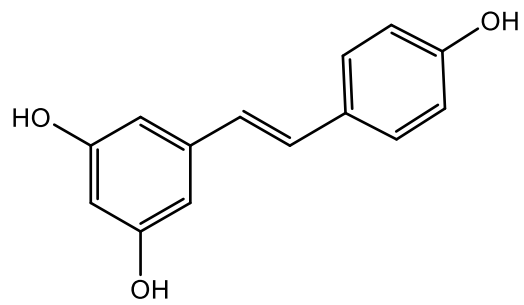
Indole-3-carbinol



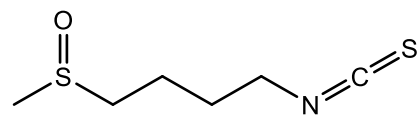
Lycopene



Resveratrol



Sulforaphane



Research into phytochemicals is focused not only on their effects on health, but also on the necessary doses and actual amounts that people ingest as food, bioavailability and ways to synthesize these compounds. The potency and bioavailability of natural products can also be increased by producing synthetic analogues i.e. EF24, the synthetic analogue of curcumin, showed a 10-fold potency increase (Amin *et al.* 2009).

1.2.2 Polyphenols

Polyphenols are the biggest group of phytochemicals (Tsao, 2010). They are produced by plants for their protection. The structure of polyphenols can vary a lot and the complexity of the structure is also highly variable. The simplest polyphenols can occur as simple phenolic molecules such as catechol while the complex polyphenols are highly polymerized molecules with large molecular size such as raspberry ellagitannin. In nature, these compounds are present in conjugated form i.e. glycosides with one or more sugar residues substituting hydroxyl groups. The sugar residue can be monosaccharide, disaccharide, or polysaccharide (Bravo, 1998). These compounds suppress formation and neutralise already formed free radicals by absorbing and delocalising an electron from ROS. Also, they can stop damage caused by highly reactive hydroxyl radicals by reducing the rate of Fenton reaction. The positive health effects that polyphenols exhibit is considered complex. It is assumed that these chemicals also act as cell-signalling modulators, inhibitors of xanthine oxidase and inducers of superoxide dismutase, glutathione peroxidase and catalase (Tsao, 2010). They have features of phenolic structure and can be classified based on their function, source or chemical properties. Chemical subgrouping of polyphenols includes phenolic acids, flavonoids, polyphenolic amides and other polyphenols (Tsao, 2010).

Phenolic acids can be found in free form in vegetables and fruits, while in seeds and grains they are mostly in the bound form. Hydrobenzoic acids can be found in vanilla, tea, raspberries, rhubarb etc., while hydroxycinnamic acids can be found in cinnamon, coffee, plums, kiwi, and wheat bran.

Capsaicin found in chilli peppers is one of the most investigated phenolic amides. Another member of this group, avenanthramide, is found in oats. Resveratrol, curcumin and ellagic acid belong to the miscellaneous group of polyphenols and can be found in grapes and wine, turmeric and berries, respectively. This group also includes lignans found in sesame seeds

and grains (Thomas *et al.* 2015). Citrus fruits also contain polyphenolic compounds and the concentration of the polyphenolic compounds in citrus fruits depends upon the variety of the fruit as well as the growing conditions (Muscatello *et al.* 2018). Neohesperidosides are found in grapefruits, bergamot and bitter oranges. The bitter taste of these fruits is partially due to the bitter taste of Neohesperidosides. Rutinosides are tasteless polyphenols that are found in mildly tasting citrus fruits such as oranges, lemons, and tangerines.

The activity of flavonoids as antioxidant chemicals varies based on their chemical structure and glycosylation patterns. Their biggest subcategory and also the one most often found in plants comprises flavones (e.g. apigenin, acacetin), flavonols (e.g. kaempferol, quercetin), flavanones (e.g. naringenin, pinocembrin) and flavanonols (e.g. taxifolin) (Thomas *et al.* 2015). Less commonly found in plants are neoflavonoids, while the greatest source of isoflavones are leguminous plants. Black rice and red, blue and purple coloured parts of plants contain anthocyanidins. Proanthocyanidins are condensed tannins, while flavanols with strong antioxidant activity (catechin and epicatechin) are the main phytochemicals found in tea and chocolate and are known as tannins (Tsao, 2010; Thomas *et al.* 2015).

Flavonoids

Flavonoids constitute approximately 4,000 natural polyphenolic compounds, predominantly found in plants. Some of the properties like carcinogen inactivation, anti-oxidation, anti-Alzheimer's disease, anti-proliferation, cell cycle arrest, induction of apoptosis and differentiation, inhibition of angiogenesis, and multidrug resistance reversal make flavonoids a significant subject of research (Krishnadhas, Santhi & Annapurani, 2016). The compounds of flavonoids can be categorised as flavones, flavonols, flavanones, isoflavones and anthocyanidins (Hamed *et al.* 2019). Flavonoids constitute diverse chemical structures that contain 15 carbon atoms and exhibit the framework of C6-C3-C6, formed using two A-B aromatic rings, which are linked with a three carbon unit (Awouafack, Tane & Eloff, 2013).

Extraction of flavonoids

The extraction of flavonoids is generally used using the processes of refluxing, heating and boiling. However, before the extraction process is applied to the plants, the samples need to be prepared. Samples from different parts of the plants are dried and ground for the purpose of extraction of flavonoids (Rabeta & Lin, 2015). The yields on extraction of flavonoids are influenced by multiple factors including temperature, time duration, and ratio of water to solvents in case of aqueous mixtures (Tan *et al.* 2014). Some of the methods used for the

extraction of flavonoids from natural products include maceration, infusion, decoction, percolation, hot continuous extraction (Soxhlet), ultrasound-assisted extraction and microwave-assisted extraction. While undertaking these extraction processes, a number of solvents are used like water, methanol, ethanol, acetone, *n*-butanol, chloroform and ethyl acetate. Several studies have also shown that the processes of maceration and infusion are mostly used to extract flavonoids from the plants (Munhoz *et al.* 2014). For instance, the study by Jäger *et al.* (2010) found that the maceration and infusion were utilised to prepare herbal tea from *Viscum album L.*, which yielded about 30-40% of flavonoids- substances. Another process used for extraction is decoction, which is known as a simple, convenient and cheap method of extracting flavonoids. The study by Chaisawangwong & Gritsanapan (2009) proved that the use of decoction method provided with the maximum flavonoids extractions at 17.54 mgRE/g, as compared to any other methods in dried-young flowers. Similarly, Vaidya *et al.* (2014) had undertaken the extraction of flavonoids contents from the seeds of *Ziziphus mauritiana* using different methods like maceration, decoction, Soxhlet extraction and sonication. The study reported that the maximum contents of flavonoids are extracted using sonication extraction method.

Furthermore, the microwave-assisted technique is another extraction process which is considered superior than these conventional extraction processes. The key difference is that in the microwave-assisted technique, the heat and mass gradients during the process move from inside to outside (Veggi *et al.* 2013). In this extraction process, the solvent penetrates into the solid matrix, then the constituents breaks down or solubilize, and the solvent transports outside the matrix and then to solution, and finally, the extract and solid separates and discharges (Aguilera, 2003). The research by Zheng *et al.* (2016) extracted flavonoids from corn silk (*Zea mays L.*) using microwave-assisted solid-liquid method, and found a good yield of 1.13% and recommended the use of the plant for the development of natural antioxidant reagents in food products.

However, Zhang *et al.* (2011) claims that many useful compounds are lost during these extraction processes of flavonoids majorly owing to the chemical reactions of oxidation and hydrolysis and long- time of extraction process. Further study by Rodríguez-Pérez *et al.* (2015) entails that the efficacy of ultrasound is effective in extracting the active compounds while processing flavonoids, since ultrasonic amplifiers exhibit strength that breaks down the cell walls and release compounds in liquid extraction.

Structural characterisation of flavonoids (NMR or MS)

The flavonoids once extracted are elucidated for spectroscopic spectra using different techniques like Nuclear Magnetic Resonance (NMR), Mass Spectrometry (MS), spectrophotometric ultra-violet (UV) and infrared (IR). Some of the structural properties of flavonoids that are observed include melting point, circular dichroism and optical rotatory power. The nuclear magnetic resonance technique can be undertaken using 1D or 2D analyses, such that the former check for the protons signals and carbon summary and types.

The basic structural skeleton of flavonoids is presented in Figure 8.

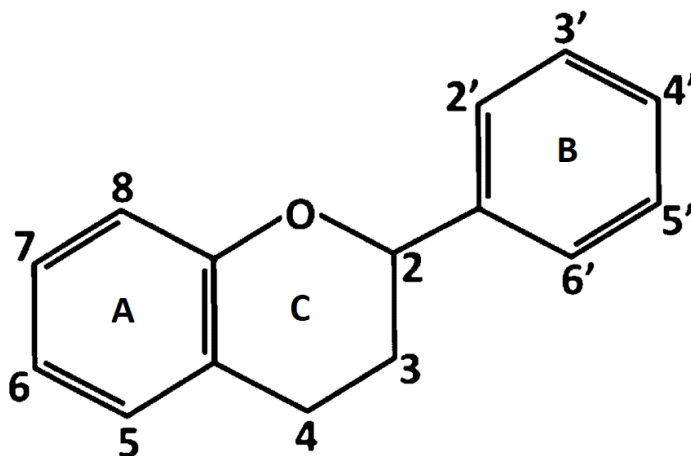


Figure 8 Structural backbone of flavonoids (C6-C3-C6) showing a chromane ring (A and C) attaching a second aromatic ring (B) in position 2, 3 or 4. Source: Balentine et al. 2015

Markham and Mabry (1975) provided the values of chemical shift values of protons and carbons using NMR in certain flavonoids, which are summarised in Table 3 below. Furthermore, 2D NMR techniques are employed in order to assess the correlation of proton-proton or other NMR nuclei, as follows: COSY (homonuclear correlated spectroscopy) shows the correlation between protons coupled to each other, HMQC (heteronuclear multiple quantum coherence) shows the correlation between protons and carbon signals (including longer range couplings), HSQC (heteronuclear single quantum coherence) provides information on C-H correlations with high resolution for carbon signals, HMBC (heteronuclear multiple bond connectivity) shows proton-carbon correlations that are 2 or 3 bonds away from each other, NOESY (the nuclear over-hauser spectroscopy) shows signal correlations between protons that are close to each other in space, while a TOCSY technique (total

correlated spectroscopy) can reveal even smaller proton couplings that COSY cannot (Awouafack *et al.* 2017).

Table 3 Chemical shifts (ppm) assigned to proton and carbon atoms in a flavonoid structure. Source: Markham & Mabry, 1975

Chemical shifts (ppm)	¹ H
2 - 3	H-3 (flavanone), CH ₃ aromatic
4 - 6	H-2 (flavanone, dihydroflavonol)
6 - 8	A- and B-ring protons
8 - 8.5	H-2 isoflavone
12 - 14	5-OH when C=O at C-4 (usually observed in DMSO-d)
Chemical shifts (ppm)	¹³ C
210 - 170	C=O
165 – 155 (no ortho/para oxygenation)	Oxygenated aromatic carbons
150 – 130 (with ortho/para oxygenation)	Oxygenated aromatic carbons
135 – 125 (para substitution)	Non-oxygenated aromatic carbons
125 – 90 (with ortho/para oxygenation)	Non-oxygenated aromatic carbons
80 - 40	Non-oxygenated (C-2, C-3 flavanone/flavanol)
28 - 35	C-4, flavanol

Another important technique of analysis is infrared spectroscopy. The research by Awouafack *et al.* (2017) showed that the flavonoids with hydroxyl groups exhibits maxima large band absorptions, estimated at 3300-3600 cm⁻¹. The study also shows that the flavonoids with carbonyl groups show intense band absorption at 1680 cm⁻¹, and shifts to 1620 cm⁻¹ when hydroxyl and carbonyl groups are chelated. It has also been found that due

to the aromatic double bands, the flavonoids form sharp and intense absorption bands in the range of 1600 cm⁻¹ and 1500 cm⁻¹.

Furthermore, ultraviolet absorption (UV) spectroscopy usually shows two absorption ranges for the two bands I and II from A- and B- rings. The results show that the maxima absorption in these cases is achieved at a range of 300 - 250 nm and 240 - 285 nm, respectively (Awouafack *et al.* 2013). The detailed results as obtained by Markham (1982) for the two bands using ultraviolet spectroscopy in different flavonoids are shown in Table 4.

Table 4 Wavelength bands typical for various classes of flavonoids. Source: Markham, 1982, pp. 144

Band II (nm)	Band I (nm)	Flavonoid class
250 - 280	310 – 350	Flavone
250 - 280	330 – 360	Flavonols (3-OH substituted)
250 - 280	350 – 385	Flavonols (3-OH free)
245 – 275	310 – 330 shoulder	Isoflavone
	320 peak	Isoflavones (5-deoxy-6,7-dioxygenated)
275 – 295	300 – 330 shoulder	Flavanones and dihydroflavonols
230 – 270	340 – 390	Chalcones
230 - 270	380 – 430	Aurones
270 - 280	465 - 560	Anthocyanidins and anthocyanins

1.2.3 Terpenoids

Terpenoids are a class of isoprenoids that consist of two or more *isoprene* units (C₅H₈) (Sarker and Nahar, 2007, p. 331). They are isolated from plant sources and used commercially as artificial flavour, fragrance, antimalarial drugs as well as anticancer drugs (Martin *et al.* 2003). Terpenoids are derived from terpenes with multicyclic structures and O-containing functional groups (Nič *et al.* 2009). Terpenoids represent a diverse group of phytochemicals that are linear or cyclical and can be classified into monoterpenoids (2 *isoprene* units), sesquiterpenoids (3 *isoprene* units), diterpenoids (4 *isoprene* units), triterpenoids (6 *isoprene* units, e.g. sterols) and tetraterpenoids (8 *isoprene* units) (Huang *et al.* 2012). Sometimes, they are classified as carotenoids (members of the tetraterpenoids

subgroup) and non-carotenoid terpenoids (Thomas *et al.* 2015). Subclasses and their representative compounds, as well as their effects on health, mechanisms of action in cancer and cancer localizations they show effect in are described in Table 3 (Huang *et al.* 2012). Still, it is thought that the full potential of terpenoids as anticancer agents is not fully investigated yet and needs further confirmation in interventional studies (Huang *et al.* 2012).

Table 5 Subclasses of terpenoids and their chemopreventive properties (Source: Huang *et al.* 2012)

Terpenoids subclass	Subclass representative	Sources	Health-related properties	Chemopreventive action	Localizations for anti-cancer effect
Monoterpenoids	Limonene	Citrus oils	Anticancer	Anti-angiogenic; proapoptotic; antioxidant	Breast; liver; pancreas; stomach; colorectal
	Cantharidin	Chinese blister beetles (<i>Mylabris phalerata</i> , <i>Mylabris cichorii</i>)	Anticancer; toxicity	Proapoptotic	Leukaemia; colorectum; bladder; breast
Sesquiterpenoids	Artemisinin	<i>Artemisia annua</i> L.	Treats infections; immunosuppressant; anticancer	Inhibition of cancer cells proliferation; chemotherapy sensitizer; proapoptotic	Leukemia; breast; ovary; prostate; colon; stomach; lung
Diterpenoids	Tanshinones	<i>Salvia miltiorrhiza</i> Bunge	Treats cardiovascular diseases; anticancer	Induction of cancer cell differentiation; anti-metastatic activity (↓MMP2, ↓MMP9, ↓NF-kB); anti-angiogenic	Leukaemia; breast; colon; liver

	Triptolide	<i>Tripterygium wilfordii</i> Hook. f	Immunosuppressant; anti-inflammatory; anticancer	Anti-proliferative	All cancer cell lines
	Pseudolaric acid B	<i>Pseudoalari kaempferi</i>	Antifungal; anticancer	Anti-angiogenic; Microtubule blockage; modulation of cancer cell-signaling	Lung; colon; breast; brain; kidney
	Andrographolide	<i>Andrographis paniculata</i>	Anti-inflammatory; ↓plasma glucose; anti-cancer	NF-κB signaling blockage; anti-proliferative; proapoptotic; anti-metastatic	Tongue
	Oridonin	<i>Rabdosia rubescens</i>	Anticancer	Proapoptotic; ↓AP-1, ↓NF-κB, ↓PI3K/Akt	Liver; skin; colorectum
Triterpenoids	Celastrol/tripterine	<i>Tripterygium wilfordii</i> Hook. f	Anticancer; anti-inflammatory	Tumour growth suppression; anti-angiogenic	Prostate; stomach
	Cucurbitacin	<i>Cucumis melo</i> L	Anti-inflammatory; hepatoprotective; anticancer	Induction of JAK/STAT3 dysfunction	Uterus; Ovary, Lung; Nasopharynx
	Alisol	<i>Alisma orientalis</i> (Sam.) Juzep	Antihypertensive; ↓lipids; anticancer	Proapoptotic	Ovary; Colon

Tetraterpenoids	Lycopene	Tomatoes	Anticancer	Anti-proliferative; anti-angiogenic	Prostate
	β -carotenes	Carrots, spinach, sweet potatoes	Anticancer	Pro-apoptotic	Breast

1.2.4 Organosulfur compounds

Organosulfur compounds or thiols comprise glucosinolates, allylic sulfides and indoles. A sulfhydryl functional group characterizes their chemical structure. Thiols manifest chemopreventive activity through ROS scavenging (Huber and Parzefall, 2007). Cruciferous vegetables are rich in glucosinolates, sulphur-containing glycosides, which are precursors of isothiocyanates and indoles. Besides their anticancer properties, glucosinolates are being investigated in cardiovascular and neurological disorders. Research shows that they modulate phase I and upregulate phase II enzymes via Keap1-Nrf2-ARE pathway repression. They also modulate the NF- κ B signaling pathway (Fuentes *et al.* 2015). Sulforaphane, via epigenetic mechanisms and induction of cytoprotective mechanisms, can help in cancer prevention (Dinkova-Kostova and Kostov, 2012). Among indoles, the most studied one is indole-3-carbinol, which can be found in Brussel sprouts and broccoli (Dinkova-Kostova and Kostov, 2012).

1.2.5 Phytochemicals as chemopreventive agents

Significant variations in cancer prevalence worldwide have led researchers to investigate the epidemiology of cancer (Chikara *et al.* 2017). Longitudinal observational studies, which noted characteristics and habits of individuals and cancer incidence, highlighted diet as a significant factor in both onset and progression of cancer (Russo *et al.* 2010). Research shows that about one third of cancers can be linked to improper dietary habits (Ullah and Ahmad, 2016). This resulted in numerous studies, which investigated the effects of phytochemicals on cancer cells.

The primary chemopreventive phytochemicals that have been intensively studied include polyphenols and sulphur-containing compounds (isothiocyanates and organosulfur compounds) (Nair *et al.* 2007). In mice, pigallocatechin-3-gallate (EGCG), a polyphenolic green tea component, increases HO-1 level in endothelial cells, whereas the curcumin from turmeric increases the expression of GST, glutathione reductase, epoxide hydrolase, HO-1 and NQO1 in liver, small intestine and kidney tissues (Shen *et al.* 2006; Gopalakrishnan and Kong, 2008). It has also been suggested that diallyl sulphides from garlic and onions are strong inducers of the Nrf2/ARE pathway and can induce NQO1 and HO-1. Also, other phytochemicals such as indole-3-carbinol (I3C), coffee diterpenes such as cafestol and sesquiterpenes such as parthenolide, have been indicated to have potential chemopreventive properties by inducing anti-oxidative stress genes through the Nrf2 pathway (Gopalakrishnan and Kong, 2008).

One of the sulphur containing compounds which has been extensively studied for its antioxidant and anti-inflammatory action is an isothiocyanate-sulforaphane (SFN). SFN induces the blocking genes (NQO-1, GST, γ -GCS, and UDP-glucuronosyltransferases (UGT) through Nrf2 pathway. Studies with Nrf2 knockout mice proved the dependence of chemo-preventative activity of SFN on Nrf2 pathway as the upregulation of antioxidant genes is blunted in knockout mice. For this study, wild-type Nrf2 mice (*nrf2*^{+/+}) and Nrf2 knock out mice (*nrf2*^{-/-}) were given 9 μ mol of SFN every day. The wild type mice showed upregulation of antioxidant and detoxification genes while the knockout mice did not show any difference in gene expression, which was measured through transcriptional profiling (Thimmulappa *et al.* 2002). Another study performed by McWalter *et al.* (2004) also reported similar results with Nrf2 knockout mice as they also observed increased antioxidant and detoxification activities in wild type mice when fed with broccoli based diet but not in knockout mice. The increase of antioxidant and detoxification activity as well as upregulation of gene expression of blocking genes indicates that SFN plays a vital role in blocking of cancer initiation by inhibiting the high oxidative and inflammatory activities in body.

One study by Almagami *et al.* (2014) showed that extracts of *Acanthus ilicifolius*, a mangrove plant, significantly decreased lipid peroxidation in rat colon cells, due to its high content of phenolics and flavonoids, reducing the number of azoxymethane-induced aberrant crypt foci (AOM-induced ACF). Consistent results were obtained in other studies, which also showed that isolated phytochemicals such as curcumin (Rao *et al.* 1993a), caffeic acid (Rao *et al.* 1993b) and diosgenin (Jayadev *et al.* 2004) could reduce AOM-induced ACF, and also colon adenocarcinoma.

The potential chemopreventive mechanisms of phytochemicals include antioxidant and anti-inflammatory activities, and regulation of cell cycle and apoptosis (Figure 9). Many natural products such as coumarins, diterpenes, indoles, curcuminoids, isothiocyanates or plant extracts, e.g., *Syzygium formasanum*, induce cellular phase II defence enzymes through the activation of Nrf2 signaling pathway. They achieve this by inhibiting the proteosomal degradation of Nrf2 or by inducing upstream signalling cascades (MAPK, PI3K, PKC, PERK), which enhances the translocation of Nrf2 to the nucleus and the subsequent expression of detoxifying enzymes such as glutathione-S-transferase (GST), NAD(P)H quinone oxidoreductase (NQO1), heme oxygenase 1 (HO-1), glutamylcysteine synthetase (GCS), and other antioxidant enzymes *via* the ARE/EpRE (antioxidant-responsive element/electrophile-responsive element) (Gopalakrishnan and Kong, 2008; Neerghen *et al.* 2010; Iqbal *et al.* 2018).

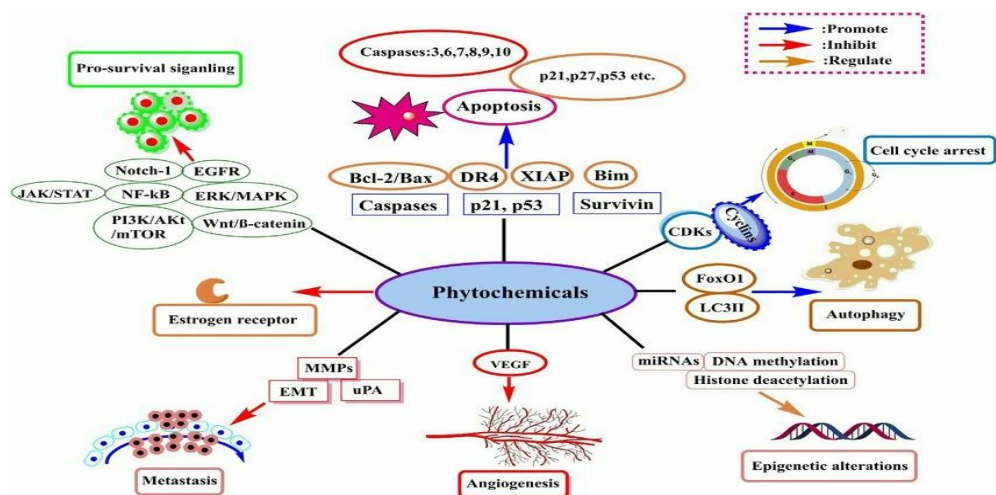


Figure 9 Mechanisms of chemoprevention exhibited by phytochemicals (Source: Iqbal et al. 2018)

Another important aspect is that phytochemicals have also been shown to work as chemo- and radiosensitizers, enhancing the effect of chemotherapeutic agents by promoting cell apoptosis. For example, resveratrol, a polyphenol from grapes, increased significantly the antiproliferative effect of paclitaxel, but also enhanced the radiation effects by altering the cell-cycle progression (Deorukhkar *et al.* 2007). Also, a terpenoid oridonin makes cells of hepatocellular carcinoma more susceptible to arsenic trioxide (Huang *et al.* 2012).

Phytochemicals, such as soy isoflavones, could prevent adverse effects in bladder and bowel caused by radiation, as well as erectile dysfunction (Ahmad *et al.* 2008).

In vitro research as well as numerous epidemiological studies support the cancer chemopreventive role of dietary phytochemicals. Lower risk of breast, pancreatic and ovarian cancer correlated with higher carotenoids intake, while a lower risk for prostate cancer was linked with a higher intake of tomatoes and cruciferous vegetables. Research shows that dark chocolate intake was linked to lower risk of colon cancer, coffee consumption reduces the risk of skin cancer, and people who drink green tea have lower risk of prostate, breast and ovarian cancer. Reduction in lung cancer risk was noted in those consuming flavonoids-rich food (Thomas *et al.* 2015).

Dietary phytochemicals are potent epigenetic regulators, a function investigated both in cancer and other health disorders. Inhibitors of DNA methyltransferases such as curcumin, catechin, epicatechin, lycopene, isoflavone daidzein and quercetin have been linked with risk reduction for prostate cancer, as well as different levels of antitumour activity. Curcumin, apigenin, lycopene, diallyl disulphide, indole-3 carbinol and resveratrol show anti-cancer

properties by altering miRNA levels (Meeran, Ahmed and Tollefsbol, 2010; Shankar *et al.* 2016).

1.3 Selected Non-Dietary Plants

1.3.1 *Centaurea asiatica*, *Centaurea dichroa*, *Centaurea kirdigensis*, *Centaurea pamphylica*, *Arctium lappa* (Asteraceae)

The Asteraceae family is the largest family of flowering plants, and it is found all around the world, especially in North America, the Mediterranean region, central Asia and China (Panero and Crozier, 2016).

This family of plants, also called Compositae, encompasses many species of economic and medicinal importance. Among these, there are species used for their oils: sunflower oil - *Helianthus annuus* L., safflower oil - *Carthamus tinctorius* L.; for their medicinal importance: anti-malarial - *Artemisia annua* L., immunity - *Echinacea purpurea*; for industrial purposes: sweetener, *Stevia rebaudiana*, orange dye, *Carthamus tinctorius* L. and *Tagetes patula* L., insecticides, Anthemideae; for consumption: artichoke, *Cynara cardunculus* L., endive, *Cichorium endivia* L., lettuce, *Lactuca sativa* L. and tarragon, *Artemisia dracunculus* L. (Dempewolf *et al.* 2008).

Compounds of essential oils from the Asteraceae species, including camphor, α -pinene, β -eudesmol, *Artemisia* ketone and thujone, have antibacterial properties against *Staphylococcus aureus*, *Salmonella typhimurium*, *Escherichia coli*, *Pseudomonas aeruginosa* and *Streptococcus pneumoniae* (Rai and Kon, 2013). Lacier *et al* used disc diffusion method to determine the antimicrobial activity of *Artemisia echegarayi* essential oil. Discs diffused with 10 μ l of essential oil were used to check the antimicrobial activity and for positive control gentamicin discs (10 μ g, Britania, Argentina) were used. The inhibition zones after 24 h incubation at 37 °C showed that the essential oil was more effective against gram positive bacteria. *A. echegarayi* EO showed highest toxicity towards *L. monocytogenes* CLIP 74903 and *B. cereus* as their MIC were lowest MIC = 2.4 μ g/ml. (Laciar *et al.* 2009).

Many members of the *Centaurea* genus (Figure 10) are used as herbal remedies. *Centaurea amanicola* oil shows antibacterial activity against *Staphylococcus aureus*, particularly its sesquiterpenoids. The high content of oxygenated sesquiterpenes in oils from *Centaurea chamaerhaponticum* is responsible for antibacterial activity against *Staphylococcus aureus*, *Streptococcus epidermidis*, *Escherichia coli* and *Salmonella ser. typhimurium* (Rai and Kon, 2013). Leaves of *Centaurea ragusina* L. exhibit both

antibacterial as well as cytotoxic properties, which are mostly attributed to isolated sesquiterpene lactones (Grienke *et al.* 2018).



Figure 10 Photo of *Centaurea* sp. Source: Jouko Lehmuskallio at <http://www.luontoportti.com>

Aside from the anti-inflammatory and antioxidant activity, chlorogenic acid found in the Asteraceae is effective in carcinogenesis by decreasing cancer cell migration (Belkaid *et al.* 2006). Extracts of species of *Centaurea* have shown antiproliferative and anticancer effects, mainly attributed to flavonoids and sesquiterpenes. Apigenin, a flavone found both in extracts of *Centaurea borysthena* and *Centaurea daghestanica*, showed cytotoxic activity against myeloma cells, and acted synergistically with chemotherapy (Korga *et al.* 2017). Pincomebrin, a flavonoid isolated from *Centaurea eryngioides*, has shown antibacterial, anti-inflammatory and anticancer properties (Rasul *et al.* 2013). The major targets for the anticancer activity of this flavonoid are ROS and NOS downregulation (in colon cancer cells) and interference with caspases and Fas/Fas ligand apoptotic pathway (upregulation in the case of leukaemia) (Rasul *et al.* 2013). Fas and Fas Ligand (FasL) are two molecules involved in the apoptosis regulation. They are responsible for the apoptosis of thymocytes that fail to properly rearrange the TCR genes as well as self-antigen recognizing cells (Volpe *et al.* 2016).

Bioactive components found in extracts of the aerial parts of *Centaurea pamphylica* (matairesinoside, arctim, matairesinol and pterodontriol) showed significant antioxidant activity (Shoeb *et al.* 2007). Arctiin, arctigenin's glycoside, was isolated from several *Centaurea* species (*C. pamphylica*, *C. americana*, *C. melitensis*, *C. albonitens*), and it has numerous pharmacological properties including antibacterial, antidiabetic, antioxidative, antiproliferative and antitumour activity (Hamedeyazdan *et al.* 2017).

Arctium lappa L. (Figure 11), most often found in China, Japan and Korea, is used in traditional medicine as an anti-inflammatory, antioxidant, diuretic and antihypertension remedy. Aside from being consumed as tea or a vegetable, *A. lappa* has been used for its antibacterial and antiviral properties (Sun *et al.* 2014). This plant represents an anti-influenza remedy frequently used in Asia (Gao, Yang and Zuo, 2018). Arctigenin and arctiin from this plant have also been widely investigated for their effects on metabolic disorders and different nervous system disorders such as neurodegeneration, cerebral ischemia and Alzheimer's disease (Gao *et al.* 2018).



Figure 11 Photo of *Arctium lappa*. Source: <http://www.herbgarden.co.za/mountainherb/seedinfo.php?id=201>

The fruit of *Arctium Lappa* L. contains arctigenin, a lignan that shows anticancer activity via Akt signaling regulation and NF- κ B inhibition (Sun *et al.* 2014, Feng *et al.* 2017) and antimetastatic activity in human breast cancer cells via downregulation of enzymes involved in cell invasion, migration and angiogenesis - matrix metalloproteinases and heparanase (Lou *et al.* 2017). Further, it was found that arctigenin from this plant inhibits STAT3 in triple-negative breast cancer cells, (Feng *et al.* 2017). Interestingly, this compound does not have a uniform anti-cancer mechanism of action across different cancer types, so it was found that in lung adenocarcinoma (non-small-cell lung cancer) cells it acts by affecting cell cycle via inhibition of NPAT expression and subsequent modulation of expression of histones (Susanti *et al.* 2013). A Phase I trial in patients with advanced pancreatic cancer who received GBS-01, an *A. lappa* L. extract rich in arctigenin, showed promising results (Ikeda *et al.* 2016). Another constituent extracted from the seeds of this plant, lappaol F, was found to induce cell-cycle arrest in human cancer cells, inhibit growth, activate caspases and induce cell death in tumour cells (Sun *et al.* 2014).

1.3.2 *Equisetum arvense* (Equisetaceae)

The Equisetaceae family has a single surviving genus with around 15 species. Usually, *Equisetum* plants can be found in damp and shaded places and are distributed all around the world. The presence of silica on the stems of these plants is the reason for their historical use in cleaning and polishing kitchenware because of their abrasiveness, and they are also used as dyes (Saslis-Lagoudakis *et al.* 2015). In traditional medicine, they are used for diuretic effects, kidney and bladder stones and wound healing (Menkovic *et al.* 2011).

Phytochemistry of *Equisetum arvense* (Figure 12) is characterised by the presence of caffeic acid derivatives, kaempferol, quercetin glycosides, apigenin, chlorogenic acid and luteolin. These compounds show wound healing properties (Ali *et al.* 2014). A randomized double-blind placebo-controlled clinical trial showed that ointment with *E. arvense* led to significant decrease in pain intensity and improvement in wound healing in women following episiotomy (Asgharikhatooni *et al.* 2015). The essential oil of *E. arvense* contains mainly fragrant acetones and thymol and has shown significant antibacterial activity against *Staphylococcus aureus*, *Pseudomonas aeruginosa* and *Escherichia coli* (Ali *et al.* 2014). Antioxidant activity is attributed to high levels of flavonoids and phenolic acids (Ali *et al.* 2014).



Figure 12 Photo of *Equisetum arvense*. Source: Bobby Hattaway at https://www.discoverlife.org/mp/20p?see=I_TQBH11687&res=640

Significant radical scavenging activity was described for *E. arvense* extracts. Main constituents responsible for this antioxidative activity are phenolic compounds. HeLa cells (Human cervical cancer) were most sensitive to the effects of different *E. arvense* extracts, but with a biphasic antiproliferative activity (Četojević-Simin *et al.* 2010).

1.3.3 *Gardenia ternifolia* (Rubiaceae)

The Rubiaceae family is mostly distributed in the tropics region. As one of the largest in the *Magnoliopsida* class, it ranks fourth in diversity of species among Angiosperms and it includes approximately 637 genera and 13000 species. This plant family has an important economic, ornamental and medicinal role among the Brazilian flora, with 120 genera and 1400 species. Representative members of this plant family include coffee (*Coffea* species), ipecac (*Carapichea ipecacuanha*) used as an emetic, and quinine (*Cinchona* species), a drug used for treating malaria (Karou *et al.* 2011).

The taxonomic classification of the Rubiaceae family is complex, but recent studies suggest this family is divided into three subfamilies: *Rubioideae*, *Cinchonoideae* and *Ixoroideae* (Martins and Nunez, 2015). This family is a source of a large diversity of substances such as anthraquinones, carotenoids, coumarins, flavonoids, indole alkaloids, iridoids, proanthocyanidins, saponins, tannins, terpenoids (diterpenes and triterpenes) and other phenolic derivatives and also bioactive alkaloids such as N,N-dimethyltryptamine (Figure 13), harmine, and tetrahydroharmine (Karou *et al.* 2011; Martins and Nunez, 2015).

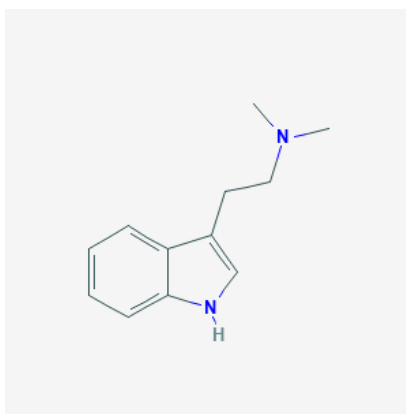


Figure 13 Chemical structure of N,N-dimethyltryptamine from the Rubiaceae
(Source: <https://pubchem.ncbi.nlm.nih.gov/compound/6089#section=2D-Structure>)

Studies have identified antibacterial, antihypertensive, antimalarial, antidiabetic, anti-inflammatory and antioxidant properties in plants from the Rubiaceae family (Karou *et al.* 2011). *Gardenia ternifolia* Schumach.& Thonn. (Figure 14) can be found in sub-Saharan Africa (Togo, Mali, Guinea) and it has been used in the treatment of malaria and jaundice (roots), infectious diseases (root bark) and as an anti-hypertensive agent (leaves and bark) (Karou *et al.* 2011). Gerdenifolins (neolignans), isolated from *Gardenia ternifolia* Schumach. and Thonn., showed cytotoxic activity against HeLa cells, inhibiting cancer cell proliferation and inducing apoptosis (Tshitenge *et al.* 2017).



Figure 14 Photo of *Gardenia ternifolia* Schumach.& Thonn. Source: D.C.H. Plowes at www.zambiaflora.com

1.3.4 *Gypsophila pilulifera* (Caryophyllaceae)

The Caryophyllaceae family of angiosperms comprises about 85 genera and 2,630 species. They can be found in Europe, North America, Asia and Australia, but particularly in the north hemisphere, and are known for surviving in unwelcoming habitats such as deserts. Members of this family are mostly known as ornamental plants, but they also have important roles in medicine and toxicology. *Spergularia rubra* has been used in traditional medicine in cases of cystitis, while *Saponaria officinalis* is thought to aid with skin problems (Chandra and Rawat, 2015).

Phytochemistry of the Caryophyllaceae is characterised by the presence of anthocyanin pigments (petals), high level of saponins (roots), phytoecdysteroids, isoprenoids and fatty acid derivatives. Ethnomedicinal use of different members of the Caryophyllaceae family includes treatment of gastric problems, inflammation of urinary and respiratory tract, fever, rheumatism. Pharmacological properties of various Caryophyllaceae species include antibacterial, antifungal, antiviral, antioxidant and anti-inflammatory activity. Anticancer properties have been described for many plants from this family, including *Dianthus caryophyllus*, *Saponaria vacaria* L., *Sileneae* (Chandra and Rawat, 2015).

Anticancer properties have been noted across different members of the *Gypsophila* species (Figure 15). Extracts of *Gypsophila arrostii* contain gypsogenins and their derivatives, which have antiproliferative effects and cause cell cycle arrest and cell death in various cancer cell lines (colorectal cancer, breast cancer, cervical cancer etc.). Compounds found in *Gypsophila oldhamia* have exhibited apoptotic activity in human hepatoma cells via activation of caspase-3 and MAPK signaling pathways (Chandra and Rawat, 2015). Extract

of *G. pilulifera* Boiss.& Heidr. contains atriterpenoid saponin which exhibits significant cytotoxic activity against human pulmonary adenocarcinoma cells (Arslan *et al.* 2012).



Figure 15 Photo of *Gypsophila fastigiata*. Source: Jouko Lehmuskallio at <http://www.luontoportti.com>

1.3.5 *Hyssopus officinalis* (Lamiaceae)

The Lamiaceae family includes about 186 genera and 7,200 species. These plants have cosmopolitan distribution, but are most commonly found in the Mediterranean. They are widely used in cuisine, industry (perfumes and food flavouring) as well as in medicine, and are considered the plants with the largest variety in use (Tamokou *et al.* 2017).

Remarkable members of the Lamiaceae family include lavender (*Lavandula officinalis* – perfume industry), culinary herbs such as rosemary (*Rosmarinus officinalis*), thyme (*Thymus vulgaris*), basil (*Ocimum basilicum*), oregano (*Ocimum vulgare*), marjoram (*Ocimum majorana*), medicinal plants such as *Salviae*, *Marrubium vulgare*, the *Stachys* genus and *Prunella vulgaris*. Peppermint originates from *Mentha piperita*, menthol from *Mentha arvensis* and spearmint from *Mentha spicata* (Tamokou, 2017).

Phytochemistry of the members of the Lamiaceae family is characterized by the presence of quinones, coumarins, saponins, tannins, phenolic compounds, polyphenols, alkaloid and iridoids. Pharmacologically, these plants exhibit antioxidant and antimicrobial activity (Tamokou *et al.* 2017).

Hyssopus officinalis (Figure 16) is used as a medicinal plant in people with respiratory and intestinal disorders. Essential oils from this plant showed strongest antimicrobial activity against *Klebsiella* sp. and *Pseudomonas aeruginosa* isolated from human sputum (Stanković *et al.* 2016), while another study found strong activity against *Staphylococcus*

aureus, *Candida albicans*, *Escherichia coli* and *Streptococcus pyogenes* (Kizil *et al.* 2010). Yet, the antioxidant activity of this oil was low (Kizil *et al.* 2010; Stanković *et al.* 2016). The main components of essential oil of *Hyssopus officinalis* are 1,8-cineole, isopinocampone, β -pinene, terpinen-4-ol and pinocarvone (Kizil *et al.* 2010; Stanković *et al.* 2016).



Figure 16 Photo of *Hyssopus officinalis*. Source: Jouko Lehmuskallio at <http://www.luontoportti.com>

1.3.6 *Kitaibelia balansae* (Malvaceae)

The Malvaceae family (order *Malvales*) comprises around 244 genera and 4,225 species (Christenhusz and Byng, 2016). Most of these species can be found worldwide (Taia, 2009). Different systems of classification exist for this family of plants, and taxonomy is complex. Some authors have included the *Hibiscus* genus into this family, while others have moved it to Bombacaceae, which they consider a separate family (Taia, 2009). The most important species when it comes to economic value are cacao (*Theobroma cacao*), cotton (*Gossypium* species), baobab (*Adansonia digitata* L.) and hibiscus (Dzoyem *et al.* 2017).

Plants from this family have been used in folk medicine, specifically as antiseptics, diuretics, medicines used for respiratory diseases, antifertility drugs (abortifacient), and remedies for skin disorders, and also gastrointestinal disorders due to their carminative activity (Toyin *et al.* 2014; Vadivel, 2016). Phytochemicals behind these effects include phenolic acids, flavonoids and polysaccharides. Namely, important compounds encompass kaempferol, luteolin, quercetin, thiamine, riboflavin, entriacontane and myricetin, among others (Toyin *et al.* 2014; Vadivel, 2016).

Flowers of the plants in the genus *Kitaibelia* contain these phytochemicals, as well as apigenin and chrysoeriol (Vadivel, 2016). Extract of *Kitaibelia vitifolia* shows antibacterial activity, as well as antioxidant activity by acting as a free-radical scavenger and inhibitor of lipid peroxidation (Mašković *et al.* 2011). Extracts of *K. balansae* Boiss. (Figure 17), plant used as a pain remedy, show significant antiviral activity against herpes simplex virus type 1 (Dikilitas and Duman, 2018).



Figure 17 Photo of *Kitaibelia balansae*. Source: Prof. Avinoam Danin at <https://flora.org.il/en/plants/KITBAL/>

1.3.7 *Solanum anguivi* (Solanaceae)

The Solanaceae family of plants has cosmopolitan distribution. It includes about 98 genera and 2,700 species (Yadav *et al.* 2016). Many of the plants in this family are economically important, including potato (*Solanum tuberosum*), tomato (*Solanum lycopersicum*), eggplant (*Solanum melongena*), tobacco (*Nicotiana tabacum et rustica*) and peppers (*Capsicum* sp.) (Oyeyemi *et al.* 2015; Yadav *et al.* 2016). Many are important for their toxicological properties, such as nightshades, belladonna (*Atropa belladonna*) and jimsonweed (*Datura stramonium*) (Yadav *et al.* 2016).

This family produces wide range of secondary metabolites, among which the alkaloids are the most prominent ones. These compounds include tropanes, solanine, scopolamine, capsaicin, atropine and nicotine. Capsaicin has shown potent anticancer activity across different cancers including lung, breast, stomach, prostate cancer and leukaemia (Zheng *et al.* 2016). The mechanisms of action for anticancer effects of capsaicin involve anti-metastatic effects, NF- κ B inhibition, inhibition of MMPs expression, induction of apoptosis and upregulation of RIP3 (Zheng *et al.* 2016). Moreover, steroidal glycoalkaloids (α -tomatine, α -solanine, α -chaconine etc.) from the Solanaceae plants have antitumour effects (Sucha and Tomsik, 2016).

Fruits of the *Solanum anguivi* (Figure 18), found mainly in Africa, contain many important phytochemicals, including flavonoids, tannins, phenols, alkaloids, triterpenoids, steroids and saponins (Oyeyemi *et al.* 2015). This plant has been used as food and in folk medicine as an antihypertensive agent, pain ailment, cough expectorant and remedy for skin disorders (Oyeyemi *et al.* 2015). Polyphenolic compounds found in this plant (rutin, caffeic acid, chlorogenic acid, gallic acid, quercetin) exhibit antioxidant activity (Elekofehinti *et al.* 2013).



Figure 18 Photo of *Solanum anguivi*. Source: Robert v. Blittersdorff at <http://www.africanplants.senckenberg.de>

1.3.8 *Ziziphus mucronata* (Rhamnaceae)

The Rhamnaceae family has a cosmopolitan distribution and comprises around 50 genera and over 900 species (Chen and Schirarend, 2007). Members of this family have been used as laxatives, dyes and drugs (*Rhamnus* species). Interestingly, timber of *Hovenia*, *Alphitonia* and *Ziziphus* species has been used for musical instruments and fine furniture. Besides being used as ornamentals, some plants are also used as food (*Ziziphus* species and *Hovenia dulcis*) (Chen and Schirarend, 2007).

There are around 100 *Ziziphus* species, found mostly in Asia, America and Africa. Most important phytochemical constituents include phenolics, flavonoids, tetracyclic triterpenoid saponins and proanthocyanidins (Mokgolodi *et al.* 2011). *Ziziphus mucronata* contains cyclopeptide alkaloids (mucronine J, abussenine A and franguloline) (Mokgolodi *et al.* 2011; Ibrahim *et al.* 2012).

Ziziphus mucronata (Figure 19) is found in Africa. Ethnomedicinal uses of this plant involve relief for chest pain, topical application for wounds, remedy for cough, parasitoses and gastrointestinal disorders (Mokgolodi *et al.* 2011; Ibrahim *et al.* 2012). Extracts exhibit antidiabetic and antibacterial activity (Ibrahim *et al.* 2012). Extracts of *Ziziphus mucronata* were found to improve cell viability and reduce the harmful effects of amyloid-beta peptide on neurons, a protein involved in the pathogenesis of Alzheimer's disease (Adewusia *et al.* 2013). Experimental results indicate that administration of root extracts of *Z. mucronata* led to an increase in serum insulin and lower level of blood glucose (Ibrahim and Islam, 2017). Extracts of this plant have shown significant antioxidant activity as radical scavengers, with ethyl acetate leaf extract yielding the highest content of phenols (Ibrahim *et al.* 2012).

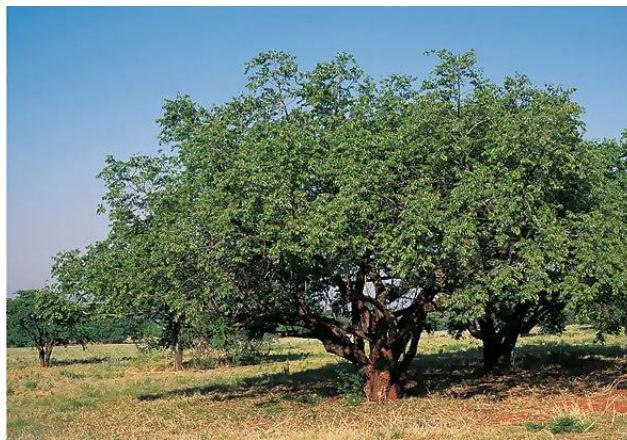


Figure 19 Photo of mature *Ziziphus mucronata*. Source: Michael Briza at http://www.krugerpark.co.za/africa_buffalothorn.html

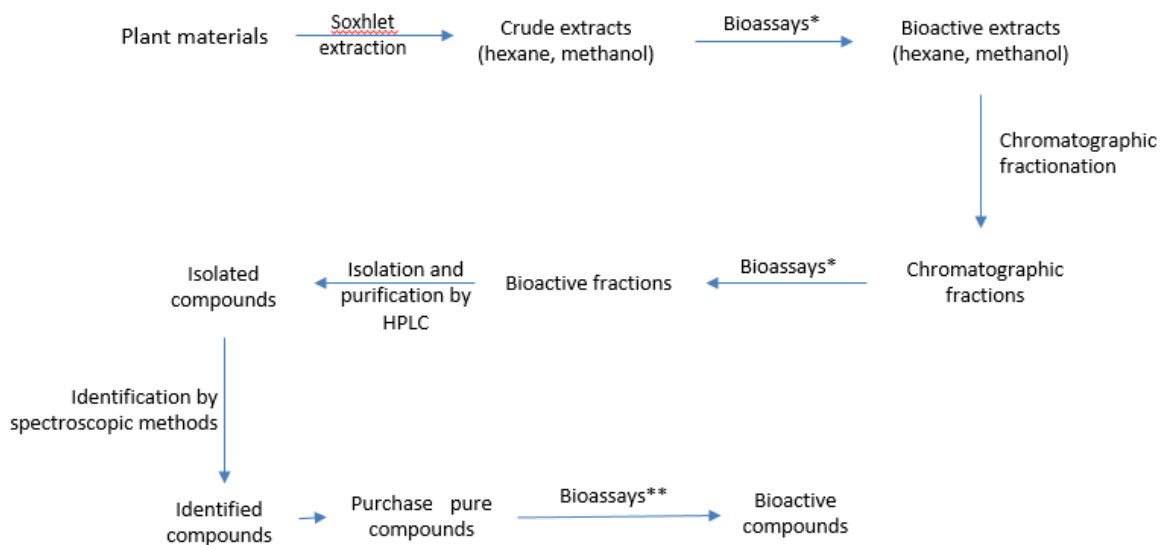
1.4 Aims and research outlines

The aim of this research project was to focus on non-dietary plants in search for bioactive compounds that can modulate the Nrf2/ARE signaling pathway, in a positive manner to provide cancer chemoprevention effects, or in a negative manner to inhibit Nrf2 activation that could be useful for chemoresistant cancers (Wang *et al.* 2008). The research was designed as a bioassay-guided investigation, using the MTT assay followed by a luciferase reporter gene assay at each step to measure Nrf2 gene induction. The AREc32 reporter cell line is a stable cell line derived from MCF-7 cells that contains a luciferase gene construct under the control of the Antioxidant Response Elements (ARE) (Wang *et al.* 2006) - so that an Nrf2 inducer activating the ARE would cause a quantifiable increase in luciferase activity (bioluminescence signal). Untransfected MCF-7 cells, a stable human breast adenocarcinoma-derived cell line, was chosen for Western blotting of the NAD(P)H:quinone oxidoreductase 1 (NQO1) protein and for the study of cytoprotective properties of selected bioactive compounds against ethacrynic acid (ETA).

Selected plant material will be extracted by refluxing hot solvents (Soxhlet extraction) using *n*-hexane and methanol in the order of lower to higher polarity. The resulting solvent, mixed with extracted crude mixtures, will be forced to evaporate, and the crude extracts will be assayed for cytotoxicity using the MTT assay. Throughout the bioassay-guided investigation, the least cytotoxic concentrations will be used in the luciferase reporter gene assay as treatment of AREc32 cells. tBHQ (*tert*-butylhydroquinone), a synthetic derivative of hydroxyquinone and a known activator of the Nrf2 transcription factor, will be used as positive control for the induction of Nrf2 in the AREc32 assays.

The extracts will also be assayed for free-radical scavenging properties using the DPPH (2,2-diphenyl-1-picrylhydrazyl) assay. The flavonol quercetin will be used as positive control because of its reproducible free radical scavenging activity against DPPH *in vitro*. A diagram describing the research process is presented in Figure 20.

After identification of bioactive extracts, these will be further fractionated, either by solid-phase extraction (SPE) with methanol and water for methanol extracts, or by vacuum-liquid chromatography (VLC) using a ethyl acetate and *n*-hexane solvent system for *n*-hexane crude extracts.



*Bioassays performed were MTT assays, luciferase assays and DPPH assays

**Bioassays performed were MTT assays followed by luciferase assays, Western blotting for NQO1 detection and MTT assay for quantifying the effect of pretreatment with selected flavonoids on the cytotoxicity of ethacrynic acid (ETA) in MCF-7 cells.

Figure 20 Flow diagram of the bioassay-guided investigation

Fractions will be tested in AREc32 cells via luciferase assay for Nrf2/ARE induction and also screened for free radical scavenging properties using the DPPH assay. Methanol fractions that are most bioactive in the luciferase assay will further be screened for separation of components using HPLC, while the *n*-hexane fractions will be further separated using preparative TLC. The isolated compounds will also undergo screening with the luciferase reporter gene assay using AREc32 cells, as well as further investigational tests such as the detection of the NQO1 protein, a Phase II enzyme whose expression is controlled by Nrf2 activity.

Selected phytochemicals will also be tested for cytoprotective activity against ETA, as oxidative stress inducer, using the MCF-7 cell line, thus gaining a better view of the biological role that individual compounds from bioactive mixtures have in cancer chemoprevention.

CHAPTER 2 Materials and Methods

2.1 Phytochemical Methods

2.1.1 Plant materials

Aerial parts of *Arctium lappa* L. (Asteraceae), *Equisetum arvense* L. (Equisetaceae) and *Hyssopus officinalis* L. (Lamiaceae) were sourced from Romania, Dambovită region. Whole dry aerial parts of *Centaurea pamphylica* Boiss.& Heldr. (Asteraceae) were collected from West and East Anatolia, Turkey and the voucher specimen (PHSH0011) exists in the herbarium of Plant and Soil Science Department of the University of Aberdeen, UK, and Canakkale Onsekiz Mart University, Turkey (COMU). Roots of *Gypsophila pilulifera* Boiss.& Heldr (Caryophyllaceae) and aerial parts of *Kitaibela balansae* Boiss. (Malvaceae) were also received from Turkey, as well as the *n*-hexane and methanol extracts of *Centaurea asiatica*, *Centaurea dichroa* Boiss.& Heldr. and *Centaurea kirdigensis*. Aerial parts of *Gardenia ternifolia* Schumach.& Thonn. (Rubiaceae), roots of *Solanum anguivi* Lam. (Solanaceae) and bark of *Ziziphus mucronata* Willd. (Rhamnaceae) were received from Kenya. Voucher specimens of all plants used in this project are kept at the Centre for Natural Products Discovery, the Liverpool John Moores University, UK.

2.1.2 Soxhlet extraction

All aerial parts of plants were air-dried and ground into powder using a regular spice grinder. Thimbles made of thick cellulose filter paper were prepared by hand, filled with ground plant material and placed in the Soxhlet apparatus as shown in Figure 21 below.



Figure 21 Soxhlet apparatus at the end of a reflux cycle (500 ml)

Soxhlet extraction was performed on all plant materials, with the exception of *Centaurea asiatica*, *Centaurea dichroa* and *Centaurea kirdigensis*, for which extracts were received.

The solvent extraction was performed with 900 ml of *n*-hexane and methanol (Fisher Scientific) successively, using a 500 ml Soxhlet apparatus, for the following plants: *Centaurea pamphylica*, *Gardenia ternifolia*, *Gypsophila pilulifera*, *Solanum anguivi* and *Ziziphus mucronata*. For the other plants, a 250 ml Soxhlet apparatus was used, refluxing 500 ml of solvent.

The solvent extraction was performed for 12 reflux cycles with each solvent for each plant material.

The amounts of ground plant material loaded into the thimbles are shown in Table 6.

Table 6 Amounts of plant materials used for Soxhlet extraction

Plant	Amount in extraction thimble (g)
<i>Arctium lappa</i> L (root)	91.94
<i>Centaurea pamphylica</i> (aerial parts)	56.98
<i>Equisetum arvense</i> (aerial parts)	33.52

Plant	Amount in extraction thimble (g)
<i>Gardenia ternifolia</i> (aerial parts)	110
<i>Gypsophyla pilulifera</i> (roots)	105.52
<i>Hyssopus officinalis</i> (aerial parts)	78.8
<i>Kitaibelia balansae</i> (aerial parts)	41.94
<i>Solanum anguivi</i> (roots)	73.84
<i>Ziziphus mucronata</i> (bark)	100.67

2.1.3 Sample cleaning and separation

The resulting compound-rich solvents were filtered using filter paper to remove traces of plant material (impurities) and samples were concentrated by solvent evaporation using a rotary evaporator at 45°C, as depicted in Figure 22. Samples were then left overnight to dry out further using an air-pump.



Figure 22 Evaporation of methanol from an extract fraction using a rotary evaporator

Methanol extracts were further fractionated by solid phase extraction (SPE) with a step gradient, as exemplified in Table 7 (Chima *et al.* 2014). Using Strata cartridges, pre-packed with reversed-phase silica C₁₈ (10 g), fractions of 250 ml (F1, F2, F3, F4) were collected in

flasks, evaporated and reconstituted at various concentrations to be used in HPLC and cell culture assays.

Table 7 SPE solvent gradient steps

Step gradient (methanol %)	Water (ml)	Methanol (ml)	Volume of fraction (ml)
20	200	50	F1 = 250
50	125	125	F2 = 250
80	50	200	F3 = 250
100	0	250	F4 = 250

Samples were prepared by dissolving approximately 1 g of crude methanol (MeOH) extract in a 10 ml solution of 10-20% MeOH in water and then added to the cartridge.

Dissolution conditions for methanol extracts were 1 g of crude extract to 10 ml of 10/20% methanol in water, as each sample had slightly different solubility.

The SPE was performed three times in similar conditions for each extract and resulting fractions were pooled in together, before undergoing solvent evaporation using the rotary evaporator as shown above.

2.1.4 Analytical TLC and free-radical scavenging assay (DPPH qualitative and quantitative assay)

The analytical TLC performed in this study had the qualitative purpose of observing the type of compounds in the *n*-hexane and methanol plant extracts.

Sheets of silica gel on aluminium, 20x20 cm (Sigma Aldrich), were spotted with *n*-hexane and methanol solvent extracts and also with quercetin (1 mg/ml) as positive control. The spotting was made using microcapillary tubes, 3 successive spottings for quercetin, 3 times for the undiluted MeOH extracts and 10 times for the *n*-hexane extracts, both diluted to 10 mg/ml.

The solvent system used was *n*-hexane:ethylacetate 4:1 for *n*-hexane extracts and *n*-hexane:ethylacetate 3:2 for methanol extracts. The development time was around 40 min. Visualisation was performed on developed and dried TLC plates using an UV lamp in

shortwave (254 nm) and longwave (365 nm) UV, followed by visualisation with the aid of a universal spray reagent of anisaldehyde, which can identify steroids, phenols, terpenes and sugars (Touchstone and Dibbons, 1978, p.205). After spraying, the chromatoplates were heated in the oven at 110°C for 5 min until full development of spots.

The anisaldehyde reagent used for derivatisation was prepared fresh before spraying the chromatoplates, with ingredients from Sigma Aldrich. The solution was a mix of 10 ml glacial acetic acid, 5 ml of sulphuric acid and 55 ml of methanol, cooled to room temperature before adding 0.5 ml of *p*-anisaldehyde mixed in 30 ml of methanol.

A qualitative DPPH assay was performed by spraying a developed TLC plate with DPPH solution (80 µg/ml) and observing a colour change from purple to yellow on spots. This colour change shows that the stable free-radical DPPH can be reduced by some extracted phytochemicals that can act as free-radical scavengers.

A further quantitative DPPH test was performed with the aim of calculating the concentration at which an extract, fraction or compound exerts a 50% inhibition on the free radical DPPH. The positive control used for this assay was quercetin.

A series of four 10-fold dilutions of the test sample were prepared from a stock solution of 1 mg/ml. Then, 1 ml of each test solution was mixed with 1 ml of DPPH solution (80 µg/ml) and left in the dark for approximately 30 min. A standard of 1 ml MeOH and 1 ml DPPH solution was also prepared. A Cole-Palmer spectrophotometer was blanked with a sample of methanol and absorbance values were read at 517 nm.

The readings provided data for curve-plotting of absorbance vs %inhibition and the IC₅₀ was calculated (Chima *et al.* 2014) using the following formula:

$$\%Inh = \frac{(Abs_{Std} - Abs_S)}{Abs_{Std}} \times 100,$$

where Abs_{Std} was the absorbance value of the standard, Abs_S was the absorbance value of the test sample and $\%Inh$ was the % inhibition of DPPH exerted by the test sample relative to the standard.

2.1.5 Isolation and identification of phytochemicals

Isolation of phytochemicals

HPLC analysis of methanol fractions resulting from SPE fractionation was carried out on Agilent Technologies 1260 Infinity, equipped with a Diode Array Detector (DAD) to record UV-Vis absorption spectra. Prior to HPLC analysis, samples were dissolved in MeOH.

Method optimisation for the separation of compounds from mixtures was carried out on the preparative Agilent 1260, using a semiprep Phenomenex column (Luna 5 μ m C₁₈, 150x10 mm, serial no. 210456-1), fitted with a guard column (Hichrom). The flow was set to 2 ml/min and the injection volumes varied between 50 and 200 μ L.

To isolate compounds, peaks were collected in glass beakers as they eluted through the Hichrom prep column (ACE 5 μ m C₁₈ phase, 150x21.2 mm, serial no. A121687) at a flow rate of 10 ml/min, following injections of 200 to 900 μ L, while the concentration of samples always aimed to be around 100 mg/ml.

The purity of isolated compounds was checked on the analytical 1260 Agilent HPLC, using a Phenomenex Kinetex column (EVO 5 μ m C₁₈ phase, 150x4.6 mm, batch no. 5720-0051), fitted with a 'SecurityGuard' guard column. The flow was adjusted between 0.8 and 1 ml/min and the injection volume between 10 and 30 μ L for samples at 10 mg/ml.

The optimal method for separation of semi-polar compounds resulted from methanol Soxhlet extraction is shown in Table 8.

Table 8 Preparative HPLC gradient method

Time (min)	Water (%)	Methanol (%)
0	70	30
30	0	100
40	0	100 (cleaning step)
42	70	30 (re-equilibration step)

Water and MeOH used for HPLC experiments were sourced from Fisher Scientific and were of HPLC grade. Prior to use, trifluoroacetic acid (TFA) was added to solvents to make up a 0.1% concentration. Bottles were then degassed using helium and the HPLC system was always kept free of air bubbles by purging before each experiment.

The software used to visualise data on computers linked to the Agilent HPLC system was ChemStation.

Identification of phytochemicals

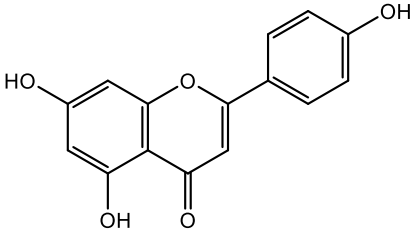
NMR (Nuclear Magnetic Resonance) spectroscopy techniques were employed in order to characterise the molecular structure of the isolated compounds. For NMR, minimum available amounts (1 mg - 10 mg) of isolated compounds were dissolved in deuterated methanol (CD₃OD, Cambridge Isotope Laboratories) and analysed on a 400 MHz Bruker at the Liverpool John Moores NMR laboratory and on a 600 MHz Bruker AMX 600 at the University of Botswana. The experiments performed were 1D (one dimensional) and 2D (two dimensional) and included the following techniques: ¹H (Proton), ¹³C (Carbon), DEPTQ (Distorsionless Enhancement by Polarization Transfer Including the Detection of Quaternary Nuclei), ¹H -¹H COSY (Correlated Spectroscopy), ¹H -¹³C HSQC (Heteronuclear Single Quantum Coherence Spectroscopy), ¹H-¹³C HMBC (Heteronuclear Multiple Bond Correlation Spectroscopy) and NOESY (Nuclear Overhauser and Exchange Spectroscopy). The interface to the NMR equipment was the TopSpin 3 software from Bruker.

Following tentative assignment of molecular formulas using NMR, samples were sent to EPSRC UK, the National Mass Spectrometry Facility at Swansea University, UK. Mass spectrometry data was acquired on Xevo G2-S ASAP or LTQ Orbitrap XL 1 spectrometers.

2.1.6 Selected phytochemical compounds (flavonoids) used for bioassays

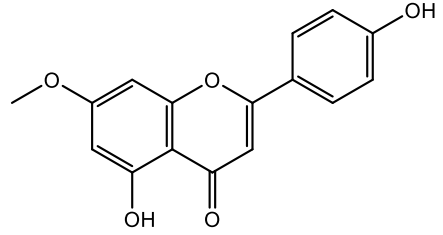
Genkwanin, naringenin, kaempferol and luteolin were purchased from Cayman Chemical Company, USA. Apigenin and quercetin were purchased from Sigma Aldrich, Germany, whereas hesperetin, hispidulin and velutin were purchased from Henan Allgreen Chemical, China. Sakuranetin was isolated from methanolic fraction F3 (80% MeOH/water) of "GT-Me". Table 9 below contains structural details of the compounds.

Table 9 Polyphenolic phytochemicals used in bioassays and their chemical structure. Structures generated in ChemDraw

Phytochemical compound	Chemical structure
Apigenin (4',5,7-trihydroxyflavone)	

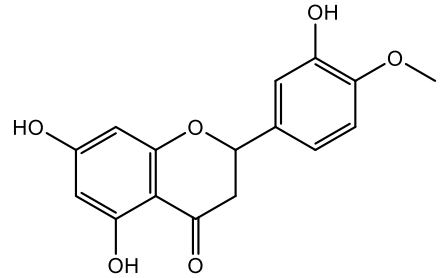
Genkwanin

(4',5-dihydroxy-7-methoxyflavone)



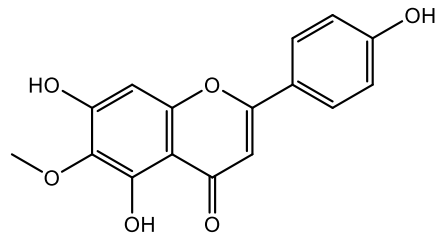
Hesperetin

(3',5,7-trihydroxy-4'-methoxyflavanone)



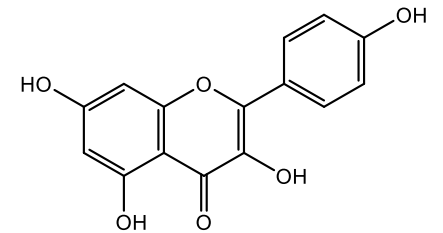
Hispidulin

(4',5,7-trihydroxy-6-methoxyflavone)



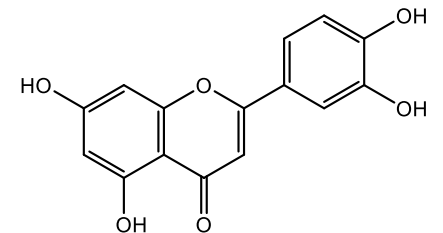
Kaempferol

(3,4',5,7-tetrahydroxyflavone)



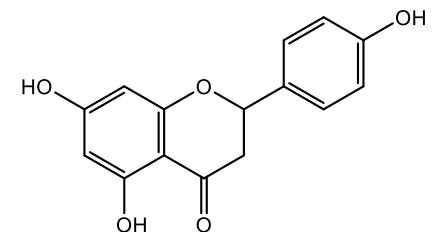
Luteolin

(3',4',5,7-tetrahydroxyflavone)



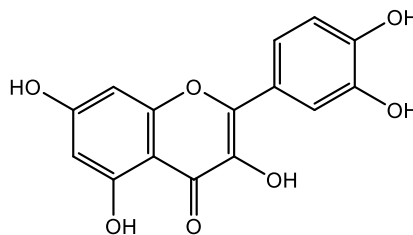
Naringenin

(4',5,7-trihydroxyflavanone)



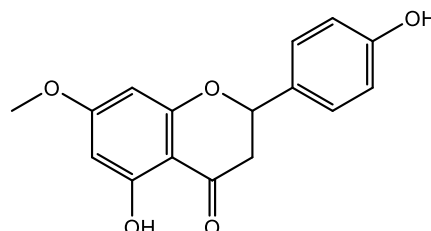
Quercetin

(3,3',4',5,7-pentahydroxyflavone)



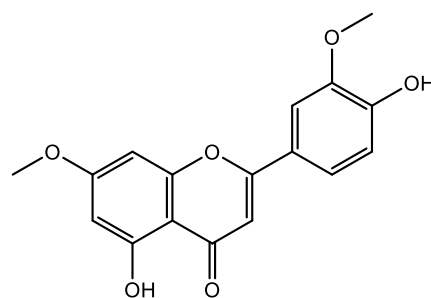
Sakuranetin/F3GT-Me-PA

(4'-5-Dihydroxy-7-methoxyflavanone)



Velutin

(4',5-dihydroxy-,3',7-dimethoxyflavone)



2.1.6 Sample naming convention

Table 10 shows the code names allocated to test samples generated such as the crude extracts and resulting fractions.

Table 10 Code names of plant extracts and fractions

Full plant name	Plant name code	Crude extract code	
		<i>n</i> -hexane	methanol
<i>Arctium lappa</i>	AL	AL-He	AL-Me
<i>Centaurea asiatica</i>	CA	CA-He	CA-Me
<i>Centaurea dichroa</i>	CD	CD-He	CD-Me
<i>Centaurea kirdigensis</i>	CK	CK-He	CK-Me
<i>Centaurea pamphylica</i>	CP	CP-He	CP-Me
<i>Equisetum arvense</i>	EA	EA-He	EA-Me
<i>Gardenia ternifolia</i>	GT	GT-He	GT-Me

Full plant name	Plant name code	Crude extract code	
		<i>n</i> -hexane	methanol
<i>Gypsophila pilulifera</i>	GP	GP-He	GP-Me
<i>Hyssopus officinalis</i>	HO	HO-He	HO-Me
<i>Kitaibelia balansae</i>	KB	KB-He	KB-Me
<i>Solanum anguivi</i>	SA	SA-He	SA-Me
<i>Ziziphus mucronata</i>	ZM	ZM-He	ZM-Me

2.2 Cell Biology And Biochemical Methods

2.2.1 Cell culture

AREc32 cells were obtained from Prof. Roland Wolf from the University of Dundee. AREc32 cells were cultured in T25 or T75 flasks with vented caps in 5 ml or 15 ml, respectively, of complete medium: Dulbecco's Modified Eagles Medium High Glucose supplemented with 10% fetal bovine serum, 1% penicillin-streptomycin (Sigma Aldrich), 1% glutamine and 0.8 mg/ml of antibiotic G418 (Sigma Aldrich). Incubation conditions were 37°C with 5% CO₂ in a humidified atmosphere. Cells were split and passaged twice a week.

For each experiment, cells were removed from flasks when they showed a confluence of at least 80%. They were washed twice with PBS (37°C) and detached from the flasks by adding trypsin (Sigma Aldrich) and leaving it for 2 min. Trypsin was then removed and flasks incubated for 5 min to allow complete detachment. Cells were seeded in 96-well plates at a density of 1.2×10^4 cells per well in 200 µL of complete medium. Seeded cells were incubated for 24 h before treatment. After treatment, experiments were performed following another 24 h incubation period.

For the experiments where the MCF-7 cell line was used, cell culture was performed as described for AREc32 cells. MCF-7 cells were obtained from Dr. Andrew Evans from the Liverpool John Moores University.

2.2.2 Cytotoxicity Assay

Cytotoxicity assays on treated cells were performed at every step of the bioassay-guided investigation to determine a suitable non-cytotoxic concentration of the extract, fraction or compound that could be used in further cell-based assays.

Cytotoxic activities were profiled using the MTT (3-(4,5-dimethylthiazol-2-yl)-2,5-diphenyltetrazoliumbromide) assay, a colourimetric assay for revealing cell metabolism activity. A volume of 20 µL MTT solution (5 mg/ml) was added to each treated well and the plate was incubated in the dark for approximately 4 h. The vehicle was then removed by vacuum aspiration and 100 µL DMSO were added for solubilisation of the purple formazan precipitate.

Absorbances were read at 570 nm on a ClarioStar microplate reader with multidetection capabilities (BMG LABTECH, Durham, USA). To normalise the experiment, the average absorbance value of blank wells was subtracted from the absorbance value of each control and treated well.

For the MTT assay, all experiments were performed in triplicate and cell viability was calculated relative to control (untreated cells). Data was analysed and visualised in Microsoft Excel.

2.2.3 Cell treatment schedules for the MTT assay

The treatment of cells with compounds of known molecular weight was performed using dilutions of molar concentrations. Typically, a stock solution of 1 mM in complete medium containing 10% DMSO (Stock 1) would be prepared first and used to prepare a second stock solution of 0.1 mM/1% DMSO (Stock 2) that would be used for treating cells directly into the wells.

The treatment of cells with crude extracts or compounds of unknown molecular weight was performed using dilutions of mass concentrations. Typically, a stock solution of 1 mg/ml in complete medium would be prepared first, containing 0-10% DMSO (Stock 1), depending on the solubility of the compound. Stock 1 solution was used to prepare a second stock solution of 0.1 mg/ml (Stock 2) if lower concentrations were required.

2.2.4 Luciferase Assay for measuring Nrf2/ARE induction

The luciferase assay was performed 24 h after treatment of AREc32 cells using the Dual-Luciferase Reporter Assay System kit (Promega, UK) containing lysis buffer, luciferase assay substrate and buffer. The vehicle was removed from each well of the seeded plate and then washed with 100 μ L of PBS before adding 20 μ L of 5X Passive Lysis Buffer diluted to 1X with distilled water. For the lysis to take place, the plate was frozen immediately (-20°C) and thawed right before the bioluminescence reading. After reconstituting the luciferase substrate with the buffer, thawed wells were transferred to an opaque 96-well plate and 20 μ L of substrate were added to 6 wells at a time, recording the bioluminescence readings with a ClarioStar microplate reader.

2.2.5 Western Blotting

To determine if compounds induced NQO1, an indicative marker of Nrf2 activity, Western Blotting was used in order to show the presence of the NQO1 protein. The cell line used for this experiment was MCF-7 and it was cultured in the same manner as in 2.2.1 above, without the addition of the G418 antibiotic to the culture medium.

The cytotoxicity assay described in 2.2.2 was also performed on MCF-7 cells, with a change in seeding density to 1×10^4 cells/well in 96-well plates. Cells were treated for the MTT assay with varying concentrations up to 50 μ M.

Once the optimal non-cytotoxic concentration had been calculated (no more than 10% toxicity), MCF-7 cells were seeded at 0.3×10^6 cells/well in 6-well plates. Twenty-four hours after seeding, the cells were incubated with bioactive compounds for 0, 3, 6, and 24 h. For each time point, untreated cells were harvested to produce control samples. Table 11 shows the compounds used to treat MCF-7 cells and the respective concentrations applied.

Table 11 Concentrations (μM) of bioactive compounds used, with tBHQ as positive control

Bioactive compound	Concentration (μM)
Naringenin	5
Sakuranetin	20
tBHQ	10

Cell harvest

For cell harvest, the culture plate was placed on ice and cell monolayers were washed 3 times with ice cold PBS. After PBS was aspirated, 300ul of RIPA lysis buffer was added to each well. Adherent cells were scraped off with a plastic cell scraper and placed in pre-cooled 1.5 ml micro centrifuge tubes. The micro centrifuge tubes containing the cell lysates were placed in a tube mixer at 4°C and left for 30 min at constant agitation, followed by centrifugation at 14000 rpm for 20 min. The supernatant was removed and aliquoted to be kept at -20°C.

Protein determination

The Bradford assay was used for protein determination, following the 2 ml microassay procedure from the Bio-Rad protocol, Quick Start™ Bradford Protein Assay.

Firstly, BSA protein standards (1.25 – 20 $\mu\text{g/ml}$) were prepared from a stock solution of 2 mg/ml, with RIPA buffer (Sigma-Aldrich) as diluent. Cell lysates were also diluted 10, 100 and 1000 times with RIPA buffer to a volume of 1 ml. One ml of protein standard and 1 ml of 1X Bradford Dye reagent (Sigma-Aldrich) were added to 2 ml disposable cuvettes and incubated in the dark at RT for 20 min. Similarly was performed for cell lysate samples.

Absorbance readings were recorded at 595 nm using a Cole-Parmer Visible Spectrophotometer, blanked with diluent. A standard curve of absorbance versus concentration of BSA standard was prepared each time before SDS electrophoresis and the linear equation and concentrations of lysates were calculated in Excel.

Sodium Dodecyl Sulphate-Polyacrylamide Gel Electrophoresis (SDS-PAGE)

In order to resolve the cell lysates, a separation of proteins based on their molecular weight was performed using 12% precast polyacrylamide gels with 10 well combs (Mini-Protean TGX Stain-Free, Bio-Rad).

The comb was removed and two precast gels were placed in a Mini-PROTEAN® Tetra Cell (Bio-Rad). The cell and wells were filled with running buffer (25 mM Tris, 192 mM glycine, 0.1% w/v SDS).

For protein preparation, cell lysates were diluted with RIPA buffer to a concentration of 2 µg/µL and then mixed with an equal amount of 2x Laemlli sample buffer (Bio-Rad), containing 10% 2-mercaptoethanol. Samples were heated at 95°C for 5 min, centrifuged for 1 min in a mini centrifuge at 6000 rpm and loaded into wells (5 µg) along with a prestained molecular weight marker (10-250 kDa). The electrophoresis cell was set to run at 200 V for almost 3 h.

Protein transfer from gel to PVDF membrane

Proteins were transferred onto 0.2 µm PVDF membranes using the Trans-Blot® Turbo™ Transfer System from Bio-Rad. Typically, the membrane was equilibrated (activated) by soaking it in methanol for 3 min and then rinsed with transfer buffer (25 mM Tris, 192 mM glycine, 0.04% w/v SDS, 20% v/v methanol).

A semi-dry transfer method was used, with the gel and membrane stacked between two filter papers saturated with transfer buffer and making sure no air bubbles were trapped between the layers.

Antibody probing

After transfer, the membrane was blocked for 1 h at RT in blocking buffer (1X Tris buffered saline, 0.1% Tween 20, 5% skimmed powder milk) The membrane was then incubated at 4°C overnight, in 10 ml of blocking buffer containing the anti-NQO1 primary antibody (Abcam, 1:1000). After incubation with the primary antibody, the membrane was washed with TBST (1X Tris buffered saline, 0.1% Tween 20) 3 times, each time for 5 minutes. After washing, the membrane was further incubated at RT for 3 h, in 10 ml of blocking buffer containing HRP-conjugated secondary antibody (rabbit anti-mouse IgG, 1:1000). Following incubation with the secondary antibody, the membrane was washed again 3 times, 5 minutes each time, before signal detection. Throughout the incubation steps, the membranes were placed on an orbital shaker to maintain agitation of the buffer and an even spread of the antibody.

Imaging

To image the blot, 2 ml of the chemiluminescent substrate (Amersham ECL Western Blotting Detection Reagent, GE Healthcare) was applied to the whole membrane. The immunoblot was then covered with plastic film and immediately placed in the CCD imager (ChemiDoc XRS+, Bio-Rad) which was controlled by the Image Lab software.

Reprobing step

After the first imaging step, a second Western blot was performed in order to reveal the control bands of beta-actin. For this, the membrane was sealed in plastic foil with 10 ml harsh stripping buffer (20 ml 10% SDS, 12.5 ml Tris HCl pH 6.8 0.5M, 67.5 ml dH₂O, 0.8 ml 2-mercaptoethanol for 100 ml) and placed in a waterbath for 30 min at 50°C. The membrane was washed 5 times with TBST, 5 min each time.

A second round of antibody probing was performed, as described previously, with the distinction that the secondary antibody was anti-beta actin (Abcam, 1:1000).

2.2.6 Cytotoxicity profile (LD₅₀) of ethacrynic acid following pretreatment with bioactive compounds

MCF-7 cells were seeded in 96-well plates at a density of 1×10^4 cells/well and left to recover for 24 h. Afterwards, the cells were pre-treated with bioactive compounds at non-cytotoxic concentrations for 24 h prior to incubation with ethacrynic acid (ETA), a known GSH inhibitor and ROS inducer, at the following concentrations: 0, 3.125, 6.25, 12.5, 25, 50, 100, 150, 250, 350, 500 and 1000 μ M for 24 h. Cytotoxicity was then assessed using the MTT assay as described in section 2.2.2. This cytotoxic assessment was carried out on two occasions, with a total of 6 test wells per ETA concentration.

A logarithmic graph was generated for concentration of ETA against cell viability and the LD₅₀ was calculated using nonlinear regression (least squares fitting method). LD₅₀ values corresponding to wells treated with bioactive compounds were then compared to the LD₅₀ of the wells treated with ethacrynic acid only. Two-way ANOVA was also performed on the data sets obtained to see the effects of the pretreatment conditions at the various concentrations of ETA applied. All data analysis was performed in GraphPad Prism 8.3.1. Results were considered significant if $P < 0.05$.

CHAPTER 3 Results and Discussion

Nine plants were subjected to successive Soxhlet extractions with *n*-hexane and methanol to yield the starting crude extracts. These extracts were then qualitatively screened for components using thin-layer chromatography. The extracts were also tested for DPPH inhibition, as an indication of free-radical scavenging activity. See results in Study 1: Sample preparation and Soxhlet extraction of plant materials followed by screening of phytochemical composition (TLC) and free-radical scavenging activity of crude extracts (DPPH assay), page 87.

The starting crude extracts were also tested for cytotoxicity in AREc32 cells before being screened for Nrf2 induction using a luciferase reporter assay. See results in Study 2: Cytotoxicity assay and luciferase reporter assay of methanol and *n*-hexane extracts of selected plants and precipitated compounds, page 94.

The bioactive crude extracts were further fractionated depending on the available material and the fractions were also subjected to the previously mentioned assays. See results in Study 3: Chromatographic fractionation of bioactive crude methanol extracts of *Centaurea dichroa* (CD), *Centaurea pamphylica* (CP), *Gardenia ternifolia* (GT) and *Ziziphus mucronata* (ZM), followed by cytotoxicity assay and luciferase assay using AREc32 cells and DPPH assay of fractions, page 117.

Main compounds from methanol fractions showing good separation in the HPLC screening were isolated and further subjected to spectroscopic techniques (mass spectrometry and nuclear-magnetic resonance spectroscopy). See results in Study 4: Identification of compounds from bioactive fractions of methanol extracts by means of UV-Vis, nuclear magnetic resonance (NMR) and mass spectrometry (MS) analysis, page 127. Similar compounds were then purchased to be used in cell-based bioassays and the results are presented and discussed in Study 5 of this chapter: Cytotoxicity assay and luciferase assay in AREc32 cells of selected polyphenolic compounds: apigenin, genkwanin, hesperetin, hispidulin, kaempferol, luteolin, naringenin, quercetin, sakuranetin and velutin, page 145.

The selected polyphenolic compounds were tested for Nrf2 activity and then for the expression of NQO1 in MCF-7 cells (naringenin and sakuranetin), a protein whose expression is mediated via Nrf2 induction. See results in Study 6: Determination of NQO1 gene expression induced by selected phytochemical compounds, page 153.

Finally, Study 7 (Effect of selected flavonoids on ethacrynic acid-induced oxidative stress in MCF-7 cells, p. 161) presents the results of an investigative experiment into the effect of the selected flavonoids in MCF-7 cells under increased oxidative stress induced by ETA.

3.1 Study 1: Sample preparation and Soxhlet extraction of plant materials followed by screening of phytochemical composition (TLC) and free-radical scavenging activity of crude extracts (DPPH assay)

Soxhlet extraction yielded various amounts of crude extracts and Table 12 presents a comprehensive summary of the starting amount of plant materials and the resulting amounts and yields of the *n*-hexane and methanol extracts.

Table 12 Summary of crude extracts resulted after Soxhlet extraction. Note that as different sample materials have different densities, the masses contained in the same thimble vary.

Plant material Weight (g)	Extract (g)/%Yield as result of:	
	<i>n</i> -hexane extraction	methanol extraction
<i>Centaurea pamphylica</i> (CP) 56.98	0.34/0.59%	4.87/8.55%
<i>Gypsophila pilulifera</i> (GP) 105.52	0.30/0.28%	26.15/24.78%
<i>Gardenia ternifolia</i> (GT) 110	0.44/0.39%	14.70/13.36%
<i>Solanum anguivi</i> (SA) 73.84	0.21/0.29%	7.12/9.64%
<i>Ziziphus mucronata</i> (ZM) 100.67	0.36/0.35%	26.38/26.2%
<i>Equisetum arvense</i> (EA) 33.52	0.12/0.37%	3.85/11.48%
<i>Kitaibelia balansae</i> (KB) 41.94	0.17/0.41%	6.88/16.40%

<i>Hyssopus officinalis</i> (HO)	0.35/0.45%	8.54/10.83%
78.8		
<i>Arctium lappa</i> (AL)	0.25/0.28%	16.49/17.93%
91.94		

The highest yields of extraction were reached only for the extraction with methanol, ranging from the lowest yield of 8.55% for *Centaurea pamphylica* up to 26.2% for *Ziziphus mucronata*. The *n*-hexane extracts registered very low extraction yields of less than 0.5% of the amount of raw material.

During the methanol extraction of GP, GT and ZM, precipitates could be observed. They were re-dissolved and concentrated in the case of GP, or filtered out, as in the case of GT and ZM. Samples were then sent for NMR and MS analysis for identification. The precipitated compounds were labelled as GPS1, GTS1/GTS2, and ZMPH1/ZM1. See Section 4.1 for identification results and Appendix B for NMR and MS spectra.

Moreover, analytical TLC of all extracts revealed that they contain a variety of compounds and Tables 13 and 14 on the next page show their retention factors (R_f). The solvent system of 20% ethyl acetate in *n*-hexane worked well for the non-polar extracts, as compounds moved from the baseline and were not put close to the solvent front. On the other hand, the 40% ethyl acetate in *n*-hexane solvent system used for methanol extracts failed to move compounds off the baseline and some were found on the solvent front. Streaking was also observed for AL-Me, GT-Me, KB-Me and ZM-Me, which points out that the sample was too concentrated when applied to the plate.

Derivatisation with anisaldehyde reagent revealed in visible light mostly violet and pink/purple spots for methanol extracts, indicative of phenolic compounds, but also terpenes (mono-, di- or triterpenes) or steroids (Agatonovic-Kustrin *et al.* 2019). *n*-Hexane extracts also showed pink/purple spots.

Table 13 TLC retention factors (R_f) of compounds observed at 254 nm and 366 nm for n-hexane and methanol extracts. A 1:4 ethyl acetate:n-hexane solvent system was used for non-polar extracts and a 2:3 ethyl acetate:n-hexane for methanol extracts. Extra spots were observed after spraying with anisaldehyde reagent.

	<i>n</i> -Hexane extracts					Methanol extracts				
	Solvent front = 8.3 cm					Solvent front = 9.1 cm				
	CP-He	GP-He	GT-He	SA-He	ZM-He	CP-Me	GP-Me	GT-Me	SA-Me	ZM-Me
	0.06	0.16	0.09	0.06	0.39	0.04	0.80	0.04	0.05	0.32
	0.12	0.36	0.21	0.22	0.51	0.25	-	0.85	-	-
R_f	0.25	0.38	0.32	0.36	0.59	0.94	-	0.96	-	-
	0.30	0.51	0.36	0.38	-	-	-	-	-	-
	0.36	0.57	0.51	0.50	-	-	-	-	-	-
	0.38	-	0.65	0.59	-	-	-	-	-	-

Table 14 TLC retention factors (R_f) of compounds observed at 254 nm and 366 nm for n-hexane and methanol extracts. A 1:4 ethyl acetate:n-hexane solvent system was used for non-polar extracts and a 2:3 ethyl acetate:n-hexane for methanol extracts. For non-polar extracts extra spots were observed after spraying with anisaldehyde reagent.

	<i>n</i> -Hexane extracts				Methanol extracts			
	Solvent front = 8.7 cm				Solvent front = 9.3 cm			
	EA-He	KB-He	HO-He	AL-He	EA-Me	KB-Me	HO-Me	AL-Me
	0.07	0.05	0.16	0.04	0.05	0.14	0.04	0.17
R_f	0.11	0.36	0.28	0.28	0.17	0.89	0.34	0.58
	0.21	0.41	0.42	0.39	0.94	-	0.45	0.86
	0.27	0.52	0.54	0.49	-	-	0.89	-
	0.39	-	0.67	0.65	-	-	-	-
	0.55	-	-	-	-	-	-	-

After spraying the TLC plates with DPPH solution for qualitative assay of free-radical scavenging activity, colour changes from purple to white/yellow were observed for most of the methanol extracts, with the exception of GP-Me.

For the next step, using the quantitative free-radical scavenging assay method described, the DPPH assay was carried out on all crude extracts. Out of all the crude extracts tested only the methanol extracts of AL-Me, CD-Me, CP-Me, EA-Me, GT-Me, HO-Me, SA-Me and ZM-Me exceeded the threshold of 50% DPPH inhibition (Figures 25 and 26).

Centaurea asiatica, *Centaurea kirgidensis* and *Gypsophila pilulifera* (CA-Me, CK-Me and GP-Me) methanol extracts did not show significant free-radical scavenging and the results were not reported.

Chima *et al* (2014) reports an IC₅₀ value for the methanol extract of the stems of *Gypsophila pilulifera* in the DPPH assay of 0.02 mg/ml and of almost 0.003 mg/ml for the 50% MeOH SPE fraction, compared to the positive control quercetin, which showed 50% inhibition of DPPH at 0.0025 mg/ml.

Quercetin, as a positive control, reached 50% inhibition of DPPH at a concentration between 0.001 and 0.01 mg/ml. ZM-Me reached 50% inhibition between 0.01 and 0.1 mg/ml, whereas CP-Me, GT-Me and SA-Me at a concentration between 0.1 and 1 mg/ml (Figure 23).

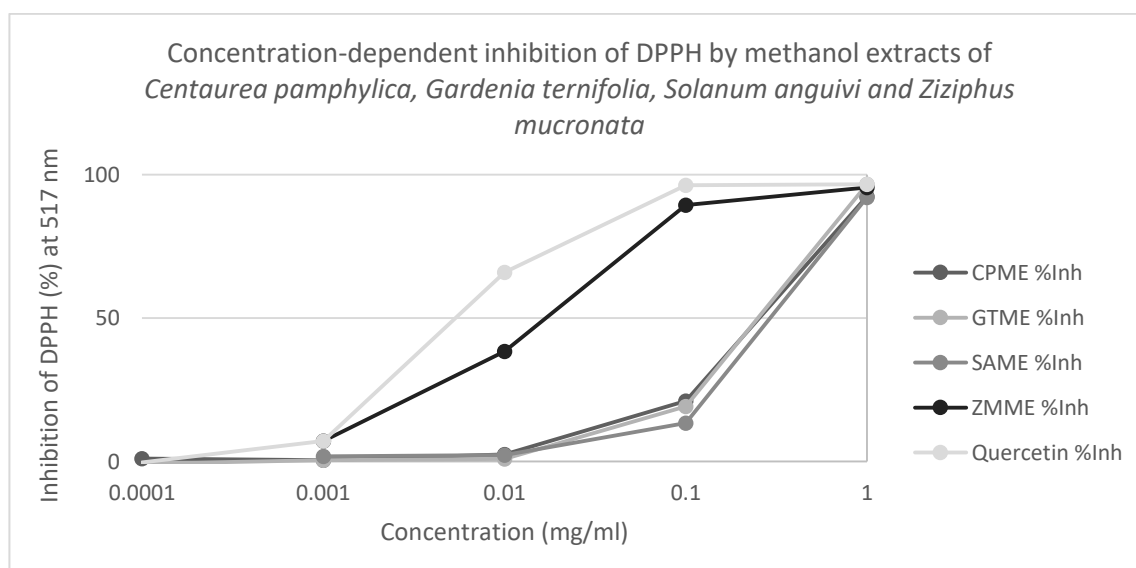


Figure 23 %Inhibition of DPPH by methanol extracts of CP, GT, SA, ZM and quercetin at 10-fold dilutions between 0.0001 and 1 mg/ml. Graph shows the average values of triplicate experiments.

In another assay (Figure 26), quercetin showed 50% inhibition of DPPH at a concentration between 0.001 and 0.01 mg/ml.

Figure 24 also shows that AL-Me exhibited a 50% inhibition at the lowest concentration, between 0.01 and 0.1 mg/ml, out of the methanol extracts tested. EA-Me, HO-Me and CD-Me caused a 50% inhibition of DPPH between the concentrations 0.1 and 1 mg/ml, representing the lowest IC_{50} , along with CP-Me, GT-Me and SA-Me.

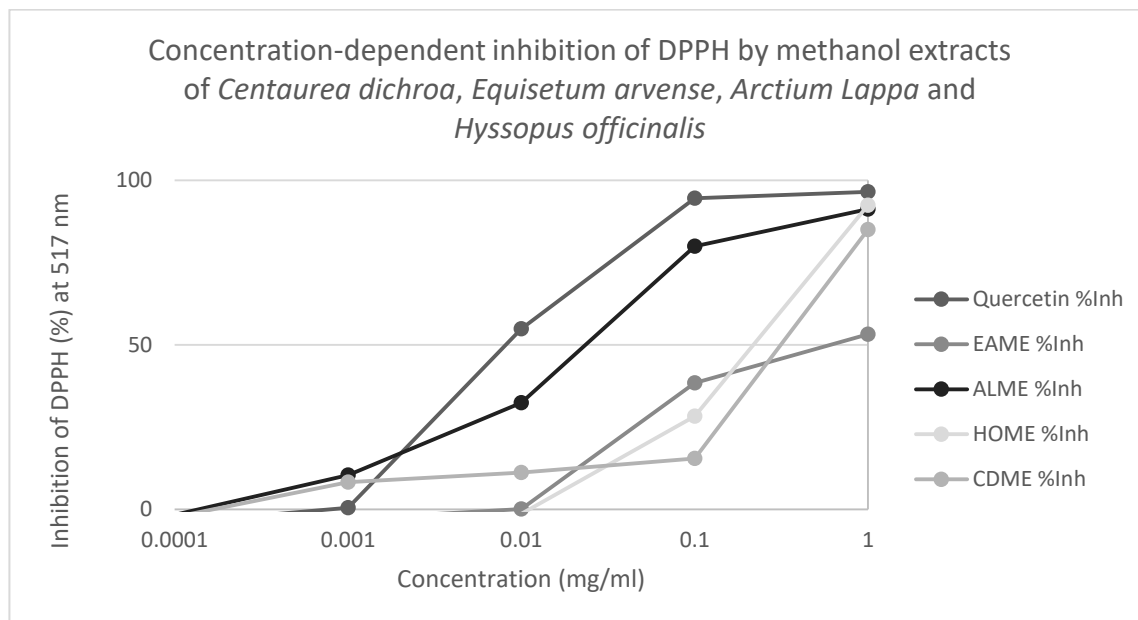


Figure 24 %Inhibition of DPPH by methanol extracts of *Equisetum arvense*, *Arctium Lappa*, *Hyssopus officinalis*, *Centaurea dichroa* and the positive control quercetin at concentrations between 0.0001 and 1 mg/ml. Graph shows the average values of triplicate experiments.

To increase the precision of the IC_{50} results, the DPPH assay was performed again for the samples that exceeded 50% inhibition at 1-fold dilutions in the range of concentrations identified previously.

Figure 25 shows the concentration-dependent inhibition of DPPH by quercetin at concentrations between 0.001 and 0.01 mg/ml, resulting in an IC_{50} of 0.002 mg/ml.

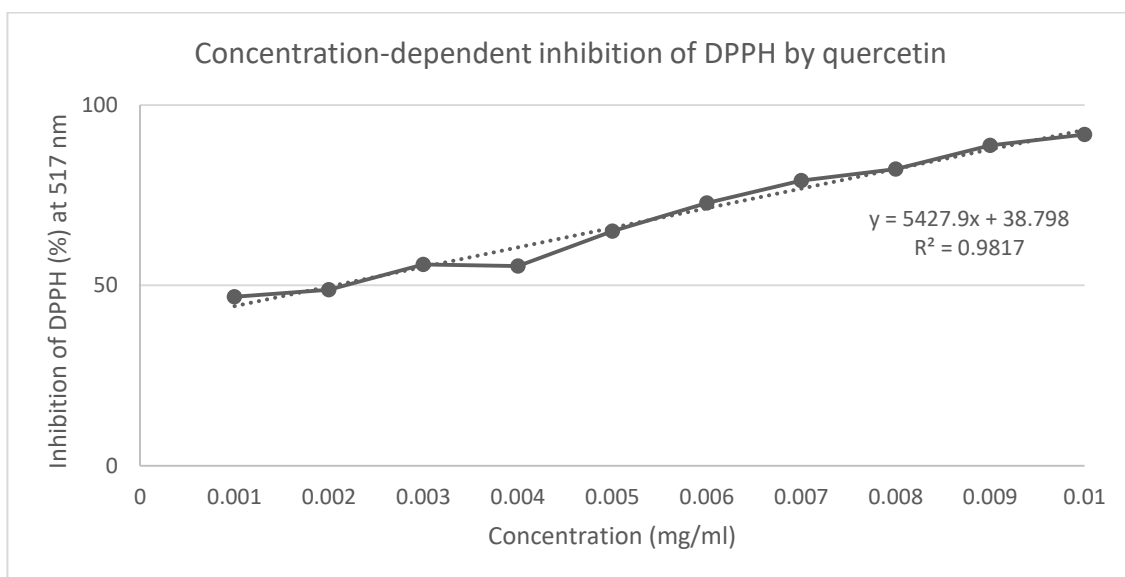


Figure 25 %Inhibition of DPPH by quercetin at 1-fold dilutions between 0.001 and 0.01 mg/ml. Graph shows the average values of duplicate experiments.

Similarly, Figure 26 shows the dose-dependant DPPH inhibition of CP-Me, GT-Me, SA-Me, EA-Me and HO-Me at concentrations between 0.1 and 1 mg/ml. The IC₅₀ values calculated are presented in Table 13.

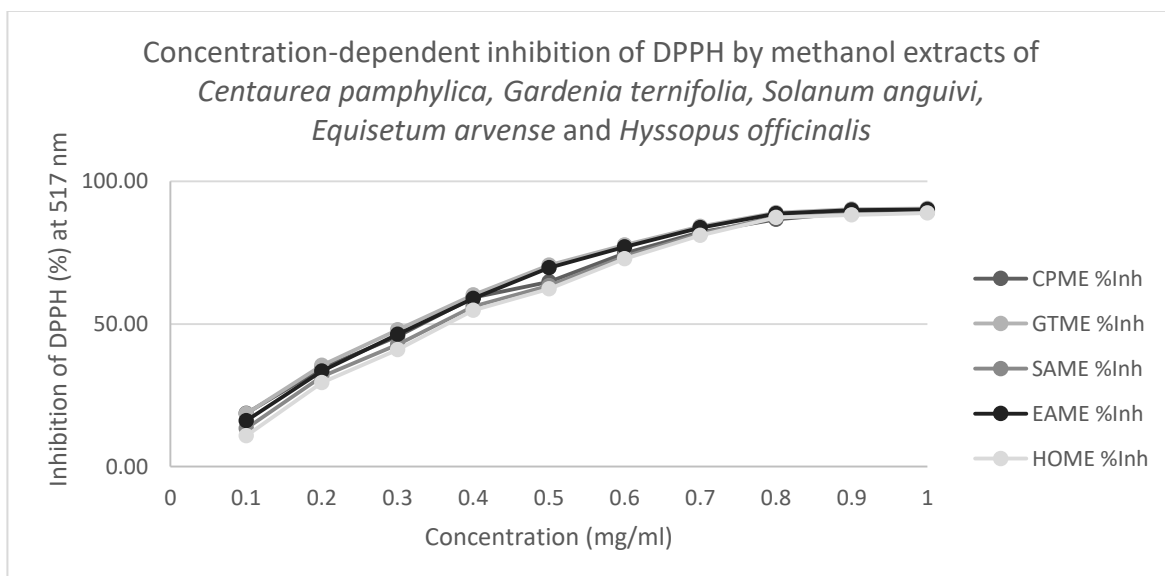


Figure 26 %Inhibition of DPPH by CP-ME, GTME, SAME, EAME and HOME at concentrations of 1-fold dilutions between 0.1 and 1 mg/ml. Graph shows the average values of duplicate experiments.

Furthermore, ZM-Me and AL-ME exhibited 50% DPPH inhibition at concentrations between 0.01 and 0.1 mg/ml and Figure 27 shows the concentration-inhibition curves. The IC₅₀ values calculated are presented in Table 15.

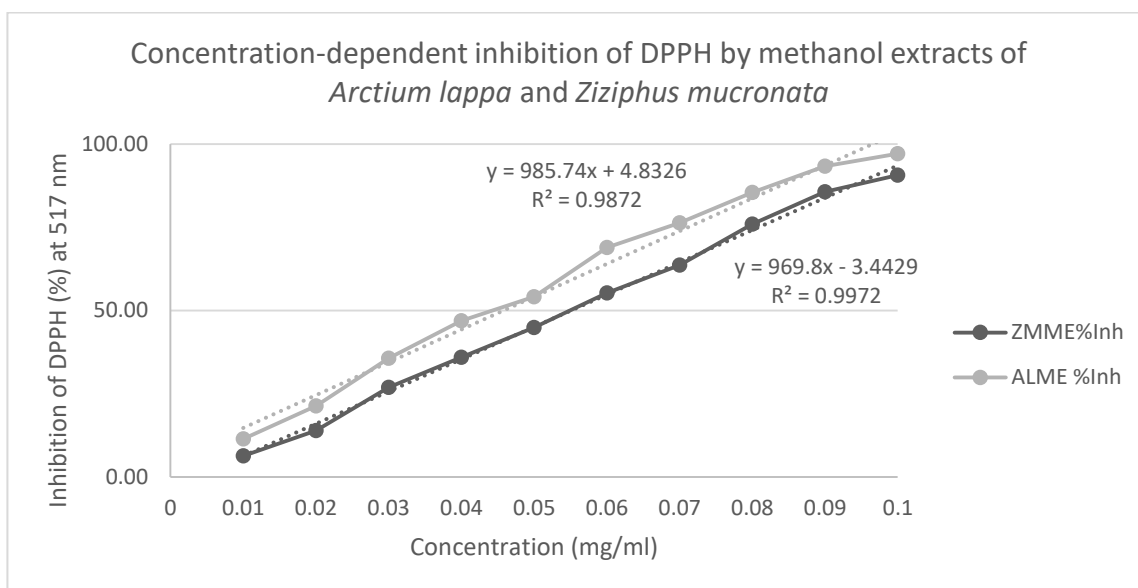


Figure 27 Graph showing the %inhibition of DPPH by ZM-Me and AL-Me at 1-fold dilutions between 0.01 and 0.1 mg/ml. Graph shows the average values of duplicate experiments

Using the line equations provided in MS Excel for each concentration curve, $y = ax + b$, the IC_{50} values of the positive control, as well as of the methanol extracts of AL, CP, GT, SA, EA, HO and ZM were calculated as:

$$IC_{50} (mg/ml) = \frac{50-b}{a}, \text{ and are shown in Table 15:}$$

Table 15 The DPPH IC_{50} values (mg/ml) of methanol extracts of *Arctium lappa*, *Ziziphus mucronata*, *Gardenia ternifolia*, *Equisetum arvense*, *Centaurea pamphylica*, *Solanum anguivi* and *Hyssopus officinalis*, and positive control quercetin

Positive control/Extract	IC_{50} (mg/ml)
quercetin	0.002
AL-Me	0.045
ZM-Me	0.055
GT-Me	0.344
EA-Me	0.362
CP-Me	0.366
SA-Me	0.398
HO-Me	0.415

According to the IC₅₀ values determined from the DPPH assay it was observed that the most bioactive methanol extracts with free-radical scavenging capability relative to the positive control quercetin were AL-Me and ZM-Me at 0.045 and 0.055 mg/ml concentrations, almost 25 times higher than the IC₅₀ value of quercetin.

The methanol extract of *Ziziphus mucronata*, which showed significant free-radical scavenging potential, second after that of *Arctium lappa* by 0.01 mg/ml, was also identified by Olajuyigbe and Afolayan (2011), who confirm that its bioactivity (IC₅₀ approx 0.04 mg/ml) is due to the phenolic compounds found in the bark of this plant.

3.2 Study 2: Cytotoxicity assay and luciferase reporter assay of methanol and *n*-hexane extracts of selected plants and precipitated compounds

The methanol and *n*-hexane extracts of the selected plants obtained from Soxhlet extraction were tested for cytotoxicity in AREc32 cells and the cell viability values for each concentration tested are shown in the sections below. After identifying a safe and non-cytotoxic concentration of the crude extracts, they were then applied at the respective doses to AREc32 cells for treatment; 24 h later the cells were subjected to a luciferase assay to assess the Nrf2-inducing capabilities of the crude extracts.

Another aim was to check if the free-radical scavenging capabilities showed by the methanol extracts of *Arctium lappa*, *Ziziphus mucronata* and *Gardenia ternifolia* in Study 1 would correlate with a potential Nrf2-inducing capacity.

3.2.1 Cytotoxicity (MTT assay) of tBHQ and luciferase activity induction in AREc32 cells

Firstly, the positive control tBHQ was screened for cytotoxicity in AREc32 cells at concentrations likely to be used for *in vitro* assays, between 10 µM and 100 µM (Zhang *et al.* 2005).

Figure 28 shows the cytotoxic profile of tBHQ in AREc32 cells, which lowered cell viability to 27.75% at the highest concentration applied of 100 µM. At 50 µM tBHQ the cell viability was kept at 78.04%, while treatment with 10 µM and 25 µM did not seem to disrupt the cell viability, as this was 101.81% and 99.95%.

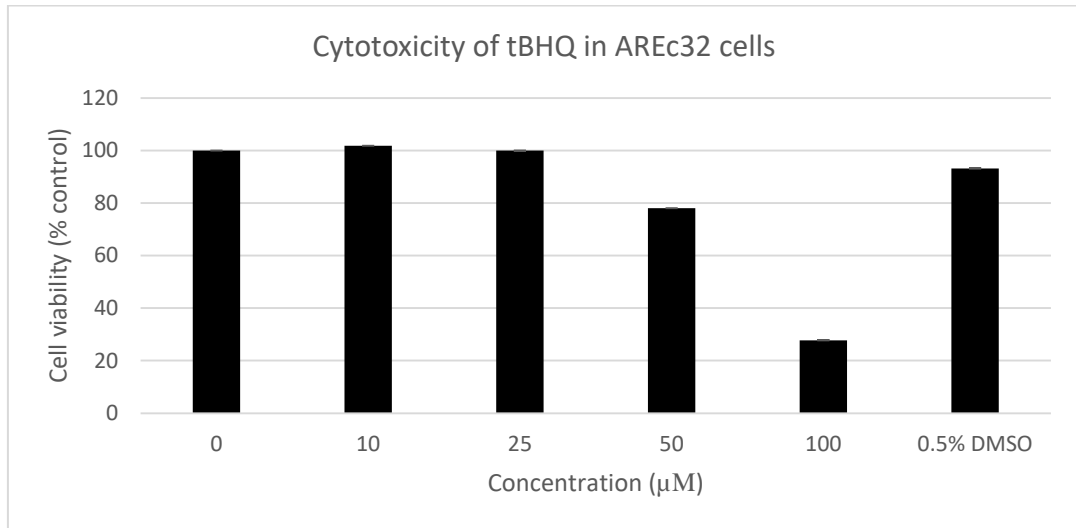


Figure 28 Cell viability as percentage to control (0 mg/ml) observed after treatment of AREc32 cells for 24 h with tBHQ (10-100 μM). DMSO represents the vehicle control and its concentration is expressed as v/v%. Results show the mean +/- SEM (n=12)

Therefore, both concentrations of 10 μM and 25 μM of tBHQ were chosen to be assayed for induction of luciferase activity linked to Nrf2/ARE activity, along with the 50 μM concentration which had been successfully used in other studies (Zhang *et al.* 2005).

Figure 27 below shows the results of the luciferase assay. The highest fold to control induction recorded for tBHQ was an average of 27.3-fold, at 50 μM concentration. In a dose-dependent manner, the 25 μM dose elicited an induction of luciferase activity of 11.39-fold to control, followed by the 10 μM dose with the lowest luciferase induction of 4.47-fold control.

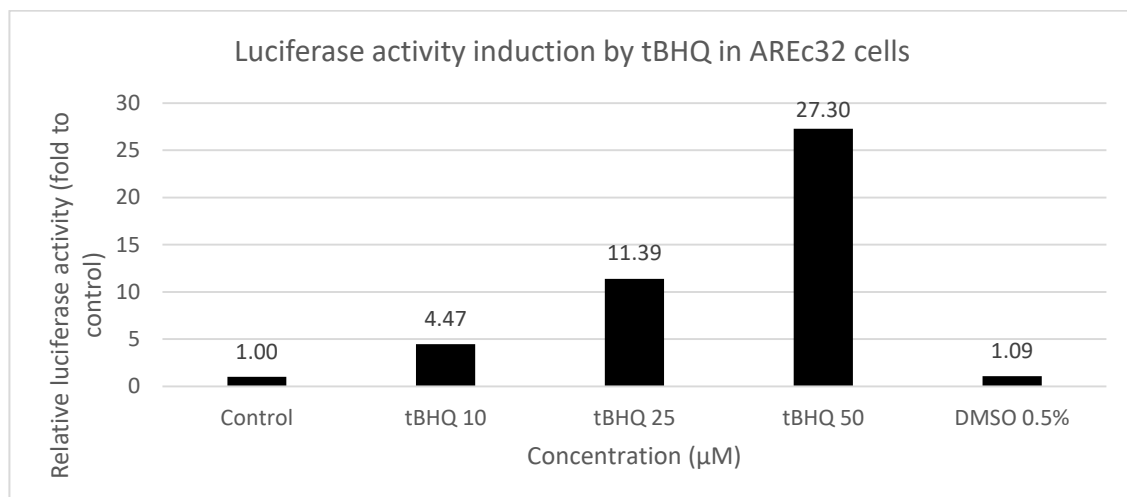


Figure 29 Effect of tBHQ on the induction of luciferase activity. AREc32 cells were incubated for 24 h with non-cytotoxic concentrations of tBHQ (10-50 μM). DMSO represents the vehicle control and its concentration is expressed as v/v%. Values show the average of n=3.

Reviewing the results of tBHQ in AREc32 assays, a scale for Nrf2 induction was set: an induction of less than 5-fold to control would be considered representative of a low cancer induction potential, an induction between 5 and 10-fold would be considered a medium potential, while an induction of over 10-fold would be considered high. Moreover, tBHQ at 10 μ M was used as positive control during all luciferase assays for characterisation of Nrf2/ARE activity induction.

3.2.2 Cytotoxicity (MTT assay) and Nrf2 induction results (luciferase assay) of crude methanol extracts

Crude methanol extracts of AL, CA, CD, CK, CP, EA, GP, GT, HO, KB, SA and ZM (see section 2.1.6 in Chapter 2 for naming convention) were tested using the MTT assay to identify a non-cytotoxic concentration suitable to be used in the luciferase assay. Figures 32 to 45 show the percentage viability of AREc32 cells treated with various concentrations of crude extracts, using DMSO as vehicle control.

AL-Me showed a low increase in cytotoxicity with a cell viability starting to decrease from 98.07% at the lowest concentration of 10 μ g/ml down to 61.11% μ g/ml at 1000 μ g/ml (Figure 30).

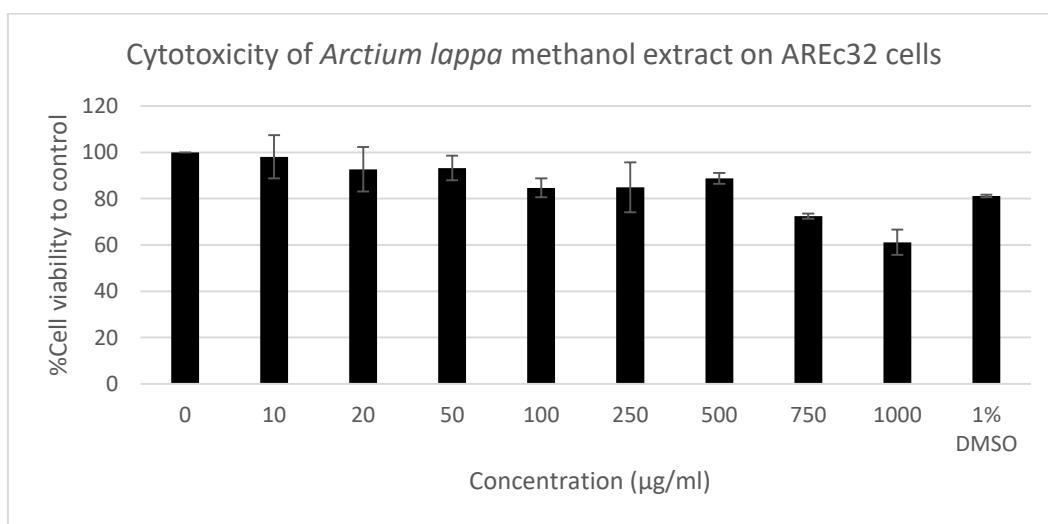


Figure 30 Cell viability as percentage to control (0 mg/ml) observed after treatment of AREc32 cells for 24 h with AL-Me (0.01-1 mg/ml). DMSO represents the vehicle control and its concentration is expressed as v/v%. Results show the mean \pm SEM (n=3, 3 replicates)

The first cell viability measurement in the range of concentrations tested that reached to over 90% in cell viability was recorded for the effect of the 50 μ g/ml dose, which was used for the subsequent luciferase assay.

Figure 31 shows that the methanol extract of *Centaurea asiatica* lowered the cell viability to 60.15% at the highest concentration of 1000 µg/ml. At the concentration of 50 µg/ml the cell viability was maintained at 94.32%, compared to 78.27% cell viability caused by the next highest concentration of 100 µg/ml and it was chosen for further luciferase assay.

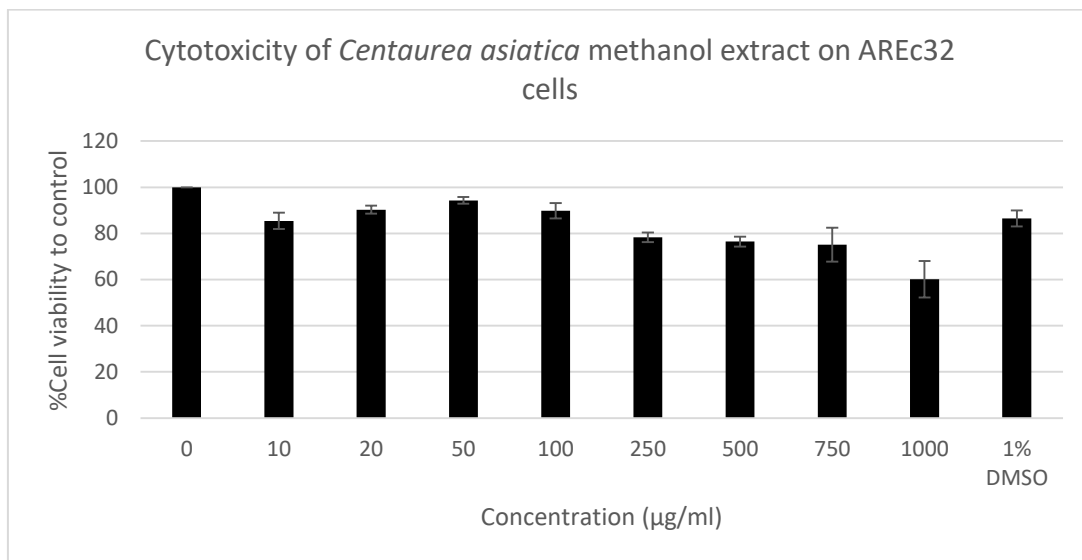


Figure 31 Cell viability as percentage to control (0 mg/ml) observed after treatment of AREc32 cells for 24 h with CA-Me (0.01-1 mg/ml). DMSO represents the vehicle control and its concentration is expressed as v/v%. Results show the mean +/- SEM (n=3, 3 replicates)

Centaurea dichroa caused a higher drop in cell viability of AREc32 cells after overnight treatment at concentrations between 10 and 1000 µg/ml (Figure 32). The cell viability dropped to as low as 29.01% to untreated control at the maximum concentration of 1000 µg/ml. Between 10 and 250 µg/ml the cell viability was maintained around 90%, so that 250 µg/ml was considered the most suitable concentration of CD-Me to be assayed for Nrf2/ARE induction.

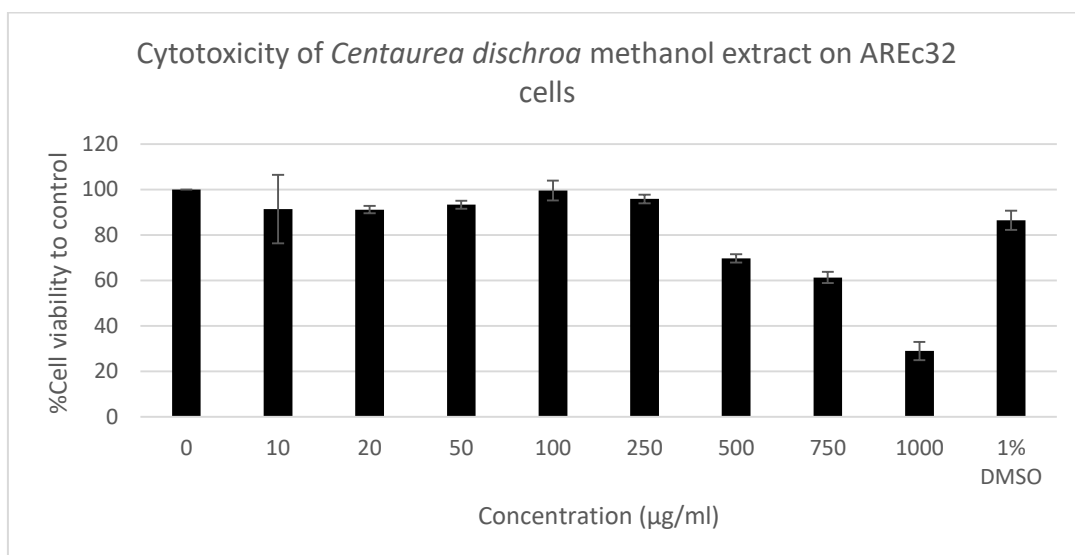


Figure 32 Cell viability as percentage to control (0 mg/ml) observed after treatment of AREc32 cells for 24 h with CD-Me (0.01-1 mg/ml). DMSO represents the vehicle control and its concentration is expressed as v/v%. Results show the mean +/- SEM (n=3, 3 replicates)

On the other hand, the cytotoxicity profile of the methanol extract of *Centaurea kirgidentis* show low effects on the AREc32 cell viability (Figure 33), with the highest concentration of 1000 µg/ml lowering the cell viability to 75.74%. Overall, the cell viability was maintained between 76.10% at 100 µg/ml and 91.84% at 10 µg/ml and the latter dose was used in the following luciferase assay.

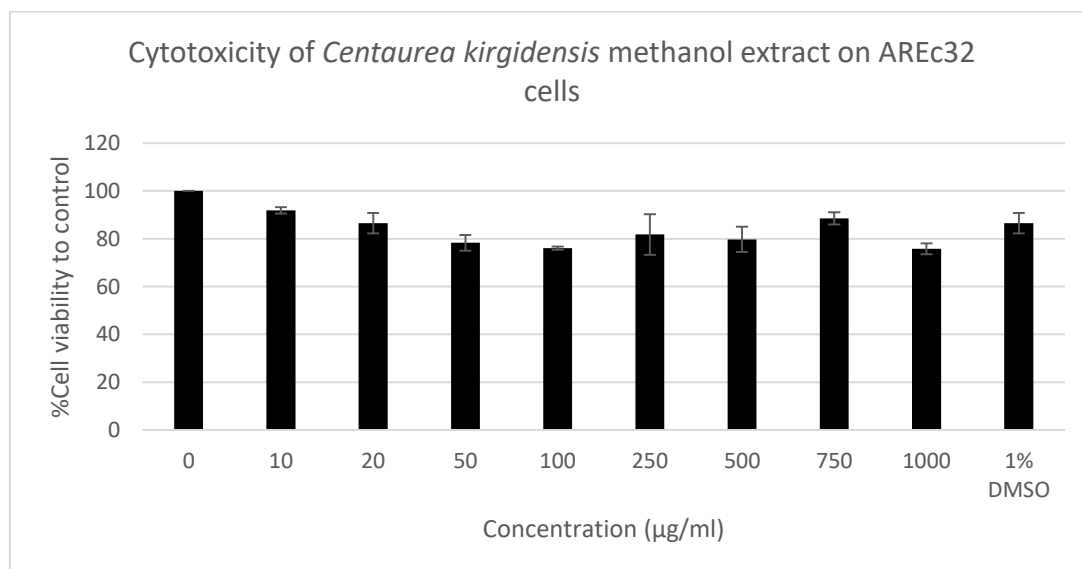


Figure 33 Cell viability as percentage to control (0 mg/ml) observed after treatment of AREc32 cells for 24 h with CK-Me (0.01-1 mg/ml). DMSO represents the vehicle control and its concentration is expressed as v/v%. Results show the mean +/- SEM (n=3, 3 replicates)

Between 25 µg/ml and 750 µg/ml, CP-Me (Figure 34) caused a decrease in cell viabilities, from 97.5% to 86.6%, but as the concentrations increased from 1 to 6 mg/ml, cell viability

values decreased consistently to under 47.3% and 0.1 mg/ml was considered the appropriate dose for the luciferase assay.

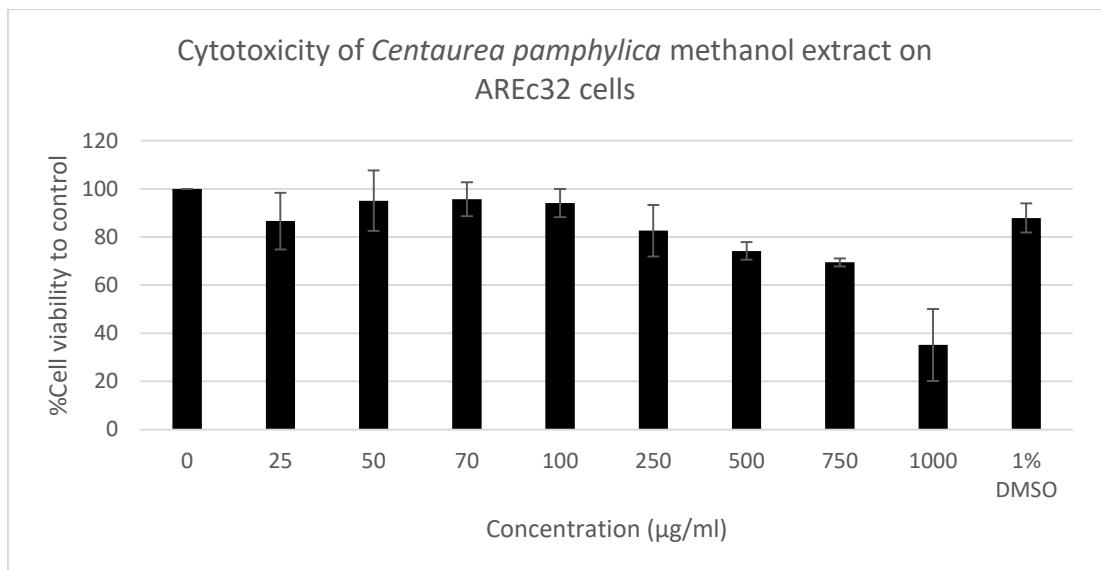


Figure 34 Cell viability percentage of control (0 mg/ml) observed after treatment of AREc32 cells for 24 h with CP-Me (0.025-1 mg/ml). DMSO represents the vehicle control and its concentration is expressed as v/v%. Results show the mean +/- SEM (n=3, 3 replicates)

Figure 35 below shows that the methanol extract of *Equisetum arvense* had a low cytotoxicity in AREc32 cells, varying between 99.51% at 10 µg/ml and 81.97% at the highest concentration of 1000 µg/ml. However, only at doses lower than 50 µg/ml could the cell viability be maintained at over 90%. Therefore the concentration of 50 µg/ml was considered the most appropriate for further testing in the luciferase assay.

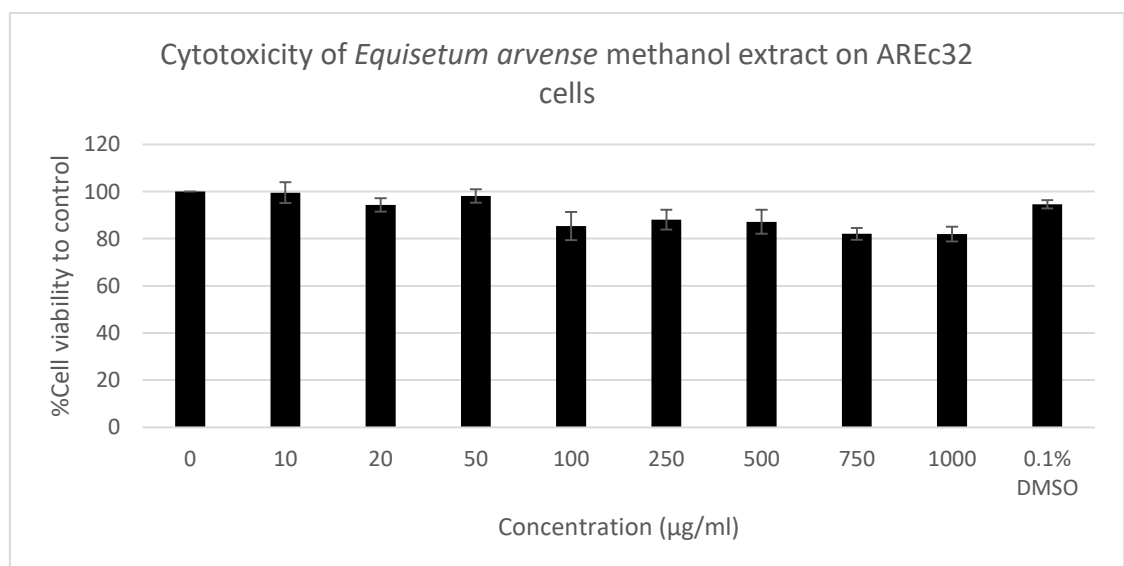


Figure 35 Cell viability percentage of control (0 mg/ml) observed after treatment of AREc32 cells for 24 h with EA-Me (0.01-1 mg/ml). DMSO represents the vehicle control and its concentration is expressed as v/v%. Results show the mean +/- SEM (n=3, 3 replicates)

Moreover, the treatment of AREc32 cells overnight with a range of concentrations of GP-Me (Figure 36), caused the cell viability to decrease steadily from 94.82% to 78.78% over the range of 25 µg/ml to 70 µg/ml. Between 100 µg/ml and 1000 µg/ml the cell viability was maintained between 84% and 89%, so that the most suitable dose was identified at 25 µg/ml, this being the only concentration that could ensure a cell viability of over 90%.

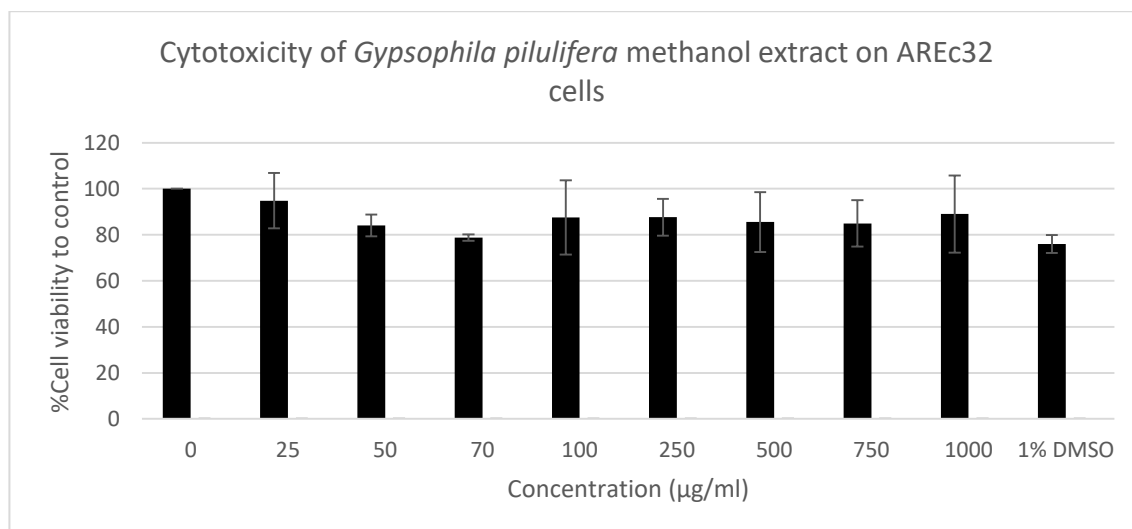


Figure 36 Cell viability percentage to control (0 mg/ml) observed after treatment of AREc32 cells for 24 h with GP-Me (0.025-1 mg/ml). DMSO represents the vehicle control and its concentration is expressed as v/v%. Results show the mean \pm SEM (n=3, 3 replicates)

Furthermore, AREc32 cells treated with the GT-Me extract at concentrations between 25 and 1000 µg/ml showed varying viabilities between 117.23% and 89.96%, as shown in Figure 37. Higher error bars were recorded for the effects of the concentrations in the mid-range, 70 to 750 µg/ml, as well as cell viabilities of over 100%. This could be down to variation in the sample preparation, including poor mixing of the plate during formazan dissolution in DMSO. It could also be noted that a high \pm SEM was also recorded for the cell viability% exerted by GT-Me at 1000 µg/ml. This could mean that at concentrations of over 100 µg/ml the phytochemical extract solubilises with more difficulty and creates highly variable results in the MTT assay, but also that the GT-Me extract might have a direct interaction with the MTT molecules, reducing it to excess formazan. Altogether, 25 µg/ml was considered a safe non-cytotoxic concentration of GT-Me that could be assayed for luciferase activity in AREc32 cells.

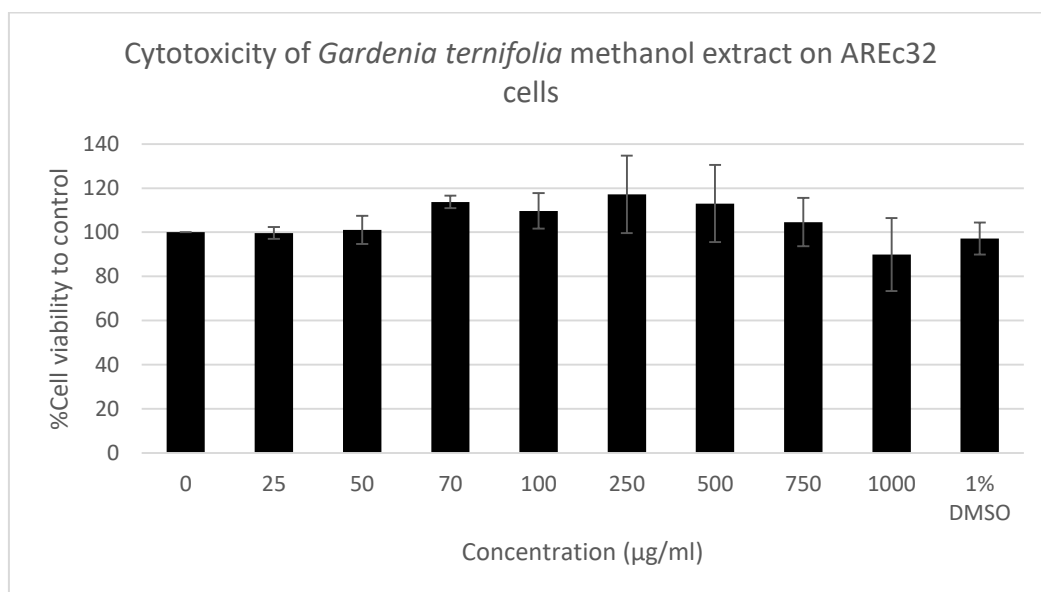


Figure 37 Cell viability percentage to control (0 mg/ml) observed after treatment of AREc32 cells for 24 h with GT-Me (0.025-1 mg/ml). DMSO represents the vehicle control and its concentration is expressed as v/v%. Results show the mean +/- SEM (n=3, 3 replicates)

The methanol extract HO-Me (Figure 38) exhibited a very high cytotoxicity at concentrations 750 µg/ml (27.48% cell viability) and 1000 µg/ml (7.88% cell viability), otherwise maintaining a steady decline from 99.52% at 10 µg/ml to 78.92% at 500 µg/ml. It was determined that the concentration of 100 µg/ml of HO-Me which caused a 97.84% viability of AREc32 cells would be appropriate for the luciferase assay, as the next highest concentration, 250 µg/ml, lowered the cell viability to 81.83%.

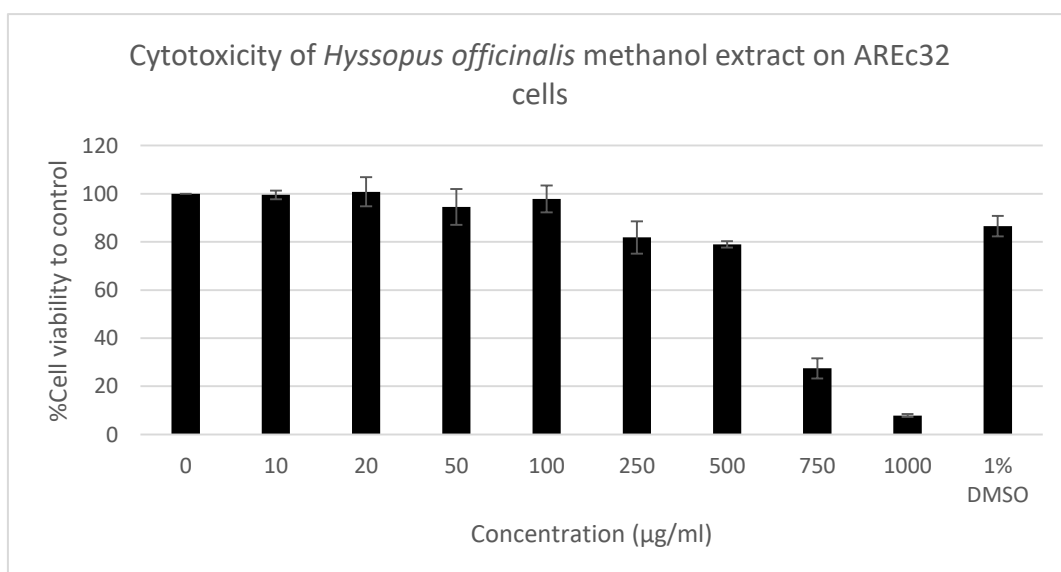


Figure 38 Cell viability percentage to control (0 mg/ml) observed after treatment of AREc32 cells for 24 h with HO-Me (0.01-1 mg/ml). DMSO represents the vehicle control and its concentration is expressed as v/v%. Results show the mean +/- SEM (n=3, 3 replicates)

Another methanol extract tested for cytotoxicity, KB-Me, (Figure 39) showed a very high cytotoxicity at concentrations between 500 µg/ml (1.60% cell viability) and 1000 µg/ml (3.76% cell viability). Overall, 10 µg/ml proved to be the highest dose that reached a cell viability of over 90%, namely 94.69% and was considered suitable for the luciferase assay in AREc32.

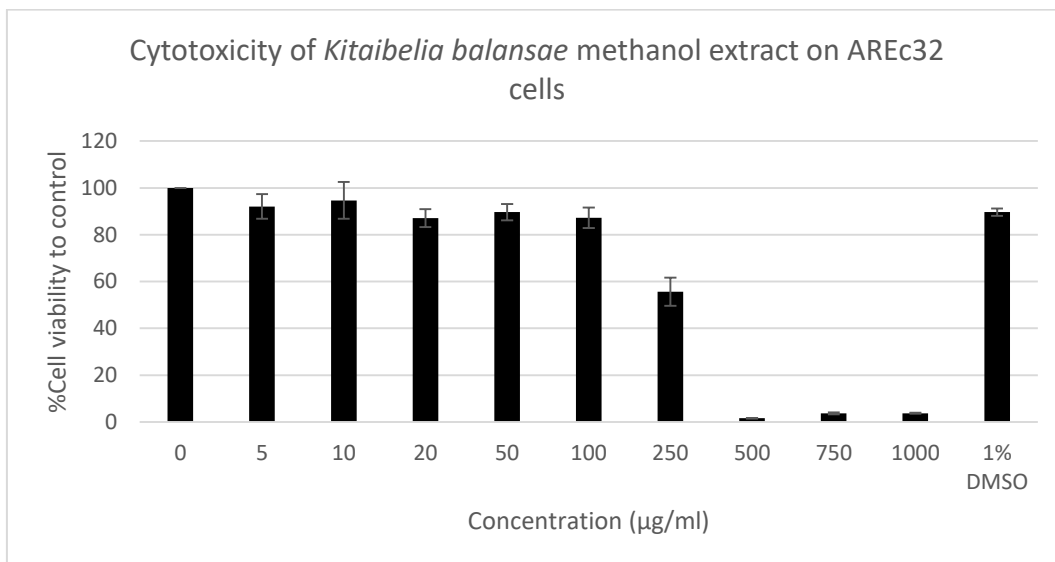


Figure 39 Cell viability percentage to control (0 mg/ml) observed after treatment of AREc32 cells for 24 h with KB-Me (0.005-1 mg/ml). DMSO represents the vehicle control and its concentration is expressed as v/v%. Results show the mean +/- SEM (n=3, 3 replicates)

The MTT assay for methanol extract of *Solanum anguivi*, SA-Me (Figure 40), showed a high decrease in cell viability from 105.90% at the lowest concentration of 5 µg/ml to 9.11% at 1000 µg/ml. The second lowest concentration of 10 µg/ml caused a cell viability of 84%, which was considered too low to be used in the luciferase assay, therefore the 5 µg/ml concentration was considered more suitable.

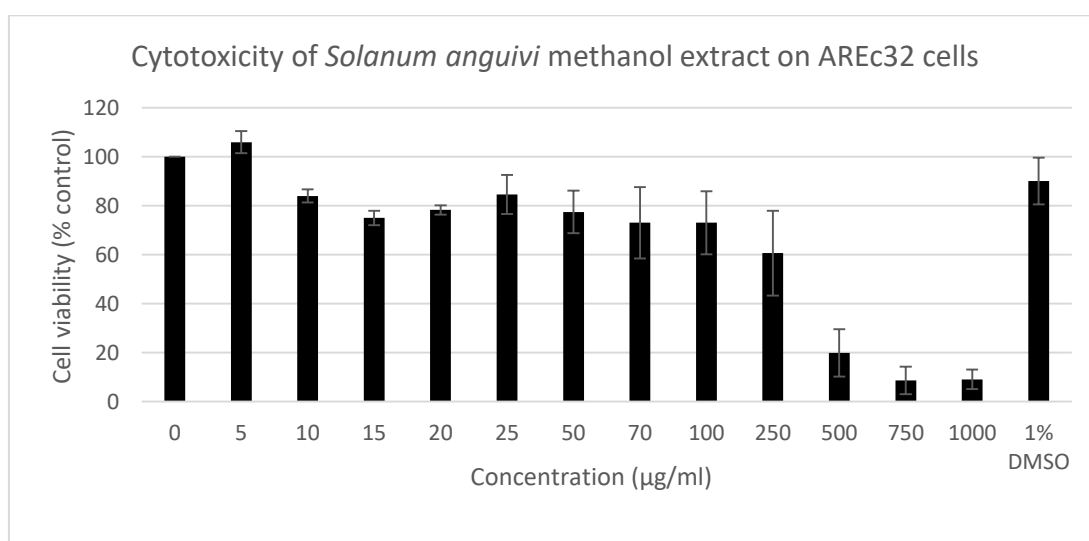


Figure 40 Cell viability as percentage to control (0 mg/ml) observed after treatment of AREc32 cells for 24 h with SA-Me (0.005-1 mg/ml). DMSO represents the vehicle control and its concentration is expressed as v/v%. Results show the mean +/- SEM (n=3, 3 replicates)

For the *Ziziphus mucronata* methanol extract, ZM-Me, (Figure 41), cell viabilities varied between 120.43% and 99.09% at concentrations between 25 µg/ml and 1000 µg/ml with relatively high \pm SEM throughout.

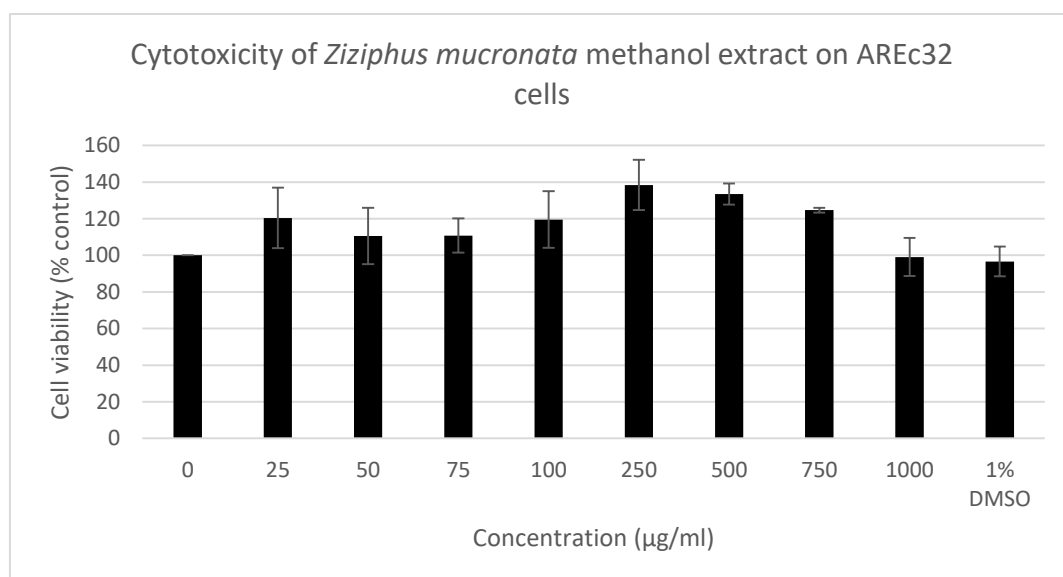


Figure 41 Cell viability as percentage to control (0 mg/ml) observed after treatment of AREc32 cells for 24 h with ZA-Me (0.025-1 mg/ml). DMSO represents the vehicle control and its concentration is expressed as v/v%. Results show the mean \pm SEM (n=3, 3 replicates)

During the cell viability assay of ZM-Me, a visual observation was made soon after adding MTT solution to the vehicle in the wells: the vehicle would exhibit a dose-dependent purple colour similar to that of solubilised formazan so that with increased extract concentration applied, the more intensely the colour would be observed. This observation was inconsistent with the fact that a higher concentration normally causes a low cell viability, hence a lighter colourisation. Compared to the development of other plates, this was the only case of vehicle colourisation, which meant that the cell culture wells should be washed at least two times with PBS before replacing the culture medium and adding the MTT solution, as phytochemicals could react with the tetrazolium salt in the well, reducing it. This possibility has in fact been reported by Bruggisser *et al.* (2001).

Thus, to confirm that the methanol extract of ZM-Me reduced the MTT by direct interaction in the cell culture medium, the hypothesis was tested by tailoring a mock-cell viability assay where no cells would be seeded. Figure 42 shows that the hypothesis proved to be true, as the extract reduced the MTT in a dose-dependent manner in the absence of cells.

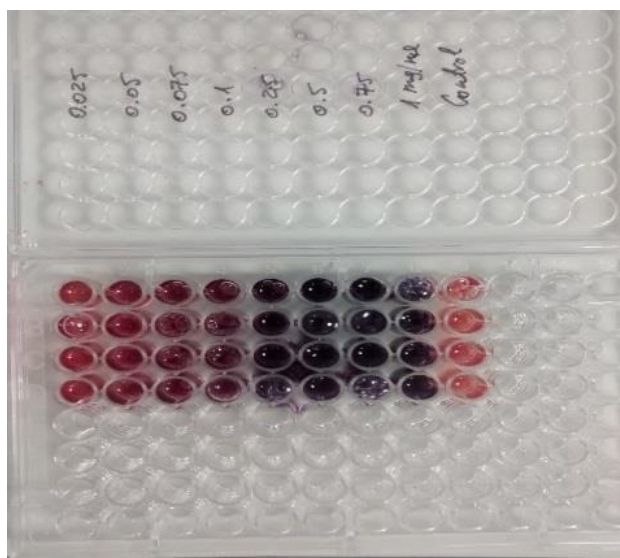


Figure 42 Simulation of MTT assay on ZMME extract (0.025-1 mg/ml) without seeded cells. The methanol extract reacts with the MTT in the culture medium in a concentration-dependent manner.

Finally, a new MTT assay was performed where the culture medium was removed from the wells prior to a washing step with PBS and adding fresh medium containing MTT. Figure 43 below shows the results of the second MTT assay where the results were consistent with expectations; the cytotoxicity was markedly increased throughout the range of concentrations used for treatment of AREc32 cells. Moreover, the cytotoxicity exhibited at the highest concentration of 1000 $\mu\text{g/ml}$ dropped 72.2% down to 26.88%, whereas at the lowest concentrations of ZM-Me, 25 and 30 $\mu\text{g/ml}$, the cell viability was maintained at over 100%, decreasing to 91.57% at 40 $\mu\text{g/ml}$ and under 77.28% from 50 $\mu\text{g/ml}$ to 1000 $\mu\text{g/ml}$.

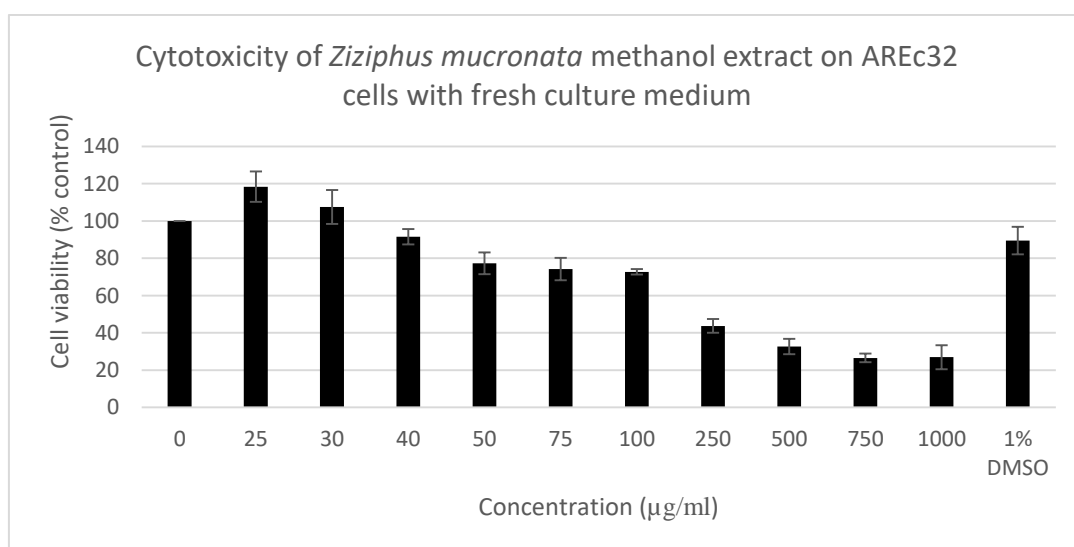


Figure 43 Cell viability percentage to control (0 mg/ml) observed after treatment of AREc32 cells for 24 h with ZM-Me (0.025-1 mg/ml). DMSO represents the vehicle control and its concentration is expressed as v/v%. Results show the mean \pm SEM (n=3, 3 replicates).

Therefore, the most appropriate concentration of ZM-Me to be used in the luciferase assay for Nrf2 induction screening was 40 µg/ml.

3.2.3 Results of luciferase assays of crude methanol extracts in AREc32 cells

Following the MTT assays, the methanol extracts were tested in the luciferase assay for assessing their Nrf2 induction capabilities.

As Figure 44 shows, four methanol extracts distinguish themselves out of twelve methanol extracts tested, with the positive control tBHQ (10 µM) showing 5.6-fold to control induction.

The methanol extract of *Centaurea dichroa*, CD-Me (250 µg/ml), exhibited the highest luciferase induction with 22.8-fold to control, followed by the methanol extract of *Centaurea pamphylica*, CP-Me (100 µg/ml), with 11.2-fold to control induction.

The methanol extract of *Gardenia ternifolia*, GT-Me (750 µg/ml), showed medium cancer chemopreventive potential and it was the third most bioactive methanol extract, with a 8.9-fold to control induction of luciferase activity, followed by the methanol extract of *Ziziphus mucronata*, ZM-Me (40 µg/ml), which reached a fold induction of 3.7, lower than that of the positive control tBHQ.

CA-Me and CK-Me showed similar luciferase activity, 2.2-fold to control, although CA-Me was applied at a higher concentration than CK-Me (50 vs 10 µl).

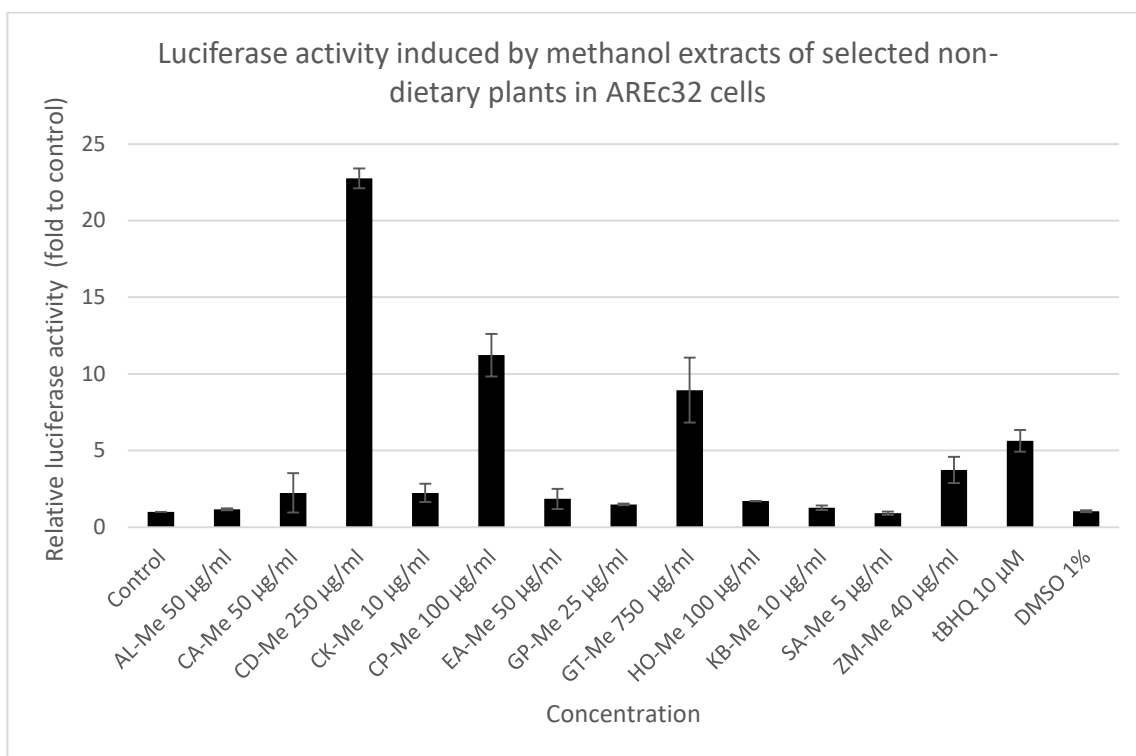


Figure 44 Effect of methanol extracts on the induction of luciferase activity and tBHQ as positive control. AREc32 cells were incubated for 24 h with non-cytotoxic concentrations of methanol extracts of AL, CA, CD, CK, CP, EA, GP, GT, HO, KB, SA and ZM. DMSO represents the vehicle control and its concentration is expressed as v/v%. Values show mean \pm SEM (n=3, 3 replicates), control=1.

The methanol extracts that showed the lowest cancer chemopreventive potential (less than 5-fold induction to control, arbitrarily set at 1) were: EA-Me (1.85-fold), HO-Me (1.7-fold), GP-Me (1.48-fold), AL-Me (1.17-fold), KB-Me (1.27-fold) and SA-Me (0.92-fold).

An inverse correlation was observed between the free-radical scavenging properties of the methanol extracts and their cancer chemopreventive potential. So that CD-Me, CP-Me and GT-Me showed the lowest DPPH %inhibition, with IC_{50} values between 0.1 and 1 mg/ml, while increasing luciferase activity over 10-fold in AREc32 cells at concentrations in the same range.

For ZM-Me the same trend was observed; while it showed high free-radical scavenging compared to other extracts (second to AL-Me), it increased luciferase activity less than the positive control tBHQ (5.6-fold). ZM-Me had an IC_{50} of 0.055 mg/ml in the DPPH assay, while the concentration used in the luciferase assay was 0.04 g/ml.

DMSO used at 1% v/v in the well to help dissolution of phytochemicals showed an effect on cell viability after 24 h of treatment, as the cell viability decreased to 75% in the case of the *Gypsophila pilulifera* methanol extract. However, DMSO did not show any effect on the luciferase activity in AREc32 cells, measuring a 1-fold to control induction, which can indicate the possibility that a higher dose of GP-Me could have exerted a higher effect on

the luciferase activity. In the context of low bioavailability of dietary phytochemicals, the concentrations used for *in vitro* assays should also be of the lowest achievable concentration that can exert a quantifiable effect.

3.2.3 Cytotoxicity (MTT assay) and Nrf2 induction (luciferase assay) of crude *n*-hexane extracts

All *n*-hexane extracts were assessed for cytotoxicity using the MTT assay, at concentrations between 5 and 1000 µg/ml, before screening them for luciferase activity induction, an indicator for activation of the Nrf2/ARE signaling pathway that upregulates the expression of cytoprotective genes and enzymes to protect against reactive species (Kumar *et al.* 2014)

The *n*-hexane extract of *Arctium lappa* proved highly cytotoxic from 100 µg/ml upwards to 1000 µg/ml with decreasing cell viabilities from 59.67% to 1.52% respectively (Figure 45). Between 5 and 50 µg/ml the cell viability was maintained at over 78% at 50 µg/ml up to 90.01% at 5 µg/ml, the latter being the safest concentration of AL-Me tested in AREc32 cells.

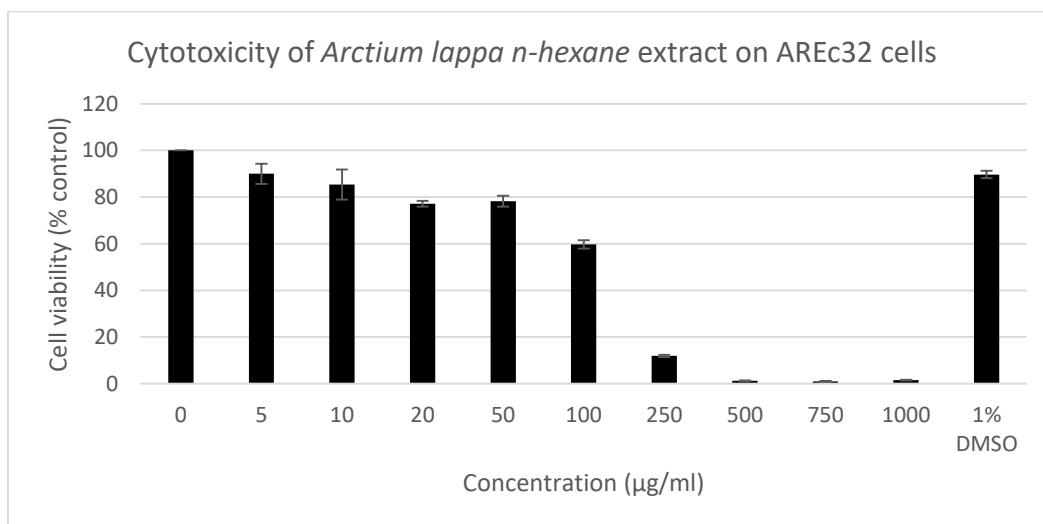


Figure 45 Cell viability as percentage to control (0 µg/ml) observed after treatment of AREc32 cells for 24 h with AL-He (5-1000 µg/ml). DMSO represents the vehicle control and its concentration is expressed as v/v%. Results show the mean +/- SEM (n=3, 3 replicates)

Another *n*-hexane extract tested for cytotoxicity in AREc32 cells was that of *Centaurea asiatica* (Figure 46), which dropped slowly from 101.96% at 10 µg/ml to 88.25% at 750 µg/ml. At the highest concentration of 1000 µg/ml CA-Me caused a cell viability of 37.41%. Overall, the most suitable concentration for the luciferase assay was considered to be 250 µg/ml, which maintained a cell viability of over 90%, at 95.47%.

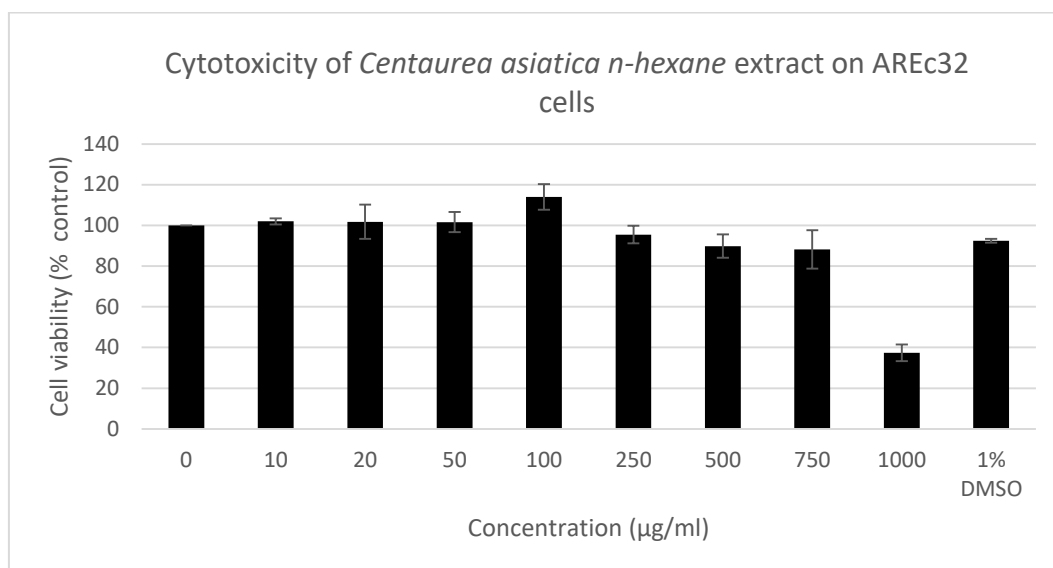


Figure 46 Cell viability as percentage to control (0 µg/ml) observed after treatment of AREc32 cells for 24 h with CA-He (10-1000 µg/ml). DMSO represents the vehicle control and its concentration is expressed as v/v%. Results show the mean +/- SEM (n=3, 3 replicates)

Figure 47 shows the cytotoxicity profile of the *n*-hexane extract of *Centaurea kirdigensis* which recorded a minimum cell viability of 55.35% at the highest concentration of 1000 µg/ml. However, at 50 µg/ml CK-He maintained a cell viability of 99.99%, making it the most suitable candidate dose for the luciferase assay.

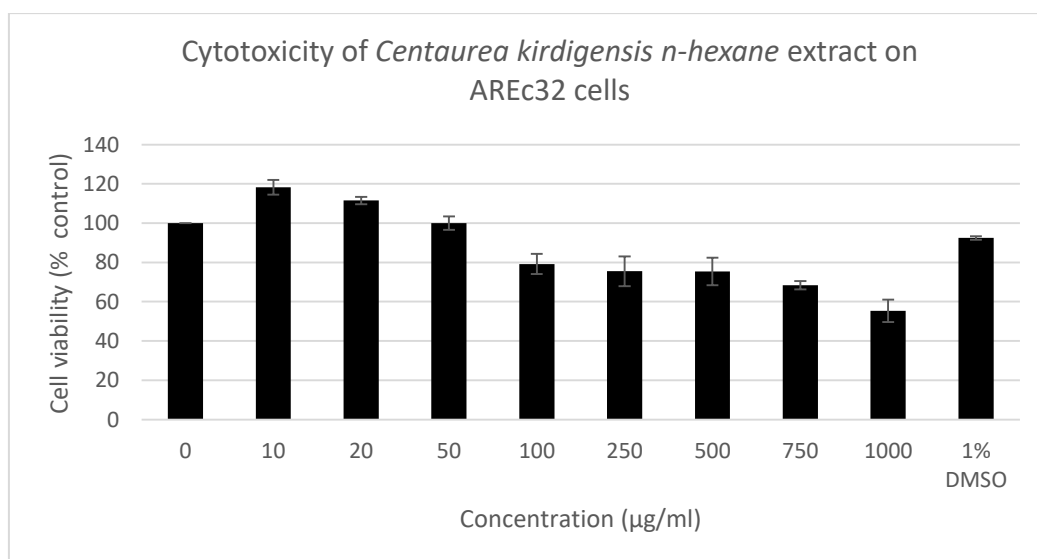


Figure 47 Cell viability as percentage to control (0 µg/ml) observed after treatment of AREc32 cells for 24 h with CK-He (10-1000 µg/ml). DMSO represents the vehicle control and its concentration is expressed as v/v%. Results show the mean +/- SEM (n=3, 3 replicates)

The *n*-hexane extract of *Centaurea pamphylica*, CP-He, maintained a steady decrease in cell viability from 106.22% at 5 µg/ml to 79.44% at 250 µg/ml (Figure 48). A sharp decrease then followed from 79.44% to 26.04% cell viability at 500 µg/ml CP-He, going as low as 2.8%

at the highest concentration of 1000 µg/ml. Ultimately, CP-He was tested for luciferase activity at 20 µg/ml (93.06% cell viability).

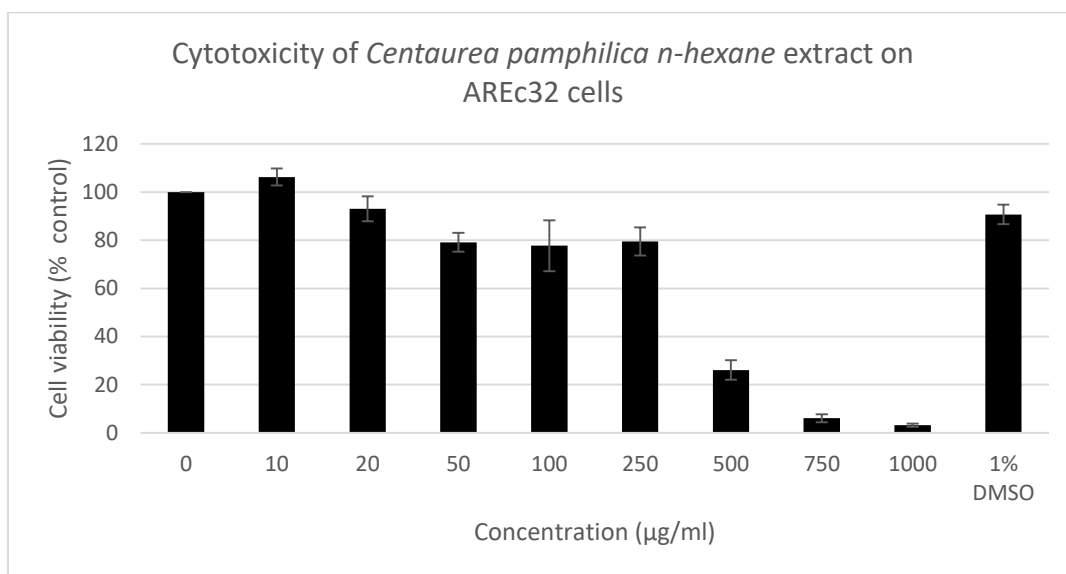


Figure 48 Cell viability percentage to control (0 µg/ml) observed after treatment of AREc32 cells for 24 h with CP-He (10 - 1000 µg/ml). DMSO represents the vehicle control and its concentration is expressed as v/v%. Results show the mean +/- SEM (n=3, 3 replicates)

Equisetum arvense recorded a decrease in cell viability from 104.94% at the lowest concentration of 5 µg/ml to 21.61% cell viability at the highest concentration of 1000 µg/ml (Figure 49). The steepest decrease in cell viability was noted between the concentrations 500 µg/ml and 750 µg/ml, of 32%.

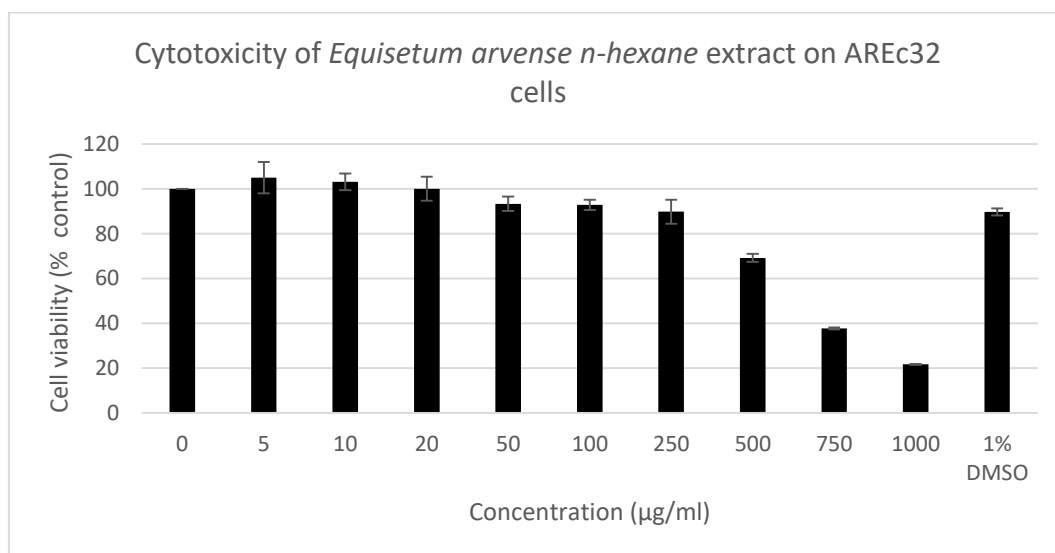


Figure 49 Cell viability percentage to control (0 µg/ml) observed after treatment of AREc32 cells for 24 h with EA-He (5-1000 µg/ml). DMSO represents the vehicle control and its concentration is expressed as v/v%. Results show the mean +/- SEM (n=3, 3 replicates)

At 250 µg/ml dose of EA-He the cell viability was slightly below 90%, at 89.75 µg/ml, so that the next lower concentration of 100 µg/ml maintained a cell viability of 92.83% and it was most suitable for use in the AREc32 luciferase assay.

Furthermore, Figure 50 shows that GP-He, the *n*-hexane extract of *Gypsophila pilulifera* maintained a high cell viability between 10 µg/ml and 100 µg/ml, of around 100%, with 96.20% at 100 µg/ml. From 250 µg/ml to 1000 µg/ml the cell viability of AREc32 cells was strongly affected by GP-Me, decreasing from 38.70% to 3.69% cell viability. Thus, the 100 µg/ml concentration was chosen for the luciferase assay (96.20%).

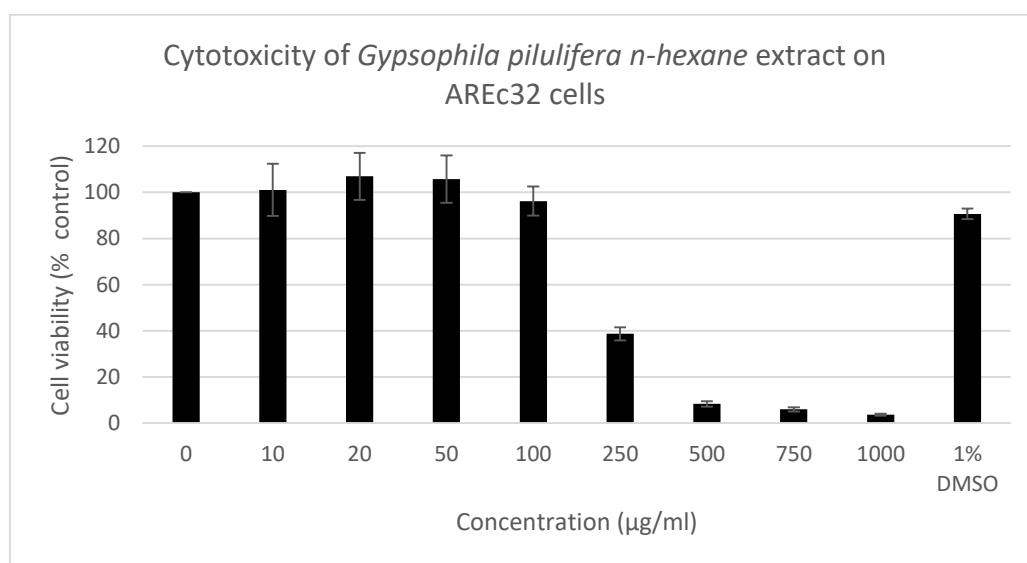


Figure 50 Cell viability percentage to control (0 µg/ml) observed after treatment of AREc32 cells for 24 h with GP-He (10-1000 µg/ml). DMSO represents the vehicle control and its concentration is expressed as v/v%. Results show the mean +/- SEM (n=3, 3 replicates).

The *n*-hexane extract of *Gardenia ternifolia*, GT-He, caused a steady decrease in cell viability (Figure 51), from 94.54% to 84.82% between the lowest concentration of 5 µg/ml going up 50 µg/ml. A steep decrease to 38.32% at 100 µg/ml followed, after which the cytotoxicity became more pronounced, causing a cell viability of 10.94% at the highest concentration of 1000 µg/ml. Thus the concentration suitable for the luciferase assay was 10 µg/ml (99.79%).

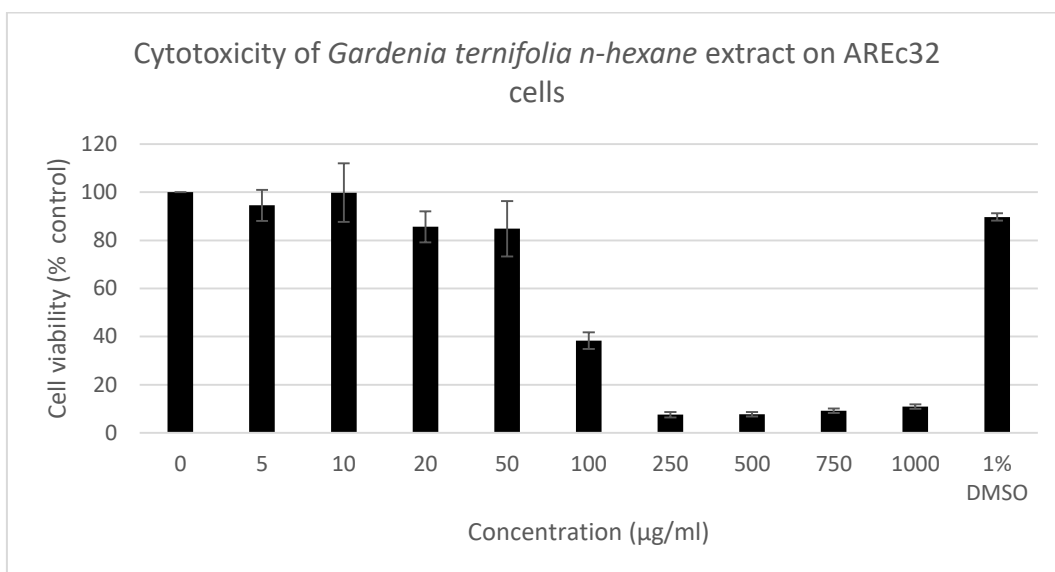


Figure 51 Cell viability percentage to control (0 µg/ml) observed after treatment of AREc32 cells for 24 h with GT-He (5-1000 µg/ml). DMSO represents the vehicle control and its concentration is expressed as v/v%. Results show the mean +/- SEM (n=3, 3 replicates).

HO-He, the *n*-hexane extract of *Hyssopus officinalis*, also showed a steady cell viability from the starting dose of 5 µg/ml to 100 µg/ml, between 92.98% and 93.95%, respectively. Marked cytotoxicity was noted between the doses of 250 µg/ml and 1000 µg/ml, where the cell viability dropped further from 63.30% to 4.50%. Therefore, the non-cytotoxic concentration of 100 µg/ml was used in the subsequent luciferase assay (Figure 52).

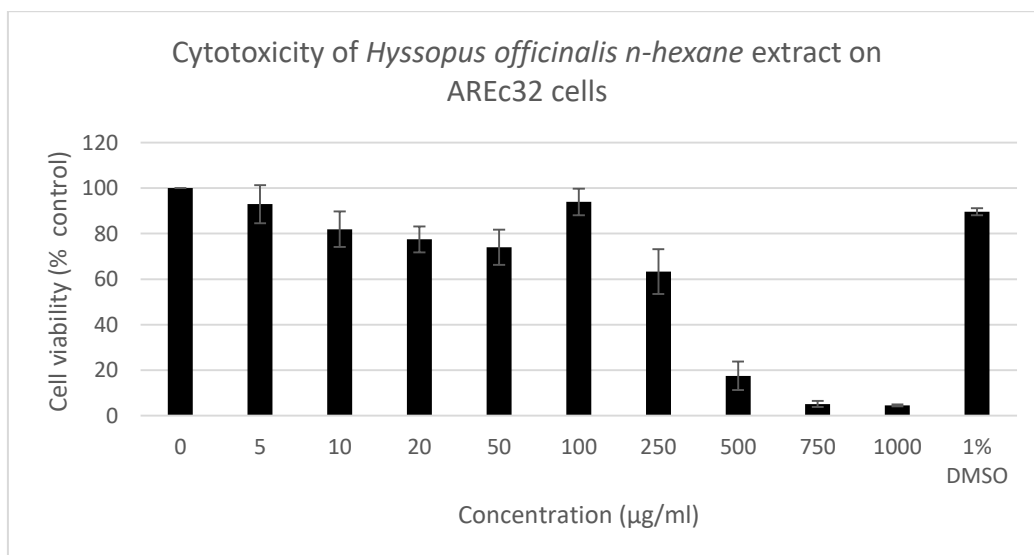


Figure 52 Cell viability percentage to control (0 µg/ml) observed after treatment of AREc32 cells for 24 h with HO-He (5-1000 µg/ml). DMSO represents the vehicle control and its concentration is expressed as v/v%. Results show the mean +/- SEM (n=3, 3 replicates)

As it can be observed in Figure 53 below, the *n*-hexane extract of *Kitaibelia balansae* showed significant cytotoxic properties against AREc32 cells at doses between 250 µg/ml and 1000 µg/ml, as the cell viability was measured at maximum 2.88% and 1.50%

respectively. However, only at 5 and 10 µg/ml was the cell viability over 90%, with 94.23% cell viability noted at 10 µg/ml, which was the chosen concentration for the luciferase assay.

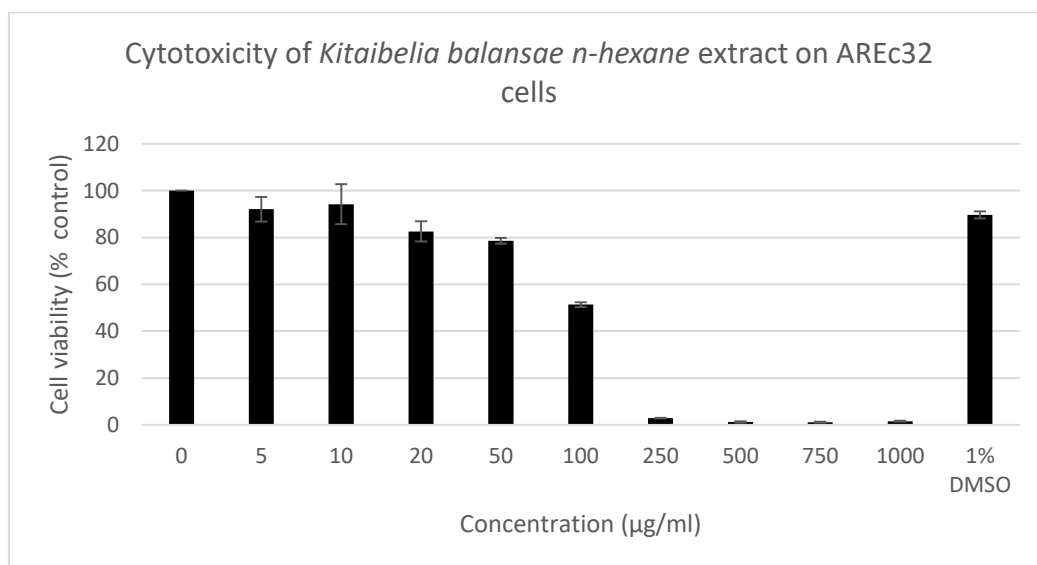


Figure 53 Cell viability percentage to control (0 µg/ml) observed after treatment of AREc32 cells for 24 h with HO-He (5-1000 µg/ml). DMSO represents the vehicle control and its concentration is expressed as v/v%. Results show the mean +/- SEM (n=3, 3 replicates)

Figure 54 below shows the cytotoxicity produced by SA-He, the *n*-hexane extract of *Solanum anguivi*, in AREc32 cells. SA-He caused cell viabilities between 121.76% and 97.80% at concentrations between 5 µg/ml and 100 µg/ml. A sudden drop in cell viability from 109.45% (100 µg/ml) to 53.95% cell viability (250 µg/ml) was then noted, followed by markedly high cytotoxicity, driving the cell viability to less than 9.86% at concentrations between 500 and 1000 µg/ml. Overall, the safest concentration of SA-He to be used in the luciferase assay was 100 µg/ml.

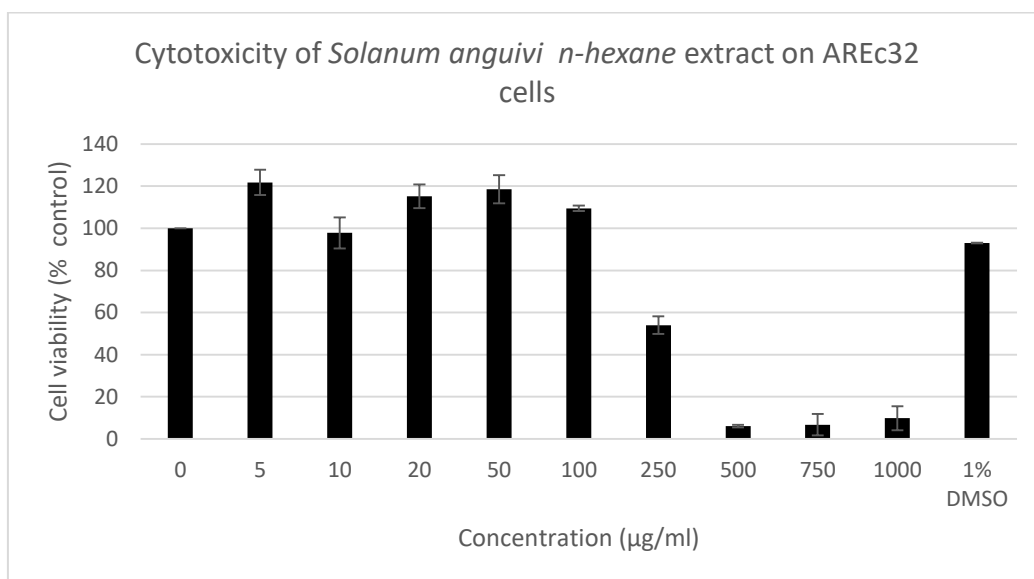


Figure 54 Cell viability percentage of control (0 µg/ml) observed after treatment of AREc32 cells for 24 h with SA-He (5-1000 µg/ml). DMSO represents the vehicle control and its concentration is expressed as v/v%. Results show the mean +/- SEM (n=3, 3 replicates).

Finally, the *n*-hexane extract of *Ziziphus mucronata*, ZM-He, showed a steady decrease in cell viability (Figure 55), from 103.61% to 36.05%, as concentrations decreasing from 5 to 1000 µg/ml. The non-cytotoxic concentration of ZM-He chosen for the subsequent luciferase assay was 100 µg/ml, which caused a viability of 94.05%, before decreasing to 81.60% at 250 µg/ml.

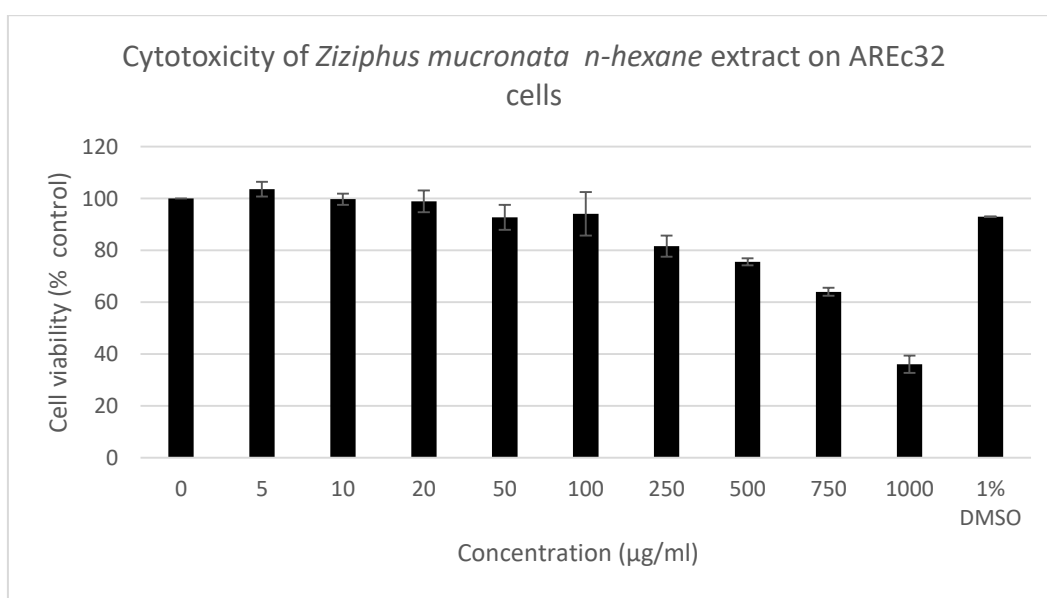


Figure 55 Cell viability percentage of control (0 µg/ml) observed after treatment of AREc32 cells for 24 h with ZM-He (5-1000 µg/ml). DMSO represents the vehicle control and its concentration is expressed as v/v%. Results show the mean +/- SEM (n=3, 3 replicates).

Lastly, the final *n*-hexane extract tested for cytotoxicity in AREc32 cells was CD-He, the *n*-hexane extract of *Centaurea dichroa*. Having observed from previous MTT assays that the

n-hexane extracts would exert high cytotoxicity at concentrations higher than 500 µg/ml, the range of concentrations was lowered to 1 – 500 µg/ml.

Figure 56 below shows that CD-He affected the cell viability of AREc32 to 90.08% at the lowest concentration of 1 µg/ml, before decreasing it to 56.01% at the highest concentration of 500 µg/ml. Because the second lowest concentration of CD-He, 5 µg/ml, also maintained a cell viability of over 90% (90.78% cell viability), this was eventually considered the most suitable concentration for further luciferase assay tests.

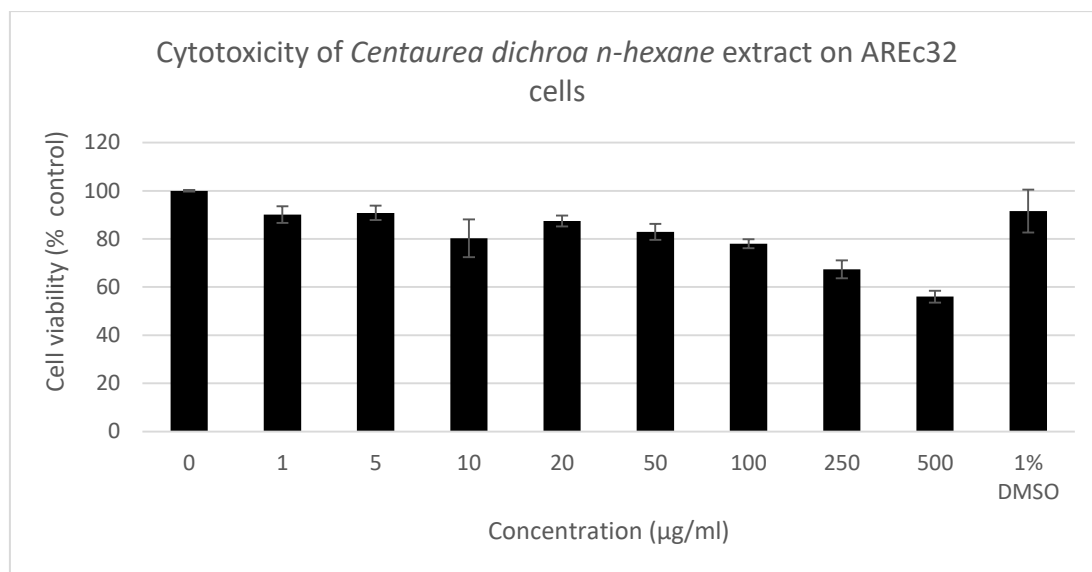


Figure 56 Cell viability as percentage to control (0 µg/ml) observed after treatment of AREc32 cells for 24 h with CD-He (1-500 µg/ml). DMSO represents the vehicle control and its concentration is expressed as v/v%. Results show the mean +/- SEM (n=3, 3 replicates)

All the *n*-hexane extracts of the selected plants were screened for Nrf2/ARE induction at non-cytotoxic concentrations using AREc32 cells after a 24 h treatment. The results are presented in Figure 57 below.

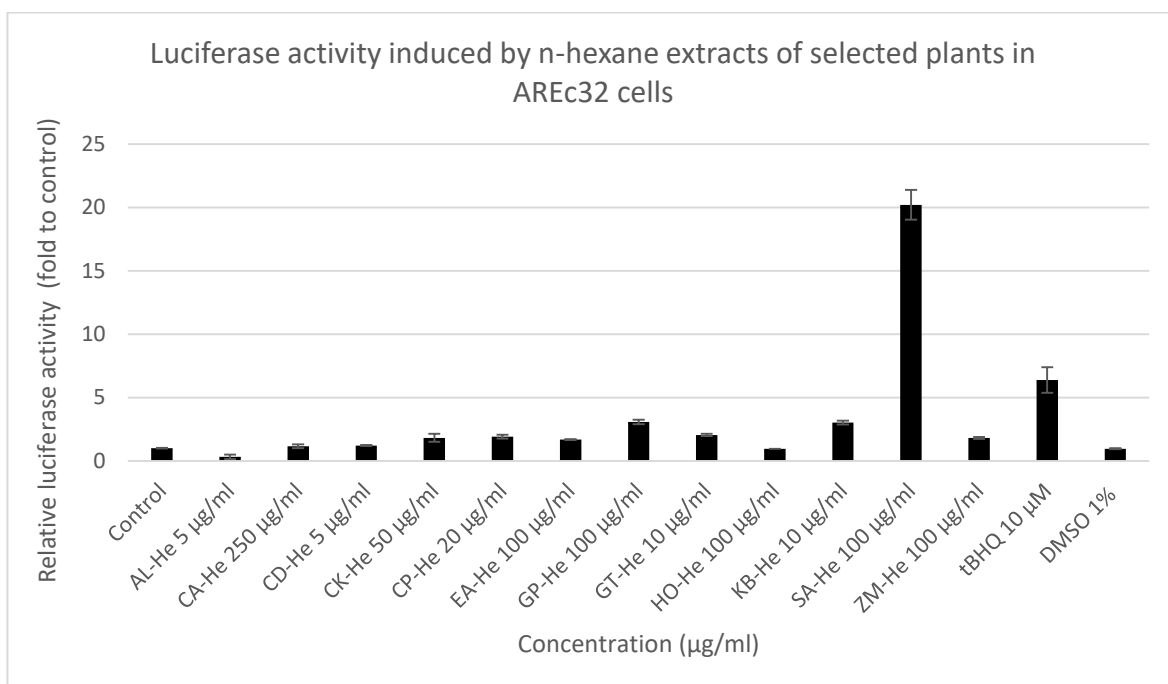


Figure 57 Effect of n-hexane extracts on the induction of luciferase activity and tBHQ as positive control. AREc32 cells were incubated for 24 h with non-cytotoxic concentrations of AL-He, CA-He, CD-He, CK-He, CP-He, EA-He, GP-He, GT-He, HO-He, KB-He, SA-He and ZM-He. DMSO represents the vehicle control and its concentration is expressed as v/v%. Values show mean \pm SEM (n=3, 3 replicates), control=1.

One *n*-hexane extract was noted for exhibiting a very high potential of Nrf2/ARE activation, namely SA-He, showing a 20.2-fold to control luciferase induction.

The other *n*-hexane extracts tested showed a luciferase induction of less than half of that of the induction recorded for the positive control tBHQ, of 6.32-fold. The *Gypsophila pilulifera* *n*-hexane extract exhibited the second highest luciferase induction of 3.08-fold, followed by the *n*-hexane extract of *Kitaibelia balansae* with 3.03-fold to control induction. The only other *n*-hexane extract that achieved a luciferase induction of more than 2-fold was that of *Gardenia ternifolia*, GT-He, with a 2.05-fold to control induction.

AL-He, CA-He, CD-He, CK-He, CP-He, EA-He, HO-He, ZM-He did not show a significant luciferase induction, with results of maximum 1.9-fold to control.

Ultimately the analysis was constrained by the lack of crude extract needed for VLC (at least 2 g) and the lack of plant raw material for a new Soxhlet extraction.

Apart from SA-He, no other non-polar crude extract exhibited a luciferase fold induction of over 20%. Although, GP-He and KB-He did show a fold induction of approximately 3-fold to control, which indicates a potential for Nrf2/ARE activation.

3.2.4 Cytotoxicity and luciferase assay results for compounds precipitated during the Soxhlet extraction of *Gypsophila pilulifera*, *Gardenia ternifolia* and *Ziziphus mucronata*

One of the precipitates, GPS1, resulted from the methanol extraction of *Gypsophila pilulifera* and a second compound, GTS1/GTS2, precipitated out of solution during the methanol extraction of *Gardenia ternifolia*. These compounds were pure and they were tested on AREc32 cells using the MTT assay at a range of concentrations between 0.625 and 40 μM . For structural characterisation details see Study 4 in Section 3.4.

The cell viability was consistently high (140.8% to 96.4%, $n=3$, 4 replicates) over a range of concentrations between 5 and 40 μM . The compounds were then tested at 40 μM in the luciferase assay where no significant results in Nrf2 induction were recorded. Cell viabilities exceeding 100% could be due to uneven seeding of cells, causing the control to have a lower value, relative to which cell viabilities were calculated.

On the other hand, the precipitate, ZMPH1, resulted from the *n*-hexane extraction of *Ziziphus mucronata* was tested in the MTT assay at concentrations starting at 0.625 μM (Figure 58). Cell viabilities decreased steadily from 95.9% to 62.3% as the concentration increased to 40 μM , and the concentration of 2.5 μM , which was responsible for 92.6% cell viability, was considered non-cytotoxic at an appropriate level for the luciferase assay.

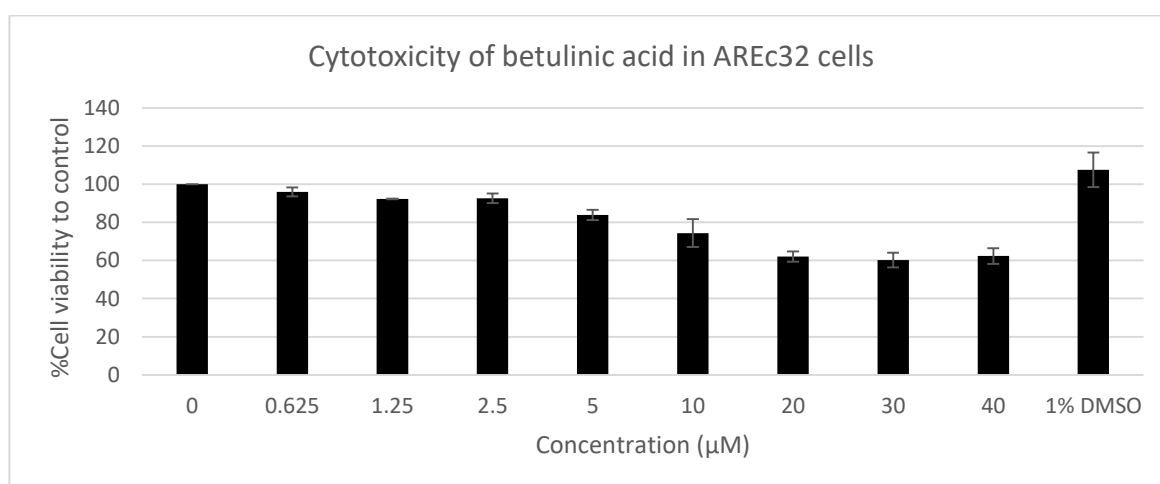


Figure 58 Cell viability as percentage of control (0 mg/ml) observed after treatment of AREc32 cells for 24 h with betulinic acid (0.625-40 μM). DMSO represents the vehicle control and its concentration is expressed as v/v%. Results show the mean \pm SEM ($n=3$, 4 replicates)

Betulinic acid exhibited an Nrf2 induction of 1.08-fold to control (SEM = 0.075, $n = 3$, 3 replicates) and was considered not to be capable of up-regulating the Nrf2/ARE signaling pathway.

3.3 Study 3: Chromatographic fractionation of bioactive crude methanol extracts of *Centaurea dichroa* (CD), *Centaurea pamphylica* (CP), *Gardenia ternifolia* (GT) and *Ziziphus mucronata* (ZM), followed by cytotoxicity assay and luciferase assay using AREc32 cells and DPPH assay of fractions

Guided by the results of Study 2, methanol extracts that showed significant Nrf2 induction levels were further fractionated using appropriate chromatographic separation techniques. The fractions obtained were assayed again using the luciferase assay using AREc32 cells in order to measure Nrf2 induction.

As all *n*-hexane extracts showed insignificant luciferase activity, further purification was performed only on the methanol extracts of *Centaurea dichroa* (CD-Me), *Centaurea pamphylica* (CP-Me), *Gardenia ternifolia* (GT-Me) and *Ziziphus mucronata* (ZM-Me).

Methanol extracts were fractionated by solid phase extraction (C₁₈) with a step gradient of methanol in water (%MeOH/H₂O): 20% - F1 (fraction 1), 50% - F2 (fraction 2), 80% - F3 (fraction 3) and 100% - F4 (fraction 4). Fractions of solvent mix containing dissolved phytochemicals were collected in flasks, evaporated and reconstituted with culture medium to be used in the cytotoxicity and luciferase assays using AREc32 cells.

Fractions F1 always resulted in a higher amount, 200-300 mg, following solid phase extraction of 1 g of starting material, while fractions F2 and F3 were separated with a much lower weight of around 40 to 100 mg. Fractions F4 weighed between 10 and 40 mg with an overall recovery of the extraction of approximately 40%.

3.3.1 Cytotoxicity results for methanol fractions of *Centaurea dichroa* (CD-Me), *Centaurea pamphylica* (CP-Me), *Gardenia ternifolia* (GT-Me) and *Ziziphus mucronata* (ZM-Me) in AREc32 cells

The experiment was performed three times and results were recorded for three wells for each repetition of the experiment. No DMSO was required at this stage, as samples solubilised readily in the culture medium at 37°C using a sonication bath.

The methanol extract sample of *Centaurea dichroa* was received at a later date than the preparation of the other extracts; so that after reviewing the MTT assay results of CP-Me (Figure 60), GT-Me (Figure 61) and ZM-Me (Figure 59) it could be observed that the cytotoxicity of methanol fractions on AREc32 cells from concentrations of 500 µg/ml upwards was too high and more useful insight could be found in the range of 1 µg/ml to 500 µg/ml. The results of the MTT assay of fractions of CD-Me are presented in Figure 59 below.

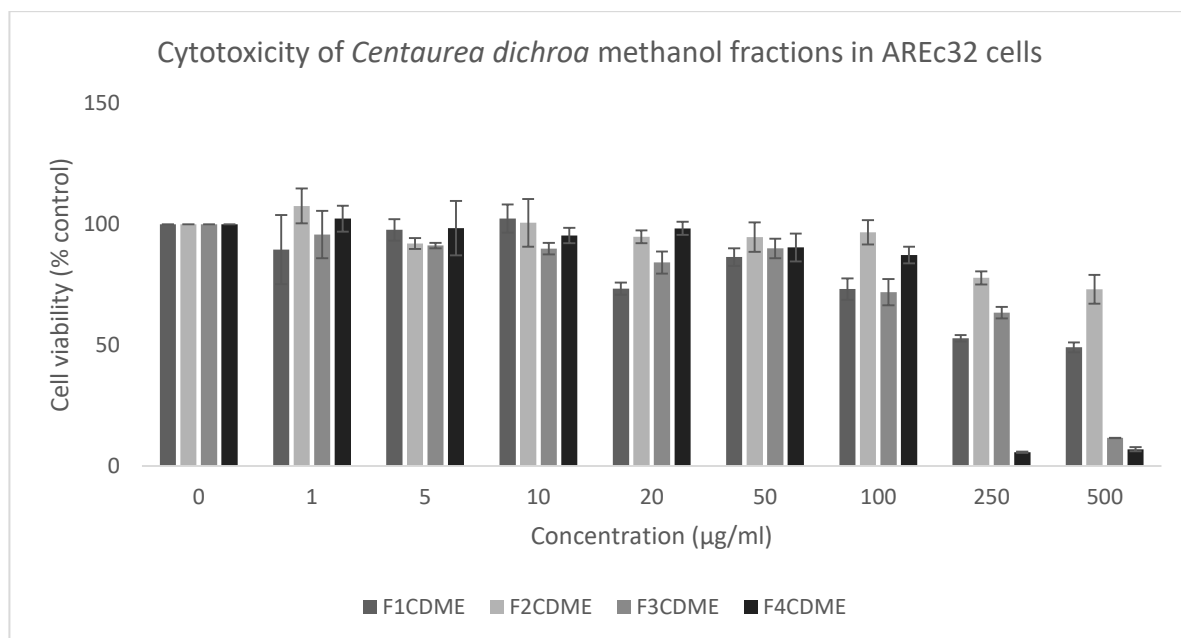


Figure 59 Cell viability as percentage to control (0 µg/ml) observed after treatment of AREc32 cells for 24 h with CD-Me fractions (1-500 µg/ml). Results show the mean +/- SEM (n=3, 3 replicates).

Fraction F1 of CD-Me at 10 µg/ml was determined appropriate for further luciferase assay as it caused a 102% cell viability, the first concentration lower than 500 µg/ml to maintain a cell viability of over 90%.

Fractions F2, F3 and F4 of CD-Me maintained cell viabilities of 97% and 90% - F2 at 100 µg/ml, F3 and F4 at 50 µg/ml. These were concentrations chosen for further luciferase assay.

All four fractions of CP-Me caused a sustained decrease in cell viability at concentrations increasing from 20 to 1000 µg/ml as shown in Figure 60, with F2 CP-Me showing the steepest decrease, from 95% to 12%.

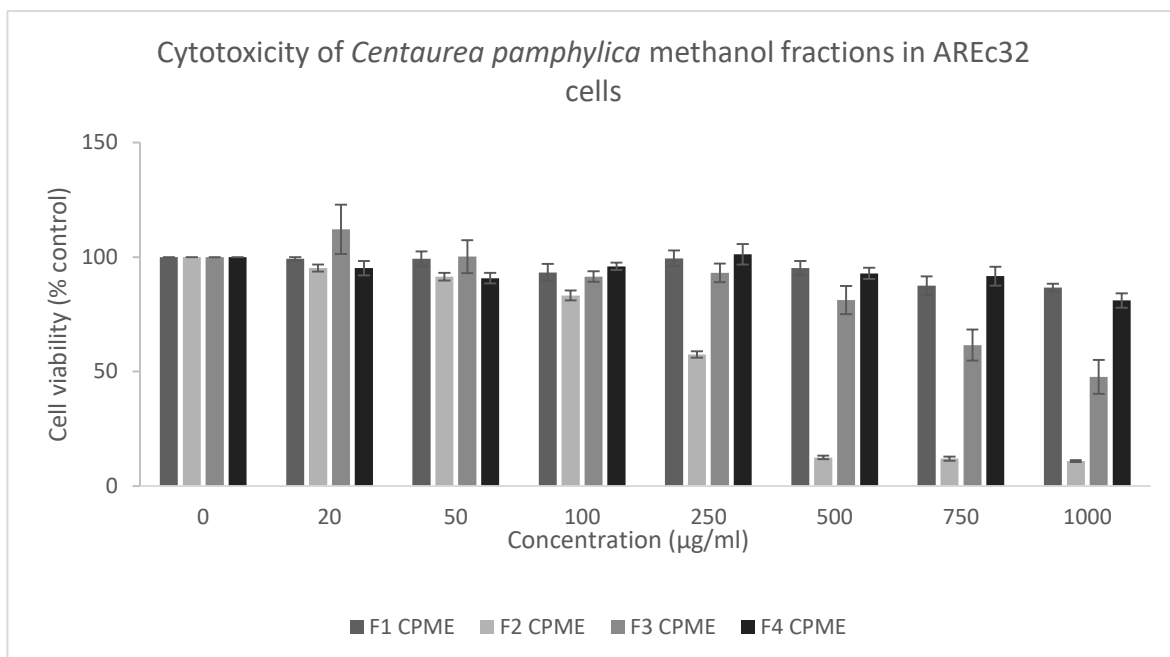


Figure 60 Cell viability as percentage to control (0 µg/ml) observed after treatment of AREc32 cells for 24 h with CP-Me fractions (20-1000 µg/ml). Results show the mean +/- SEM (n=3, 3 replicates).

The non-cytotoxic dose of F1 CP-Me was determined to be 500 µg/ml (95% cell viability), for F2 was 50 µg/ml (91%), for fraction F3 it was 250 µg/ml (93% cell viability) and for fraction F4 the appropriate concentration was determined to be 750 µg/ml (92% cell viability).

GT-Me fractions behaved in a similar fashion causing a decrease in cell viability at concentrations increasing from 20 to 1000 µg/ml as shown in Figure 61, but with fraction F4 showing a significant decrease from 116% to 16%, whereas the other fractions maintained a cell viability of over 40% at the highest dose.

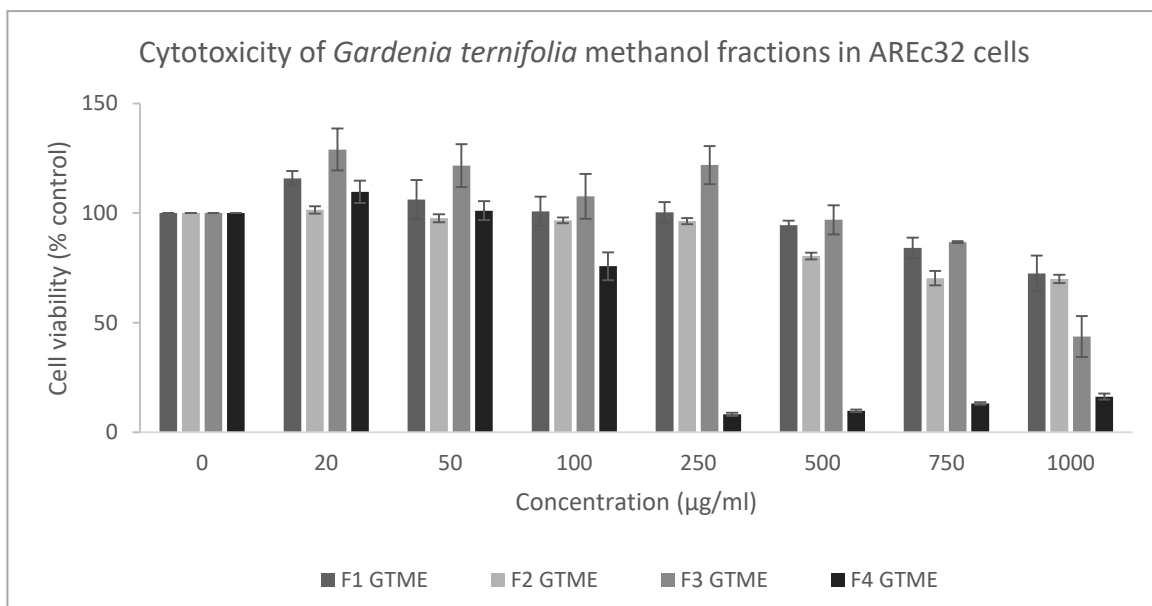


Figure 61 Cell viability as percentage to control (0 µg/ml) observed after treatment of AREc32 cells for 24 h with fractions of GT-Me (20-1000 µg/ml). Results show the mean \pm SEM (n=3, 3 replicates).

Therefore, fraction F4 of GT-Me at 50 µg/ml proved to be a safe concentration to use in the luciferase assay, as well as fractions F1 and F3 at 500 µg/ml and fraction F2 at 250 µg/ml (over 90% cell viability).

Figure 62 shows the cytotoxicity profile of the methanol fractions of the bioactive *Ziziphus mucronata* methanol extract. As discussed previously in Section 3.2.2, when the methanol extract ZM-Me was assessed for cytotoxicity in AREc32 cells, this bioactive extract also readily reduces the MTT in the culture medium to formazan, so that, as expected, the extract fractions behaved similarly, especially F2, F3 and F4, indicating cell viabilities of over 145% , 112% and 166% even at the lowest concentration of 20 µg/ml.

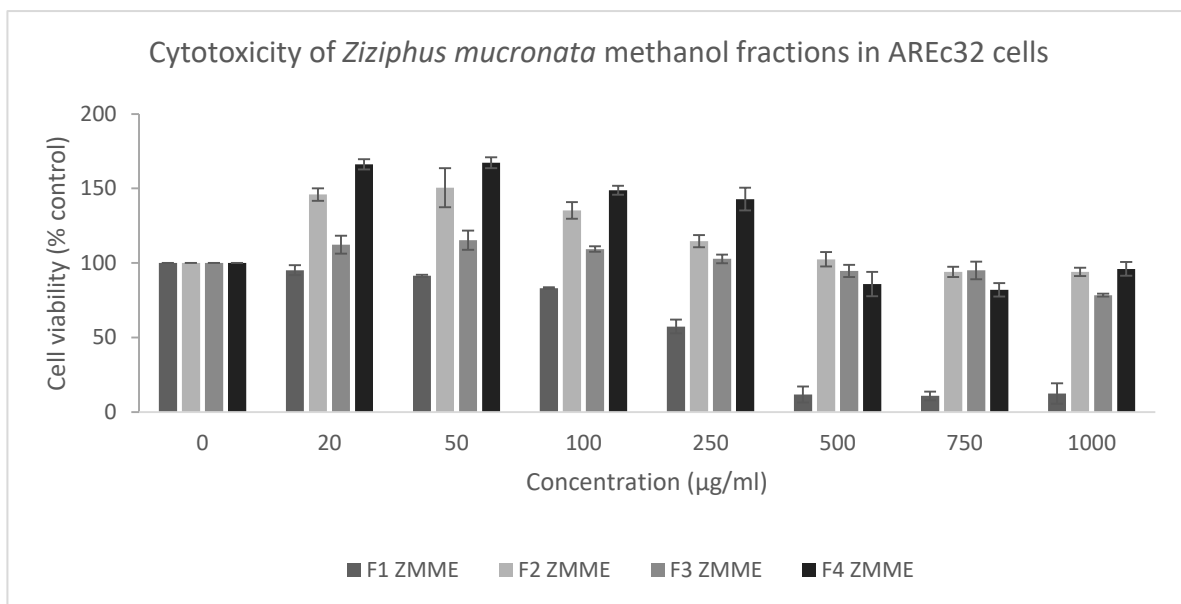


Figure 62 Cell viability as percentage to control (0 µg/ml) observed after treatment of AREc32 cells for 24 h with ZM-Me fractions (20-1000 µg/ml). Results show the mean +/- SEM (n=3, 3 replicates).

Therefore, given the known capacity of methanol fractions of ZM-Me to exhibit falsely low cytotoxicity, the concentrations to be used in the luciferase assay were determined as one step lower than the information presented in the graph. So that F1 was best to use in AREc32 cells luciferase assay at 50 µg/ml (91%) according to the graph. F3 caused a cell viability of 95% at 750 µg/ml, which continued upwards as the dose decreased, so it was chosen as a safer concentration for the luciferase assay.

Fractions F2 and F4 were least cytotoxic over the entire range of 20 µg/ml to 1000 µg/ml (Figure 62), so the concentration used in the subsequent luciferase assay was 1000 µg/ml for both fractions, as they exhibited cell viabilities of 114.67% and 142.85% respectively.

Following the MTT assay, each fraction was tested in the luciferase assay at the appropriate non-cytotoxic concentration and the results are presented in the next section. All phytochemical samples were prepared in warm culture medium before each experiment.

3.3.2 Luciferase assay results for methanol fractions of *Centaurea dichroa* (CD-Me), *Centaurea pamphylica* (CP-Me), *Gardenia ternifolia* (GT-Me) and *Ziziphus mucronata* (ZM-Me)

Figure 65 below shows that fractions F2 and F3 of the methanol extract of *Centaurea dichroa* (20 µg/ml) exhibited the highest induction of luciferase activity, which is linked to the activation of Nrf2/ARE signaling pathway in AREc32 cells. These methanolic fractions caused an increase in fold to control induction of 3.7 and 5.5, respectively.

The positive control tBHQ caused a 6.4-fold to control increase in luciferase activity, whereas Fraction 1 and Fraction 4 of CD-Me showed the lowest luciferase induction with 1.3-fold and 1.3-fold to control, respectively. Fractions F2 and F3 showed low to medium luciferase induction, 3.7 and to 5.5-fold, respectively (Figure 63).

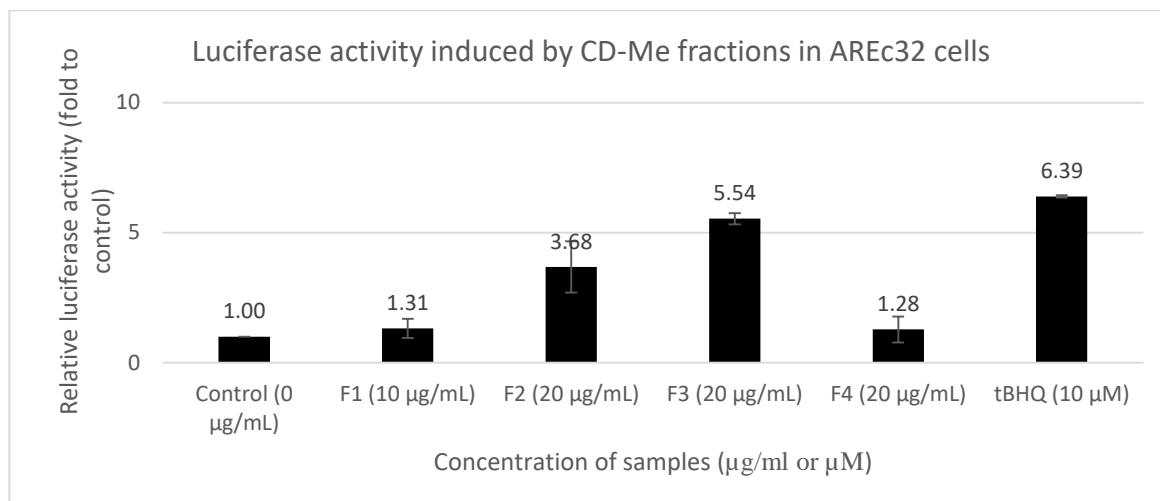


Figure 63 Effect of fractions of *Centaurea dichroa* methanol extract on the induction of luciferase activity and of tBHQ as positive control. AREc32 cells were incubated for 24 h with non-cytotoxic concentrations of CD-Me. Values show mean +/- SEM (n=3, 3 replicates), control=1.

CP-Me fractions showed, in Figure 66 below, the highest increase in luciferase activity than all other *Centaurea* species tested, with F3 (500 µg/ml) and F4 (750 µg/ml) reaching induction folds of 12.5 and 13.4, respectively. Fraction 2 (50 µg/ml) exhibited a medium induction of luciferase with 6.4-fold to control increase, close to the 5.6-fold to control induction reached by the positive control tBHQ (at least 50% lower than the highest fold induction recorded by Fraction 3 and Fraction 4 of CP-Me).

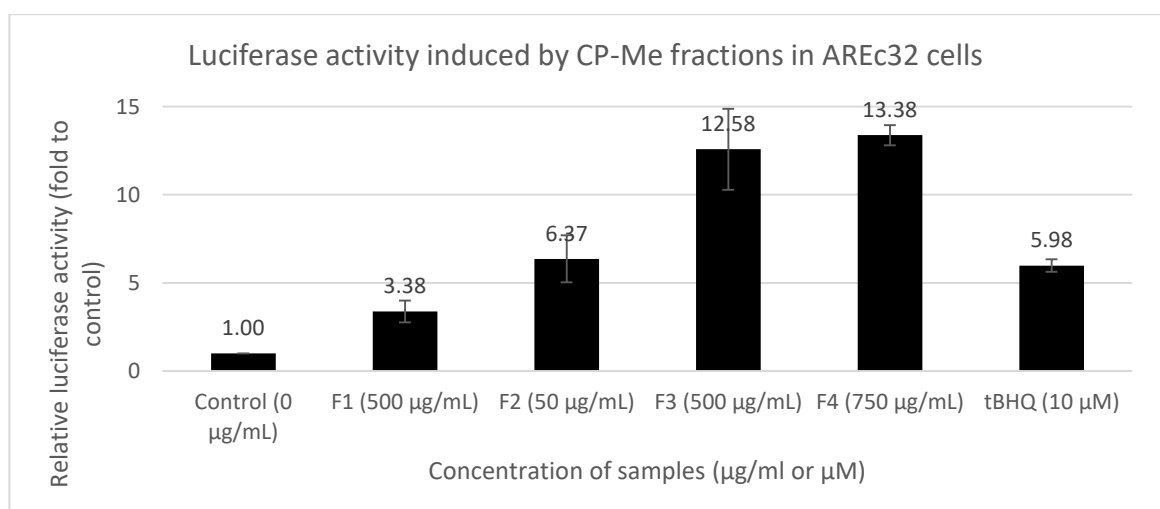


Figure 64 Effect of fractions of *Centaurea pamphilica* methanol extract on the induction of luciferase activity and of tBHQ as positive control. AREc32 cells were incubated for 24 h with non-cytotoxic concentrations of CP-Me. Values show mean +/- SEM (n=3, 3 replicates), control=1.

GT-Me fractions exhibited similar results (Figure 65) with F3 (500 µg/ml) and F4 (100 µg/ml) reaching high induction folds of 11.6 and 12.6, respectively. These results are also almost 50% higher than the induction achieved by the positive control tBHQ, of 5.6-fold to control luciferase activity induction.

On the other hand, fractions F1 (500 µg/ml) and F2 (250 µg/ml) of GT-Me exhibited a low level of Nrf2 induction with 1.1 and 2.9-fold to control (Figure 65).

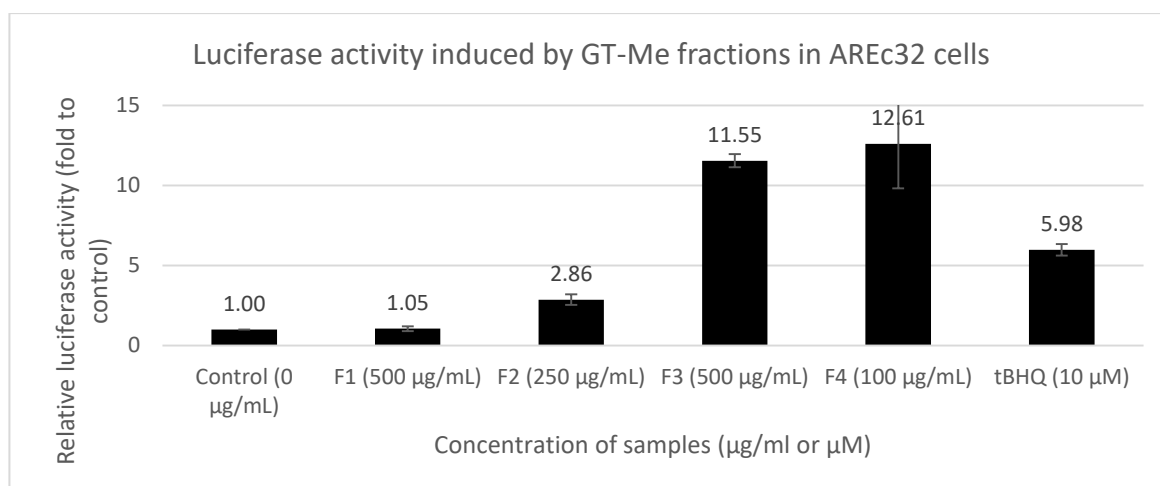


Figure 65 Effect of fractions of *Gardenia ternifolia* methanol extract on the induction of luciferase activity and tBHQ as positive control. AREc32 cells were incubated for 24 h with non-cytotoxic concentrations of GT-Me. Values show mean +/- SEM (n=3, 3 replicates), control=1.

The methanol fractions of ZM-Me did not show any significant fold increase in luciferase activity (Figure 66), with fraction F2 (1000 µg/ml) exhibiting the highest fold to control induction of 2.3-fold, compared to the positive control induction of 5.6-fold to control induction.

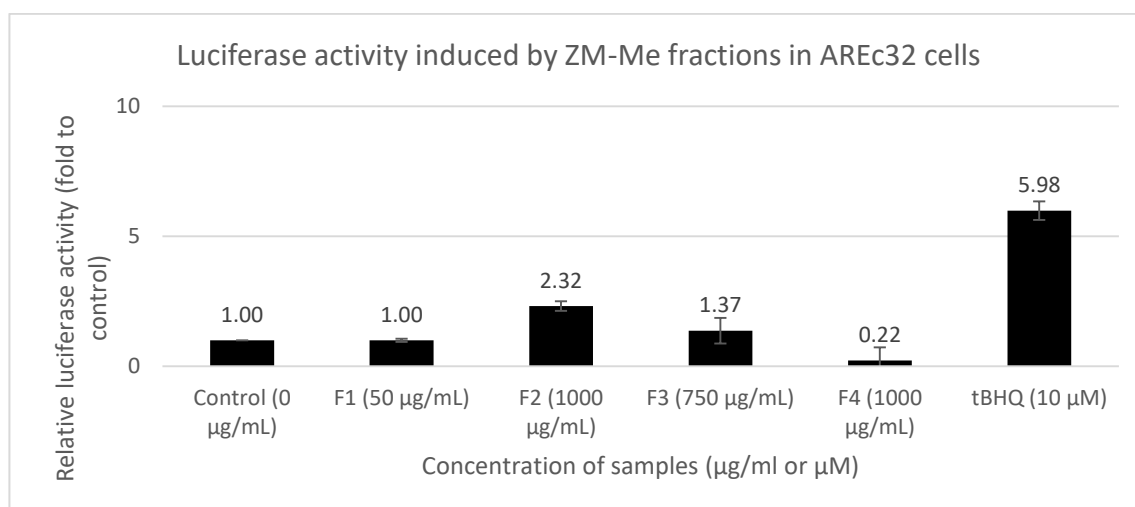


Figure 66 Effect of fractions of *Ziziphus mucronata* methanol extract on the induction of luciferase activity and tBHQ as positive control. AREc32 cells were incubated for 24 h with non-cytotoxic concentrations of ZM-Me. Values show mean +/- SEM (n=3, 3 replicates), control=1.

3.3.3 DPPH assay results for bioactive methanol fractions of *Centaurea dichroa* (CD-Me), *Centaurea pamphylica* (CP-Me), *Gardenia ternifolia* (GT-Me) and *Ziziphus mucronata* (ZM-Me)

The methanol fractions of the above mentioned plant species that showed high fold induction in the luciferase assay in AREc32 were also tested in the DPPH assay to check their potential as free radical scavengers. Quercetin was used as positive control in every experiment.

Because the fractions F4 of the methanol extracts identified previously as bioactive (CP-Me and GT-Me) did not reach a 50% inhibition of DPPH, these results were not shown.

Figure 67 below shows the dose dependent inhibition of DPPH by fractions F3 of bioactive methanol extracts of *Centaurea dichroa*, *Centaurea pamphylica* and *Gardenia ternifolia*, as well as that of quercetin.

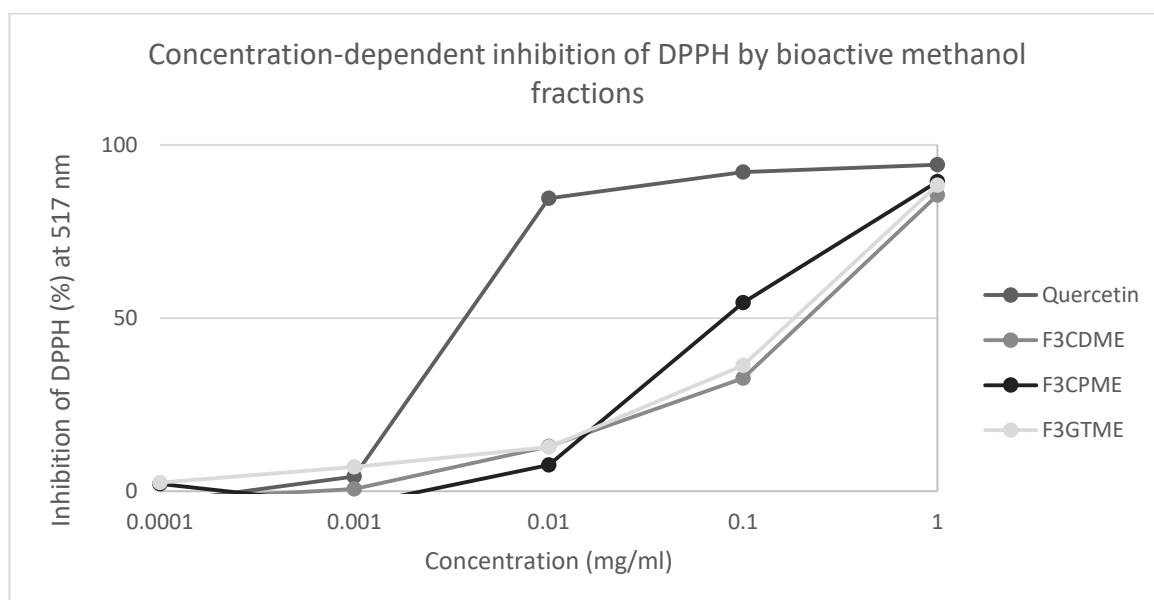


Figure 67 %Inhibition of DPPH by fractions F3 of methanol extracts of *Centaurea dichroa*, *Centaurea pamphylica*, *Gardenia ternifolia* and the positive control quercetin at concentrations between 0.0001 and 1 mg/ml. Graph shows the average values of triplicate experiments.

In Figure 67, fractions F3 of GT-Me and CD-Me both reached 50% inhibition of DPPH between 0.1 and 1 mg/ml concentrations, whereas fraction F3 of CP-Me reached the same level of inhibition at a lower concentration, between 0.01 and 0.1 mg/ml. The positive control quercetin achieved 50% inhibition of DPPH somewhere between 0.001 and 0.01 mg/ml.

Fractions F3 of GT-Me and CD-Me were further investigated for free-radical scavenging activity at 1-fold dilutions between the concentrations identified previously. So that Figure 68 shows that the IC_{50} values for these two plant extracts would be between 0.1 and 0.2

mg/ml, almost 40 times higher than the positive control quercetin with IC_{50} of 0.005 mg/ml (Figure 70).

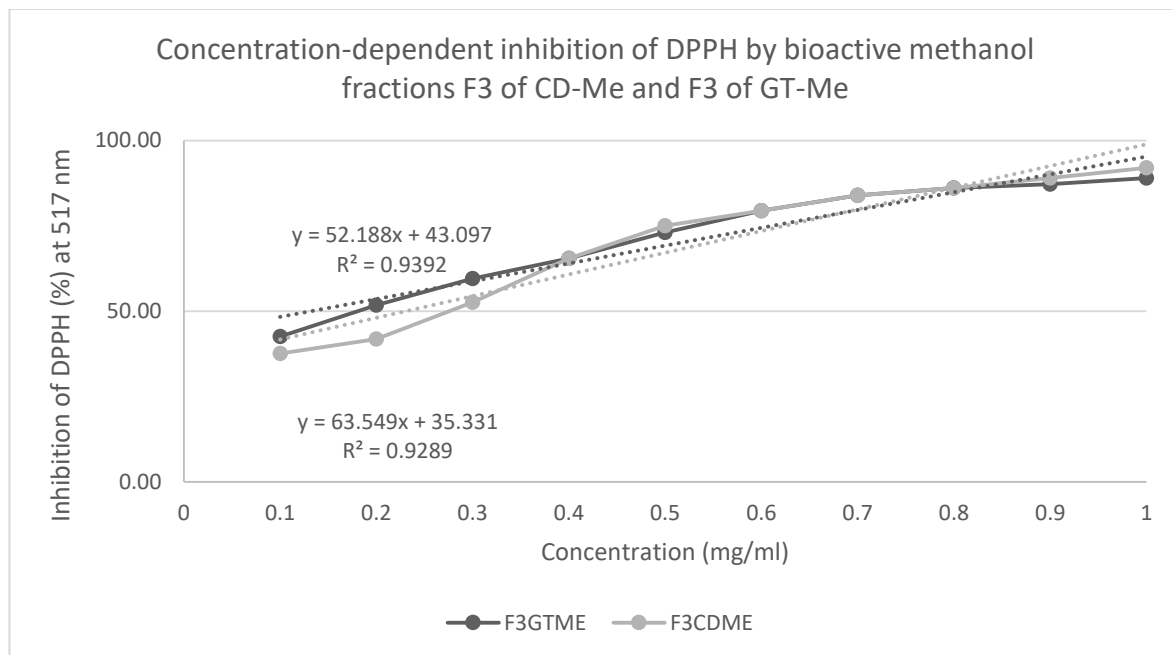


Figure 68 Graph showing the %inhibition of DPPH by CD-Me and GT-Me at 1-fold dilutions between 0.1 and 0.01 mg/ml. Graph shows the average values of duplicate experiments

The IC_{50} of fractions F3 of GT-Me and F3 CD-Me were calculated as 0.132 mg/ml and 0.230 mg/ml, respectively.

Fraction F3 of CP-Me was further assayed at concentrations between 0.01 and 0.1 and Figure 69 shows the concentration-dependent profile of percentage DPPH inhibition.

Moreover, the IC_{50} value for F3 of CP-Me was determined to be 0.072 mg/ml.

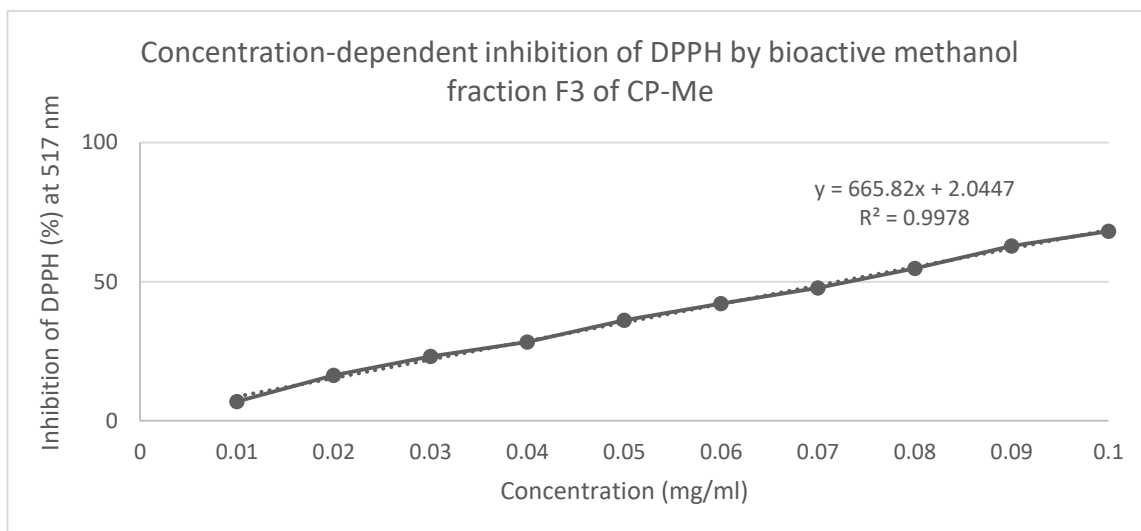


Figure 69 Graph showing the %inhibition of DPPH by CP-Me at 1-fold dilutions between 0.1 and 0.01 mg/ml. Graph shows the average values of duplicate experiments

Figure 70 shows the concentration-dependent inhibition of DPPH exhibited by positive control quercetin between the concentrations of 0.001 and 0.01 mg/ml, which indicates an IC₅₀ of 0.005 mg/ml.

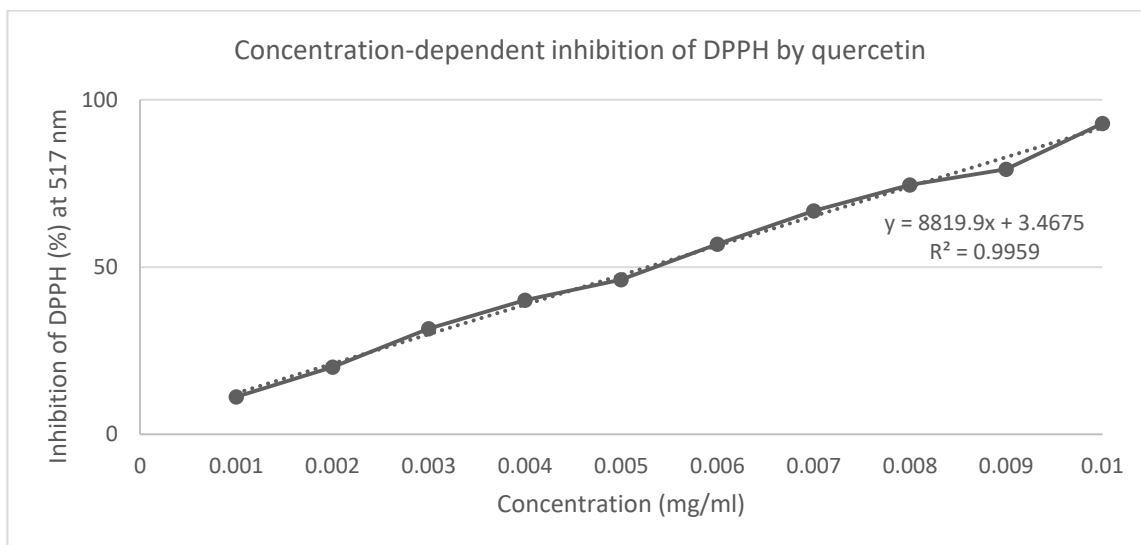


Figure 70 Graph showing the %inhibition of DPPH by quercetin at 1-fold dilutions between 0.001 and 0.01 mg/ml. Graph shows the average values of duplicate experiments.

Out of the six fractions of methanol extracts tested for free-radical scavenging activity, fraction F3 of *Gardenia ternifolia* methanol extract produced a 50% inhibition of DPPH at the lowest concentration, namely 0.132 mg/ml, 66 times higher than the IC₅₀ of 0.005 mg/ml achieved by the positive control quercetin.

3.4 Study 4: Identification of compounds from bioactive fractions of methanol extracts by means of UV-Vis, nuclear magnetic resonance (NMR) and mass spectrometry (MS) analysis

Fractions F2 and F3 of *Centaurea dichroa*, fractions F2, F3 and F4 of *Centaurea pamphylica* and F3 and F4 of *Gardenia ternifolia* methanol extracts were found to be most bioactive in terms of Nrf2 induction in the luciferase assay and they were subjected to preparative HPLC for isolation and purification of compounds. The purest compounds isolated were then analysed using NMR and MS techniques.

The aim was to characterise novel structures of phytochemicals from the plant species screened, but also to test the ability of individual compounds to modulate the Nrf2/ARE signaling pathway in AREc32 cells. However, the starting material consisting of methanol extracts and subsequent fractions was not sufficient for isolation of pure compounds for cell based assays, with the exception of F3 GT-Me-P4/PA.

3.4.1 Structural characterisation of compounds precipitated during Soxhlet extraction

3.4.1.1 Structural characterisation of GPS1 as stachyose

One of the precipitates, GPS1, resulted from the methanol extraction of *Gypsophila pilulifera*, was identified as stachyose (Figure 71), as one of the most common tetrasaccharides commonly found in woody plants, which is involved in storage and transport of sugar (Avigad and Dey, 1997).

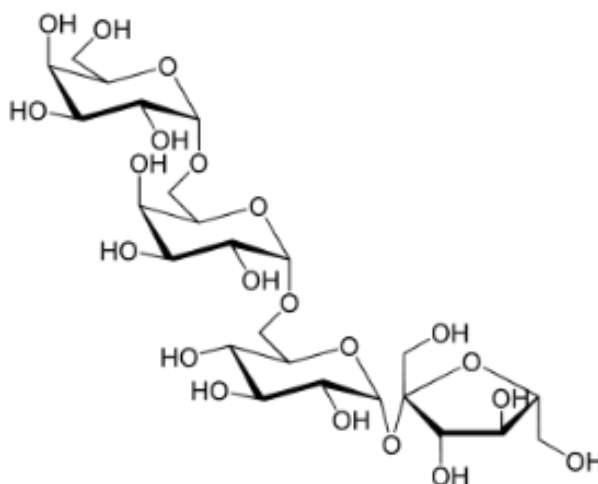
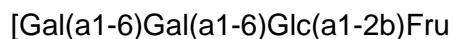
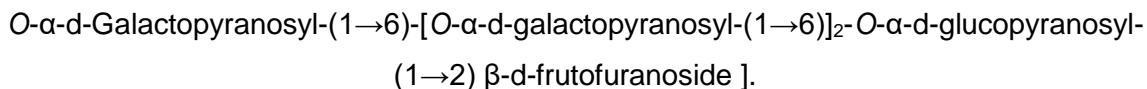


Figure 71 Chemical structure of stachyose C₂₄H₄₂O₂₁, 666 g/mol.

The NMR spectra of GPS1 indicate the formula of Stachiose (Appendix A.1):



aka



The chemical shift values in both $^1\text{H-NMR}$ and $^{13}\text{C-NMR}$ spectra are in agreement with the ones reported in the literature by MyIntyre and Vogel (1989) and Youssef *et al* (2016).

For the GPS1 precipitate assignments were based on comparison to the literature data and the correlations presented by the ^1H , COSY, HSQC, HMBC and DEPTQ experiments presented in Appendix A.1. Figure 74 depicts the assignments.

$^1\text{H-NMR}$ (D_2O , d, ppm) spectra:

Overlapped anomeric protons can be observed, at 4.95 (m, 2H, glycosidic); 5.40 (d, H glycosidic).

Peaks in the 3.4 - 4.18 ppm domain represent all the other protons (non-anomeric). While the chemical shift range is very narrow, causing signal overlapping, this region is identical to the ones observed in catalogues and reported literature.

$^{13}\text{C-NMR}$ (D_2O , d, ppm spectra):

Peaks at 61.14, 61.45, 62.46, 65.87 and 66.48 ppm may be assigned to C atoms in the -CH₂-O- groups found in positions 6 in galactose and glucose pyranosic rings and the 1 and 6 positions in the fructose furanosic ring.

Peaks at 68.30, 68.45, 68.79, 69.24, 69.51, 70.29, 70.98, 71.28, 72.39, 72.56, 72.73, 74.01, 76.37, 81.35 ppm may be assigned to C atoms in the >CH-O- groups.

Peaks at 92.10, 98.37 and 98.03 ppm may be assigned to the three anomeric C atoms in the pyranose rings, while the 103.8 ppm value is clearly attributed to the unique quaternary C atom, the fructose anomeric C-2 atom. The chemical shifts of all anomeric carbon atoms show greater values due to the deshielding produced by the oxygen atoms in the acetal >C(-O-)₂ bonds.

NMR assignments for GPS1 precipitate, as well as a comparison between the GPS1 NMR assignments (in black) and those reported in literature for stachyose are presented in Figure 72 (MyIntyre and Vogel, 1989).

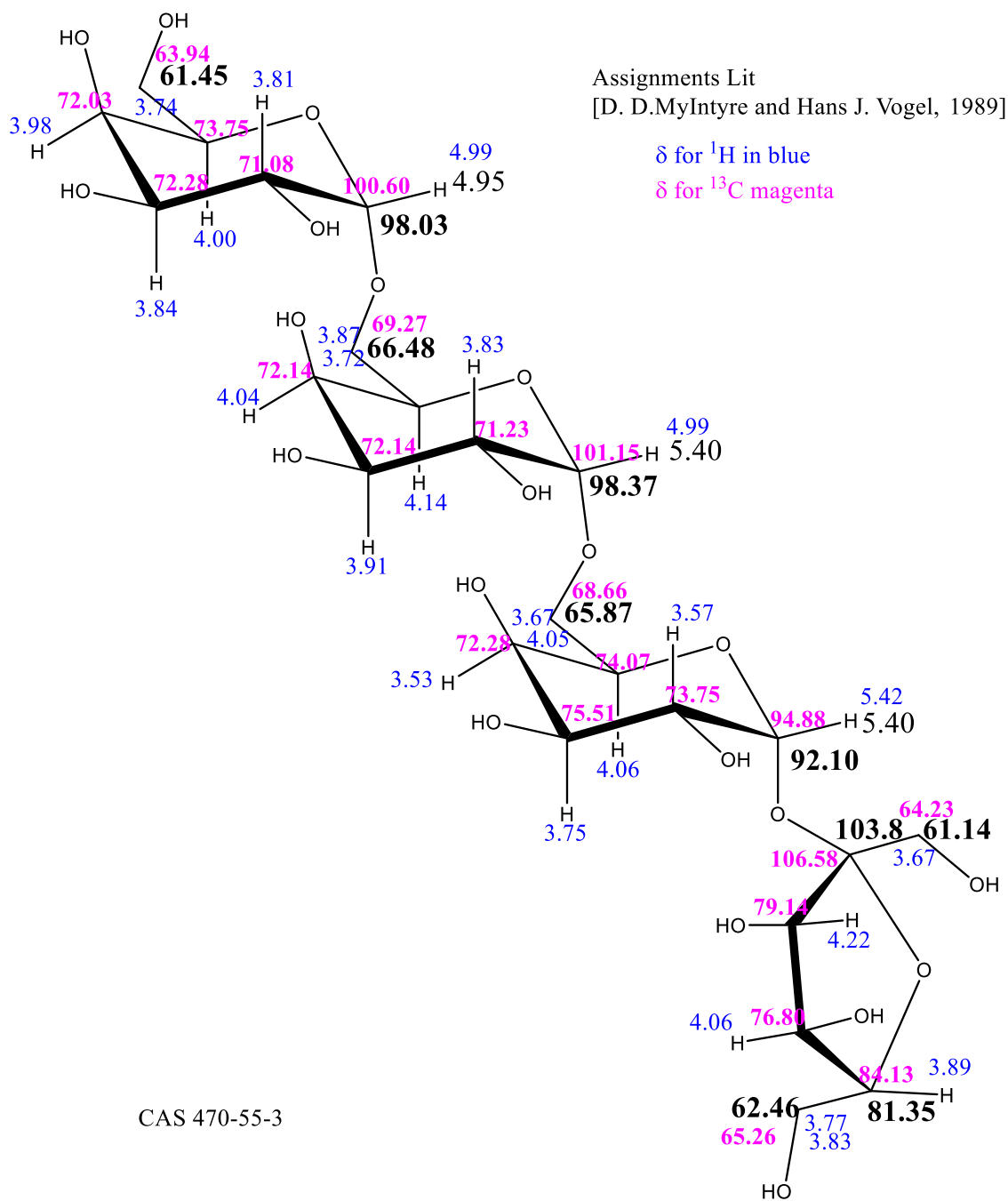


Figure 72 GPS1 experimental NMR assignments (in black) compared to those for stachiose in literature (blue and magenta in the image)

3.4.1.2 Structural characterisation of GTS1/GTS2 as mannitol

Similarly, another compound, GTS1/GTS2, precipitated out of solution during the methanol extraction of *Gardenia ternifolia* and was identified as mannitol. See the chemical structure in Figure 73.

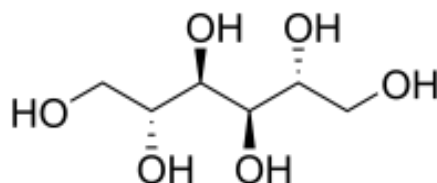


Figure 73 Chemical structure of mannitol

The $[M-H]^-$ ion at m/z 181.05 confirmed the molecular formula $C_6H_{14}O_6$. The molecular weight of mannitol is 180 g/mol. For MS spectra see Appendix A.2.

From the NMR spectra it could be observed that in D_2O , the primary alcohol groups (CH_2OH) show more shielded values for the chemical shifts of the methylene group (3.4 ppm), while the CH protons in the CH-OH groups show less shielded chemical shifts in the 3.5 - 3.62 ppm interval.

The same relation "shielded-deshielded" is also apparent in the ^{13}C spectra: the primary C atoms show peaks at 65 ppm (more shielded), while the peaks at 70 - 72 ppm can be assigned to the less shielded CH-OH carbon atoms.

The identification of the GTS1/GTS2 precipitate as mannitol was attempted by comparing the chemical shifts recorded (see NMR spectra in Appendix A.2) to the values reported in the literature by Voelter *et al* (1970) and to those from chemical compounds and spectra online databases, such as chemicalbook and molbase.

The proposed assignments of the GTS precipitate as mannitol are shown in Figure 74, compared to those from literature. More literature information is presented in Figure 75.

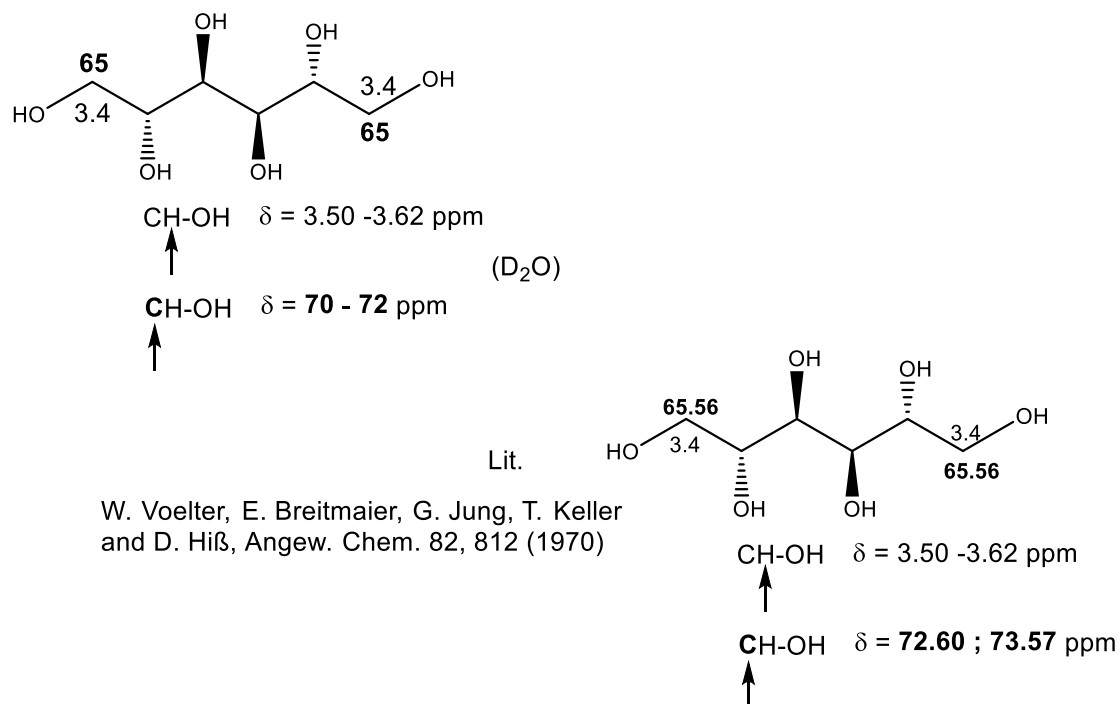
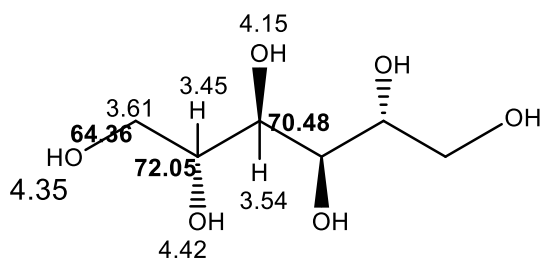
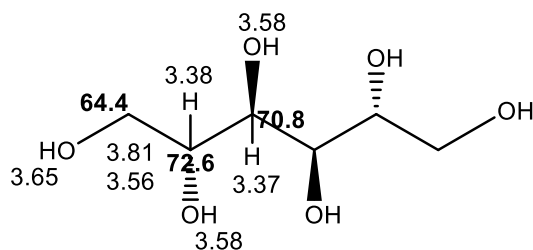


Figure 74 ¹H and ¹³C assignments for mannitol (upper left) based on NMR spectra presented in Appendix A.2; ¹H and ¹³C assignments for mannitol (lower right) based on NMR spectra from literature



https://www.chemicalbook.com/SpectrumEN_69-65-8_1HNMR.htm

https://www.chemicalbook.com/SpectrumEN_69-65-8_13CNMR.htm



http://www.molbase.com/en/hnmr_69-65-8-moldata-1500130.html#tabs

Figure 75 ¹H and ¹³C assignments for mannitol from online catalogues.

^{13}C NMR spectra also showed chemical shifts values that were in agreement with the literature and with the DEPTQ experiment (see Appendix A.3). These values are presented in bold black font in Figure 77. Values reported in the literature for ^{13}C , by Berger and Sicker (2009), are presented in bold magenta font.

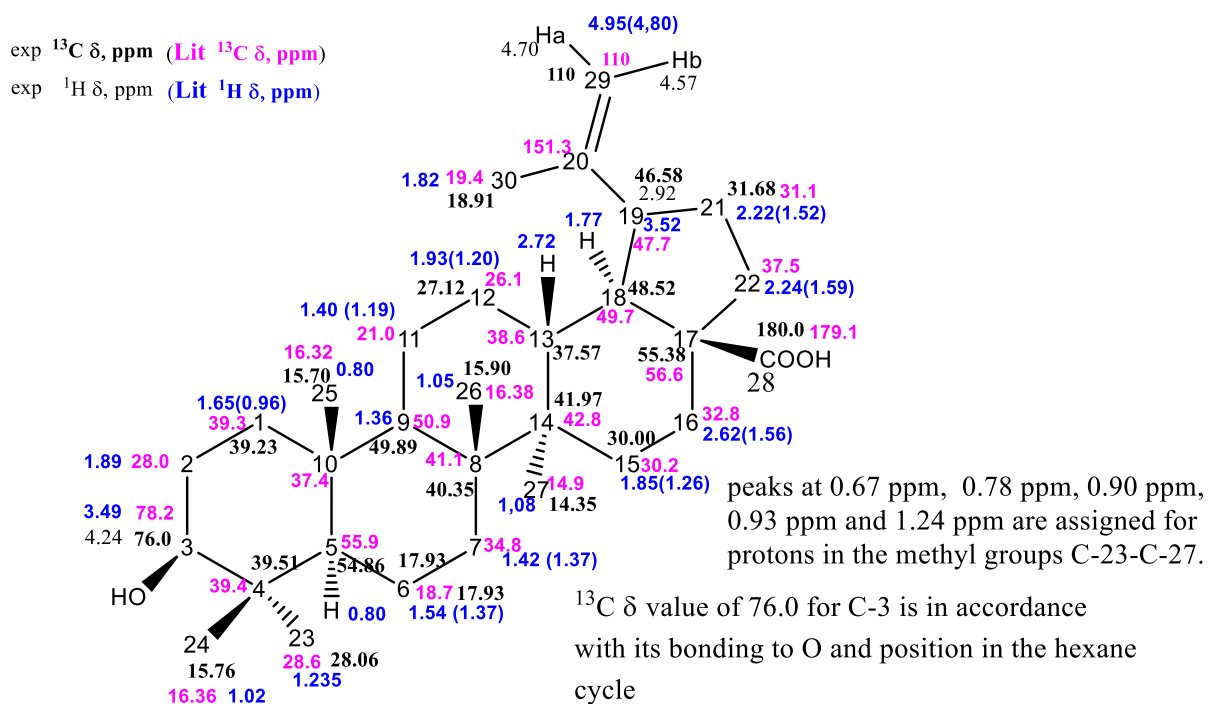


Figure 77 ^1H and ^{13}C assignments for betulinic acid based on NMR data recorded for ZMPH1 (in black) and on NMR data from literature (blue and magenta; Berger and Sicker, 2009)

3.4.2 Structural characterisation of compounds isolated from bioactive methanol fractions

3.4.2.1 Isolation of compounds from F3 CDME

The most bioactive methanol fraction of *Centaurea dichroa* was subjected to preparative HPLC and a separation of main compounds absorbing at 290 nm was observed (see Figure 78).

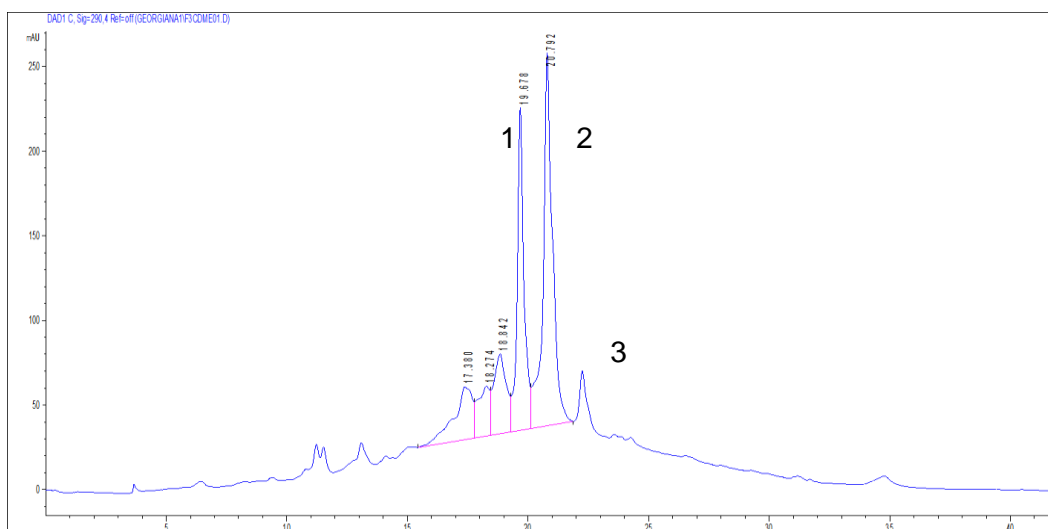


Figure 78 Preparative HPLC chromatogram of F3 CD-Me (30% to 90% MeOH in H₂O gradient solvent system, 200 μ L injection)

For Peak 1 noted in Figure 80 above, the highest absorbing values were strongest for Band I and lowest for Band II, as shown in Figure 79.

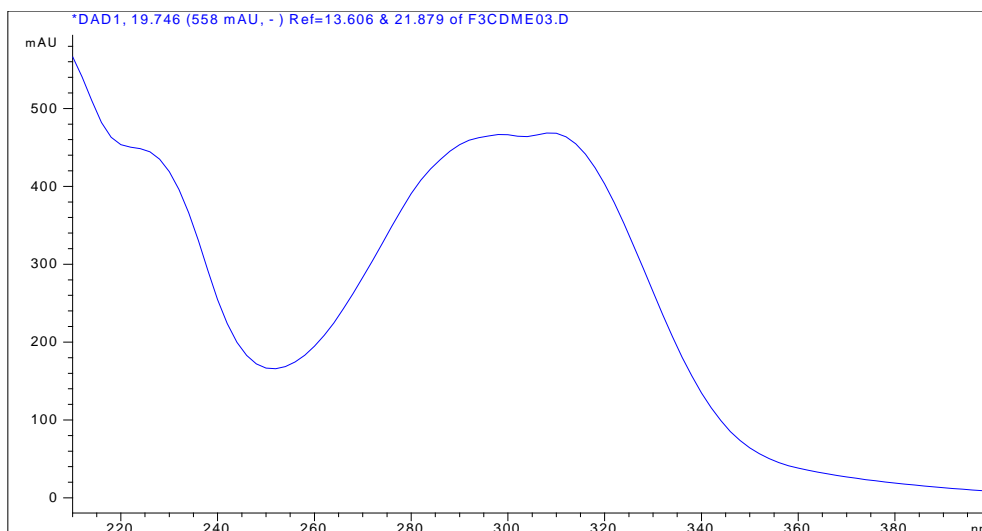


Figure 79 UV spectrum of Peak 1 of F3 CD-Me

Peaks 2 and 3 exhibited very similar UV_{max} values, although Peak 3 eluted at a much lower intensity, 50 mAU, compared to over 200 mAU for Peaks 1 and 2.

See UV spectra of Peak 2 ($t_R = 20.793$ min) and Peak 3 ($t_R = 22.233$ min) in Figures 80 and 81, respectively, as compound eluted.

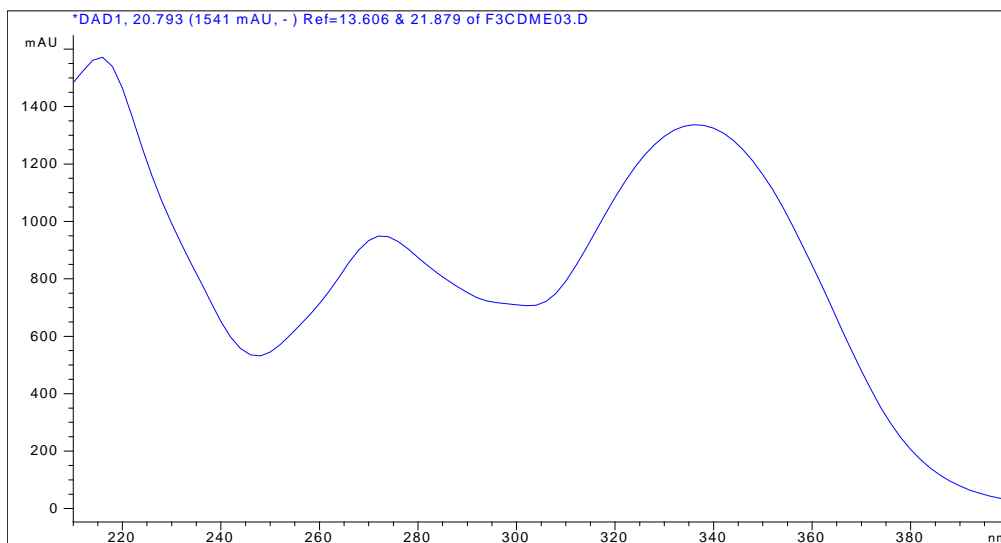


Figure 80 UV spectrum of Peak 2 of F3 CD-Me

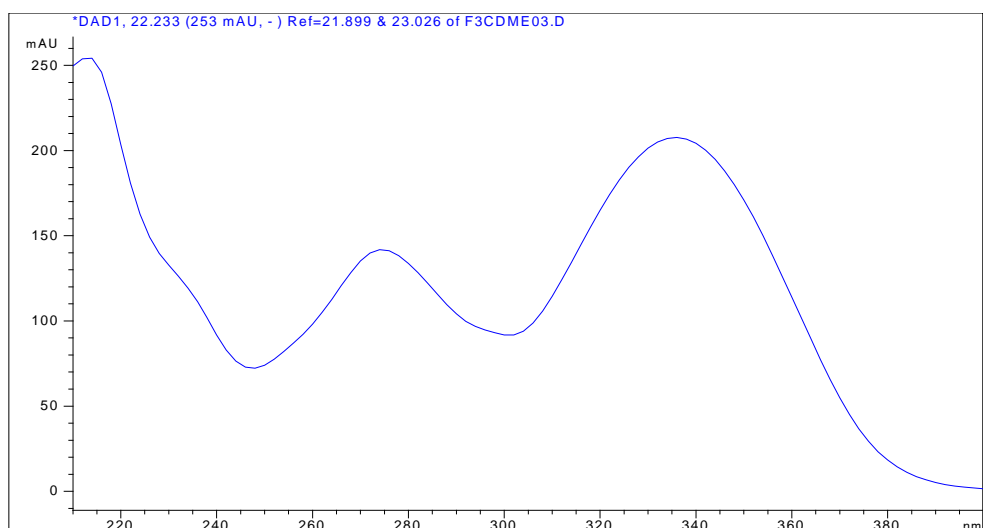


Figure 81 UV spectrum of Peak 3 of F3 CD-Me

Isolation of F3CDMe-P2

A first compound that was isolated and showed good chromatographic separation was assigned the code name F3 CD-Me-P2 and it eluted at $t_R=13.365$ min, showing UV_{max} values of 270 nm, 336 nm, identical to the UV spectrum observed in the mixture of F3CD-Me for Peak 2 (Figure 82).

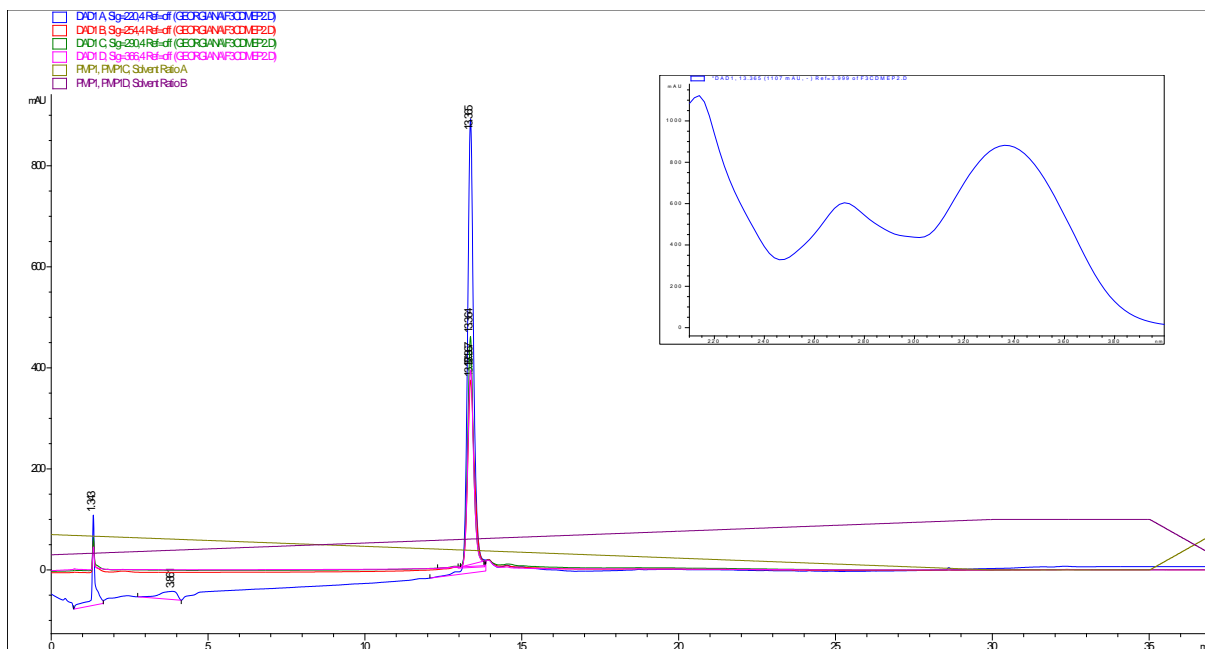


Figure 82 Analytical chromatogram of isolated compound F3CD-Me-P2, with the UV spectrum recorded on Agilent 1260 in methanol:water gradient solvent system.

The NMR spectra did not confirm a chemical structure for the possible molecular weight of 300 g/mol suggested by the MS results in Figure 83.

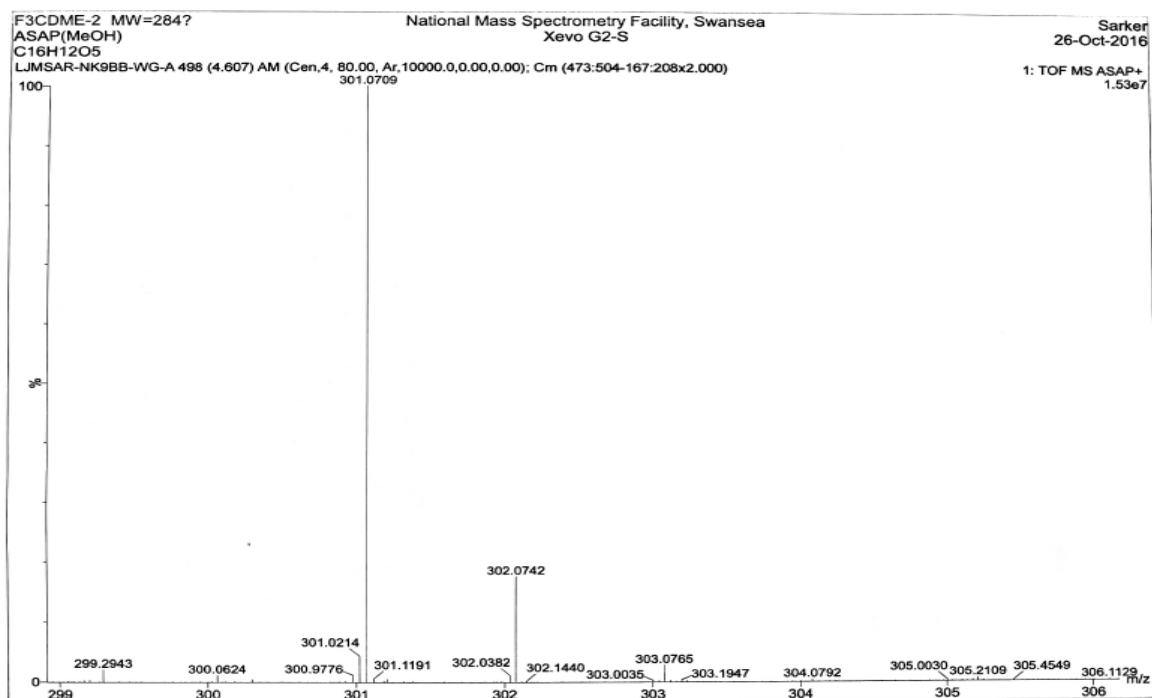


Figure 83 MS spectrum of F3CD-Me-P2

Isolation of F3CD-Me-P3

A second compound isolated from F3CD-Me eluted at $t_R=14.5$ min and its UV spectrum revealed high absorption peaks at 274 nm and 336 nm (Figure 84), typical of flavonoids and identical to the UV spectrum of Peak 3 of F3CD-Me chromatogram.

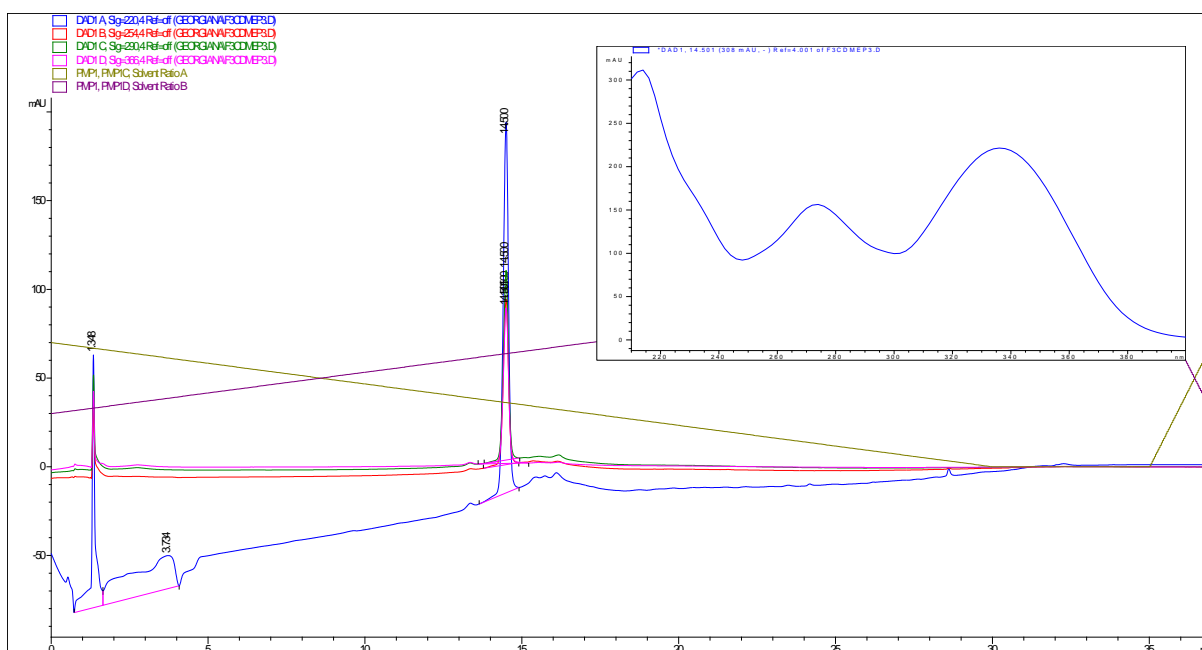


Figure 84 Analytical HPLC chromatogram of isolated compound F3CDMe-P3 in methanol/water solvent system with gradient; 10 mg/ml.

The NMR spectra did not confirm a chemical structure for the possible molecular weight of 314 g/mol suggested by the MS results in Figure 85.

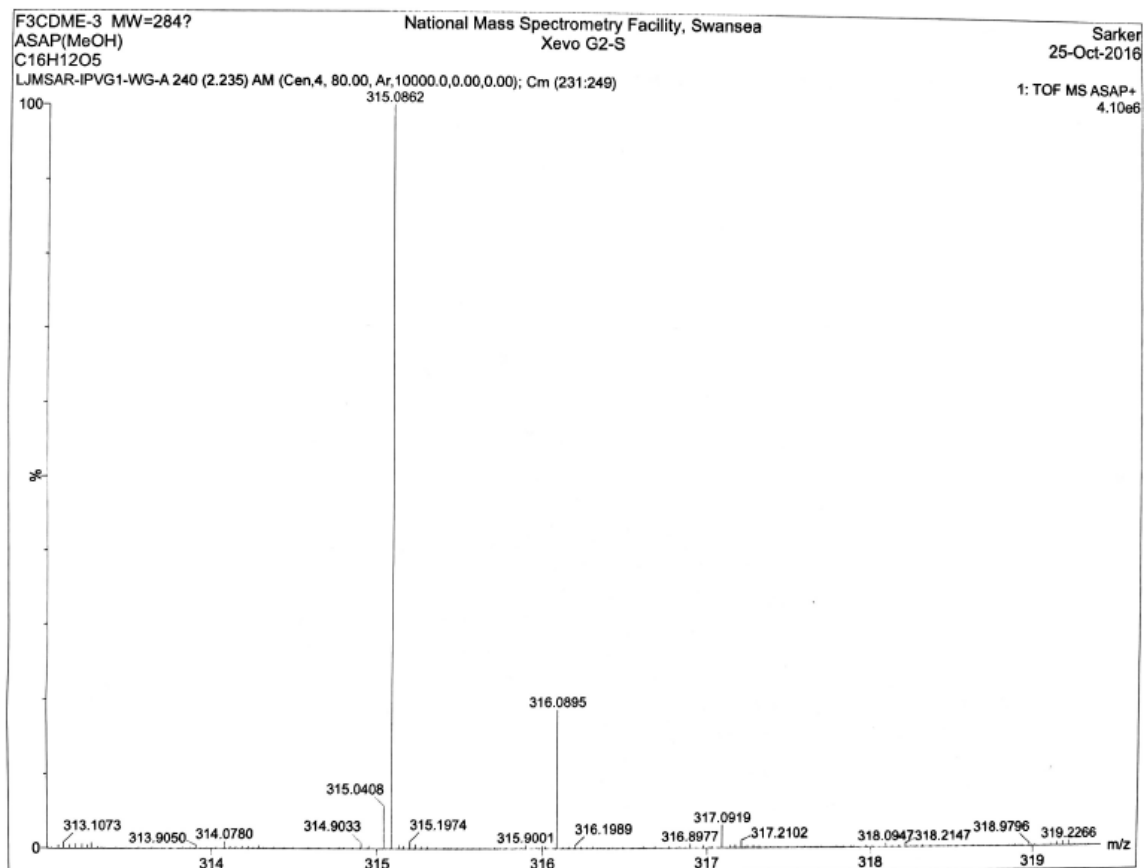
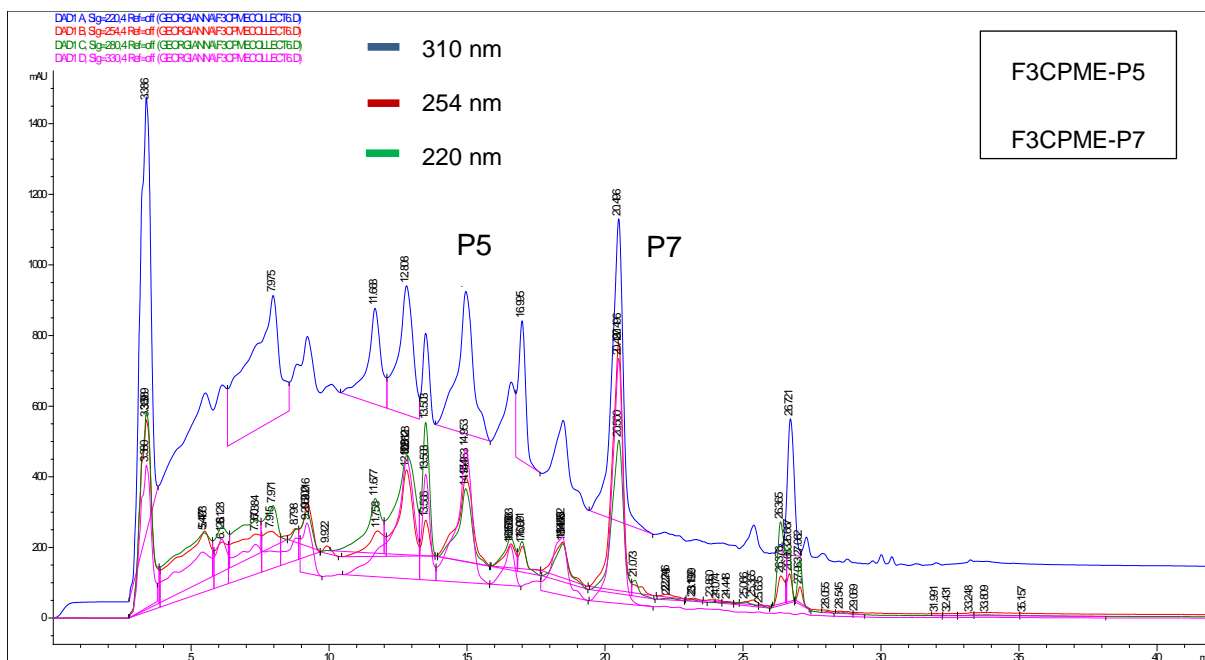


Figure 85 MS spectrum of F3CD-Me-P3

3.4.2.2 Isolation of compounds from F3 CP-Me

Because fraction F4 CP-Me yielded only 42.6 mg, an appropriate HPLC method for isolation could not be developed, given the complex mix of semi-polar compounds present in the methanol fraction.

The F3 CP-Me chromatogram (Figure 86) showed some separation between compounds using the standard gradient method and five main compounds were observed, of which compound P7 showed the best separation .



The chromatogram in Figure 90 below shows that the concentration of apigenin was higher than that of F3CP-Me-P5 and it affected the cut-off point at 2500 mAU for the second peak (Band I).

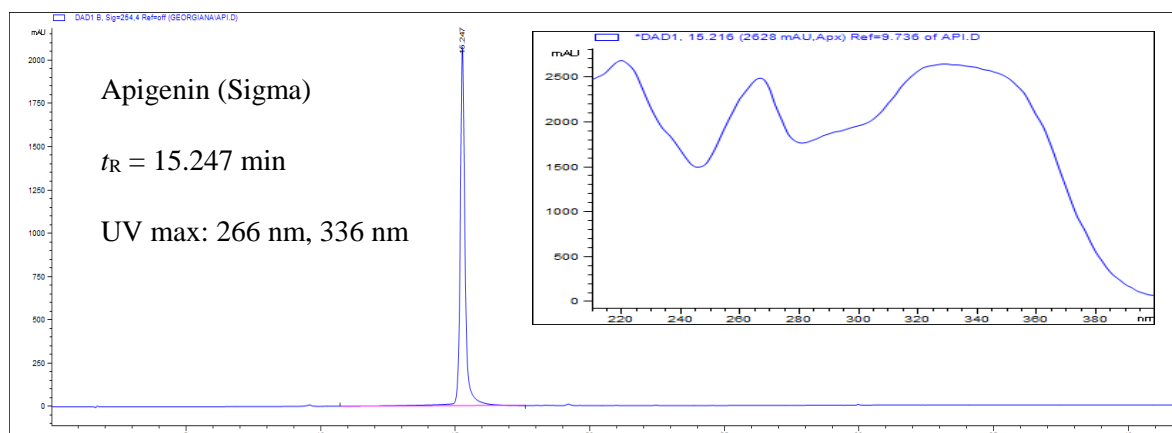


Figure 88 Analytical chromatogram of apigenin, 10 mg/ml

Because only 2.5 mg of F3CP-Me-P5 was isolated from F3CP-Me using preparative HPLC, further studies for structural elucidation or assays for bioactivity could not be carried out.

Isolation of F3 CP-Me-P7(IV)

A second compound, F3CPME-P7(IV), was isolated and purified from F3 CP-Me and Figure 91 shows the analytical chromatogram of F3CP-Me-P7(IV) in the standard solvent system.

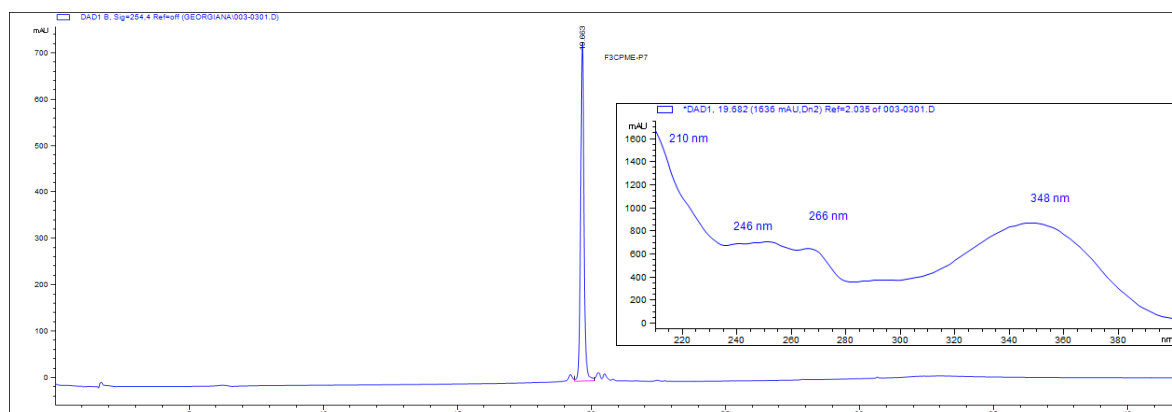


Figure 89 Analytical HPLC chromatogram of F3CP-Me-P7(IV) and recorded UV spectrum

3.4.2.3 Isolation and characterisation of compounds from F3 GT-Me

The preparative HPLC chromatogram of F3 GT-Me (Figure 90) shows the presence of two main compounds with retention times of 17.171 min and 19.981 min, respectively.

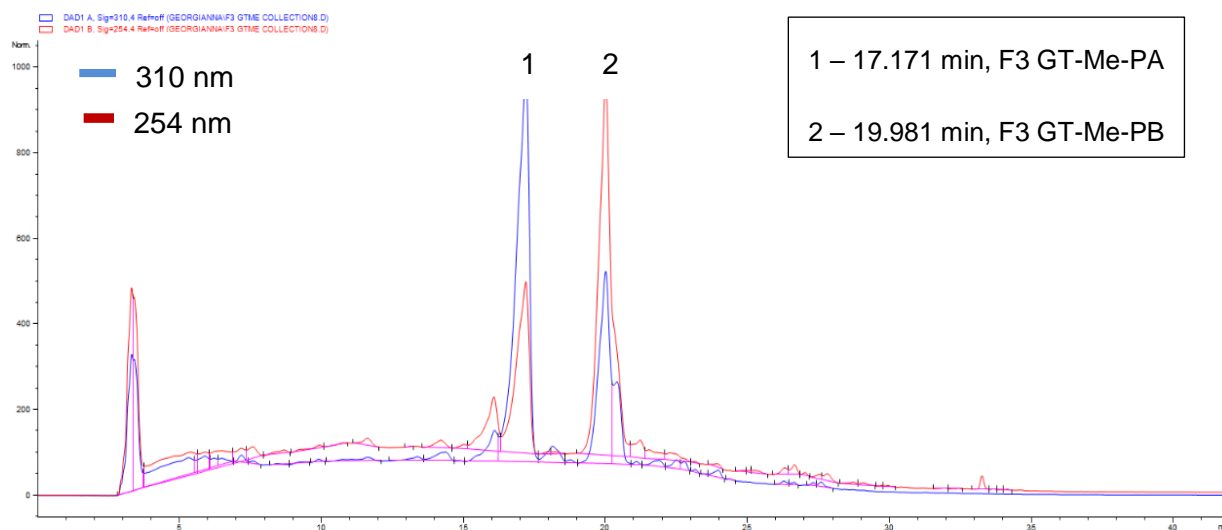


Figure 90 Preparative HPLC chromatogram for F3 GT-Me

After isolation, the weight of these compounds was 43.4 mg and 32.6 mg respectively, and the analytical HPLC chromatograms confirmed they were more than 90% pure (Figures 93 and 97).

Structural characterisation of F3 GT-Me-P4/PA

The analytical HPLC chromatogram of F3 GT-Me-P4/PA showed a pure compound with a retention time of 11.15 min, almost 6 min faster than the t_R of the same compound in the fraction mixture (Figure 91). The UV spectrum confirmed a possible isoflavone, flavanone or dihydroflavonole structure, according to Mabry, Markham and Thomas (1970, p.165-226), with a strong signal for Band II (around 280 nm) and a small shoulder for Band I.

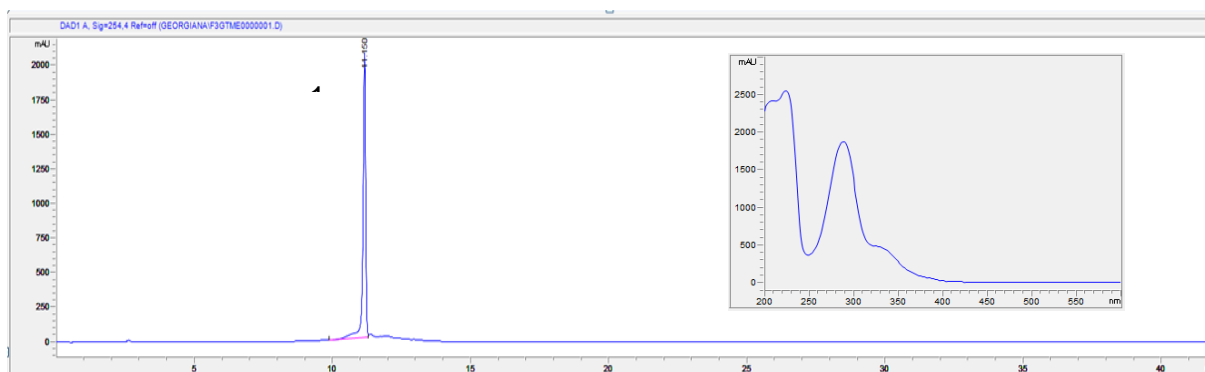


Figure 91 Analytical HPLC chromatogram for F3 GT-Me-P4/PA, 1 mg/ml

F3GTME-P4/PA was identified as the flavanone sakuranetin (Figure 92).

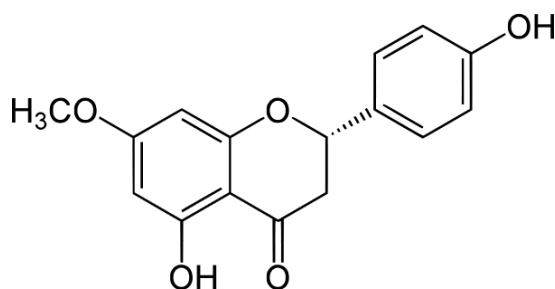


Figure 92 Chemical structure of sakuranetin C₁₆H₁₄O₅, 286 g/mol

The MS data showed a molecular ion [M-H]⁻ at *m/z* 285.07, which is compatible with the formula C₁₆H₁₄O₅ for sakuranetin and the molecular weight of 286 g/mol. The NMR spectra also confirmed the identity. See supplemental material in Appendix B.1.

The ¹H and ¹³C NMR spectra confirm precipitate F3GT-Me-P4/PA as sakuranetin (Appendix B.1).

The values of the chemical shifts identified in the NMR spectra were also compared to literature data produced by Grecco *et al* (2014), Mabry *et al* (2012, p. 330) and Agrawal (1989). The assignments are depicted in Figure 93, while Figure 94 shows the literature assignments.

The ¹H-NMR spectrum (CD₃OD, 400 MHz) revealed the CH₃-O signals at δ = 3.80 ppm (s, 3H) and also a singlet at 6.04 ppm (2H), corresponding to the C6 and C8 protons. The C2 H is a dd at 5.36 ppm (1H) since this proton couples with each of the C3 protons (J = 13.0 and 3.0 Hz), and the two geminal protons at C3 (H_a and H_b) present dd-s at 2.71 ppm and 3.14 ppm respectively. The two chemical shift values are different due to the deshielding produced by the aromatic ring on the space neighbouring H_b. The H_a proton shows J = 17.2 Hz as geminal coupling with H_b and J = 3 Hz for the coupling with H at C2. The H_b proton shows a J = 13 Hz coupling constant with C2 proton.

In the phenol ring B, protons 2' and 6' and protons 3' and 5' are equivalent. The former show a dd signal, (2H) at 7.32 ppm, J = 8.0 Hz, due to the coupling with the vicinal protons.

The ¹³C NMR spectra (CD₃OD, 400 MHz) showed peaks around δ 56.28 for the methoxy group, 165.27, 164.25, 159.11 ppm for aromatic C atoms in positions 7, 5, 8a deshielded by neighbouring O atoms. Also deshielded C atoms C4, C2, C-1' and C4' have assigned ppm values of 198.25, 80.64, 130.97, 169.58 ppm respectively. The chemical shifts and the

coupling values in the spectra are consistent with the structure of sakuranetin (5,4'-dihydroxy-7-methoxyflavanone).

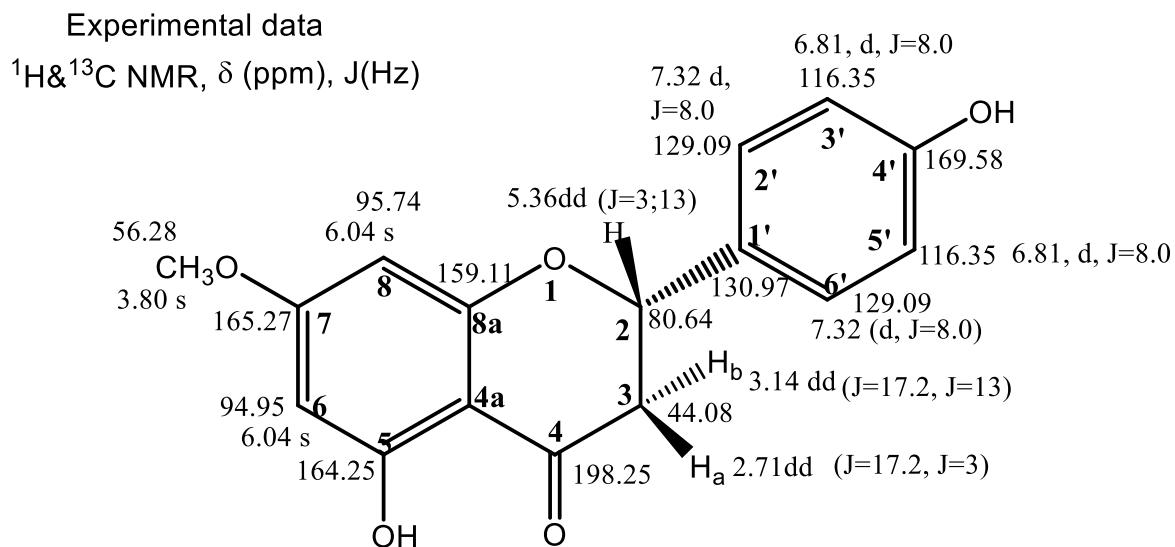


Figure 93 Experimental NMR assignments for F3GT-Me-P4/PA as sakuranetin

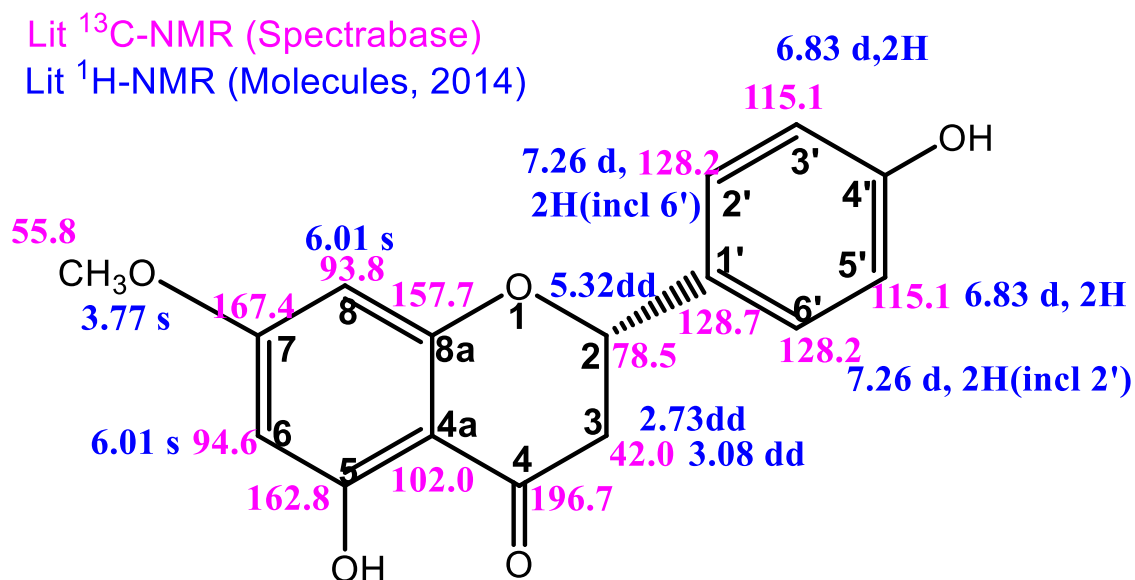


Figure 94 NMR assignments presented in literature for sakuranetin (in blue or magenta depending on source; references in text)

Isolation of F3 GT-Me-PB/P6

The isolated compound F3-GT-Me-PB eluted at 11.6 min, almost 9 minutes sooner than its elution time from the mixture F3 GT-Me (Figure 90). Figure 95 shows the analytical chromatogram after isolation.

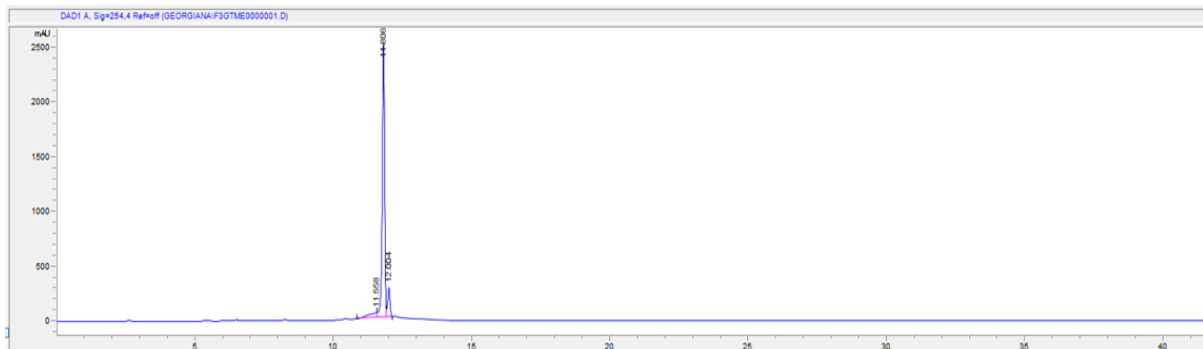


Figure 95 Analytical HPLC chromatogram for F3 GT-Me-PB/P6, 1 mg/ml

The UV spectrum showed two intense peaks corresponding to Band II, at 265 nm and for Band I at 366 nm, indicating the presence of a flavanone or flavonol (Figure 96).

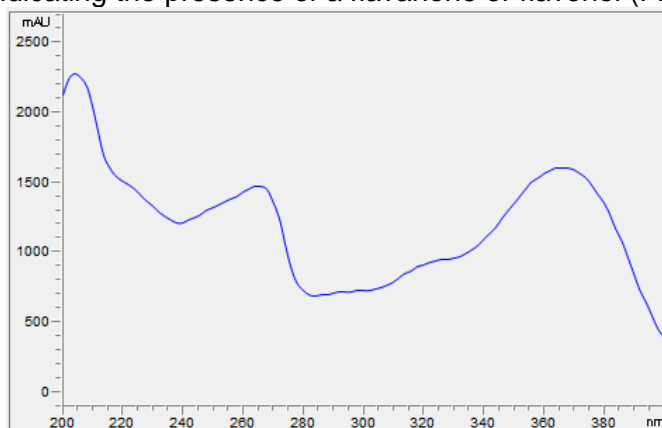


Figure 96 UV spectrum of Peak 2 as F3 GT-Me-PB/P6

3.5 Study 5: Cytotoxicity assay and luciferase assay in AREc32 cells of selected polyphenolic compounds: apigenin, genkwanin, hesperetin, hispidulin, kaempferol, luteolin, naringenin, quercetin, sakuranetin and velutin.

The flavonoids apigenin, genkwanin, hesperetin, hispidulin, kaempferol, luteolin, naringenin, quercetin, sakuranetin and velutin were tested in AREc32 cells for toxicity using the MTT assay in order to identify a non-cytotoxic concentration ($\geq 90\%$ cell viability) of each phytochemical compound to then be able to safely check their potential to activate the Nrf2/ARE signaling pathway, which translates into a measurable increase of luciferase activity in the luciferase reporter assay.

3.5.1 Cytotoxicity assay results for selected polyphenolic compounds: apigenin, genkwanin, hesperetin, hispidulin, kaempferol, luteolin, naringenin, quercetin, sakuranetin and velutin

Apigenin below (Figure 97) registered consistent cell viabilities of over 65% within 1 and 50 μM (94.39%-74.84%); and the concentration considered appropriate for the luciferase assay was 10 μM , which exerted a cell viability of 92.93%

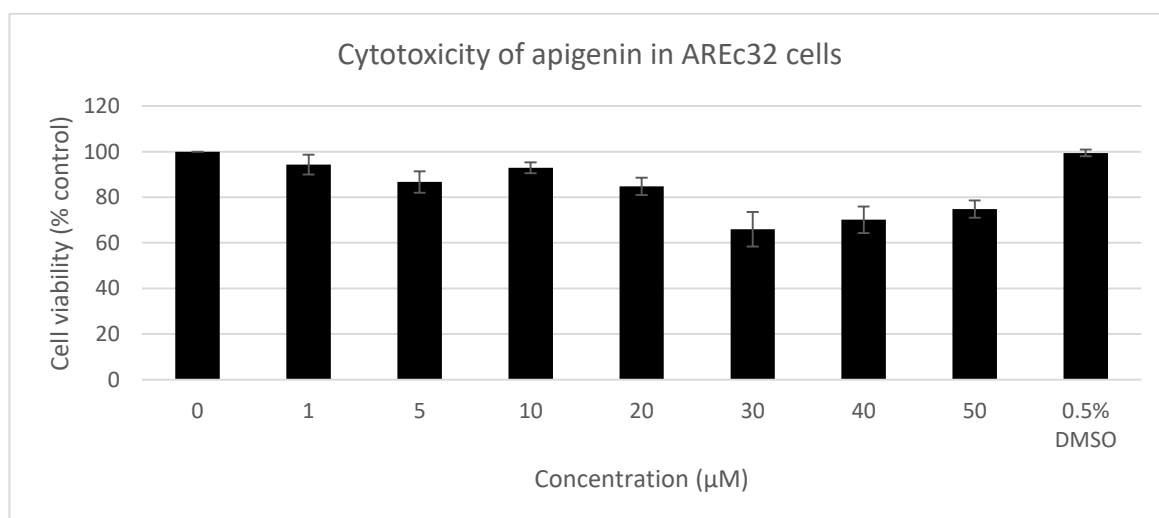


Figure 97 Cell viability as percentage to control (0 mg/ml) observed after treatment of AREc32 cells for 24 h with apigenin (1-50 μM). DMSO represents the vehicle control and its concentration is expressed as v/v%. Results show the mean \pm SEM (n=3, 3 replicates)

Genkwanin (Figure 98) showed a gradual loss of cell viability as the concentration of treatment increased from 1 μM to 50 μM , from 92.72% to 43.40% cell viability respectively. The most appropriate dose for further luciferase assay was identified as 1 μM , as this was the only dose that did not affect the cells beyond 90% cell viability, while the next dose up, at 5 μM caused a cell viability of 86.70%.

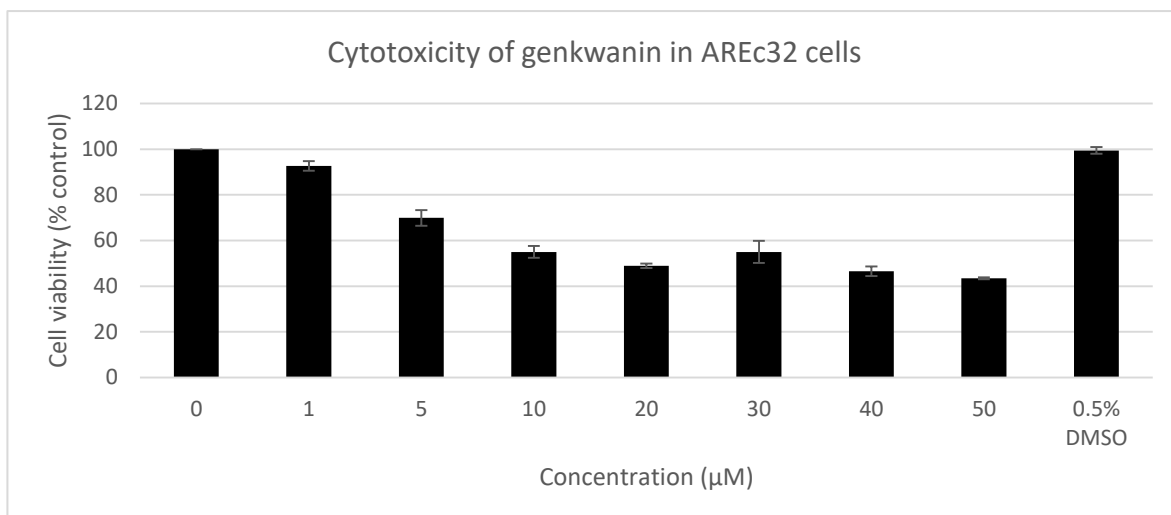


Figure 98 Cell viability as percentage to control (0 mg/ml) observed after treatment of AREc32 cells for 24 h with genkwainin (1-50 µM). DMSO represents the vehicle control and its concentration is expressed as v/v%. Results show the mean +/- SEM (n=3, 3 replicates)

Figure 99 shows that hesperetin was fairly non-cytotoxic to AREc32 at concentrations between 1 µM and 40 µM (96.79%-96.48% cell viability), although it did cause a decrease to 73.31% cell viability at the highest non-cytotoxic concentration of 40 µM. Hesperetin was therefore subsequently tested at the dose of 40 µM in the luciferase reporter assay.

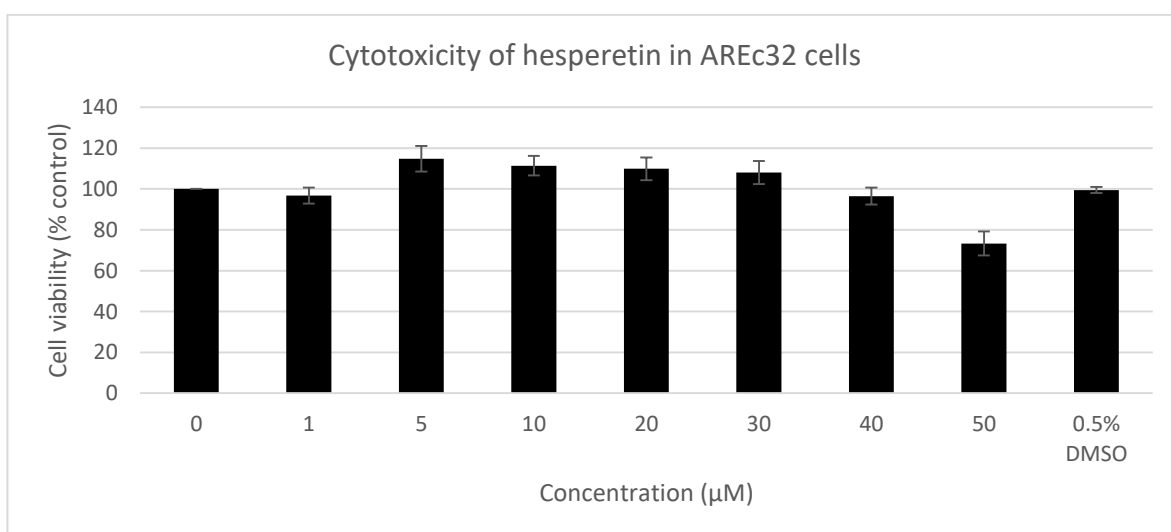


Figure 99 Cell viability as percentage to control (0 mg/ml) observed after treatment of AREc32 cells for 24 h with hesperetin (1-50 µM). DMSO represents the vehicle control and its concentration is expressed as v/v%. Results show the mean +/- SEM (n=3, 3 replicates)

Hispidulin (Figure 100) shows a range of cell viabilities that reach over 65% after treatment at concentrations between 1 µM and 50 µM. However, only the lowest concentration, 1 µM, reached a cell viability of over 90%, specifically 93.40%. This was the concentration chosen to use for treatment of AREc32 cells to measure luciferase activity linked to the Nrf2/ARE activation.

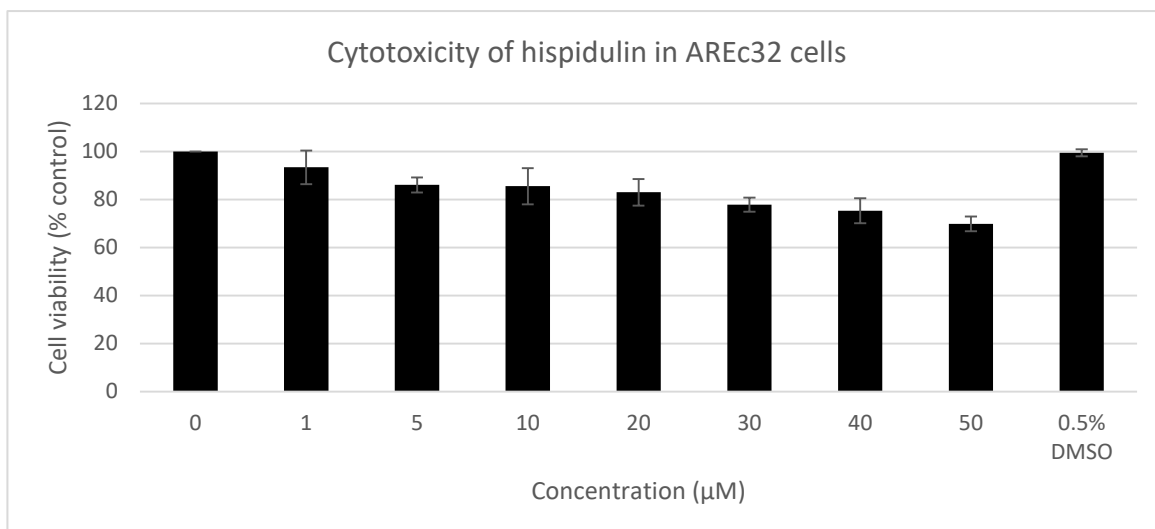


Figure 100 Cell viability as percentage to control (0 mg/ml) observed after treatment of AREc32 cells for 24 h with hispidulin (1-50 µM). DMSO represents the vehicle control and its concentration is expressed as v/v%. Results show the mean +/- SEM (n=3, 3 replicates)

AREc32 treatment with kaempferol (Figure 101) at concentrations between 1 µM and 40 µM revealed cell viabilities of over 65%, with the exception of the result of the treatment with kaempferol at 50 µM, which caused a very low cell viability of 24.71%. However, at 20 µM treatment, the cell viability went to 91.43%, before falling to 73.79% following 30 µM treatment; therefore the concentration appropriate for the luciferase assay was determined to be 20 µM for kaempferol.

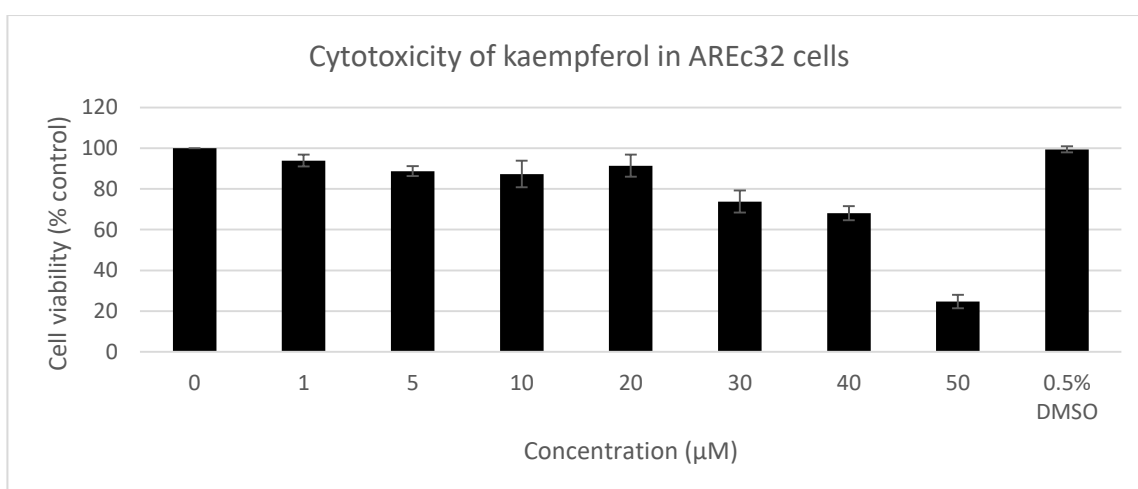


Figure 101 Cell viability as percentage to control (0 mg/ml) observed after treatment of AREc32 cells for 24 h with kaempferol (1-50 µM). DMSO represents the vehicle control and its concentration is expressed as v/v%. Results show the mean +/- SEM (n=3, 3 replicates)

Figure 102 shows the cytotoxicity exerted by luteolin in AREc32 cells over a range of dosage from 1 µM to 50 µM, resulting in 92.38% to 66.16% cell viability, respectively. Similarly to hispidulin, the most appropriate non-cytotoxic concentration of luteolin to be used in further testing was 1 µM.

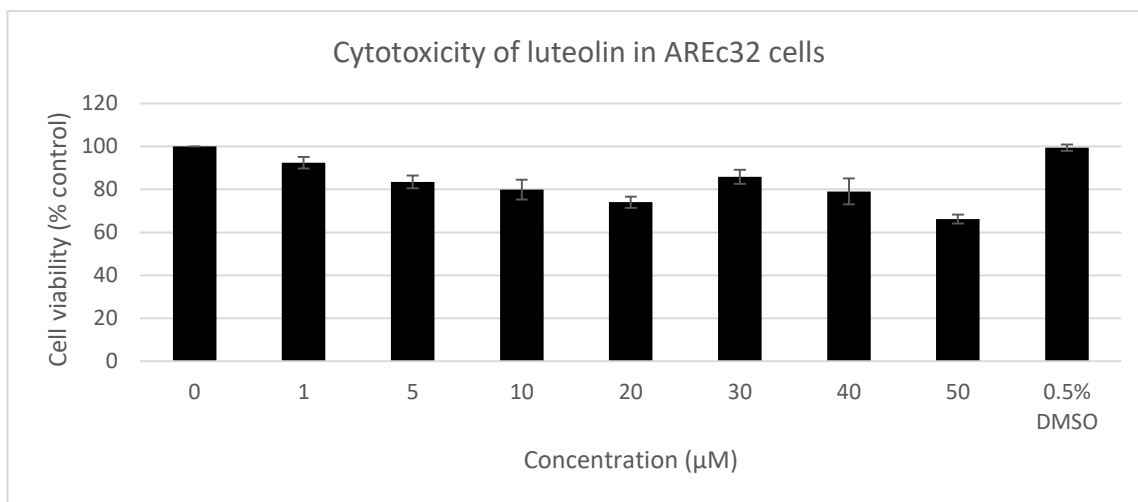


Figure 102 Cell viability as percentage to control (0 mg/ml) observed after treatment of AREc32 cells for 24 h with luteolin (1-50 µM). DMSO represents the vehicle control and its concentration is expressed as v/v%. Results show the mean +/- SEM (n=3, 3 replicates)

Naringenin (Figure 103) determined a range of cell viabilities starting from 97.64% after 1 µM treatment to as low as 57.88% after 50 µM overnight treatment. The concentration that determined a cell viability of 92% was 20 µM and it was chosen to be used in the subsequent luciferase assay, as the following concentration of 30 µM caused a slightly lower cell viability of 87.71%.

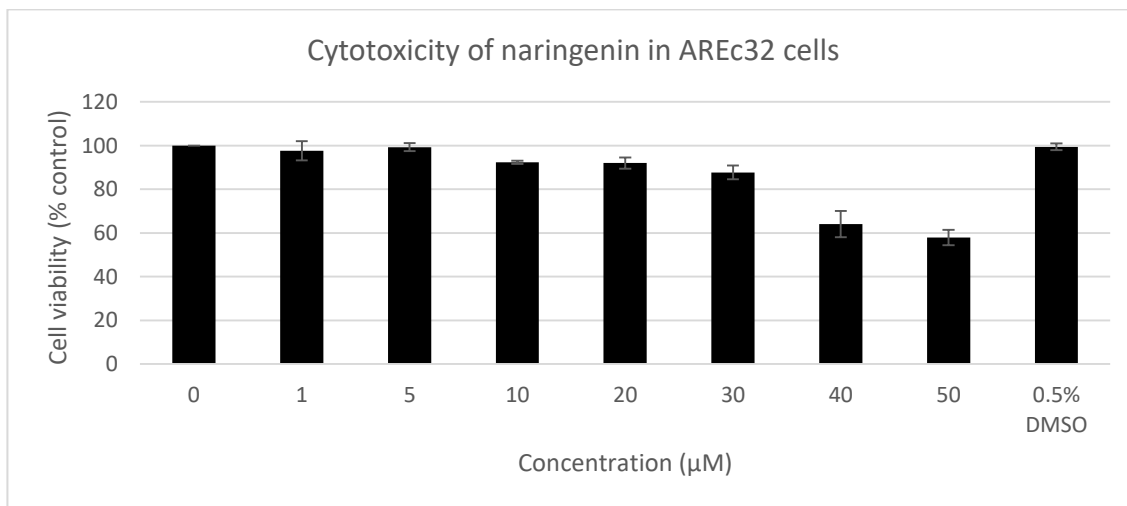


Figure 103 Cell viability as percentage to control (0 mg/ml) observed after treatment of AREc32 cells for 24 h with naringenin (1-50 µM). DMSO represents the vehicle control and its concentration is expressed as v/v%. Results show the mean +/- SEM (n=3, 3 replicates)

Quercetin (Figure 104) produced a decrease in cell viability ranging from 106.4% after treatment with 1 µM to 51.84% cell viability after 50 µM treatment. The steepest rise in cytotoxicity was marked by a 58.16% cell viability after overnight treatment of AREc32 cells with quercetin at 40 µM, noting a fall in cell viability of approximately 31% compared to the effect of the 30 µM dose treatment. Overall, the safest concentration of quercetin that could

draw forth an effect in the luciferase assay was considered to be 10 μM (94.98% cell viability).

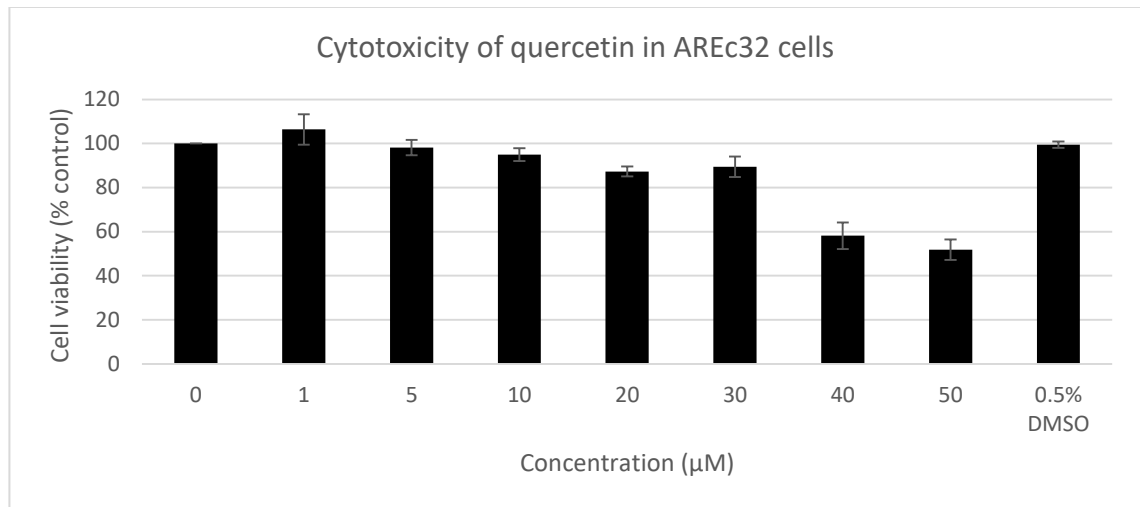


Figure 104 Cell viability as percentage to control (0 mg/ml) observed after treatment of AREc32 cells for 24 h with quercetin (1-50 μM). DMSO represents the vehicle control and its concentration is expressed as v/v%. Results show the mean \pm SEM (n=3, 3 replicates)

Figure 105 below shows the low cytotoxicity capability of sakuranetin in AREc32 cells at concentrations between 1 μM and 50 μM (100.29% - 88.59% cell viability). In this case, the most appropriate concentration of natural product to be used in the planned luciferase assay was 40 μM , which caused a cell viability of 91.70%.

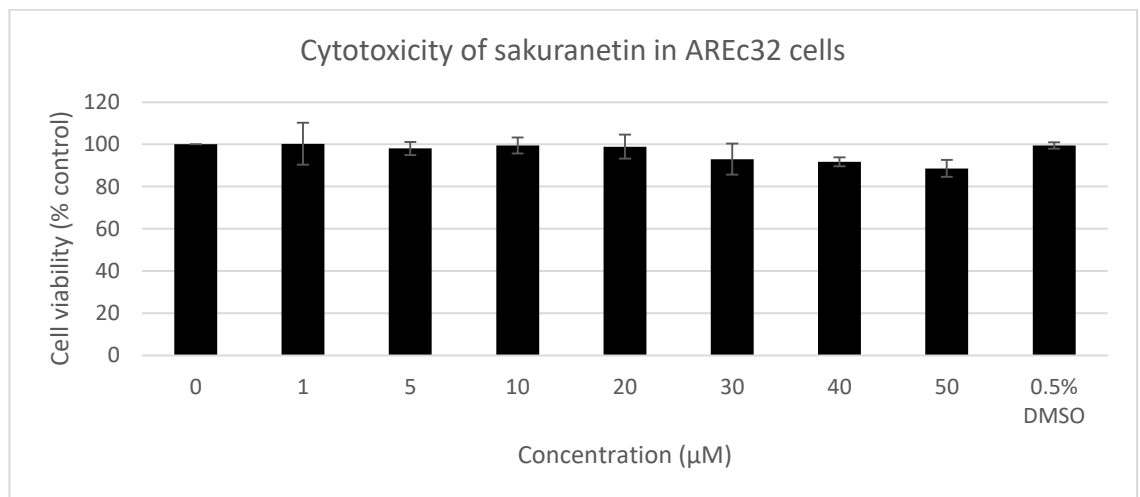


Figure 105 Cell viability as percentage to control (0 mg/ml) observed after treatment of AREc32 cells for 24 h with sakuranetin (1-50 μM). DMSO represents the vehicle control and its concentration is expressed as v/v%. Results show the mean \pm SEM (n=3, 3 replicates)

Velutin (Figure 106) showed a trend of cytotoxicity increase from 88.31% cell viability at 1 μM to 34.52% at 50 μM . Along the range of concentrations tested, only 5 μM was a dose that caused a reach over 90% of the cell viability (91.50%) after 24 h treatment. The next

concentration of velutin used was 10 μM and caused a 82.77% cell viability, which was considered too low so that 5 μM was used to treat cells for the luciferase assay.

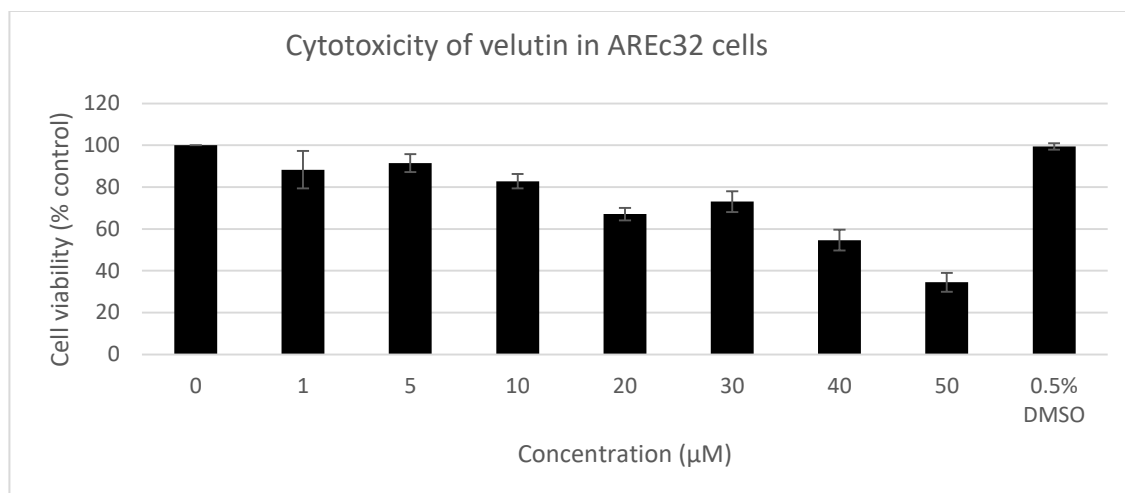


Figure 106 Cell viability as percentage to control (0 mg/ml) observed after treatment of AREc32 cells for 24 h with velutin (1-50 μM). DMSO represents the vehicle control and its concentration is expressed as v/v%. Results show the mean \pm SEM (n=3, 3 replicates)

Overall, the lowest concentration of flavonoids deemed non-cytotoxic for the luciferase assay was 1 μM (genkwain, hispidulin, luteolin), while most compounds maintained a high cell viability at concentrations between 5 μM and 20 μM . The highest concentration of flavonoids deemed non-cytotoxic for the luciferase assay was 40 μM , for hesperetin and sakuranetin.

3.5.2 Luciferase assay results on AREc32 cells for selected polyphenolic compounds: apigenin, genkwain, hesperetin, hispidulin, kaempferol, luteolin, naringenin, quercetin, sakuranetin and velutin

The relative luciferase activity of the known flavonoids that were selected for testing is presented in Figure 107 below. The figure shows that the treatment of AREc32 cells with the positive control, the known Nrf2 activator tBHQ, caused a fold increase of 7.9 times than in the absence of treatment (control).

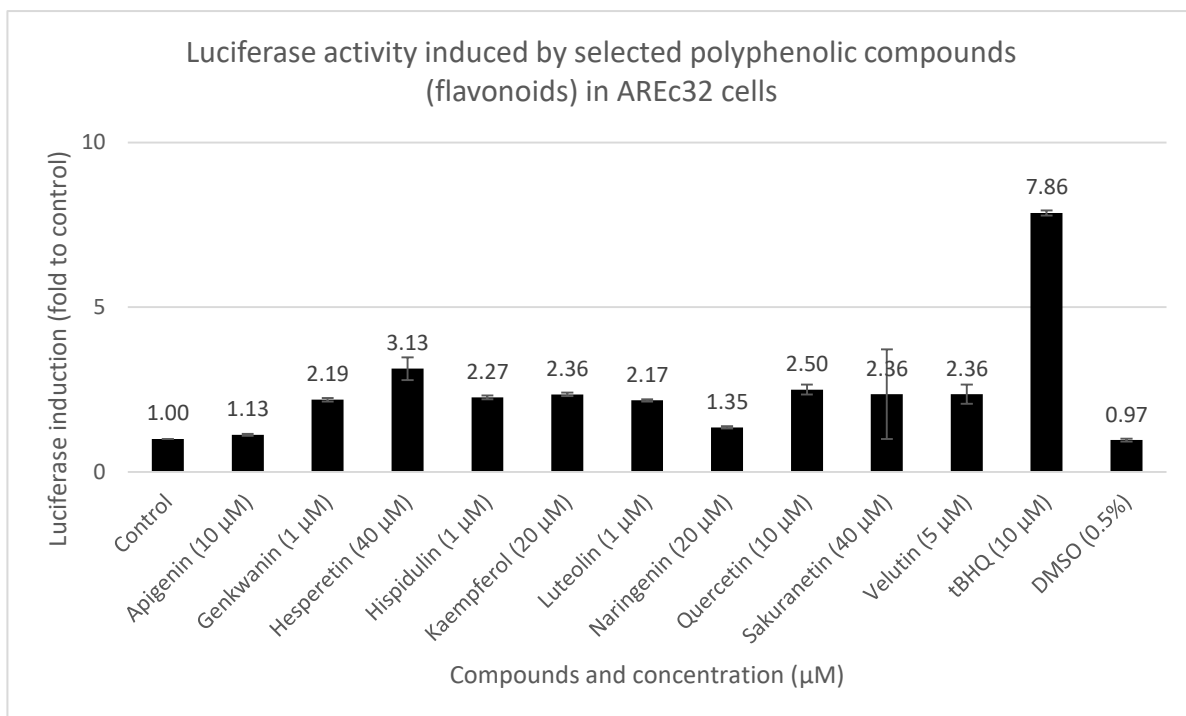


Figure 107 Effect of various flavonoids on the induction of luciferase activity and tBHQ as positive control. AREc32 cells were incubated for 24 h with non-cytotoxic concentrations of apigenin, genkwanin, hesperetin, hispidulin, kaempferol, luteolin, naringenin, quercetin, sakuranetin and velutin. DMSO represents the vehicle control and its concentration is expressed as v/v%. Values show mean \pm SEM (n=3, 3 replicates), control=1.

The bioactive phytochemicals tested showed an induction in luciferase activity between 1.1-fold, for apigenin, to 3.1-fold, for hesperetin. The highest fold-induction of luciferase activity was noted for quercetin, kaempferol, sakuranetin, velutin and hispidulin, between 2.5-fold for quercetin at 10 µM and 2.3-fold for hispidulin at 20 µM. Kaempferol (20 µM), sakuranetin (40 µM) and velutin (5 µM) all caused an induction of 2.4-fold to control.

Luteolin was previously reported as an inhibitor of the Nrf2/ARE signaling pathway by decreasing the Nrf2 expression at mRNA and protein level in A549 cells. (Tang *et al.* 2011). The luciferase activity measured in AREc32 cells after 24 h treatment with luteolin at 1 µM was 0.8 ± 0.05 fold relative to the induction caused by the vehicle control DMSO and was found to be Keap1-independent.

Tang *et al.* (2011) also reported luteolin to cause a dose-dependent reduction in the expression of the phase II detoxifying enzymes NQO1 and HO-1 in Caco2 (human colon cancer), MCF-7 (human breast cancer) and A549 (human non-small-cell lung cancer) cells. Sulforaphane was found to increase the mRNA level of NQO1 and HO-1 in Caco2 cells at a dose of 5 µM, but further RT-PCR tests would be necessary to establish if the selected flavonoids increase mRNA expression of Nrf2/ARE controlled detoxifying genes.

Because the luciferase activity exerted by tBHQ in AREc32 cells in the study by Tang *et al* (2011) was 9.7 ± 0.1 SD fold, and the average of fold induction achieved in this study was 6.46 ± 0.98 SD.

Although flavonoids have been the most studied group of compounds amongst polyphenols, it is still not fully understood how they manage to exert their effects on the Nrf2/ARE pathway in terms of transcriptional activation. However, research indicates that cytoprotective genes involved in phase 2 metabolism are largely induced by pro-oxidant compounds, such as ROS and electrophiles, and flavonoids, as well as tBHQ, show electrophilic properties (Lee-Hilz *et al.* 2006; Pandey and Rizvi, 2009).

3.6 Study 6: Determination of NQO1 gene expression induced by selected phytochemical compounds

According to Valerio *et al.* (2001), treatment of MCF-7 cells with quercetin (15 μ M for 24 h) resulted in a rise in the expression of the NQO1 gene activity, observed through increased luciferase activity, as well as increased NQO1 mRNA expression. The cells had been transfected with a reporter gene construct containing copies of the ARE element of the human NQO1 gene and it concluded in support of the hypothesis that dietary polyphenols increase the expression of phase II enzymes via a mechanism involving the ARE element. Therefore, complementary to the luciferase reporter assay screening of extracted and selected compounds with various flavonoid structures previously performed with AREc32 cells in Study 5, these Nrf2 inducers were also examined for their ability to increase the expression of NQO1 in MCF-7 cells.

3.6.1 Cytotoxicity assay of bioactive compounds on MCF-7 cells

In order to establish a safe concentration for the subsequent *in vitro* studies, all flavonoids were first assessed for cytotoxicity using the MTT assay.

The graphs below (Figures 108 – 117) represent the dose-dependent cell viability of MCF-7 cells as affected by various flavonoids.

Quercetin (Figure 108) produced a cell viability of 86.51% at 5 μ M, but at 2.5 μ M the cell viability was higher, at 93.37%. The lowest cell viability was recorded at the highest concentration and was 73.36%.

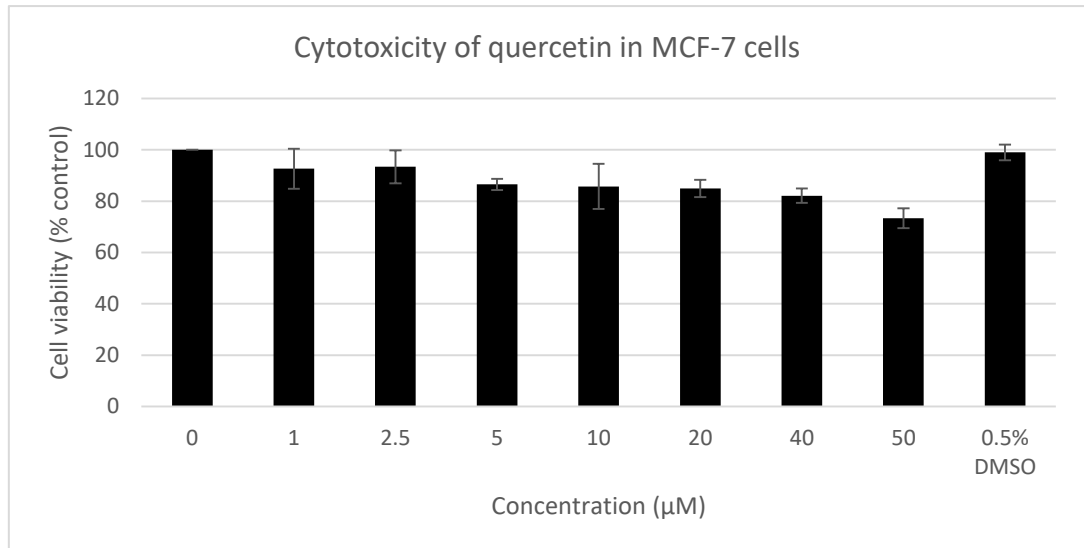


Figure 108 Cell viability as percentage to control (0 mg/ml) observed after treatment of MCF-7 cells for 24 h with quercetin (2.5 µM). DMSO represents the vehicle control and its concentration is expressed as v/v%. Results show the mean +/- SEM (n=3, 3 replicates)

Apigenin (Figure 109) was also fairly non-cytotoxic when used at the highest concentration of 50 µM, resulting in 74.83% cell viability and as the concentration dropped to 5 µM, the cell viability went up to 96.03%.

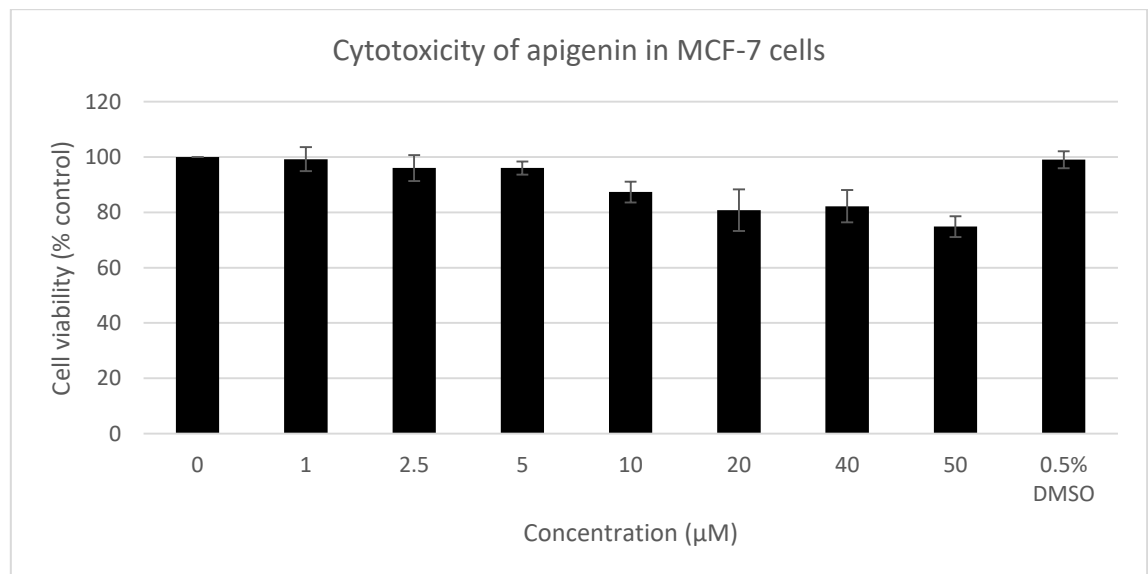


Figure 109 Cell viability as percentage to control (0 mg/ml) observed after treatment of MCF-7 cells for 24 h with apigenin (5 µM). DMSO represents the vehicle control and its concentration is expressed as v/v%. Results show the mean +/- SEM (n=3, 3 replicates)

Genkwanin (Figure 110) exhibited the highest and most consistent cytotoxicity in MCF-7 cells, starting from 10.95% after a treatment of 24 h with 50 µM, only increasing to 51% when cells were treated with 5 µM. The following lowest concentration of 2.5 µM caused a cell viability of 91.11%.

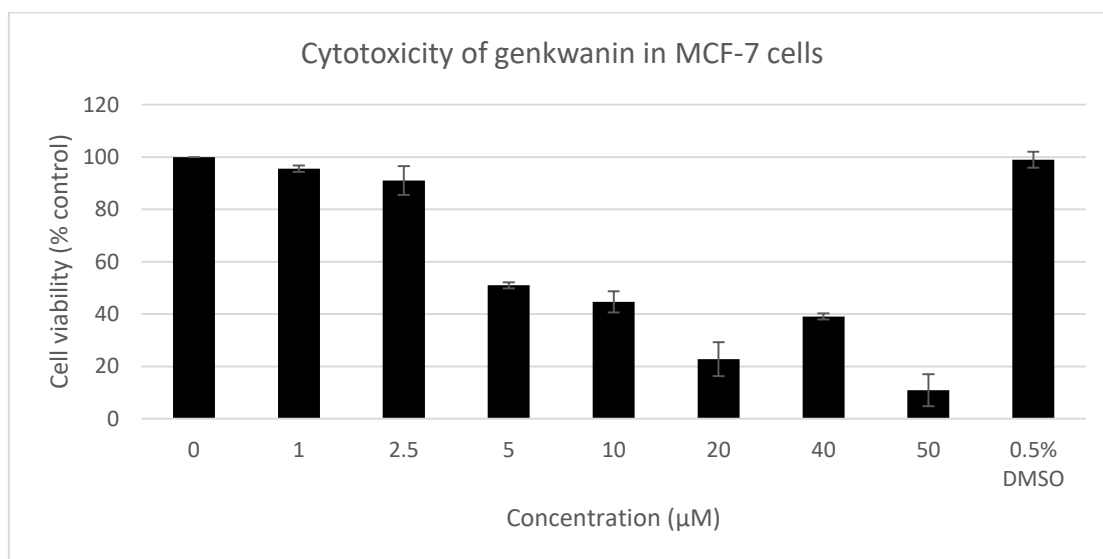


Figure 110 Cell viability as percentage to control (0 mg/ml) observed after treatment of MCF-7 cells for 24 h with genkwanin (2.50 µM). DMSO represents the vehicle control and its concentration is expressed as v/v%. Results show the mean +/- SEM (n=3, 3 replicates)

Hesperetin (Figure 111) showed a 24.33% cell viability when used at 50 µM, which increased steadily to 93.99% when hesperetin was used for overnight treatment of MCF-7 cells at 1 µM.

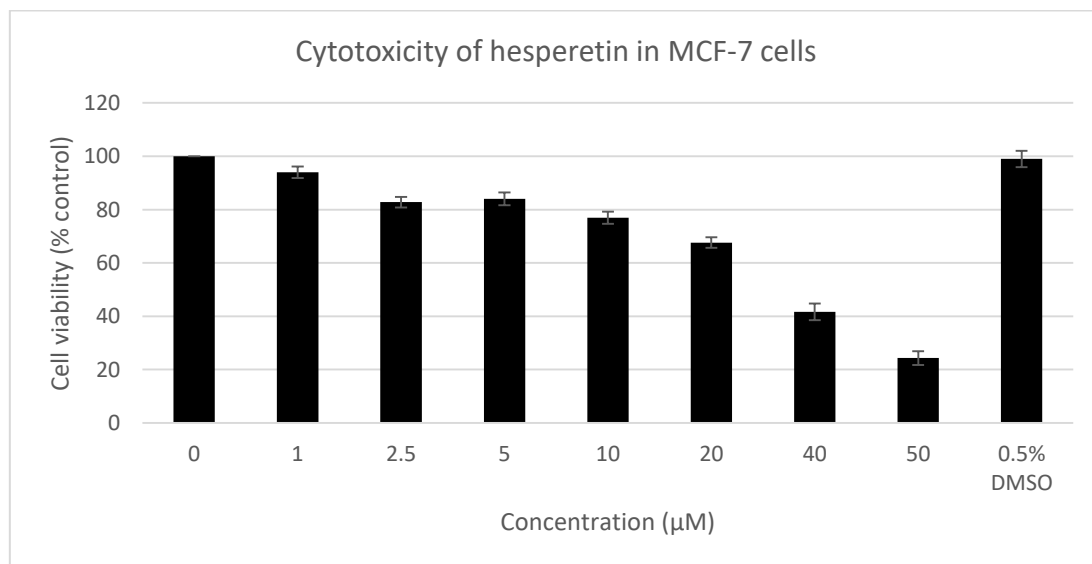


Figure 111 Cell viability as percentage to control (0 mg/ml) observed after treatment of MCF-7 cells for 24 h with hesperetin (1 µM). DMSO represents the vehicle control and its concentration is expressed as v/v%. Results show the mean +/- SEM (n=3, 3 replicates)

Figure 112 below shows that the compound hispidulin was fairly non-cytotoxic between 1 and 40 µM, reaching a cell viability of 94.76% at 2.5 µM treatment. At 50 µM hispidulin caused a 14.8% cell viability.

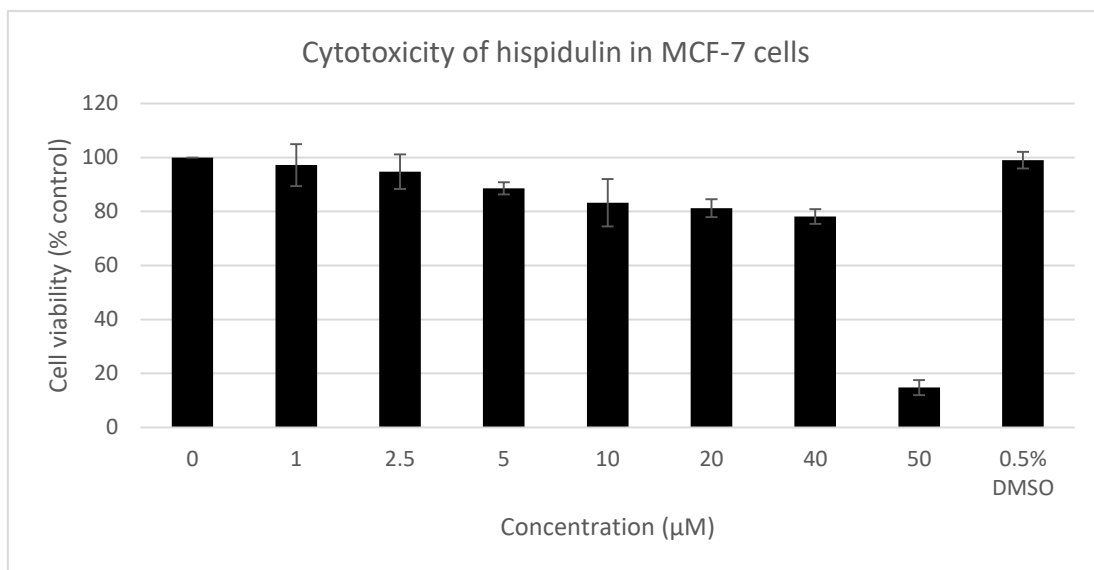


Figure 112 Cell viability as percentage to control (0 mg/ml) observed after treatment of MCF-7 cells for 24 h with hispidulin (2.5 µM). DMSO represents the vehicle control and its concentration is expressed as v/v%. Results show the mean +/- SEM (n=3, 3 replicates)

Figure 113 shows the cell viability profile created by kaempferol in MCF-7 cells and it was consistently high at concentrations applied in the range of 1-50 µM (95.56%-78.47%).

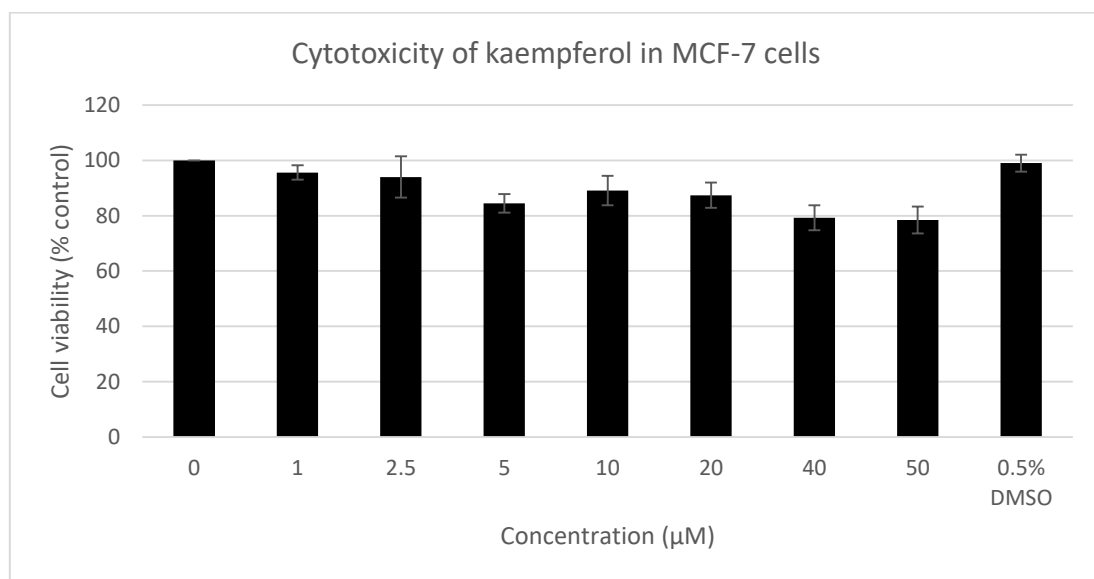


Figure 113 Cell viability as percentage to control (0 mg/ml) observed after treatment of MCF-7 cells for 24 h with kaempferol (2.5 µM). DMSO represents the vehicle control and its concentration is expressed as v/v%. Results show the mean +/- SEM (n=3, 3 replicates)

Luteolin (Figure 114) exhibited a steady cytotoxicity profile in MCF-7 cells when used between 1 and 50 µM, with cell viabilities dropping from 92.99% to 66.16% at 50 µM. The concentration of 2.5 µM of luteolin was considered non-cytotoxic, as it caused a 93.40% cell viability.

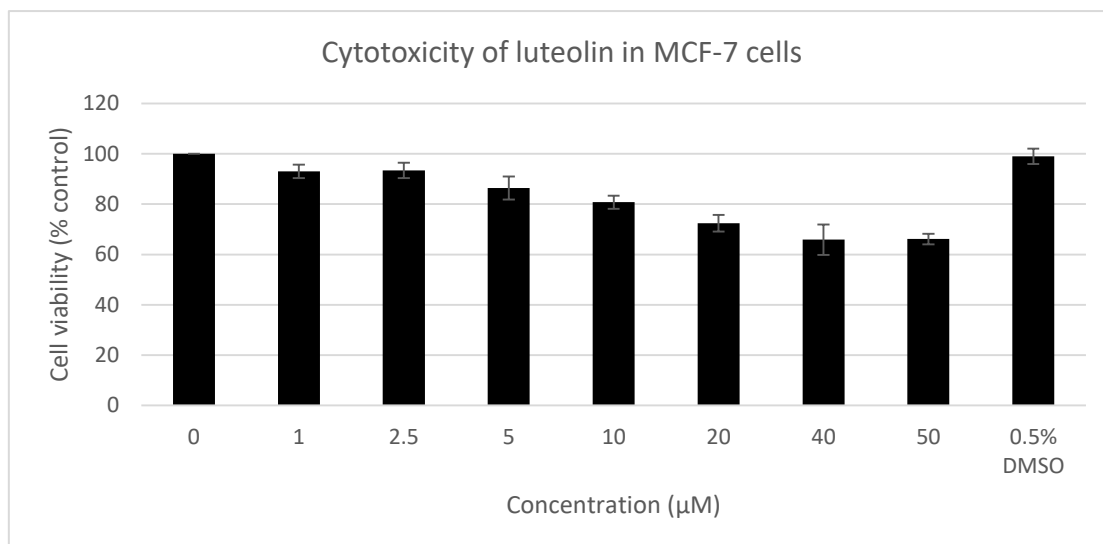


Figure 114 Cell viability as percentage to control (0 mg/ml) observed after treatment of MCF-7 cells for 24 h with luteolin (2.5 µM). DMSO represents the vehicle control and its concentration is expressed as v/v%. Results show the mean +/- SEM (n=3, 3 replicates)

Naringenin (Figure 115) was shown to exert high cytotoxicity at the highest concentrations, 40 µM and 50 µM, of 35.81% and 32.60% respectively. From the next lowest concentration of 20 µM the cell viability increased from 65.93% to 94.41% at 2.5 µM, the highest non-cytotoxic dose. At the lowest concentration of 1 µM naringenin the cell viability was 98.01%.

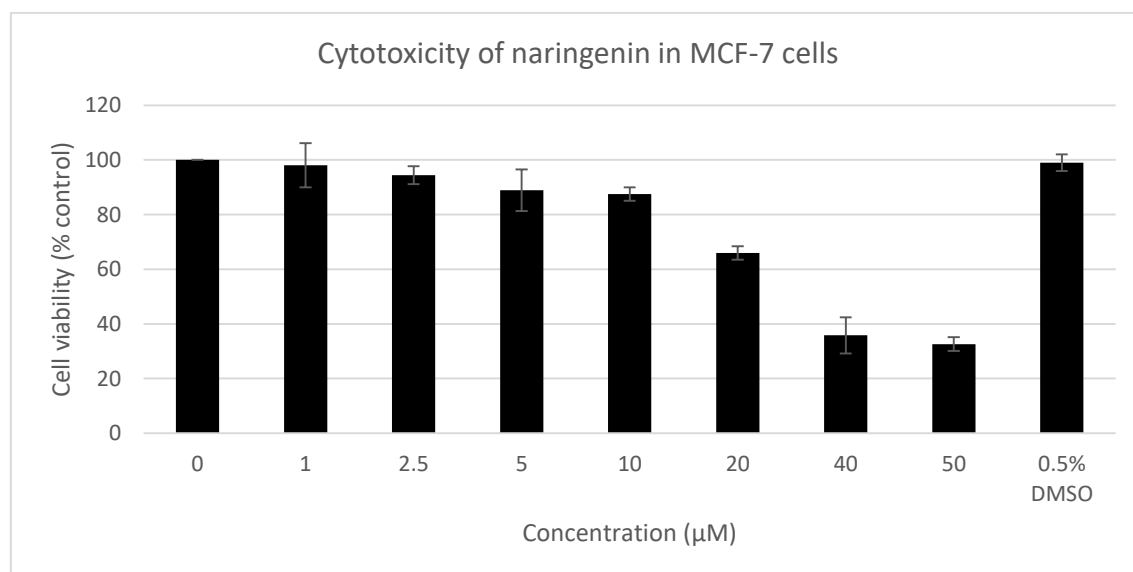


Figure 115 Cell viability as percentage to control (0 mg/ml) observed after treatment of MCF-7 cells for 24 h with naringenin (2.5 µM). DMSO represents the vehicle control and its concentration is expressed as v/v%. Results show the mean +/- SEM (n=3, 3 replicates)

Treatment of MCF-7 cells with sakuranetin (Figure 116) resulted in the highest cell viability profile out of all the flavonoids tested. The cell viability varied between 99.28% at the lowest concentration of 1 µM and 83.60% at 50 µM.

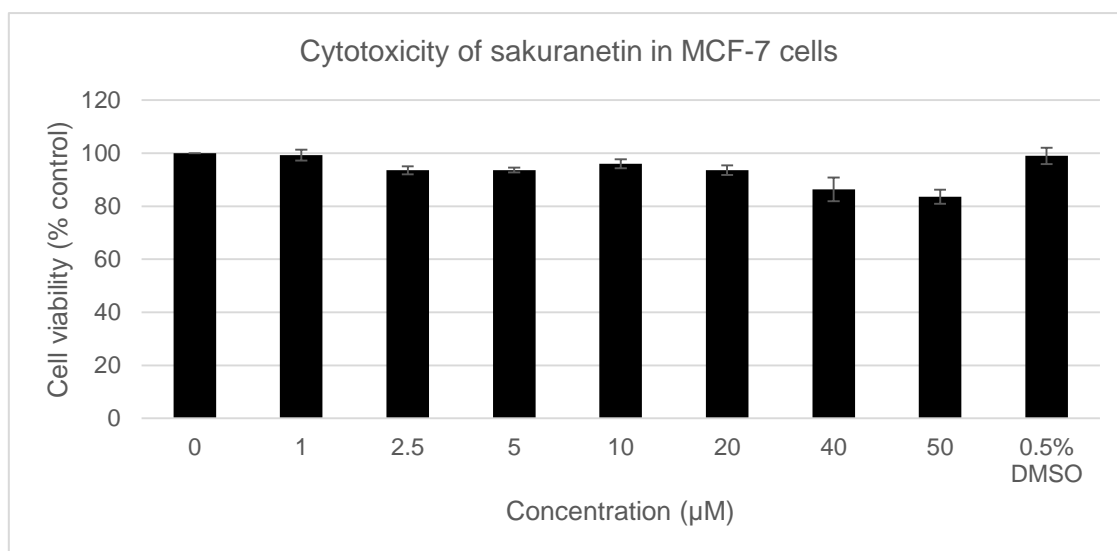


Figure 116 Cell viability as percentage to control (0 mg/ml) observed after treatment of MCF-7 cells for 24 h with sakuranetin (20 µM). DMSO represents the vehicle control and its concentration is expressed as v/v%. Results show the mean +/- SEM (n=3, 3 replicates)

Figure 117 below shows the cytotoxicity profile of velutin in MCF-7 cells at concentrations between 1 µM and 50 µM (85.85%-74.04%).

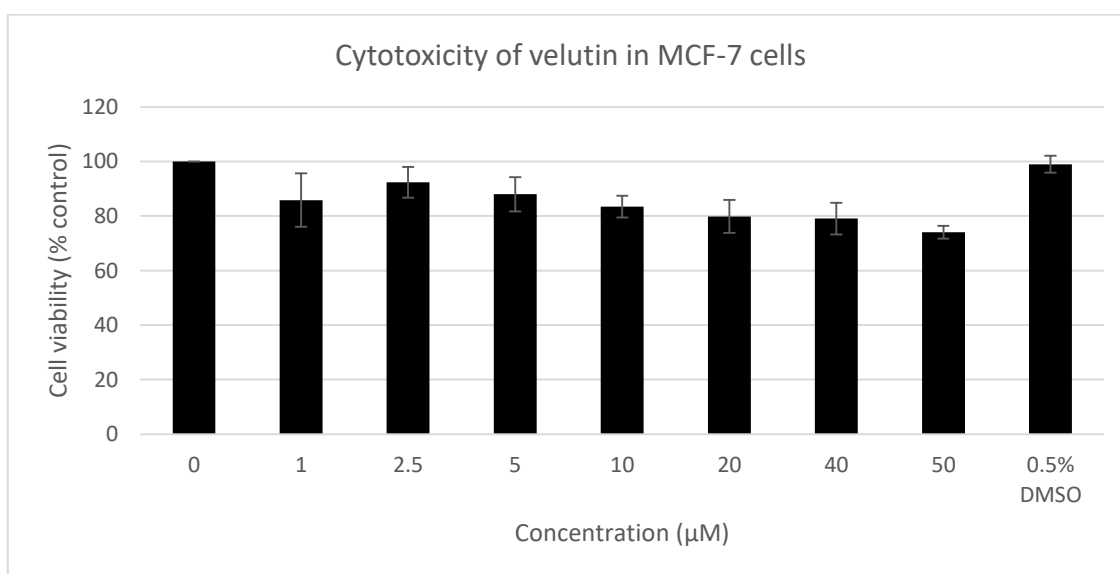


Figure 117 Cell viability as percentage to control (0 mg/ml) observed after treatment of MCF-7 cells for 24 h with velutin (1-50 µM). DMSO represents the vehicle control and its concentration is expressed as v/v%. Results show the mean +/- SEM (n=3, 3 replicates)

Overall, the cytotoxicity study of flavonoids in MCF-7 cells revealed cancer cytotoxicity potential for genkwainin (confirmed in literature), hispidulin, naringenin and hesperetin. Genkwainin (20 µM) decreased MCF-7 cell viability to 23% after 24 h treatment and hispidulin (50 µM) proved even more cytotoxic, causing 15% cell viability to control.

Li *et al* (2017) reported on the preparation of nanosuspensions of genkwanin, using D-alpha tocopherol acid polyethylene glycol succinate, as an effective formulation for an anticancer drug. The nanosuspension of genkwanin also showed increased cytotoxicity in the following cancer cell lines: HeLa, HepG2, A549, as well as MCF-7, BT-474 and MDA-MB-453 (human breast cancer cell lines).

Hispidulin has been shown to have antiproliferative properties against MCF-7 and Hep-2 cells by Talib *et al* (2012) with IC₅₀ values of 10 and 19.5 µg/ml.

In trypan blue exclusion assays, naringenin was shown to have insignificant cytotoxic effects on various breast cancer cell lines, with IC₅₀ values higher than 200 µM (Yadegarynia *et al*, 2012).

Naringenin and sakuranetin were subsequently tested for detection of expression of NQO1 protein after 24 h treatment with MCF-7 cells. The results are presented in the following section.

3.6.2 Western Blotting results for induction of NQO1 by sakuranetin and naringenin

The flavanones sakuranetin (20 µM) and naringenin (5 µM) did not induce expression of NQO1 protein after 24 h treatment, as compared to the control (untreated MCF-7 cells). Figure 120 shows the results of sampling at three time points after treatment: 3 h, 6 h and 24 h.

Control samples at time 0 h and 24 h resemble the bands revealed under treatment conditions for both compounds used.

tBHQ as positive control significantly increased the expression of the NQO1 protein after 24 h treatment with 10 µM, compared to untreated control, causing overexposure in imaging (Figure 118, b).



Figure 118 Effect of 24 h treatment of MCF-7 cells with (a) sakuranetin and (b) naringenin on NQO1 protein expression.

Western Blotting should be performed for all the bioactive compounds, including a HO1 antibody that would reveal another detoxifying enzyme at around 33 kDa. The use of densitometric analysis of the blots to produce histograms would also provide insight into the results, as a quantitative approach.

Tanigawa *et al* (2007) show that tBHQ acts to induce Nrf2/ARE by stimulating the ubiquitination of Keap 1 protein, which in turn cannot act as a substrate adaptor for conjugation with ubiquitin to form a Keap1/Nrf2 complex that would normally remove Nrf2 and inhibit ARE transcriptional activity.

Sulforaphane and quercetin, on the other hand, do not promote the ubiquitination of Keap1 (Zhang *et al*, 2005).

Moreover, as tBHQ is a synthetic Nrf2 inducer which acts by creating oxidative stress via redox cycling, which is a distinct mechanism of Nrf2/ARE activation than that of the flavonoid quercetin or the organosulfur compound sulforaphane, the positive control for future studies with phytochemicals should be a Nrf2-promoting compound typical for the class of compounds screened. In detail, because tBHQ can undergo modifications that lead to the formation of reactive oxygen species, this causes the disruption of Nrf2 degradation process via Keap1 and promote its binding instead with the ARE transcriptional elements in the nucleus.

It was also noticed that the results were in agreement with the low Nrf2 induction levels sakuranetin and naringenin demonstrated in AREc32 cells (see Section 3.5.2), with 2.4 and 1.4-fold to control induction, respectively.

3.7 Study 7: Effect of selected flavonoids on ethacrynic acid-induced oxidative stress in MCF-7 cells

Flavonoids of similar structures to compounds isolated from GT-Me, CD-Me and CP-Me were previously screened for Nrf2 induction potential using AREc32 cells, finding a maximum of 3-fold induction (see Study 5). Subsequent experiments were carried out to evaluate the NQO1 gene expression in un-transfected MCF-7 cells. The cell line was selected based on its feature of overexpressing the Nrf2 transcription factor (Zhang *et al*, 2016).

Furthermore, using the same cell line, the cytoprotective potential of the flavonoids was challenged again by examining if they can provide protection against the oxidative stress inducer ethacrynic acid (ETA). The flavonoids apigenin, genkwanin, hesperetin, hispidulin, kaempferol, luteolin, naringenin, quercetin, sakuranetin and velutin were applied at non-cytotoxic concentrations determined in Study 6.

Figure 119 below shows the cytotoxicity profile of ETA in MCF-7 cells *in vitro* as a graph of cell viability (%) against ETA concentrations (μM), starting from 3.125 μM , dose which resulted in 93.58% cell viability, and going up to 1000 μM , causing a cell viability of 3.62%.

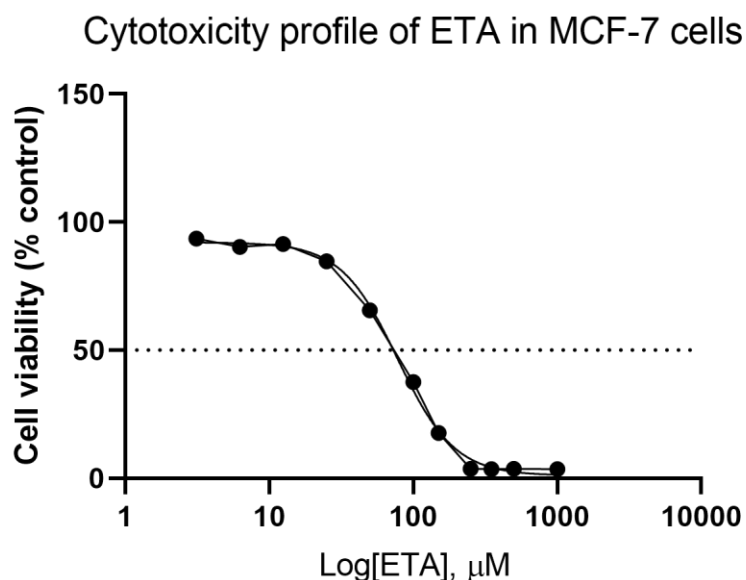


Figure 119 Cell viability as percentage to control (no treatment) observed after treatment of MCF-7 cells for 24 h with ethacrynic acid (3.125-1000 μM). Results of the MTT assay show the mean of 3 experiments (n=3, 2 replicates).

In the experimental conditions applied it was estimated that the median lethal dose of ETA in MCF-7 cells was 68.5 μM . Also to be noted is that the cytotoxicity of ETA lowered the cell viability to less than 90% starting from 25 μM and at 50 μM it decreased to 65.57%.

Figure 120 below shows the protection against ETA-induced cytotoxicity exerted by tBHQ, which was the positive control used throughout the bioassay-guided investigation as chemopreventive agent/Nrf2 inducer. MCF-7 cells pre-treated with tBHQ at 10 μM showed no cytotoxicity effect at the lowest dose of ETA (3.125 μM). The cell viability decreased to 71.63% after ETA treatment at the highest concentration of 1000 μM . The highest dose of ETA caused a cell viability 68% higher than in cells without pre-treatment.

MCF-7 cells were treated with 10 μM of tBHQ overnight before applying ETA at a range of concentrations. Figure 120 below shows the results of the cytotoxicity profile of ETA in pretreated cells, as well as in cells without pretreatment.

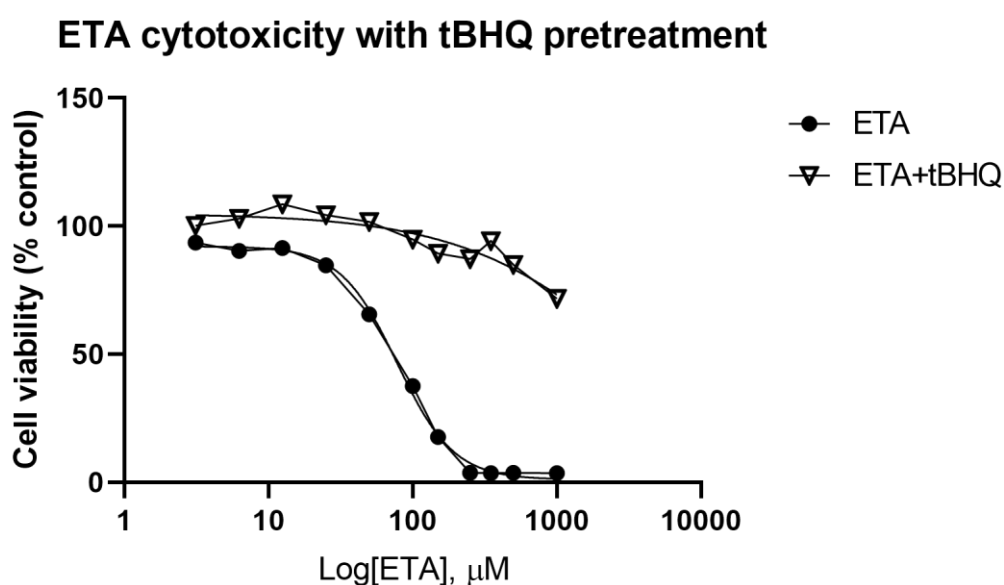


Figure 120 Cell viability as percentage to control (no treatment) observed after pre-treatment of MCF-7 cells for 24 h with tBHQ (10 μM) and ethacrynic acid (3.125-1000 μM). Results of the MTT assay show the mean of 2 experiments (total n=6). $P < .0001$, significant difference between the cytotoxicity of ETA in pretreated cells and the cytotoxicity of ETA alone.

The absolute LD_{50} of ETA in pretreated cells was 2463 μM , almost 36 times higher than the LD_{50} exhibited in cells without pretreatment.

Apigenin (Figure 121) also exerted a protective effect against ETA in MCF-7 cells, maintaining the cell viability at the highest dose of 1000 μM ETA at 53.17%, an increase of almost 50% than in the absence of pre-treatment. However, the lowest dose of ETA, 3.125 μM , caused a decrease in cell viability to 74.97%.

ETA cytotoxicity with apigenin pretreatment

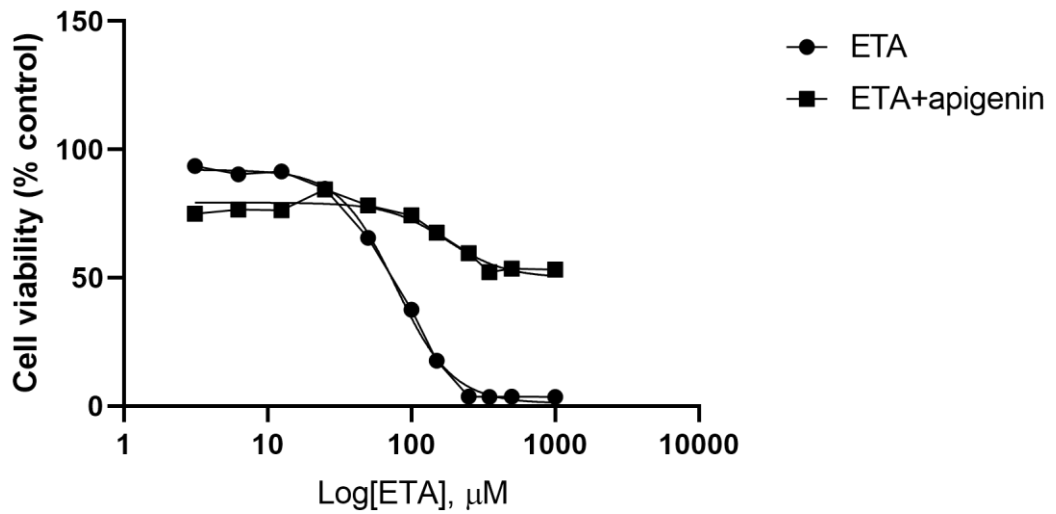


Figure 121 Cell viability as percentage to control (no treatment) observed after pre-treatment of MCF-7 cells for 24 h with apigenin (5 μM) and ethacrynic acid (3.125-1000 μM). Results of the MTT assay show the mean of 2 experiments (total n=6). P<.0001, significant difference between the cytotoxicity of ETA in pretreated cells and the cytotoxicity of ETA alone.

Genkwanin (Figure 122) also showed cytoprotective effects against ETA, causing an increased cell viability at the highest dose of ETA, from 4% to 60.7%. However, at the lowest doses of ETA, pretreated cells showed a lowered cell viability (around 80%) that of cells without genkwanin pretreatment. The LD₅₀ of genkwanin was calculated at 5384 μM, more than 70 times higher than the LD₅₀ of ETA in cells without pretreatment.

ETA cytotoxicity with genkwanin pretreatment

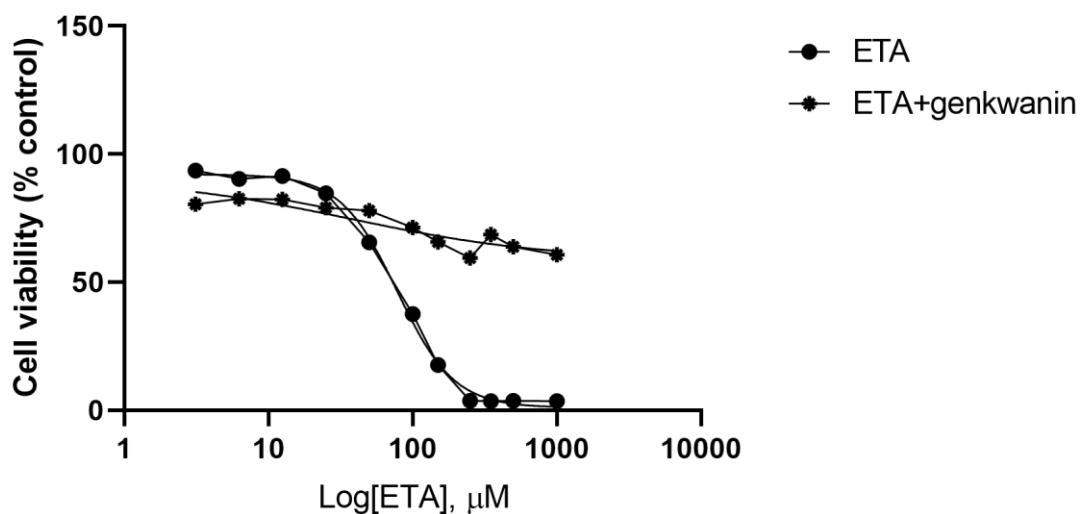


Figure 122 Cell viability as percentage to control (no treatment) observed after pre-treatment of MCF-7 cells for 24 h with genkwanin (2.5 μM) and ethacrynic acid (3.125-1000 μM). Results of the MTT assay show the

mean of 2 experiments (total n=6). $P < .0001$, significant difference between the cytotoxicity of ETA in pretreated cells and the cytotoxicity of ETA alone.

Pretreatment of MCF-7 cells with hesperetin at a dose of $1 \mu\text{M}$ offered good protection against the oxidative stress caused by ETA, with cell viabilities decreasing from 100.25% to 48.3%, increasing the LD_{50} of ETA almost 10 times, to $661 \mu\text{M}$ (Figure 123).

ETA cytotoxicity with hesperetin pretreatment

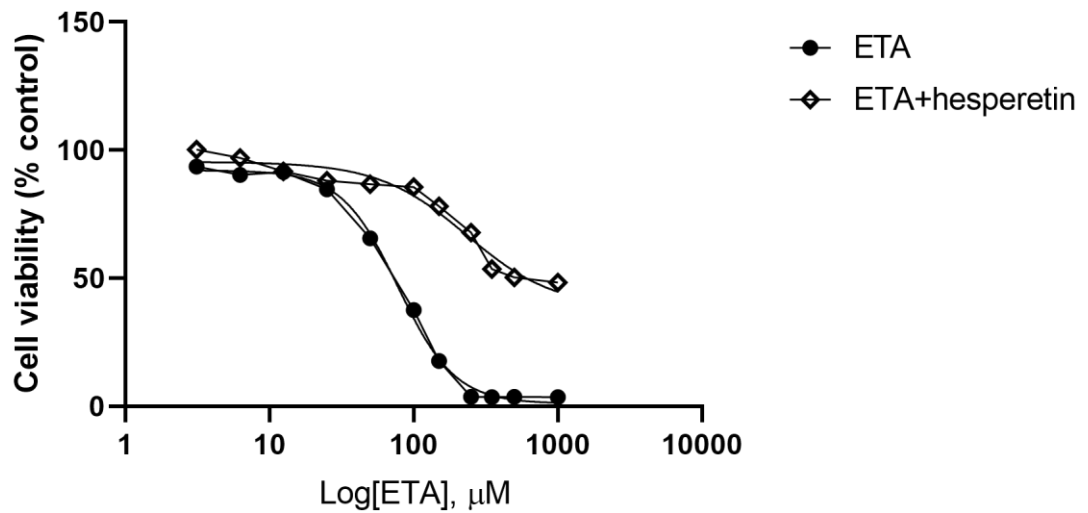


Figure 123 Cell viability as percentage to control (no treatment) observed after pre-treatment of MCF-7 cells for 24 h with hesperetin ($1 \mu\text{M}$), and ethacrynic acid ($3.125\text{--}1000 \mu\text{M}$). Results of the MTT assay show the mean of 2 experiments (total n=6). $P < .0001$, significant difference between the cytotoxicity of ETA in pretreated cells and the cytotoxicity of ETA alone.

When cells were pretreated with hispidulin at 2.5 μM , the LD_{50} of ETA increased to 2248 μM , from 68.5 μM , when measured in cells without pretreatment. Hispidulin maintained the cell viability up to 61.9%, decreasing from 97.6% (Figure 124).

ETA cytotoxicity with hispidulin pretreatment

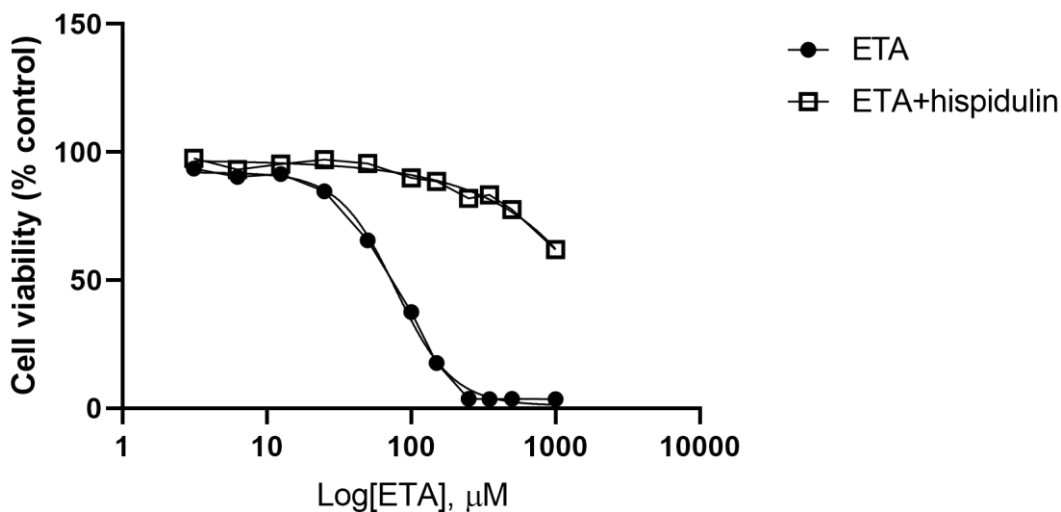


Figure 124 Cell viability as percentage to control (no treatment) observed after pre-treatment of MCF-7 cells for 24 h with hispidulin (2.5 μM) and ethacrynic acid (3.125-1000 μM). Results of the MTT assay show the mean of 2 experiments (total n=6). $P < .0001$, significant difference between the cytotoxicity of ETA in pretreated cells and the cytotoxicity of ETA alone.

Kaempferol (2.5 μM) provided good cytoprotection against ETA at doses of 50 μM and up to 150 μM , maintaining the cell viability at over 80% in this range. The most cytotoxic range of ETA was 100 μM to 1000 μM and kaempferol counteracted the effects of ETA resulting in cell viabilities between 92.50% and 62.98%, respectively (Figure 125). Moreover, the LD_{50} of ETA after kaempferol pre-treatment was more 46 times higher than that of ETA alone.

ETA cytotoxicity with kaempferol pretreatment

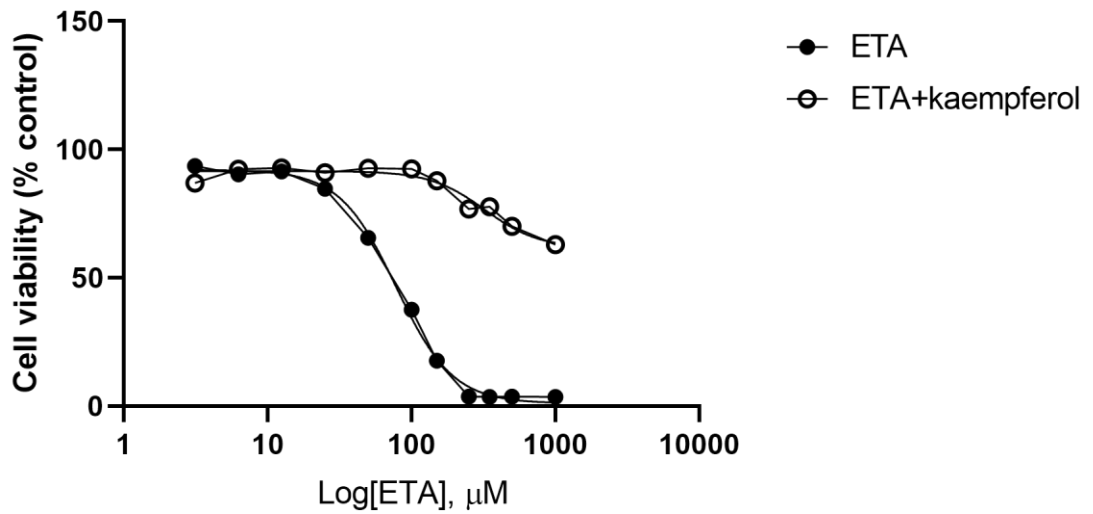


Figure 125 Cell viability as percentage to control (no treatment) observed after pre-treatment of MCF-7 cells for 24 h with kaempferol (2.5 µM) and ethacrynic acid (3.125-1000 µM). Results of the MTT assay show the mean of 2 experiments (total n=6). $P < .0001$, significant difference between the cytotoxicity of ETA in pretreated cells and the cytotoxicity of ETA alone.

Pre-treatment of MCF-7 cells with luteolin (Figure 126) at 2.5 µM offered protection against the effects of ETA, maintaining the cell viability slightly over 50% (52.63%) at the highest dose of ETA of 1000 µM. The LD₅₀ of ETA in cells pretreated with luteolin was 2094 µM, 30 times higher than that of ETA alone.

ETA cytotoxicity with luteolin pretreatment

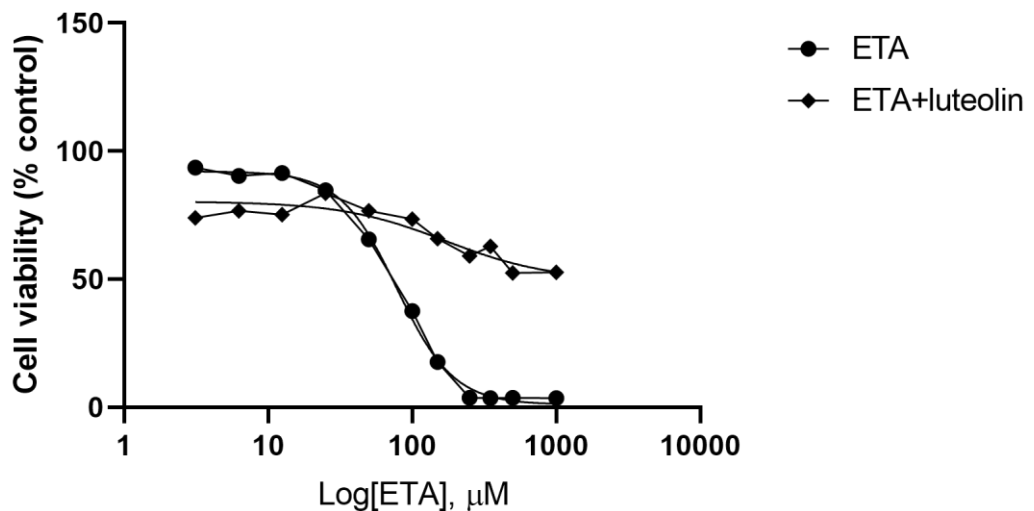


Figure 126 Cell viability as percentage to control (no treatment) observed after pre-treatment of MCF-7 cells for 24 h with luteolin (2.5 µM) and ethacrynic acid (3.125-1000 µM). Results of the MTT assay show the mean of 2 experiments (total n=6). $P < .0001$, significant difference between the cytotoxicity of ETA in pretreated cells and the cytotoxicity of ETA alone.

Figure 127 below shows the cytotoxicity profile of ETA in MCF-7 cells at a range of concentrations from 3.125 to 1000 μM , alongside its nonlinear cytotoxic profile in cells pretreated with naringenin (2.5 μM). Pretreatment with naringenin lowered the cell viability to 56.5%.

ETA cytotoxicity with naringenin pretreatment

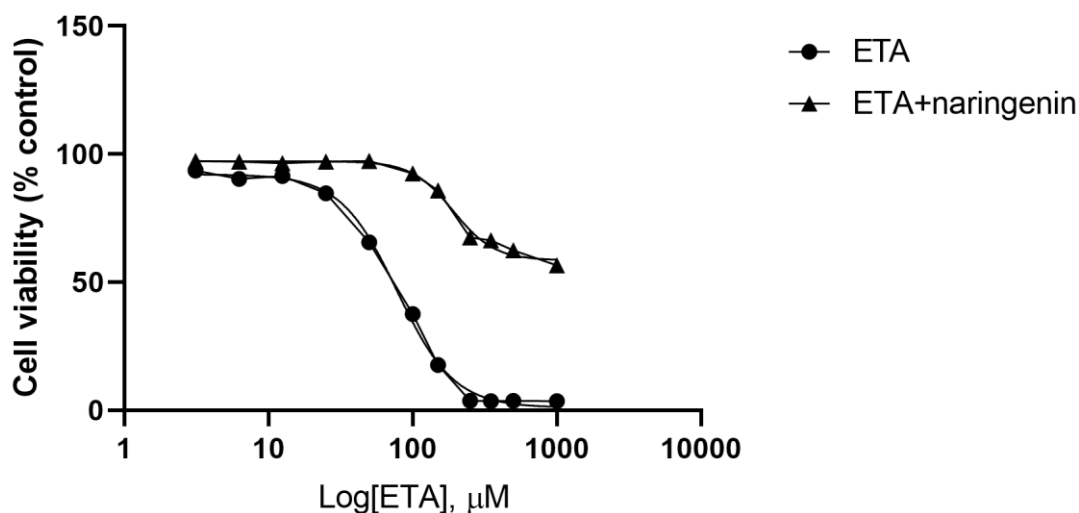


Figure 127 Cell viability as percentage to control (no treatment) observed after pre-treatment of MCF-7 cells for 24 h with naringenin (2.5 μM) and ethacrynic acid (3.125-1000 μM). Results of the MTT assay show the mean of 2 experiments (total n=6). $P < .0001$, significant difference between the cytotoxicity of ETA in pretreated cells and the cytotoxicity of ETA alone.

Figure 128 shows the cell viability response (%) in MCF-7 cells produced by one-time treatment with ETA, with and without pretreatment with sakuranetin at a dose of 20 μM . Sakuranetin exhibited cytoprotection in MCF-7 cells against ETA at concentrations higher than 25 μM . Pretreatment with sakuranetin maintained the cell viability at 90% with 25 μM ETA, decreasing to 62% at 1000 μM ETA.

ETA cytotoxicity with sakuranetin pretreatment

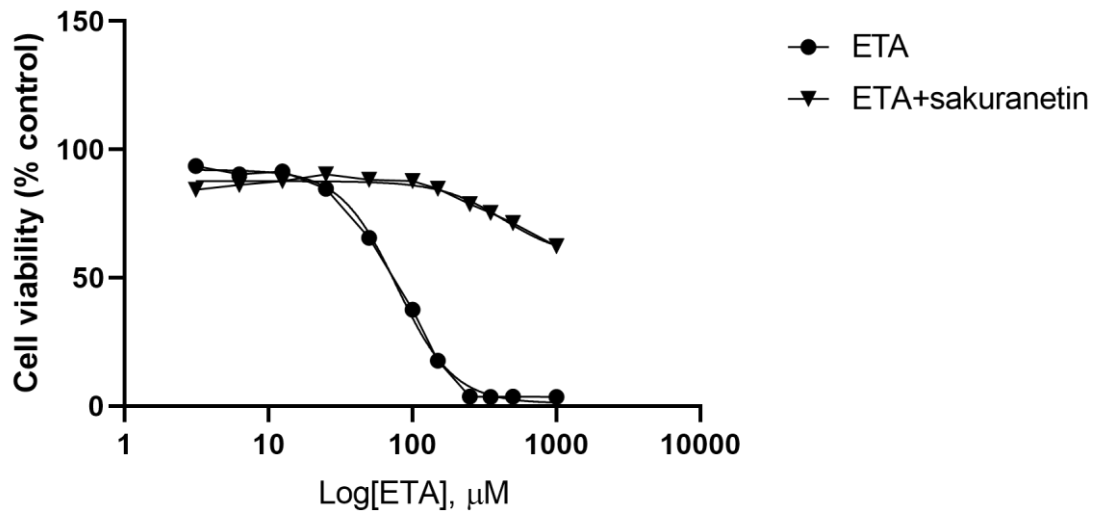


Figure 128 Cell viability as percentage to control (no treatment) observed after pre-treatment of MCF-7 cells for 24 h with sakuranetin (20 µM) and ethacrynic acid (3.125-1000 µM). Results of the MTT assay show the mean of 2 experiments (total n=6). P<.0001, significant difference between the cytotoxicity of ETA in pretreated cells and the cytotoxicity of ETA alone.

MCF-7 cells pre-treated with velutin (2.5 µM) proved more resistant metabolically to treatment with ETA for 24 h at a range of concentrations between 3.125 µM and 1000 µM, compared to treatment with ETA alone (Figure 129). Having decreased the cell viability to 66.5% at the highest dose of ETA, the LD₅₀ of ETA increased with applied pretreatment of velutin to 15496 µM, from 68.5 µM.

ETA cytotoxicity with velutin pretreatment

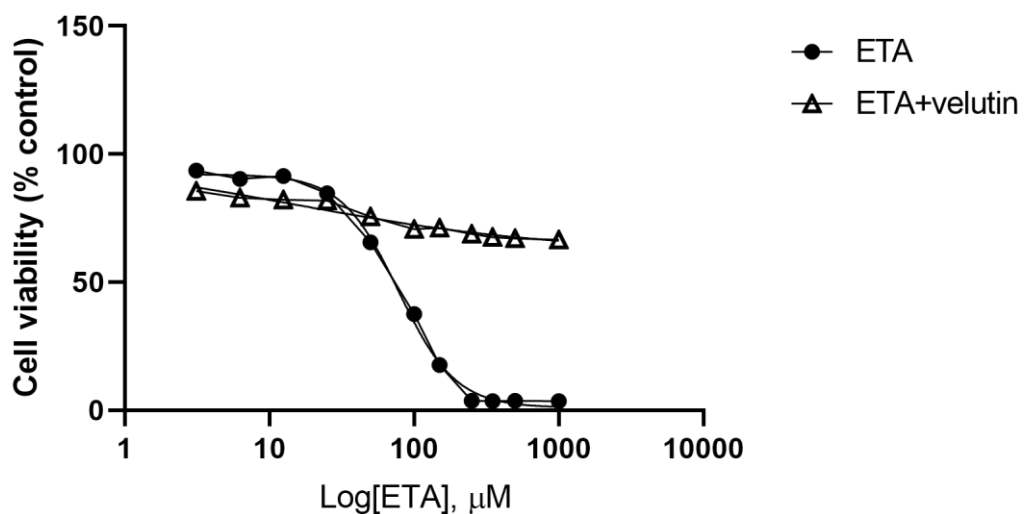


Figure 129 Cell viability as percentage to control (no treatment) observed after pre-treatment of MCF-7 cells for 24 h with velutin (2.5 µM) and ethacrynic acid (3.125-1000 µM). Results of the MTT assay show the mean

of 2 experiments (total n=6). P<.0001, significant difference between the cytotoxicity of ETA in pretreated cells and the cytotoxicity of ETA alone.

Table 16 depicts an overview of the LD₅₀ values recorded for ETA in MCF-7 cells pretreated with a selected flavonoid, tBHQ, as well as in cells without pretreatment. Overall, all flavonoids applied as pretreatment increased the LD₅₀ of ETA, used in the range of 3.125-1000 µM, at least 9 times (hesperetin, 1 µM) compared to ETA alone (68.5 µM).

Table 16 Overview of LD₅₀ of ethacrynic acid after pre-treatment with various flavonoids and without pretreatment

Compounds for pre-treatment and dose	ETA LD ₅₀ (µM)	
	w/ pre-treatment	w/o pre-treatment
Hesperetin 1 µM	661	68.5 µM
Naringenin 2.5 µM	1038	
Apigenin 5 µM	1468	
Luteolin 2.5 µM	2094	
Hispidulin 2.5 µM	2248	
tBHQ 10 µM	2463	
Kaempferol 2.5 µM	3171	
Genkwanin 2.5 µM	5384	
Sakuranetin 20 µM	10891	
Velutin 2.5 µM	15496	

The results show that with the exception of pre-treatment with hesperetin and hispidulin, all flavonoids tested caused a lower cell viability at the lowest concentration of ETA in the range tested than with ETA alone.

However, all pre-treatments with flavonoids resulted in significant protection against the cytotoxic effects of ETA applied at doses of 50 µM and higher.

Overall, 24-hour pre-treatment of MCF-7 cells with velutin, kaempferol, sakuranetin, hispidulin and genkwanin, maintained a cell viability of more than 60% and up to 66.51% in the case of velutin, when followed by treatment with ETA at the highest dose of 1000 µM. Pre-treatment with naringenin, apigenin and luteolin caused final cell viabilities between 53%

and 57%, whereas pre-treatment with hesperetin yielded the lowest cell viability, 48%, in the presence of ETA at the highest concentration of 1000 μ M.

One inference would be that ETA increased the accumulation of reactive oxygen species intracellularly and the process was inhibited by the flavonoids tested by reacting in a ROS scavenging manner and deactivating the ROS molecules. Hence, the flavonoids could have acted in a non-enzymatic way to remove the oxidative agents by reducing them to stable products (Ahmadinejad *et al*, 2017).

In addition, for the investigation of the cytoprotective effects of flavonoids it is relevant to consider the presence of metal ions, such as copper and iron, in the experimental setup. These metals have the capability to chelate and the flavonoids could enhance the DNA damage done by reactive oxygen species (Nimse and Pal, 2015).

Talalay *et al.* (1983) proposed that compounds which contain a Michael acceptor or from which a Michael acceptor can be formed during metabolism, are usually inducing agents for GST. A Michael reaction represents the addition via conjugation of a carbon anion or another carbon nucleophile, also called a Michael donor, to the carbon of a α , β – unsaturated compound, called a Michael acceptor. Michael acceptors are olefinic compounds conjugated with electron-withdrawing groups that can interact with nucleophilic compounds such as cysteine, lysine or serine (Kumar *et al*, 2014).

Considering that flavonoids also present electron-donating properties (electrophilic feature) and can undergo oxidation to quinones or semiquinones (usually when presenting a catechol moiety, which is an example of a α , β – unsaturated structure), they may cause a direct modification to Keap1, by oxidation of its cysteine residues, resulting in Nrf2 release and relocalisation (Lee-Hilz *et al*, 2006).

ETA acts as a reversible inhibitor of GST, the flavonoids tested could act by competing with ETA. Moreover, ETA also forms a ETA-GSH conjugate that is considered primarily responsible for the inhibition of GST (Awasthi *et al*, 1993; Oakley *et al*, 1997). The high cytoprotective effect shown by the flavonoids tested against ETA could also indicate that the flavonoids may interact with the ETA-GSH conjugate, disrupting it from inhibiting GST activity.

So far it has been shown that polyphenols and sulfur-containing dietary compounds act as positive modulators for regulation of detoxifying enzymes and they can trigger various signaling cascades to contribute to the accumulation of the Nrf2 protein in the nucleus increasing the expression of detoxifying enzymes (Chen *et al.* 2004).

For example, the 5,6,7-trihydroxyflavone and the 3,3',4',5,7-pentahydroxyflavone are two highly hydroxylated flavonoids, namely baicalein and quercetin. These compounds were shown to have a capacity to modulate the Nrf2/Keap pathway by preventing the ubiquitination and proteasomal degradation of the Nrf2 protein (Tanigawa *et al*, 2007 and Qin *et al*, 2014).

CHAPTER 4 Conclusions and recommendations for future work

For each study presented and discussed in Chapter 3, the conclusions and recommendations for future work for each investigational step are presented in this chapter. Final conclusions of the bioassay-guided investigation into the cancer chemopreventive properties of selected non-dietary plants and selected flavonoids close the chapter.

The selection of plants were subjected to Soxhlet solvent extraction with *n*-hexane and methanol and the crude extracts were screened for Nrf2 induction potential using a AREc32 cell-based luciferase gene reporter assay, as well as for free-radical scavenging activity using the DPPH assay.

4.1 Conclusions of Study 1

Natural products were extracted from a selection of plants and an initial phytochemical screening on the crude extracts was performed.

Overall, all methanol extracts showed a mixture of compounds during the TLC screening at 254 nm and 366 nm, with the exception of GP-Me, SA-Me and ZM-Me, which revealed only one prominent compound.

It was noted that AL-Me and ZM-Me were the samples with the highest free-radical scavenging activity in the DPPH assay, with an IC₅₀ almost 25 times lower than the positive control quercetin of 0.002 mg/ml. The third most bioactive crude extract was GT-Me, followed by EA-Me, CP-Me and SA-Me with IC₅₀ values between 0.344 and 0.398 mg/ml.

4.2 Conclusions of Study 2

The *n*-hexane extract of *Solanum anguivi* (SA-He, 100 µg/ml) caused a high Nrf2 activity of 20.2-fold to control.

However, the highest increase in Nrf2 induction was achieved by the methanol extract of *Centaurea dichroa* (CD-Me, 250 µg/ml) with a 22.7-fold to control induction. The Nrf2/ARE signaling pathway was also up-regulated by two other methanol extracts, of *Centaurea pamphylica* (CP-Me, 100 µg/ml) and *Gardenia ternifolia* (GT-Me, 750 µg/ml), with 11.2-fold and 9-fold to control luciferase induction, respectively.

Furthermore, the luciferase assay results of *n*-hexane extracts showed only one strong Nrf2 inducer. After 24 h treatment of AREc32 cells with the *Solanum anguivi* extract (SA-He) at 100 µg/ml, Nrf2 activity was increased 20.2-fold to control.

The MTT assays performed pointed out that the use of natural products for *in vitro* assays can pose a few problems, including poor water solubility of non-polar mixtures of phytochemical compounds. To this end, the solvent DMSO can be used effectively as vehicle medium for non-polar crude extracts at maximum 1% v/v per well for extract concentrations below 100 µg/ml.

4.3 Conclusions of Study 3 and recommendations for future work

The bioassay guided investigation led to further fractionation of the bioactive methanol extracts and indicated that the less polar fractions, F2-F4, were responsible for the highest Nrf2 induction in the extract mixture. The most polar fractions, F1, showed low bioactivity values, between 1 and 3.4-fold. CD-Me fractions F2 and F3 of medium polarity caused luciferase inductions between 3.7 and 5.5-fold to control, respectively, which was four times lower than the induction exerted by the CD-Me methanol extract.

Also, CP-Me fractions F3 and F4 increased Nrf2/ARE activity over 10-fold and up to 13.4-fold (max. 11.2-fold for CP-Me), whereas GT-Me fractions F3 and F4 reached luciferase activity inductions of over 10-fold, one-fold higher than the induction achieved by GT-Me.

4.4 Conclusions of Study 4 and recommendations for future work

The compounds precipitated during the Soxhlet extraction were identified as stachyose (GP-Me), mannitol (GT-Me) and betulinic acid (ZM-He).

The compounds isolated from the bioactive methanol fractions of *Centaurea dichroa*, *Centaurea pamphylica* and *Gardenia ternifolia* indicated flavonoid type structures, but because of limited starting material, various types of flavonoids such as flavones, flavanones and flavonols were eventually purchased with the purpose of screening them for Nrf2 activity in AREc32.

Compound F3GT-Me-P4/PA was identified as sakuranetin based on NMR and MS spectra and to date it has not been reported as a component of *Gardenia ternifolia* Schumach. & Thonn.

Compounds were isolated from the bioactive methanol fractions by means preparative HPLC. The chromatographic separation of peaks during prep HPLC allowed for UV-Vis spectral data to be recorded and it showed that all the compounds isolated with highest purity were flavonoids, as indicated by the two major wavelength intervals of their UV_{max} values: 240 nm – 280 nm (Band II) and 300 nm – 340 nm (Band I). The lowest wavelength interval, Band II, corresponds to the absorption of components of the A-ring system, whereas the second wavelength interval is observed because of the B-ring absorption pattern (Mabry, Markham and Thomas 1970, p.41).

Mass spectrometry, using a liquid chromatograph (LC) inlet with electrospray ionisation mode (ESI), was used as a complementary tool for structure elucidation in both positive and negative ionisation modes. The first-order mass spectra gave insight into the molecular masses of flavonoid aglycones mainly, by detecting protonated, $[M+H]^+$, or deprotonated base peak molecular ions $[M-H]^-$ (Fossen and Andersen, 2006).

Future work is recommended in order to improve the structural characterisation process. Ensuring sufficient amounts of starting material as a prerequisite is one solution. This way more analyses could be performed, such as MS, LC-MS/MS and NMR spectroscopy using different solvents, such as DMSO and $CDCl_3$, as well as infrared spectroscopy, to determine the functional groups in the molecule.

4.5 Conclusions of Study 5 and recommendations for future work

The flavonoids tested increased the Nrf2-mediated luciferase activity in AREc32 cells to no more than 3.1-fold, with most of them reaching slightly above 2-fold induction. To test for their capacity to exert effects as a result of synergistic mechanisms, the flavonoids should be tested together in the luciferase assay in various ratios and structural combinations e.g. two flavonols together vs one flavonol and one flavone together.

The flavonoids tested in the Nrf2/luciferase assay should also be tested in the DPPH assay that was performed for the crude extracts and subsequent fractions. Such a test would inform the hypothesis that a high free-radical scavenging ability of phytochemicals correlates with a low Nrf2 induction in the luciferase assay and further relationships between bioactivity levels of flavonoids, composition, concentration and chemical structure can be studied.

Future work could also be done to increase the robustness of the phytochemical isolation method by adding extra steps to the solvent reflux extraction with solvents of intermediary

polarity between those of *n*-hexane and methanol e.g. DCM. This could allow for isolation of more compounds and possibly a better chromatographic separation. The DCM extract, if Nrf2 inducing, could be screened using a TLC system (*n*-hexane:ethylacetate). Testing a third extract for Nrf2 induction could also increase specificity of the bioassay-guided investigation into non-dietary phytochemicals. Using an extraction procedure with petroleum ether instead of *n*-hexane would also be an option, as reported by Chima *et al* (2014).

4.6 Conclusions of Study 6 and recommendations for future work

In the immunoblotting assay flavanones sakuranetin and naringenin showed no significant expression of NQO1 compared to the untreated control after 24 h treatment, which was a finding consistent with the low Nrf2 induction recorded for these compounds in the luciferase assay presented in Study 5.

Because Nrf2 and Keap1 rarely mutate in cancer cells (Taguchi, Motohashi and Yamamoto, 2011), this constitutes an advantage for future investigations into the activity of Nrf2 in cancer cell lines and solid tumours to understand the mechanisms by which various types of compounds can exert a positive modulation or inhibition of the phase II detoxification phase of metabolism via the Nrf2/ARE signaling pathway.

Moreover, future investigations are also required in order to try to establish the risk for carcinogenesis induced by chronic exposure of healthy cells to Nrf2 inducers. Studying how the Nrf2/ARE signaling pathway becomes susceptible to regulation by natural products of various chemical structures is an important domain of research that adds up to the field of cancer chemoprevention and cancer research which aims to control and treat cancers as a deadly disease.

4.7 Conclusions of Study 7 and recommendations for future work

AREc32 cells pre-treated with flavonoids (apigenin, genkwanin, hesperetin, hispidulin, kaempferol, luteolin, naringenin, quercetin, sakuranetin and velutin) showed significantly higher cell viability after 24 h, compared to cells treated with ETA alone.

Observing the significant cytoprotective effects of flavonoids against ETA-induced oxidative stress at various concentrations, TUNEL assays for quantification of DNA fragmentation

could be performed in order to determine the DNA protective effects of the bioactive fractions identified in Study 3 and the resulting compounds.

4.8 Final conclusions and recommendations for future work

Plants have always been an invaluable source of bioactive compounds with a plethora of properties such as antioxidant, free-radical scavenging, cytotoxic, anti-inflammatory and also anti-viral and anti-microbial (Nijveldt *et al*, 2001).

The phytochemical isolation process was robust and efficient in pointing towards the direction of bioactive mixture of compounds or individual compounds. Out of twelve plants used as starting material in the bioassay-guided investigation, three demonstrated bioactivity in terms of Nrf2 induction in AREc32 cells.

In terms of free-radical scavenging potential, fraction F3 of CP-Me (80% MeOH/water) showed the lowest IC₅₀, of 0.072 mg/ml, followed by F3 GT-Me.

Furthermore, as a result of the DPPH assays, it was observed that mixtures or compounds with high potential for DPPH free-radical scavenging also showed low potential for Nrf2 induction in AREc32 cells. Thus, all flavonoids should be further assayed for DPPH inhibition to have a better picture over the possible inverse relationship between various cancer chemopreventive properties of phytochemicals.

Further work is necessary in order to isolate and identify the compounds in the most bioactive extract identified, in terms of Nrf2 induction quantification, namely the methanol extract of *Centaurea dichroa*. Testing to find the most efficient composition of flavonoids that is able to elicit a cancer chemopreventive response would also be useful. A chemical profiling of the bioactive extract and fractions could be performed, using HPLC coupled to MS, with a solvent system of methanol:acetic acid:water (Ferrante *et al*, 2019). This qualitative composition fingerprint could also help identify phytochemicals.

The bioassay-guided investigation also revealed that the most non-polar methanol fractions (F3 and F4) of *Centaurea pamphylica* and *Gardenia ternifolia* were most bioactive in terms of luciferase activity induction in AREc32 cells. Further research should be carried out to characterise the mixture of compounds in fractions F4 (100% MeOH).

Moreover, flavonoids tested (apigenin, genkwanin, hesperetin, hispidulin, kaempferol, luteolin, naringenin, quercetin, sakuranetin and velutin) did not show significant Nrf2 induction and this was in part confirmed by the immunoblotting of NQO1, where the

flavanones naringenin and sakuranetin did not alter the protein levels of NQO1 following treatment as compared to control.

However, the cytotoxic potential of genkwanin, naringenin and hispidulin against the breast cancer cell line MCF-7 has been confirmed following treatment with concentrations lower than 50 μ M.

The flavonoids tested also showed cytoprotective effects in MCF-7 cells as a result of ETA-induced oxidative stress. Pre-treatment of MCF-7 cells with the selected flavonoids showed potential for further testing in more cell lines, such as primary cells. Their potential for protection against DNA damage should also be assessed, as well as for the bioactive fractions identified in the luciferase assay (F3 and F4 of CP-Me and GT-Me).

The effects of Nrf2 inducers on various tissues are not entirely known yet and further studies are required, while clinical trials are underway for assessing the outcome of the Nrf2/ARE pathway activation in obesity, the progression of type 2 diabetes and cardiovascular disease such as atherosclerosis (da Costa *et al*, 2019).

Because most studied phytochemical compounds are sourced from dietary plants, studying the effects of non-dietary extract mixtures and compounds on various tissues could prove insightful with regards to the wealth of knowledge necessary for successful management of chronic disease and cancer chemoprevention strategies.

In conclusion, the studies performed in this bioassay-investigation showed and confirmed the potential for the various plant extracts and flavonoids to exert cancer chemopreventive effects by increasing Nrf2 induction, but more work is needed to support health applications for these bioactive natural products. A more focused approach to understanding the pharmacokinetics of natural products and flavonoids in particular could lead to a better understanding of the bioavailability and metabolism of flavonoids, as well as of the pharmacological effects they exert in their dual role as antioxidants/free radical-scavengers and cell signalling modulators. Further studies on the mechanisms of action of flavonoids in various cancer cell lines, as well as in primary cell cultures, and evaluating their effect on the regulation of redox homeostasis at the various stages of tumorigenesis, could support the development of novel strategies for cancer chemoprevention, management and treatment.

References

- Adewusia, E.A., Foucheb, G. and Steenkamp, V. (2013) Effect of four medicinal plants on amyloid- β induced neurotoxicity in SHSY5Y cells. *African Journal of Traditional, Complementary and Alternative Medicines*, 10(4), 6-11.
- Agatonovic-Kustrin, S., Kustrin, E., Gegechkori, V. and Morton, D. (2019). High-Performance Thin-Layer Chromatography Hyphenated with Microchemical and Biochemical Derivatizations in Bioactivity Profiling of Marine Species. *Marine Drugs*, 17(3).
- Agrawal, P.K (1989) *Carbon-13 NMR of Flavonoids*. Elsevier Science Publishers, Amsterdam, The Netherlands.
- Aguilera, J.M.(2003). *Solid-liquid extraction*. In: Tzia, C. & Liadakis, G, editors. Extraction optimization in food engineering. Marcel Dekker, New York, 35-55.
- Ahmad, I.U., Forman, J.D. and Sarkar, F.H. (2008) Reduction of adverse events by soy isoflavones in patients undergoing external beam radiation therapy for prostate cancer. *Int J Radiat Oncol Biol Phys*, 72(1), S318.
- Ahmadinejad, F., Geir Møller, S., Hashemzadeh-Chaleshtori, M., Bidkhor, G. and Jami, M.S. (2017). Molecular Mechanisms behind Free Radical Scavengers Function against Oxidative Stress. *Antioxidants*, 6(3), 51
- Ahn-Jarvis, J. H., Parihar, A., & Doseff, A. I. (2019). Dietary Flavonoids for Immunoregulation and Cancer: Food Design for Targeting Disease. *Antioxidants* (Basel), 8(7), 202.
- Ali, P., Chen, Y.F. and Sargsyan, E. (2014) Bioactive Molecules of Herbal Extracts with Anti-Infective and Wound Healing Properties. In *Microbiology for Surgical Infections*, 205-220
- Almagami, A.A., Alshawsh, M.A., Saif-Ali, R., Shwter, A., Salem, S.D. and Abdulla, M.A. (2014) Evaluation of chemopreventive effects of *Acanthus ilicifolius* against azoxymethane-induced aberrant crypt foci in the rat colon. *PloS one*, 9(5), e96004.
- Amin, A.R.M., Kucuk, O, Khuri, F.R. and Shin, D.M. (2009) Perspectives for cancer prevention with natural compounds. *Journal of Clinical Oncology*, 27(16), 2712-2725

Arslan, I., Celik, A. and Chol, J.H., (2012) A cytotoxic triterpenoid saponin from underground parts of *Gypsophila pilulifera* Boiss. & Heldr. *Fitoterapia*, 83(4), 699-703.

Asgharikhatooni, A., Bani, S., Hasanpoor, S., Alizade, S.M. and Javadzadeh, Y., (2015) The effect of *Equisetum arvense* (horse tail) ointment on wound healing and pain intensity after episiotomy: a randomized placebo-controlled trial. *Iranian Red Crescent Medical Journal*, 17(3).

Avigad, G., and Dey, P. M. (1997). *Carbohydrate Metabolism: Storage Carbohydrates. Plant Biochemistry*, p. 143–204.

Awasthi, S., Srivastava, S. K., Ahmad, F., Ahmad, H. and Ansari, G. A. S. (1993). Interactions of glutathione S-transferase- π with ethacrynic acid and its glutathione conjugate. *Biochimica et Biophysica Acta (BBA) - Protein Structure and Molecular Enzymology*, 1164(2), 173–178.

Awouafack, M.D., Tane, P. and Eloff, J.N. (2013). Two new antioxidant flavones from the twigs of *Eriosema robustum* (Fabaceae). *Phytochemistry Letters*, 6(1):62-66.

Awouafack, M.D., Tane, P. and Morita, H. (2017) Isolation and Structure Characterization of Flavonoids. *Flavonoids - From Biosynthesis to Human Health*.

Balentine, D. A., Dwyer, J. T., Erdman, J. W., Ferruzzi, M. G., Gaine, P. C., Harnly, J. M., and Kwik-Urbe, C. L. (2015) Recommendations on reporting requirements for flavonoids in research. *The American Journal of Clinical Nutrition*, 101(6), 1113–1125.

Belkaid, A., Currie, J.-C., Desgagnés, J. and Annabi, B. (2006) The chemopreventive properties of chlorogenic acid reveal a potential new role for the microsomal glucose-6-phosphate translocase in brain tumor progression. *Cancel cell International*, 6(1), 7.

Berg, J.M., Tymoczko, J.L. and Stryer, L. *Biochemistry*. 5th edition. New York: WH Freeman, 2002.

Berger, S. and D. Sicker, D. (2009) *Classics in Spectroscopy Isolation and Structure Elucidation of Natural Products*. Weinheim: Wiley.

Bradbury, K.E., Appleby, P.N. and Key, T.J. (2014) Fruit, vegetable, and fiber intake in relation to cancer risk: findings from the European Prospective Investigation into Cancer and Nutrition (EPIC)–. *The American journal of clinical nutrition*, 100(suppl_1), 394S-398S.

- Bray, F., Ferlay, J., Soerjomataram, I., Siegel, R.L., Torre, L.A. and Jemal, A. (2018) Global cancer statistics 2018: GLOBOCAN estimates of incidence and mortality worldwide for 36 cancers in 185 countries. *CA: a cancer journal for clinicians*.
- Bruggisser, R., von Daeniken, K., Jundt, G., Schaffner, W., Tullberg-Reinert, H. (2002) Interference of plant extracts, phytoestrogens and antioxidants with the MTT tetrazolium assay. *Planta medica* 68(5), 445-8.
- Četojević-Simin, D.D., Čanadanović-Brunet, J.M., Bogdanović, G.M., Djilas, S.M., Četković, G.S., Tumbas, V.T. and Stojiljković, B.T., (2010) Antioxidative and antiproliferative activities of different horsetail (*Equisetum arvense* L.) extracts. *Journal of medicinal food*, 13(2), 452-459.
- Chaisawangwong, W. and Gritsanapan, W. (2009) Extraction method for high free radical scavenging activity of Siamese neem tree flowers. *Sonklanakarinn Journal of Science and Technology*, 31(4), 419-423.
- Chandra, S. and Rawat, D.S., (2015) Medicinal plants of the family Caryophyllaceae: a review of ethno-medicinal uses and pharmacological properties. *Integrative Medicine Research*, 4(3), 123-131.
- Chen, C. and Kong, A.N. (2004) Dietary chemopreventive compounds and ARE/EpRE signaling. *Free Radic Biol Med*, 36(12), 1505-16.
- Chen, C.Y., Kao, C.L. and Liu, C.M., (2018) The Cancer Prevention, Anti-Inflammatory and Anti-Oxidation of Bioactive Phytochemicals Targeting the TLR4 Signaling Pathway. *International journal of molecular sciences*, 19(9), 2729.
- Chen, Y.L. and Schirarend, C., (2007) Rhamnaceae. *Flora of China*, 12, pp.115-168.
- Chima, N. K., Nahar, L., Majinda, R. R. T., Celik, S., and Sarker, S. D. (2014) Assessment of free-radical scavenging activity of *Gypsophila pilulifera*: assay-guided isolation of verbascoside as the main active component. *Revista Brasileira de Farmacognosia*, 24(1), 38–43.
- Chikara, S., Nagaprashantha, L.D., Singhal, J., Horne, D., Awasthi, S. and Singhal, S.S., (2017) Oxidative stress and dietary phytochemicals: role in cancer chemoprevention and treatment. *Cancer letters*.
- Cho, H.Y. and Kleeberger, S.R. (2007) Genetic mechanisms of susceptibility to oxidative lung injury in mice. *Free Radical Biology & Medicine*, 42(4), pp. 433–445.

Chow, H.S., Garland, L.L., Hsu, C.H., Vining, D.R., Chew, W.M., Miller, J.A., Perloff, M., Crowell, J.A. and Alberts, D.S., (2010) Resveratrol modulates drug-and carcinogen-metabolizing enzymes in a healthy volunteer study. *Cancer Prevention Research*, 1940-6207.

Christenhusz, M.J. and Byng, J.W., (2016) The number of known plants species in the world and its annual increase. *Phytotaxa*, 261(3), pp.201-217.

da Costa, R.M., Rodrigues, D., Pereira, C.A., Silva, J.F., Alves, J.V., Lobato, N.S. and Tostes, R.C. Nrf2 as a potential mediator of cardiovascular risk in metabolic diseases. *Frontiers in Pharmacology* 10, 382.

Dempewolf, H., Rieseberg, L.H. and Cronk, Q.C., (2008) Crop domestication in the Compositae: a family-wide trait assessment. *Genetic Resources and Crop Evolution*, 55(8), pp.1141-1157.

Deorukhkar, A., Krishnan, S., Sethi, G. and Aggarwal, B.B. (2007) Back to basics: how natural products can provide the basis for new therapeutics. *Expert Opinion Investig. Drugs*, 16(11), p.1753-1773

DiDonato, J.A., Mercurio, F. and Karin, M., (2012) NF- κ B and the link between inflammation and cancer. *Immunological reviews*, 246(1), pp.379-400.

Dikilitas, N. and Duman, R. (2018) *In vitro* Evaluation of Anti-HSV-1 Activity of Kitaibelia Balansae Boiss. (Malvaceae). *International Journal of Scientific and Technological Research*, 4(9), pp. 145-156.

Dinkova-Kostova, A.T. and Kostov, R.V., (2012) Glucosinolates and isothiocyanates in health and disease. *Trends in molecular medicine*, 18(6), pp.337-347.

Drew, D. A., Cao, Y. and Chan, A. T. (2016) Aspirin and colorectal cancer: the promise of precision chemoprevention. *Nature Reviews Cancer*, 16(3), 173–186.

Dzoyem, J.P., McGaw, L.J., Kuete, V. and Bakowsky, U. (2017) Anti-inflammatory and Antinociceptive Activities of African Medicinal Spices and Vegetables. *Medicinal Spices and Vegetables from Africa*, pp. 239-270.

Elekofehinti, O.O., Kamdem, J.P., Bolingon, A.A., Athayde, M.L., Lopes, S.R., Waczuk, E.P., Kade, I.J., Adanlawo, I.G. and Rocha, J.B.T. (2013) African eggplant (*Solanum anguivi* Lam.) fruit with bioactive polyphenolic compounds exerts *in vitro* antioxidant properties and

inhibits Ca²⁺-induced mitochondrial swelling. *Asian Pacific journal of tropical biomedicine*, 3(10), pp.757-766.

El-Gharbaoui, A., Benítez, G., González-Tejero, M.R., Molero-Mesa, J. and Merzouki, A., (2017) Comparison of Lamiaceae medicinal uses in eastern Morocco and eastern Andalusia and in Ibn al-Baytar's Compendium of Simple Medicaments (13th century CE). *Journal of ethnopharmacology*, 202, 208-224.

Fang, S., Bingyi, F., Jinlin, Q., Quan, L., Shuqian, W., Werner, H., Yinfu, C. and Xinsheng, Z., (2003) *Encyclopedic reference of traditional Chinese medicine*. Springer Science & Business Media.

Fang, Y., Yang, S. and Wu, G. (2002) Free radicals, antioxidants, and nutrition. *Nutrition*, 18(10), 872-879

Feng, T., Cao, W., Shen, W., Zhang, L., Gu, X., Guo, Y., Tsai, H.I., Liu, X., Li, J., Zhang, J. and Li, S., (2017) Arctigenin inhibits STAT3 and exhibits anticancer potential in human triple-negative breast cancer therapy. *Oncotarget*, 8(1), 329.

Ferrante, C., Zengin, G., Menghini, L., Diuzheva, A., Jekő, J., Cziáky, Z. and Orlando, G. (2019). Qualitative Fingerprint Analysis and Multidirectional Assessment of Different Crude Extracts and Essential Oil from Wild *Artemisia santonicum* L. *Processes*, 7(8), 522.

Finkel, T. and Holbrook, N. J. (2000) Oxidants, oxidative stress and the biology of ageing. *Nature*, 408(6809), 239–247.

Fitzmaurice, C., Allen, C., Barber, R.M., Barregard, L., Bhutta, Z.A., Brenner, H., Dicker, D.J., Chimed-Orchir, O., Dandona, R., Dandona, L. and Fleming, T., (2017) Global, regional, and national cancer incidence, mortality, years of life lost, years lived with disability, and disability-adjusted life-years for 32 cancer groups, 1990 to 2015: a systematic analysis for the global burden of disease study. *JAMA oncology*, 3(4), 524-548.

Fossen, T., Andersen, Ø. M. 2006. Spectroscopic techniques applied to flavonoids. Pp. 37–142 in *Flavonoids: chemistry, biochemistry, and applications*, eds. Andersen, Ø. M., Markham, K. R., CRC Press, Taylor & Francis Group, Boca Raton, USA

Fridovich, I. (1999) Fundamental aspects of reactive oxygen species, or what's the matter with oxygen?. *Annals of the New York Academy of Sciences*, 893(1), pp. 13-18

Fuentes, F., Paredes-Gonzalez, X. and Kong, A.N.T., (2015) Dietary glucosinolates sulforaphane, phenethyl isothiocyanate, indole-3-carbinol/3, 3'-diindolylmethane:

Antioxidative stress/inflammation, Nrf2, epigenetics/epigenomics and *in vivo* cancer chemopreventive efficacy. *Current pharmacology reports*, 1(3), pp.179-196.

Fulda, S. and Efferth, T., (2015) Selected Secondary Plant Metabolites for Cancer Therapy. *J Tradit Chin Med*, 1(1), pp.1-5.

Gao Q., Yang M., Zuo Z., (2018) Overview of the anti-inflammatory effects, pharmacokinetic properties and clinical efficacies of arctigenin and arctiin from *Arctium lappa* L. *Acta Pharmacol Sin*, 39: pp.787–801.

Gogvadze, V., Orrenius, S. and Zhivotovsky, B. (2008). Mitochondria in cancer cells: what is so special about them? *Trends in Cell Biology*, 18(4), 165–173.

Gopalakrishnan, A. and Kong, A.T. (2008) Anticarcinogenesis by dietary phytochemicals: cytoprotection by Nrf2 in normal cells and cytotoxicity by modulation of transcription factors NF- κ B and AP-1 in abnormal cancer cells. *Food and Chemical Toxicology*, 46, pp.1257-1270

Gordon, M.H. (2012) Significance of dietary antioxidants for health. *International Journal of Molecular Sciences*, 13(1), pp. 173-179

Gorrini, C., Harris, I.S. and Mak, T.W., (2013) Modulation of oxidative stress as an anticancer strategy. *Nature reviews Drug discovery*, 12(12), p.931.

Dos S. Grecco, S., Dorigueto, A.C., Landre, I.M., Soares, M.G., Martho, K., Lima, R., Pascon, R.C., Vallim, M.A., Capello, T.M., Romoff, P., Sartorelli, P. and Lago, J.H.G. (2014) Structural Crystalline Characterization of Sakuranetin — An Antimicrobial Flavanone from Twigs of *Baccharis retusa* (Asteraceae). *Molecules*, 19, 7528-7542.

Grienke, U., Brkanac, S.R., Vujčić, V., Urban, E., Ivanković, S., Stojković, R., Rollinger, J.M., Kralj, J., Brozovic, A. and Stojković, M.R. (2018) Biological activity of flavonoids and rare sesquiterpene lactones isolated from *Centaurea ragusina* L. *Frontiers in pharmacology*, 9.

Hamed, Y. S., Abdin, M., Akhtar, H. M. S., Chen, D., Wan, P., Chen, G., & Zeng, X. (2019). Extraction, purification by macrospores resin and *in vitro* antioxidant activity of flavonoids from *Moringa Oleifera* leaves. *South African Journal of Botany*, 124, 270–279.

Hamedeyazdan, S., Niroumand, F. and Fathiazad, F., (2017) Phytochemical analysis and antioxidative properties of *Centaurea albonitens*. *Research Journal of Pharmacognosy (RJP)*, 4(4), pp.57-64.

He, Z., He, X., Chen, Z., Ke, J., He, X., Yuan, R., Cai, Z., Chen, X., Wu, X. and Lan, P. (2014) Activation of the mTORC1 and STAT3 pathways promotes the malignant transformation of colitis in mice. *Oncology Reports*, 32(5), 1873–1880.

Hesketh, R. (2013) *Introduction to cancer biology*. Cambridge University Press.

Higgins, L.G., Kelleher, M.O., Eggleston, I.M, Itoh, K., Ymamamoto, M. and Hayes, J.D. (2009) Transcription factor Nrf2 mediates an adaptive response to sulforaphane that protects fibroblasts *in vitro* against the cytotoxic effects of electrophiles, peroxides and redox-cycling agents. *Toxicology and Applied Pharmacology*, 237, pp. 267-280.

Huang, M., Lu, J.J., Huang, M.Q., Bao, J.L., Chen, X.P. and Wang, Y.T., (2012) Terpenoids: natural products for cancer therapy. *Expert opinion on investigational drugs*, 21(12), pp. 1801-1818.

Huber, W.W. and Parzefall, W., (2007) Thiols and the chemoprevention of cancer. *Current opinion in pharmacology*, 7(4), pp.404-409.

Ibrahim, M.A. and Islam, M.S., (2017) Effects of butanol fraction of *Ziziphus mucronata* root ethanol extract on glucose homeostasis, serum insulin and other diabetes-related parameters in a murine model for type 2 diabetes. *Pharmaceutical biology*, 55(1), pp.416-422.

Ibrahim, M.A., Koorbanally, N.A., Kiplimo, J.J. and Islam, M.S., (2012) Anti-oxidative activities of the various extracts of stem bark, root and leaves of *Ziziphus mucronata* (Rhamnaceae) *in vitro*. *Journal of Medicinal Plants Research*, 6(25), pp.4176-4184.

Ikeda, M., Sato, A., Mochizuki, N., Toyosaki, K., Miyoshi, C., Fujioka, R., Mitsunaga, S., Ohno, I., Hashimoto, Y., Takahashi, H. and Hasegawa, H., (2016) Phase I trial of GBS-01 for advanced pancreatic cancer refractory to gemcitabine. *Cancer science*, 107(12), pp.1818-1824.

Iqbal, J., Abbasi, B.A., Batool, R., Mahmood, T., Ali, B., Khalil, A.T., Kanwal, S., Shah, S.A. and Ahmad, R., (2018) Potential phytochemicals for developing breast cancer therapeutics: Nature's healing touch. *European journal of pharmacology*.

Jäger, S., Beffert, M., Hoppe, K., Nadberezny, D., Frank, B. & Scheffler A. (2010). Preparation of herbal tea as infusion or by maceration at room temperature using mistletoe tea as an example. *Scientia Pharmaceutica*, 79(1):145-156.

- Jayadev, R., Jagan, M., Malisetty, V. and Rao, C. (2004) Colon cancer preventive effects of *Trigonella foenum graecum* (fenugreek) seed and its constituent diosgenin *in vivo* and *in vitro*. *Cancer Epidemiol Biomarkers Prev*, 13, p.1392-1398
- Karou, S.D., Tchacondo, T., Ilboudo, D.P. and Simpore, J., (2011) Sub-Saharan Rubiaceae: a review of their traditional uses, phytochemistry and biological activities. *Pakistan Journal of Biological Sciences*, 14(3), p.149.
- Kaur, R., Kaur, J., Mahajan, J., Kumar, R. and Arora, S. (2014) Oxidative stress--implications, source and its prevention. *Environ Sci Pollut Res Int.*, 21(3), p.1599-1613.
- Khil, M. S., Kim, S. H., Pinto, J. T., & Kim, J. H. (1996). Ethacrynic acid: A novel radiation enhancer in human carcinoma cells. *International Journal of Radiation Oncology*Biophysics*, 34(2), 375–380
- Kizil, S., Haşimi, N., Tolan, V., Kilinc, E. And Karataş, H., (2010) Chemical composition, antimicrobial and antioxidant activities of hyssop (*Hyssopus officinalis* L.) essential oil. *Notulae Botanicae Horti Agrobotanici Cluj-Napoca*, 38(3), pp.99-103.
- Korga, A., Józefczyk, A., Zgórk, G., Homa, M., Ostrowska, M., Burdan, F. and Dudka, J., (2017) Evaluation of the phytochemical composition and protective activities of methanolic extracts of *Centaurea borysthena* and *Centaurea daghestanica* (Lipsky) Wagenitz on cardiomyocytes treated with doxorubicin. *Food & nutrition research*, 61(1), p.1344077.
- Krishnadhas, L., Santhi, R. & Annapurani, S. (2016). Isolation and Identification of Flavonoid Fractions from the Leaves of *Volkameria inermis* and its In-vitro Cytotoxic Study. *International Journal of Pharmaceutical and Clinical Research*, 8(12): 1648-1653.
- Kumar, H., Kim, I., More, S.V., Kim, B.W. and Choi, D.K. (2014) Natural product-derived pharmacological modulators of Nrf2/ARE pathway for chronic diseases. *Natural Product Reports*, 31, 109-139.
- Kuno, T., Tsukamoto, T., Hara, A. and Tanaka, T., (2012) Cancer chemoprevention through the induction of apoptosis by natural compounds. *Journal of Biophysical Chemistry*, 3(02), p.156.
- Landis-Piwowar, K.R. and Iyer, N.R., (2014) Cancer chemoprevention: current state of the art. *Cancer growth and metastasis*, 7, pp.CGM-S11288.
- Lee, J.H., Shu, L., Su, Z.Y., Fuentes, F. and Kong, A.T. (2013) Cancer chemoprevention by Traditional Chinese Herbal Medicine and dietary phytochemicals: targeting Nrf2-

mediated oxidative stress/anti-inflammatory responses, epigenetics and cancer stem cells. *J Tradit Complement Med.*, 3(1), pp.69-79.

Lee-Hilz, Y. Y., Boerboom, A.-M. J. F., Westphal, A. H., van Berkel, W. J. H., Aarts, J. M. M. J. G. and Rietjens, I. M. C. M. (2006) Pro-Oxidant Activity of Flavonoids Induces EpRE-Mediated Gene Expression. *Chemical Research in Toxicology*, 19(11), 1499–1505.

Li, Y., Hong, J., Li, H., Qi, X., Guo, Y., Han, M., and Wang, X. (2017). Genkwanin nanosuspensions: a novel and potential antitumor drug in breast carcinoma therapy. *Drug Delivery*, 24(1), 1491–1500.

Lichtenberg, D. and Pinchuk, I., (2015) Oxidative stress, the term and the concept. *Biochemical and biophysical research communications*, 461(3), pp.441-444.

Liu, H.Y., Qiu, N.X., Ding, H.H. and Yao, R.Q. (2007) Polyphenols contents and antioxidant capacity of 68 Chinese herbals suitable for medical or food uses. *Food Research International*, 41(4), pp. 363–370.

Lou, C., Zhu, Z., Zhao, Y., Zhu, R. and Zhao, H., (2017) Arctigenin, a lignan from *Arctium lappa* L., inhibits metastasis of human breast cancer cells through the downregulation of MMP-2/-9 and heparanase in MDA-MB-231 cells. *Oncology reports*, 37(1), pp.179-184.

Lu, M.C., Ji, J.A., Jiang, Z.Y. and You, Q.D., (2016) The Keap1–Nrf2–ARE pathway as a potential preventive and therapeutic target: an update. *Medicinal research reviews*, 36(5), pp. 924-963.

Ma, J., Meng, Y., Kwiatkowski, D.J. *et al.* (2010) Mammalian target of rapamycin regulates murine and human cell differentiation through STAT3/p63/Jagged/Notch cascade. *J Clin Invest.* 120, 103–114.

Mabry T.J., Markham K.R. and Thomas M.B. (1970) *The Ultraviolet Spectra of Flavones and Flavonols*. In: *The Systematic Identification of Flavonoids*. Springer, Berlin, Heidelberg

Mabry, T.J., Markham, K.R. and Thomas, M.B. (2012) *The Systematic Identification of Flavonoids*, Springer Science & Business Media, 2012, p.330. Accessed at [<https://spectrabase.com/compound/7MEIVyUa8LY>].

Markham, K.R and Mabry, T.J. (1975). *Ultraviolet–visible and proton magnetic resonance spectroscopy of flavonoids*. In: Harborne, J.B., Mabry, T.J. and Mabry, H., editions. *The Flavonoids*. Chapman and Hall, London.

Markham, K.R. (1982). *Techniques of flavonoids identification*. Academic Press, London.

Martins, D. and Nunez, C., (2015) Secondary metabolites from Rubiaceae species. *Molecules*, 20(7), pp.13422-13495.

Mašković, P., Solujić, S., Mihailović, V., Mladenović, M., Cvijović, M., Mladenović, J., Aćamović-Đoković, G. and Kurćubić, V., (2011) Phenolic compounds and biological activity of *Kitaibelia vitifolia*. *Journal of medicinal food*, 14(12), pp.1617-1623.

Meeran, S.M., Ahmed, A. and Tollefsbol, T.O., (2010) Epigenetic targets of bioactive dietary components for cancer prevention and therapy. *Clinical epigenetics*, 1(3), p.101.

Menkovic *et al.* (2011) Ethnobotanical study on traditional uses of wild medicinal plants in Prokletije Mountains (Montenegro). *Journal of Ethnopharmacology*, 133(1), pp.97-107

Meyskens Jr, F.L., Mukhtar, H., Rock, C.L., Cuzick, J., Kensler, T.W., Yang, C.S., Ramsey, S.D., Lippman, S.M. and Alberts, D.S., (2015) Cancer prevention: obstacles, challenges, and the road ahead. *Journal of the National Cancer Institute*, 108(2), 309.

Mokgolodi, N.C., Hu, Y., Shi, L.L. and Liu, Y.J., (2011) *Ziziphus mucronata*: an underutilized traditional medicinal plant in Africa. *Forestry Studies in China*, 13(3), 163.

Mukhtar, H., (2012) Chemoprevention: making it a success story for controlling human cancer. *Cancer letters*, 326(2), pp.123-127.

Munhoz, V.M., Longhini, R., Souza, J.R.P., Zequi, J.A.C., Mello, E., Lopes, G.C. and Mello, J.C.P. (2014). Extraction of flavonoids from *Tagetes patula*: process optimization and screening for biological activity. *Revista Brasileira De Farmacognosia-Brazilian Journal of Pharmacognosy*, 24(5), 576-583.

Myhrstad, M.C., Carlsen, H., Nordström, O., Blomhoff, R., Moskaug, J.Ø. (2002) Flavonoids increase the intracellular glutathione level by transactivation of the gamma-glutamylcysteine synthetase catalytical subunit promoter. *Free Radical Biology&Medicine* 32(5), 386-93.

MyIntyre, D., D. and Hans J. Vogel, H.J. (1989) Complete Assignment of the ¹H-NMR Spectrum of Stachyose by Two-Dimensional NMR Spectroscopy. *Journal of Natural Products*, 52(5), 1008-1014.

Nair, S., Li, W. and Kong, A.T. (2007) Natural dietary anti-cancer chemopreventive compounds: redox-mediated differential signaling mechanisms in cytoprotection of normal cells versus cytotoxicity in tumor cells. *Acta Pharmacol Sin*, 28(4), p.459-472.

Nakajima, S., Doi, R., Toyoda, E. *et al.* (2004) N-cadherin expression and epithelial-to-mesenchymal transition in pancreatic carcinoma. *Clin Cancer Res*, 10, 4125-4133.

- Neergheen, V.S., Bahorun, T., Taylor, E.W., Jen, L.S. and Aruoma, O.I. (2010) Targeting specific cell signaling transduction pathways by dietary and medicinal phytochemicals in cancer chemoprevention. *Toxicology*, 278, p.229-241.
- Nijveldt, R.J., van Nood, E., van Hoorn, D.E.C., Boelens, P.G, van Norren, K. and van Leeuwen, P.A.M. (2001) Flavonoids: a review of probable mechanisms of action and potential applications (2001) *Am J Clin Nutr*, 74, 418–25.
- Nimse, S. B. and Pal, D. (2015). Free radicals, natural antioxidants, and their reaction mechanisms. *RSC Advances*, 5(35), 27986–28006
- Oakley, A.J., Lo Bello, M., Mazzetti, A.P., Federici, G. and Parker, M.W.(1997) The glutathione conjugate of ethacrynic acid can bind to human pi class glutathione transferase P1-1 in two different modes. *FEBS Letters* 419(1), 32-36.
- Oh, J., Hlatky, L., Jeong, Y.S. and Kim, D., (2016) Therapeutic effectiveness of anticancer phytochemicals on cancer stem cells. *Toxins*, 8(7), 199.
- Oyeyemi, S.D., Ayeni, M.J., Adebisi, A.O., Ademiluyi, B.O., Tedela, P.O. and Osuji, I.B., (2015) Nutritional quality and phytochemical studies of *Solanum anguivi* (Lam.) Fruits. *J. Nat. Sci. Res*, 5(4), pp.99-105.
- Pandey, K.B. and Rizvi, S.I. (2009) Plant polyphenols as dietary antioxidants in human health and disease
- Panero, J.L. and Crozier, B.S., (2016) Macroevolutionary dynamics in the early diversification of Asteraceae. *Molecular phylogenetics and evolution*, 99, pp.116-132.
- Patterson, S.L., Maresso, K.C. and Hawk, E., (2013) Cancer chemoprevention: successes and failures. *Clinical chemistry*, 59(1), pp.94-101.
- Ploemen, J. H. T. M., Van Schanke, A., Van Ommen, B. and Van Bladeren, P. J. (1994) Reversible Conjugation of Ethacrynic Acid with Glutathione and Human Glutathione S-Transferase PI-1. *Cancer Research* 54, 915-919.
- Qin, S., Deng, F., Wu, W., Jiang, L., Yamashiro, T., Yano, S. and Hou, D.X. (2014). Baicalein modulates Nrf2/Keap1 system in both Keap1-dependent and Keap1-independent mechanisms. *Archives of Biochemistry and Biophysics*, 559, 53–61.
- Qiong, G.A.O., Mengbi, Y.A.N.G. and Zhong, Z.U.O., (2018) Overview of the anti-inflammatory effects, pharmacokinetic properties and clinical efficacies of arctigenin and arctiin from *Arctium lappa* L. *Acta Pharmacologica Sinica*, 39, pp.787-801.

Rabeta MS, Lin SP. Effects of different drying methods on the antioxidant activities of leaves and berries of *Cayratia trifolia*. *Sains Malaysiana*. 2015;44(2):275-280

Rai, M. and Kon, K. eds., 2013. *Fighting Multidrug Resistance with Herbal Extracts, Essential Oils and Their Components*. Academic Press.

Ranger, G.S., (2014) Current concepts in colorectal cancer prevention with cyclooxygenase inhibitors. *Anticancer research*, 34(11), pp.6277-6282.

Rao, C.V., Desai, D., Simi, B., Kulkarni, N. and Amin, S. (1993b) Inhibitory effect of caffeic acid esters on azoxymethane-induced biochemical changes and aberrant crypt foci formation in rat colon. *Cancer Research*, 53, p.4182-4188.

Rao, C.V., Simi, B. and Reddy, B.S. (1993a) Inhibition by dietary curcumin of azoxymethane-induced ornithine decarboxylase, tyrosine protein kinase, arachidonic acid metabolism and aberrant crypt foci formation in the rat colon. *Carcinogenesis*, 14, p.2219-2225.

Rashid, S., (2017). *Cancer and chemoprevention: An overview*. Springer.

Rasul, A., Millimouno, F.M., Ali Eltayb, W., Ali, M., Li, J. and Li, X., (2013) Pinoцембрin: a novel natural compound with versatile pharmacological and biological activities. *BioMed research international*, 1-9.

Ríos-Arrabal, S., Artacho-Cordón, F., León, J., Román-Marinetto, E., del Mar Salinas-Asensio, M., Calvente, I. and Núñez, M.I., (2013) Involvement of free radicals in breast cancer. *Springerplus*, 2(1), 404.

Roche, J. (2018). The Epithelial-to-Mesenchymal Transition in Cancer. *Cancers*, 10(2), 52.

Rodríguez-Pérez, C., Quirantes-Piné, R., Fernández-Gutiérrez, A., Segura-Carretero, A., (2015). Optimization of extraction method to obtain a phenolic compounds-rich extract from *Moringa oleifera* Lam leaves. *Indust. Crops Prod.*, 66, 246–254

Russo, M., Spagnuolo, C., Tedesco, I. and Russo, G.L., (2010). Phytochemicals in cancer prevention and therapy: truth or dare?. *Toxins*, 2(4), pp.517-551.

Santos-Buelga, C., García-Viguera, C., Tomás-Barberán, F. A. 2003. On-line identification of flavonoids by HPLC coupled to diode array detection. Pp. 92–127 in *Methods in polyphenol analysis*, eds. Santos-Buelga, C., Williamson, G., The Royal Society of Chemistry, Cambridge, UK.

Sarker, S.D and Nahar, L. (2007) *Chemistry for Pharmacy Students: General, Organic and Natural Product Chemistry*. Jon Wiley & Sons, England.

Saslis-Lagoudakis, C. H., Bruun-Lund, S., Iwanycki, N. E., Seberg, O., Petersen, G., Jäger, A. K.. and Rønsted, N. (2015). Identification of common horsetail (*Equisetum arvense* L.; Equisetaceae) using Thin Layer Chromatography versus DNA barcoding. *Scientific Reports*, 5(1).

Sato, F. and Matsui, K. (2012). Engineering the biosynthesis of low molecular weight metabolites for quality traits (essential nutrients, health-promoting phytochemicals, volatiles, and aroma compounds). *Plant Biotechnology and Agriculture*, 443–461.

Sauer, A.G., Siegel, R.L., Jemal, A. and Fedewa, S.A., (2017) Updated review of prevalence of major risk factors and use of screening tests for cancer in the United States. *Cancer Epidemiology and Prevention Biomarkers*, p.219.

Schafer, H., Geismann, C., Arlt, A., & Sebens, S. (2014). Cytoprotection “gone astray”: Nrf2 and its role in cancer. *OncoTargets and Therapy*, 7, p.1497.

Setia, S., Nehru, B. and Sanyal, S.N., (2014) Upregulation of MAPK/Erk and PI3K/Akt pathways in ulcerative colitis-associated colon cancer. *Biomedicine & Pharmacotherapy*, 68(8), pp.1023-1029.

Shankar, E., Kanwal, R., Candamo, M. and Gupta, S., (2016) October. Dietary phytochemicals as epigenetic modifiers in cancer: promise and challenges. In *Seminars in cancer biology* (Vol. 40, pp. 82-99). Academic Press.

Sharma, N., (2014). Free radicals, antioxidants and disease. *Biology and Medicine*, 6(3), 1.

Shen, G., Xu, C., Hu, R., Jain, M.R., Gopalakrishnan, A., Nair, S., Huang, M.T., Chan, J.Y. and Kong, A.N. (2006) Modulation of nuclear factor E2-related factor 2-mediated gene expression in mice liver and small intestine by cancer chemopreventive agent curcumin. *Molecular Cancer Therapeutics*, 5, p. 39-51

Shimada, T. (2017) Inhibition of carcinogen-activating cytochrome P450 enzymes by xenobiotic chemicals in relation to antimutagenicity and anticarcinogenicity. *Toxicological research*, 33(2), 79.

Shoeb, M., Macmanus, S.M., Kong-Thoo-Lin, P., Celik, S., Jaspars, M., Nahar, L. and Sarker, S.D. (2007) 'Bioactivity of the extracts and isolation of lignans and a sesquiterpene from the aerial parts of *Centaurea pamphylica* (Asteraceae)' *DARU*, vol. 15, no. 3, 118-122.

- Shoemaker, M.L., Holman, D.M., Henley, S.J. and White, M.C., (2015) News from CDC: applying a life course approach to primary cancer prevention. *Translational behavioral medicine*, 5(2), 131-133.
- Stanković, N., Mihajilov-Krstev, T., Zlatković, B., Matejić, J., StankovJovanović, V., Kocić, B. and Čomić, L. (2016) Comparative study of composition, antioxidant, and antimicrobial activities of essential oils of selected aromatic plants from Balkan Peninsula. *Planta Med*, 82(7), pp.650-661.
- Staurengo-Ferrari, L., Badaro-Garcia, S., Hohmann, M. S. N., Manchope, M. F., Zaninelli, T. H., Casagrande, R., & Verri, W. A. (2019). Contribution of Nrf2 Modulation to the Mechanism of Action of Analgesic and Anti-inflammatory Drugs in Pre-clinical and Clinical Stages. *Frontiers in Pharmacology*, 9
- Steward, W.P. and Brown, K., (2013) Cancer chemoprevention: a rapidly evolving field. *British journal of cancer*, 109(1), pp.1.
- Su, Z.Y., Shu, L., Khor, T.O., Lee, J.H., Fuentes, F. and Kong, A.T. (2013) A perspective on dietary phytochemicals and cáncer chemoprevention: oxidative stress, Nrf2, and epigenomics. *Top Curr Chem*, 329, p.133-162
- Subhasree, B., Baskar, R., LAXmi Keerthana, R., Lijina Susan, R. and Rajasekaran, P. (2008) Evaluation of antioxidant potential in selected green leafy vegetables. *Food Chemistry*, 115(4), pp. 1213-1220
- Sucha, L. and Tomsik, P., (2016) The steroidal glycoalkaloids from solanaceae: toxic effect, antitumour activity and mechanism of action. *Planta medica*, 82(05), pp.379-387.
- Sun, Q., Liu, K., Shen, X., Jin, W., Jiang, L., Sheikh, M.S., Hu, Y. and Huang, Y., (2014) Lappaol F, a novel anticancer agent isolated from plant *Arctium Lappa* L. *Molecular cancer therapeutics*, 13(1), pp.49-59.
- Sun, S-Y., Hail, N. and Lotan, R. (2004) Apoptosis as a novel target for cancer chemoprevention. *Journal of the Ntional Cancer Institute*, 96(9), p. 662-672.
- Surh, Y-J. (2003) Cancer chemoprevention with dietary phytochemicals. *Nature Reviews*, 3(10), pp.768-780.
- Surova, O. and Zhivotovsky, B. (2013) Various modes of cell death induced by DNA damage. *Oncogene*, 32, 3789-3797.

- Susanti, S., Iwasaki, H., Inafuku, M., Taira, N. and Oku, H., (2013) Mechanism of arctigenin-mediated specific cytotoxicity against human lung adenocarcinoma cell lines. *Phytomedicine*, 21(1), pp.39-46.
- Syu, J. P., Chi, J. T. and Kung, H. N. (2016). Nrf2 is the key to chemotherapy resistance in MCF7 breast cancer cells under hypoxia. *Oncotarget*, 7(12), 14659–14672
- Taguchi, K., Motohashi, H. and Yamamoto, M. (2011). Molecular mechanisms of the Keap1-Nrf2 pathway in stress response and cancer evolution. *Genes Cells* 16, 123–140.
- Taia, W.K., (2009) General View of Malvaceae Juss. SL and Taxonomic Revision of Genus *Abutilon* Mill. in Saudi Arabia. *Journal of King Abdulaziz University-Science*, 21(2), pp.349-363.
- Talalay, P., De Long, M. J. and Prochaska, H. J. (1988). Identification of a common chemical signal regulating the induction of enzymes that protect against chemical carcinogenesis. *Proceedings of the National Academy of Sciences*, 85(21), 8261–8265.
- Talib, W. H., Zarga, M. H. A. and Mahasneh, A. M. (2012). Antiproliferative, Antimicrobial and Apoptosis Inducing Effects of Compounds Isolated from *Inula viscosa*. *Molecules*, 17(3), 3291–3303.
- Tamokou, J.D.D., Mbaveng, A.T. and Kuete, V., (2017) Antimicrobial activities of African medicinal spices and vegetables. In *Medicinal Spices and Vegetables from Africa* (pp. 207-237).
- Tan, S.P., Parks, S.E., Stathopoulos, C.E. & Roach, P.D. (2014). Extraction of flavonoids from bitter melon. *Food and Nutrition Sciences*, 5(5):458-465.
- Tang, X., Wang, H., Fan, L., Wu, X., Xin, A., Ren, H. and Wang, X. J. (2011). Luteolin inhibits Nrf2 leading to negative regulation of the Nrf2/ARE pathway and sensitization of human lung carcinoma A549 cells to therapeutic drugs. *Free Radical Biology and Medicine*, 50(11), 1599–1609
- Tanigawa, S., Fujii, M. and Hou, D. (2007). Action of Nrf2 and Keap1 in ARE-mediated NQO1 expression by quercetin. *Free Radical Biology and Medicine*, 42(11), 1690–1703
- Thomas, R., Butler, E., Macchi, F. and Williams, M. (2015) Phytochemicals in cancer prevention and management?. *British Journal of Medical Practitioners*, 8(2), pp.12-19.
- Timofte, C. (2017) Multiscale analysis of a carcinogenesis model. *Mathematics and Computers in Simulation*, 133, 298-310.

Toyin, Y.M., Olakunle, A.T. and Adewunmi, A.M., (2014) Toxicity and Beneficial Effects of Some African Plants on the Reproductive System. *Toxicological Survey of African Medicinal Plants*, 445-492.

Toyokuni, S. (2016) Oxidative stress as an iceberg in carcinogenesis and cancer biology. *Archives of Biochemistry and Biophysics*, 595, pp.46-49.

Tsao, R., (2010) Chemistry and biochemistry of dietary polyphenols. *Nutrients*, 2(12), pp.1231-1246.

Tshitenge, D.T., Feineis, D., Awale, S. and Bringmann, G., (2017) Gardenifolins A–H, scalemic neolignans from *Gardenia ternifolia*: Chiral resolution, configurational assignment, and cytotoxic activities against the HeLa cancer cell line. *Journal of natural products*, 80(5), pp.1604-1614.

Turati, F., Rossi, M., Pelucchi, C., Levi, F. and La Vecchia, C., (2015) Fruit and vegetables and cancer risk: a review of southern European studies. *British Journal of Nutrition*, 113(S2), pp.S102-S110.

Ullah, M.F. and Ahmad, A. eds., (2016) *Critical Dietary Factors in Cancer Chemoprevention*. Switzerland: Springer.

Vadivel, V., (2016) Distribution of flavonoids among Malvaceae family members—A review. *International Journal of Green Pharmacy (IJGP)*, 10(1).

Vaidya, B.N., Brearley, T.A. & Joshee, N. (2014). Antioxidant capacity of fresh and dry leaf extracts of sixteen *Scutellaria* species. *Journal of Medicinally Active Plants*, 2(3):42-49.

Valerio, L.G. Jr, Kepa, J.K., Pickwell, G.V. and Quattrochi, L.C. Induction of human NAD(P)H:quinone oxidoreductase (NQO1) gene expression by the flavonol quercetin. *Toxicology Letters*, 119(1), 49-57.

Veggi, P.C., Martinez, J. & Meireles, M.A.A. (2013). *Fundamentals of microwave extraction*. In: Chemat, F. & Cravotto, G., editors. *Microwave-assisted extraction for bioactive compounds: theory and practice, food engineering series 4*. Springer Science & Business Media, New York, 15-52.

Vidya Priyadarsini, R. and Nagini, S., (2012) Cancer chemoprevention by dietary phytochemicals: promises and pitfalls. *Current pharmaceutical biotechnology*, 13(1), pp.125-136.

- Wang, X.J., Sun, Z., Villeneuve, N.F., Zhang, S., Zhao, F., Li, Y., Zhang, D D. (2008). Nrf2 enhances resistance of cancer cells to chemotherapeutic drugs, the dark side of Nrf2. *Carcinogenesis*, 29(6), 1235–1243.
- Ward, W.M, Hoffman, J.D. and Loo, G. (2015) Genotoxic effect of ethacrynic acid and impact of antioxidants. *Toxicology and Applied Pharmacology* 286(1), 17-26.
- White, M.C., Shoemaker, M.L., Park, S., Neff, L.J., Carlson, S.A., Brown, D.R. and Kanny, D., (2017) Prevalence of modifiable cancer risk factors among US adults aged 18–44 years. *American journal of preventive medicine*, 53(3), pp.S14-S20.
- World Health Organization (2018) Cancer fact sheet [Online]. Available at: <http://www.who.int/news-room/fact-sheets/detail/cancer> (Accessed: 22 October 2018).
- Wu, X., Patterson, S. and Hawk, E., (2011) Chemoprevention–history and general principles. *Best practice & research Clinical gastroenterology*, 25(4-5), pp.445-459.
- Yadav, R., Rathi, M., Pednekar, A. and Rewachandani, Y., (2016) A detailed review on Solanaceae family. *Euro J Pharm Med Res*, 3(1), pp.369-378.
- Yadegarynia, S., Pham, A., Ng, A., Nguyen, D., Lialiukska, T., Bortolazzo, A., Sivryuk, V., Bremer, M. and White, J.B. (2012) Profiling flavonoid cytotoxicity in human breast cancer cell lines: determination of structure-function relationships. *Nat Prod Commun*. 7(10), 1295-304.
- Youssef, B.S., Fakhfakh, J., Tchoumtchoua, J., Halabalaki, M. and Allouche, N., (2016) Efficient purification and complete NMR characterization of galactinol, sucrose, raffinose, and stachyose isolated from *Pinus halepensis* (Aleppo pine) seeds using acetylation procedure. *Journal of Carbohydrate Chemistry*, 35:4, 224-237.
- Yu, X. and Kensler, T., (2005) Nrf2 as a target for cancer chemoprevention. *Mutation Research/Fundamental and Molecular Mechanisms of Mutagenesis*, 591(1), pp.93-102.
- Yuan, J., Zhang, S. and Zhang, Y., (2018) Nrf1 is paved as a new strategic avenue to prevent and treat cancer, neurodegenerative and other diseases. *Toxicology and applied pharmacology*.
- Zaynab, M., Fatima, M., Sharif, Y., Zafar, M. H., Ali, H. and Khan, K. A. (2019). Role of primary metabolites in plant defense against pathogens. *Microbial Pathogenesis*, 103728.

- Zhang, C., Wang, H. J., Bao, Q. C., Wang, L., Guo, T. K., Chen, W. L., You, Q. D. (2016). NRF2 promotes breast cancer cell proliferation and metastasis by increasing RhoA/ROCK pathway signal transduction. *Oncotarget*, 7(45), 73593–73606.
- Zhang, D. D., Lo, S.C., Sun, Z., Habib, G. M., Lieberman, M. W. and Hannink, M. (2005). Ubiquitination of Keap1, a BTB-Kelch Substrate Adaptor Protein for Cul3, Targets Keap1 for Degradation by a Proteasome-independent Pathway. *Journal of Biological Chemistry*, 280(34), 30091–30099.
- Zhang, H. S., Zhang, Z. G., Du, G. Y., Sun, H. L., Liu, H. Y., Zhou, Z. and Huang, Y. H. (2019). Nrf2 promotes breast cancer cell migration via up-regulation of G6PD/HIF-1 α /Notch1 axis. *Journal of Cellular and Molecular Medicine*, 23(5), 3451-3463
- Zhang, T.T., Lu, C.L., Jiang, J.G., Wang, M., Wang, D.M. & Zhu, W. (2015). Bioactivities and extraction optimization of crude polysaccharides from the fruits and leaves of *Rubus chingii* Hu. *Carbohydr. Polym.*, 130, 307–315.
- Zhao, C.R., Gao, Z.H. and Qu, X.J., (2010) Nrf2–ARE signaling pathway and natural products for cancer chemoprevention. *Cancer epidemiology*, 34(5), 523-533.
- Zheng, J., Zhou, Y., Li, Y., Xu, D.P., Li, S. and Li, H.B., (2016) Spices for prevention and treatment of cancers. *Nutrients*, 8(8), 495.
- Zheng, L.L., Wen, G., Yuan, M.Y. & Gao, F. (2016). Ultrasound-assisted extraction of total -flavonoids from corn silk and their antioxidant activity. *Journal of Chemistry*, 2016:1-5.
- Zheng, W. and Lee, S., (2009). Well-done meat intake, heterocyclic amine exposure and cancer risk. *Nutr Cancer*, 61(4), 437-446

Appendices

Appendix A NMR and MS spectra of precipitated compounds

Appendix A.1 NMR and MS data for precipitate GPS1 as stachyose

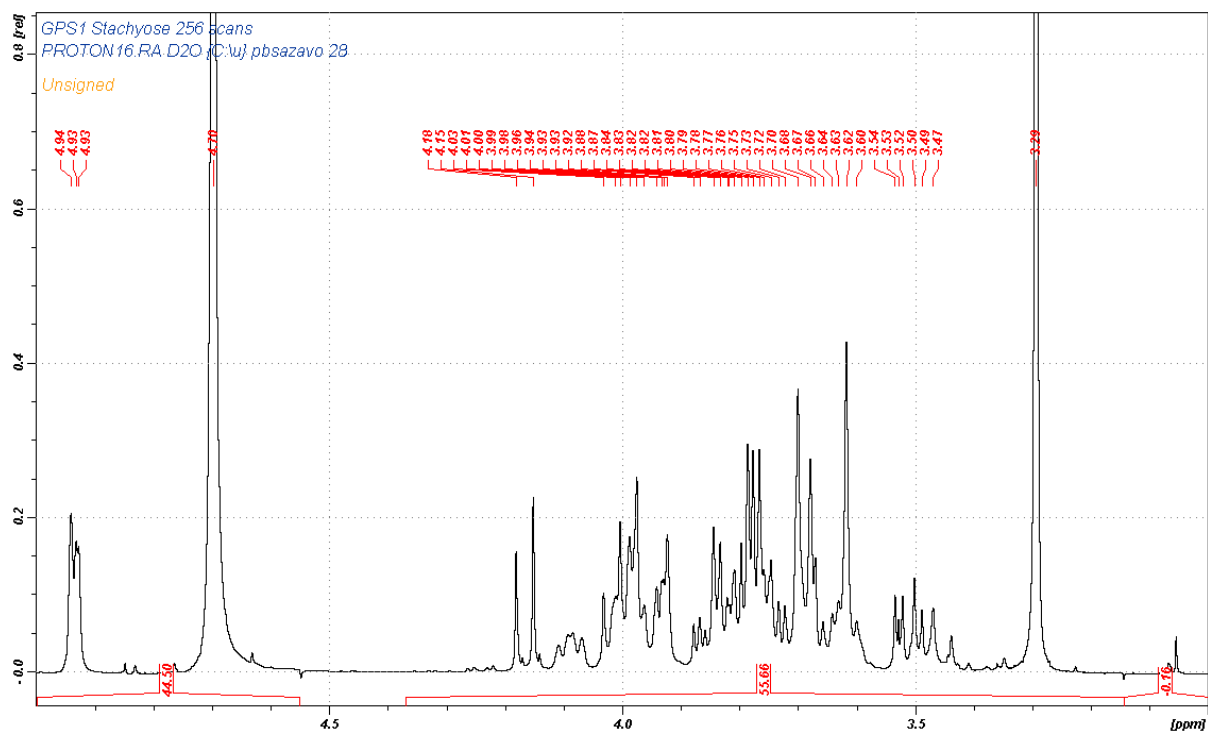


Figure 130 +H NMR spectrum of GPS1

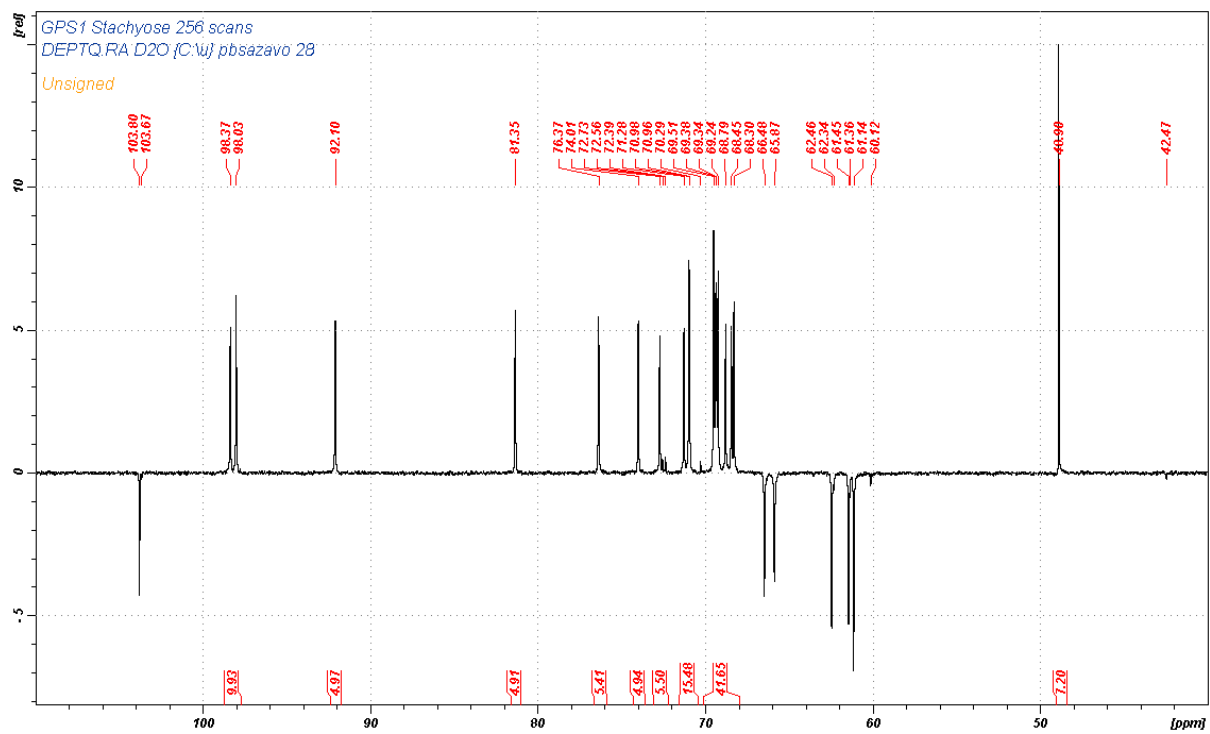


Figure 131 DEPTQ experiment spectrum of GPS1

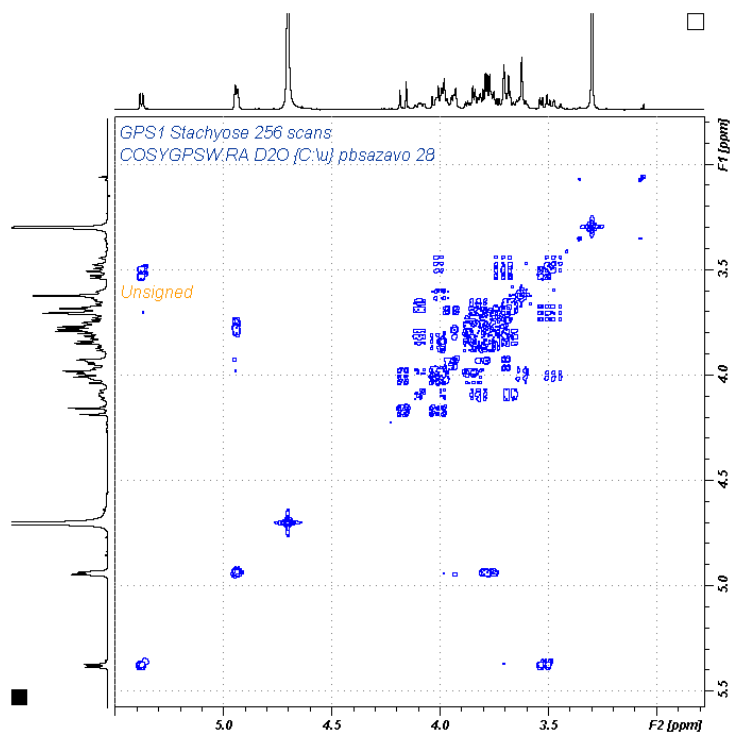


Figure 132 COSY experiment spectrum of stachyose

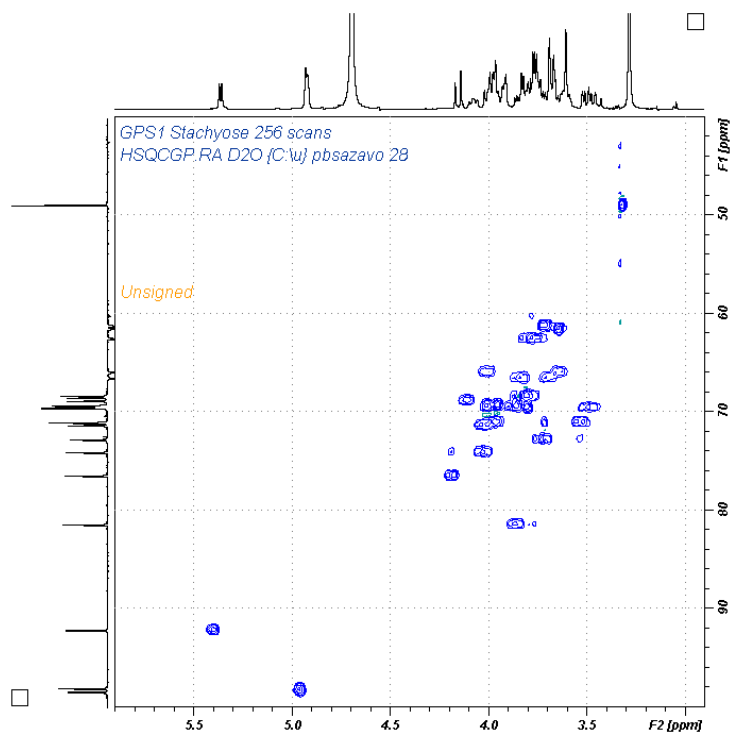


Figure 133 HSQC experiment spectrum of stachyose

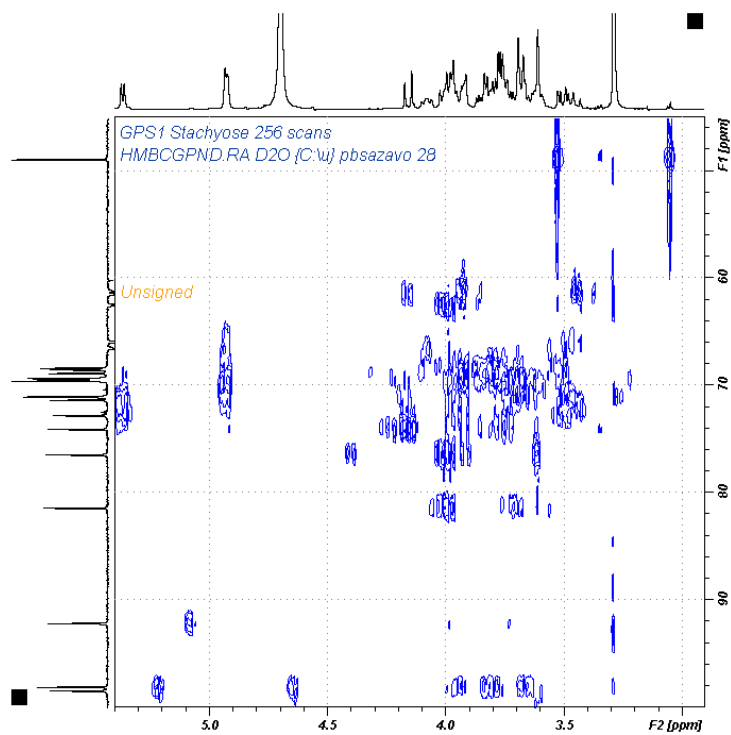


Figure 134 HMBC experiment spectrum of stachyose

Appendix A.2 NMR and MS data for precipitate GTS1/GTS2

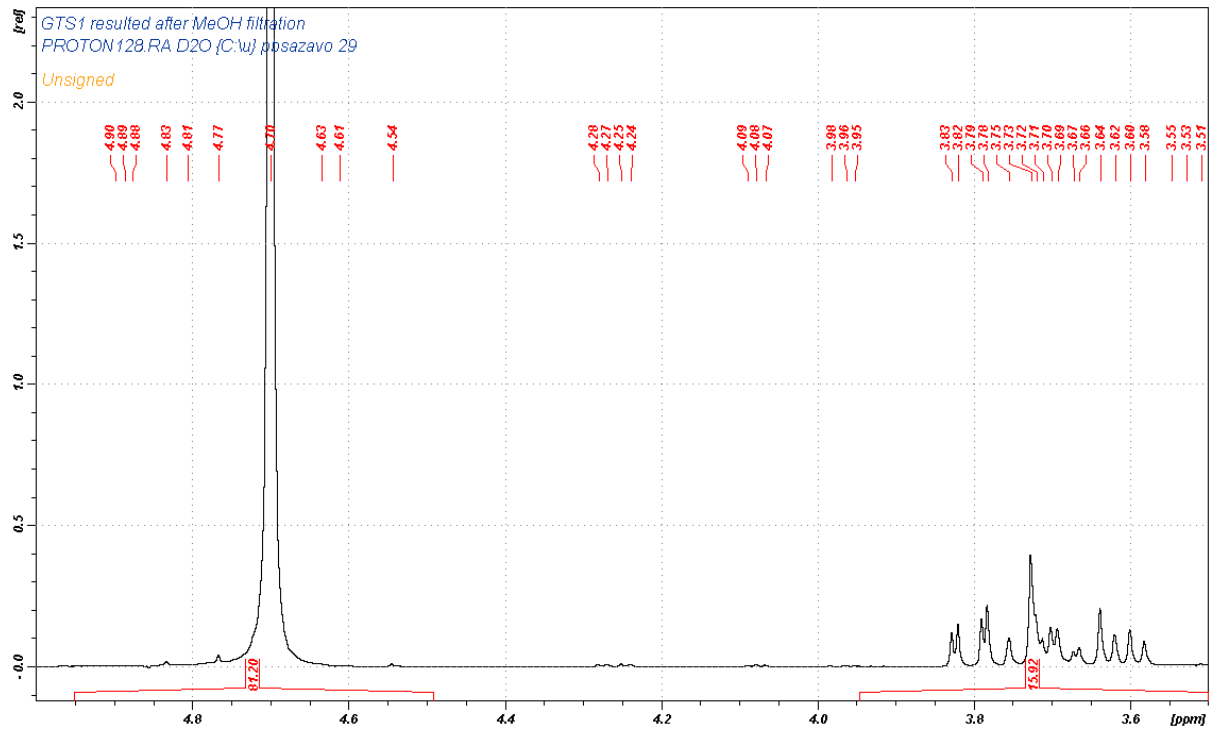


Figure 135 ¹H NMR spectrum of mannitol isolated after filtration of GT methanol extract

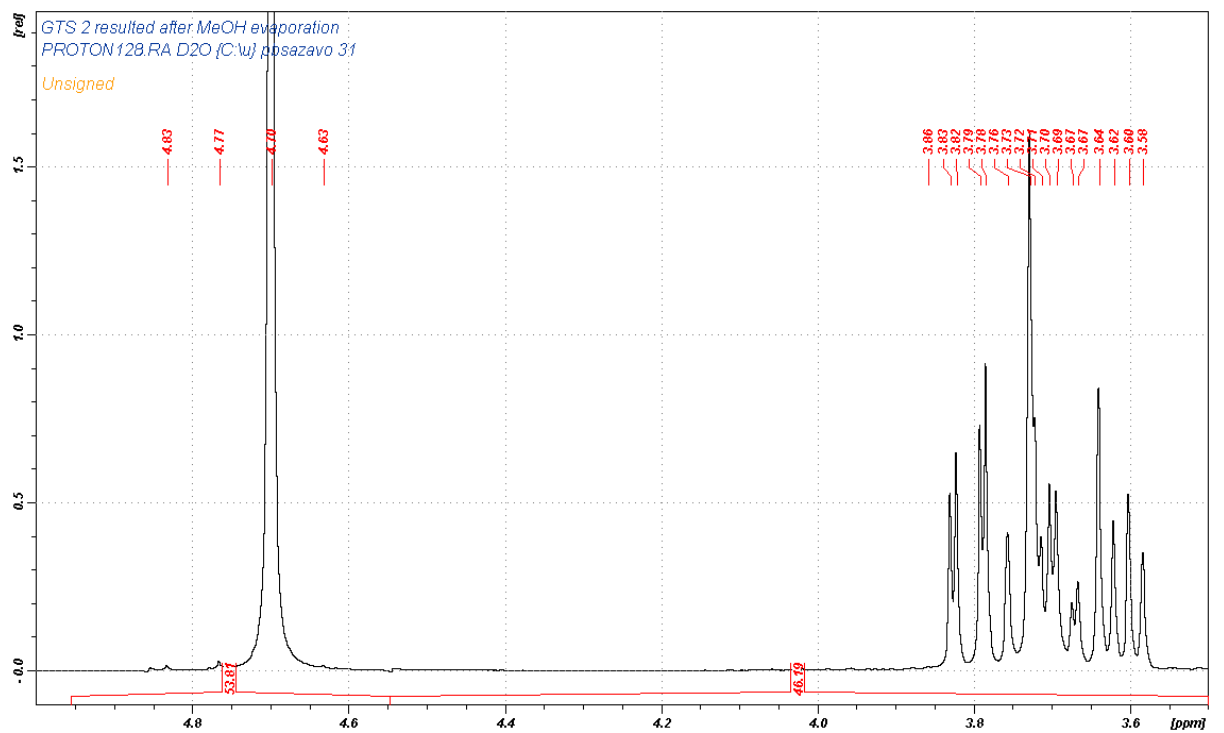


Figure 136 ¹H NMR spectrum of mannitol isolated after evaporation of GT methanol extract

Appendix A.3 NMR and MS data for precipitate ZMPH1

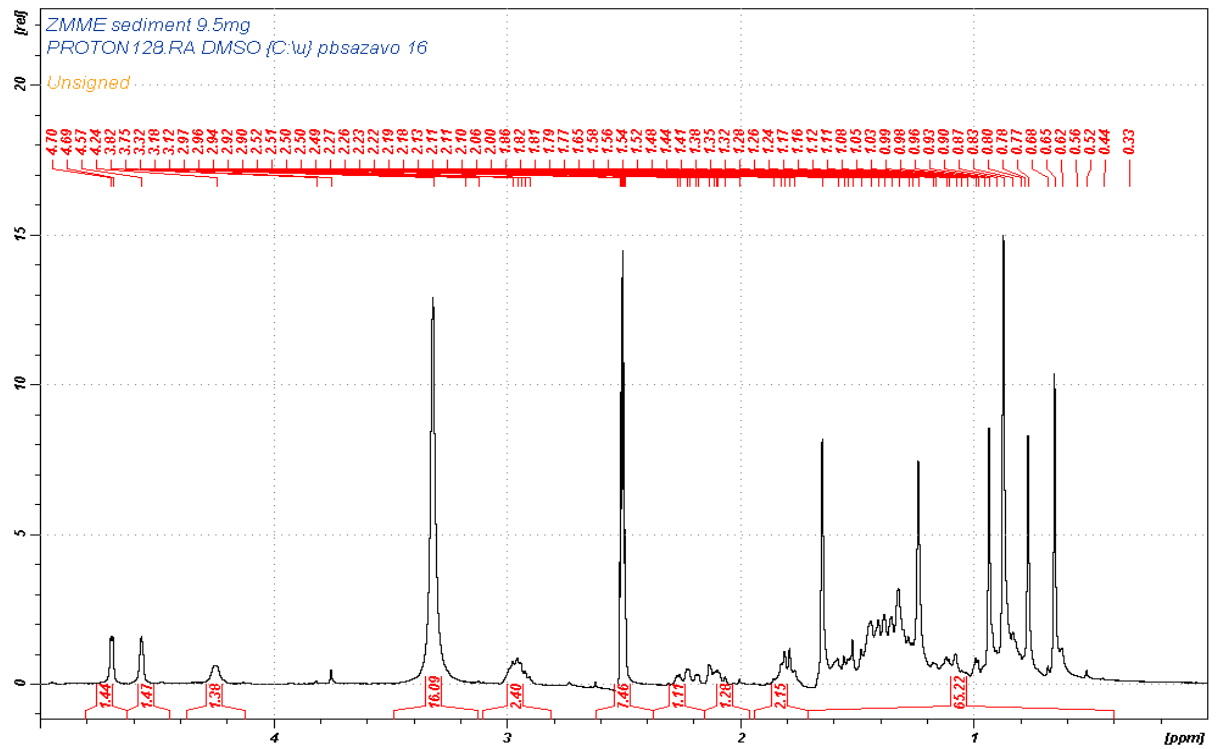


Figure 137 +H NMR spectrum of betulinic acid

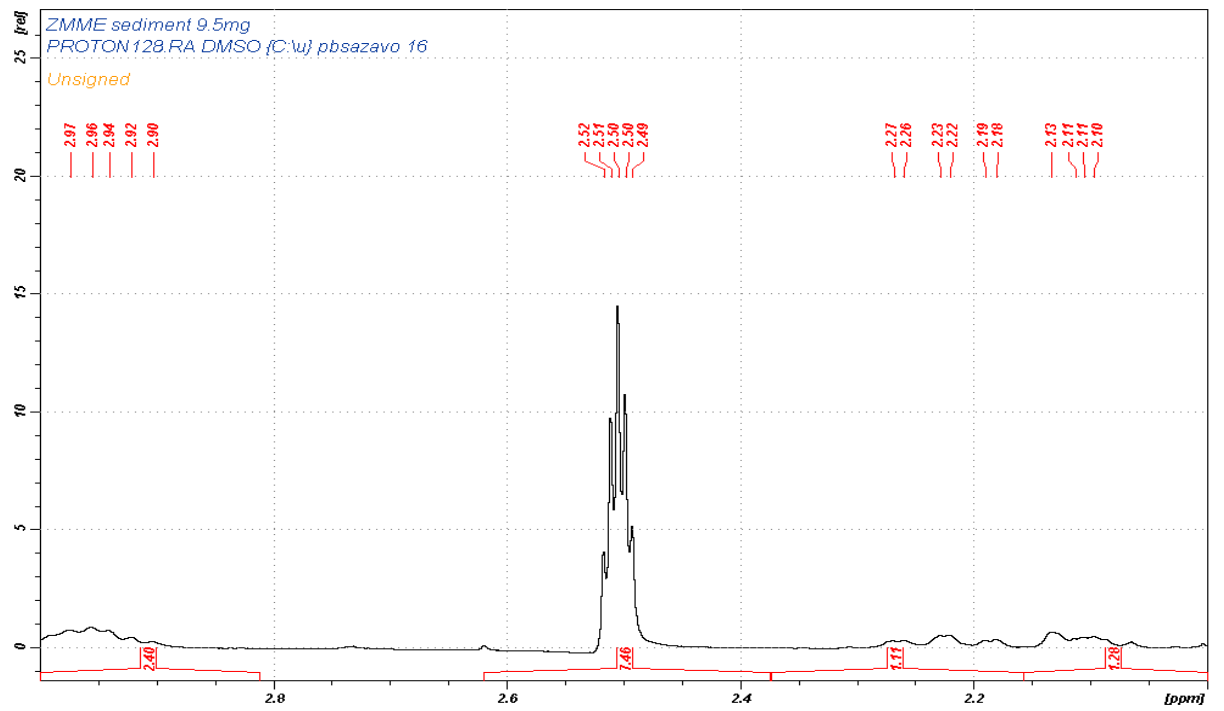


Figure 138 Expansion of +H NMR spectrum of betulinic acid

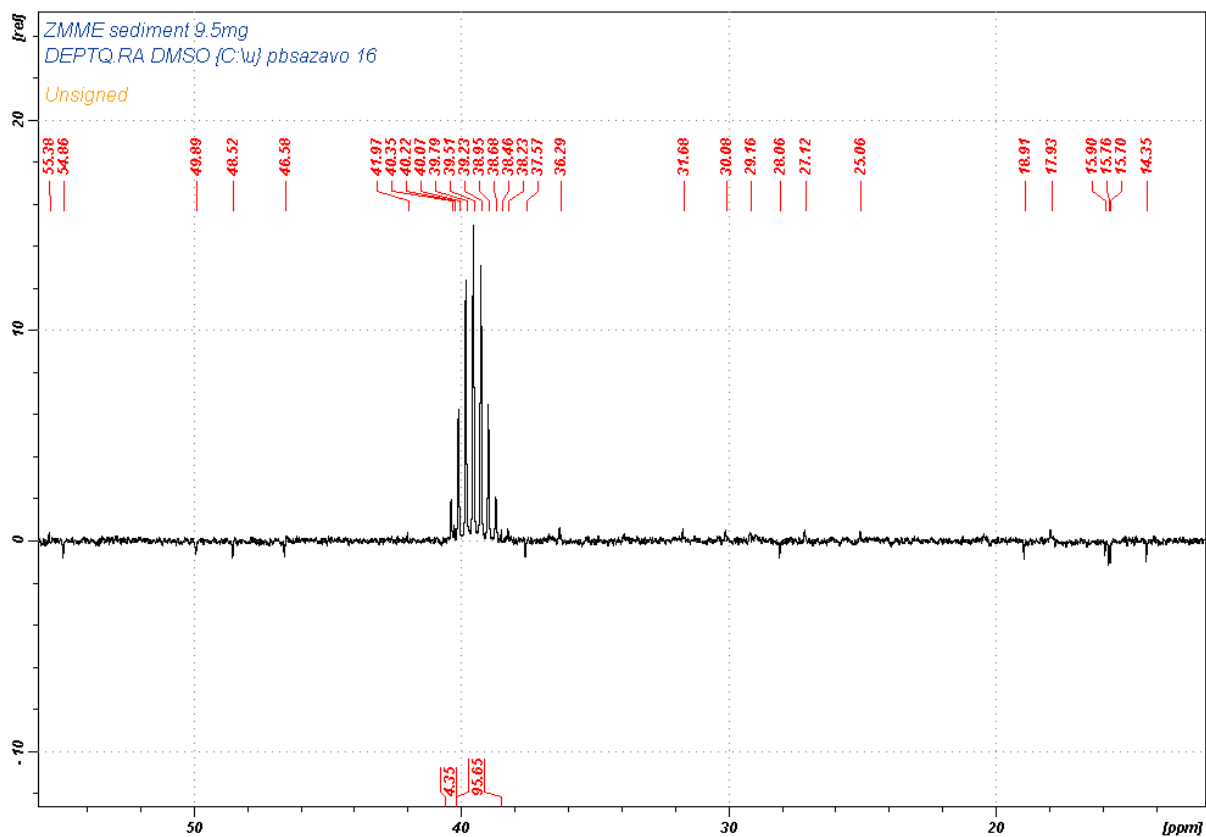


Figure 139 DEPTQ experiment spectrum of betulinic acid

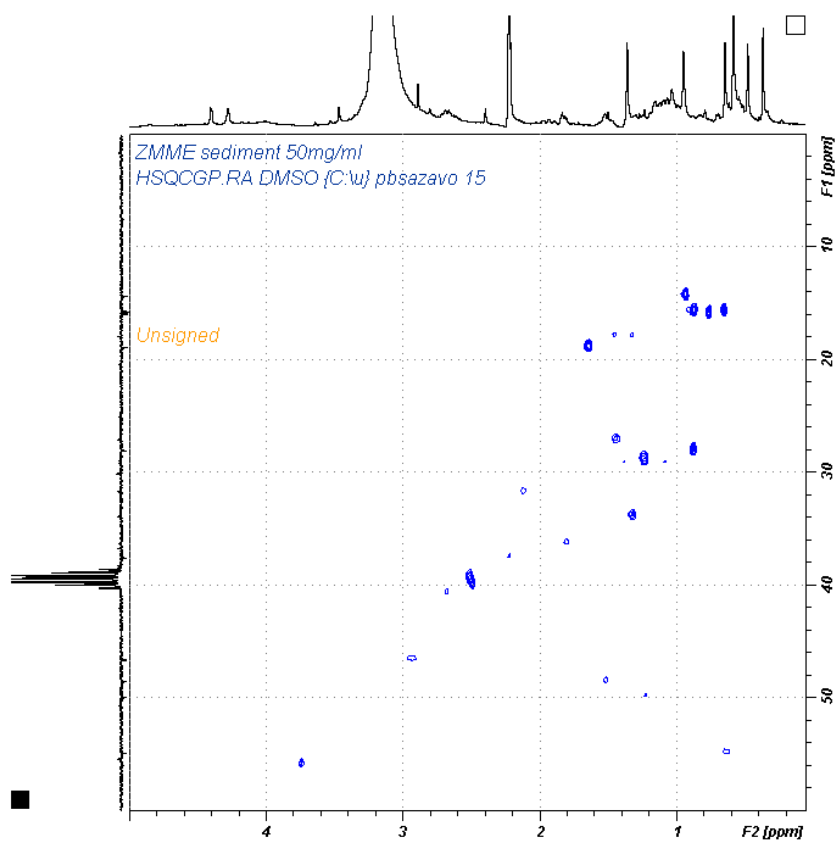


Figure 140 HSQC experiment spectrum of betulinic acid

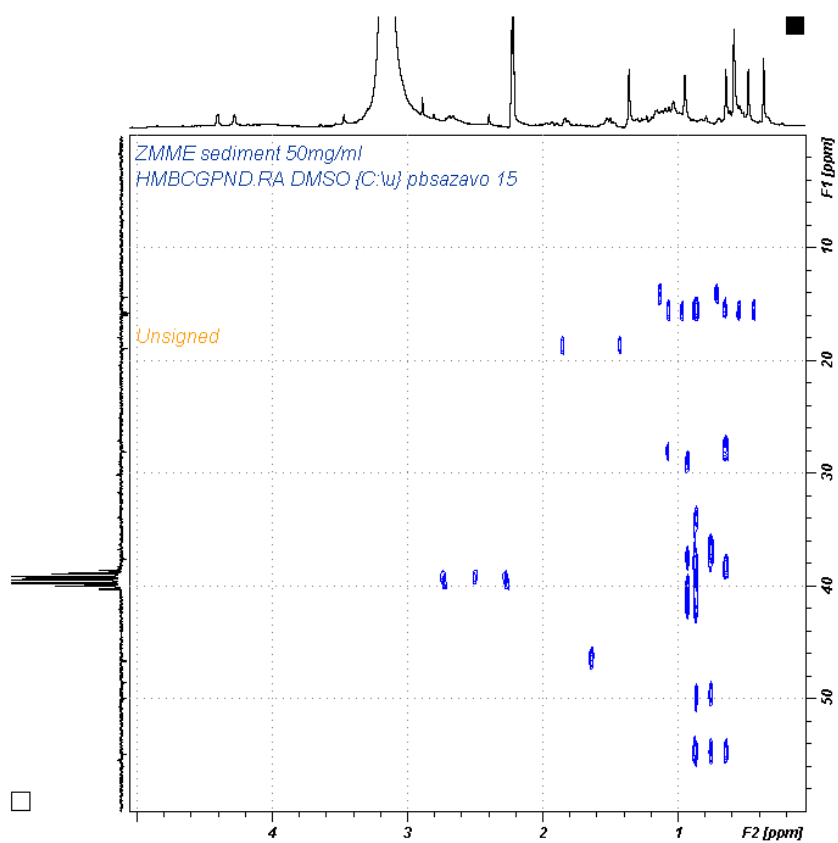


Figure 141 HMBC experiment spectrum of betulinic acid

Appendix B NMR and MS data for isolated compounds from *Gardenia ternifolia* Schumach.& Thonn. (GT-Me)

Appendix B.1 NMR and MS data for compound F3-GT-Me-PA (aka F3GTME-PA/F3GTME-P4)

F3GTME.PA
PROTON MeOD

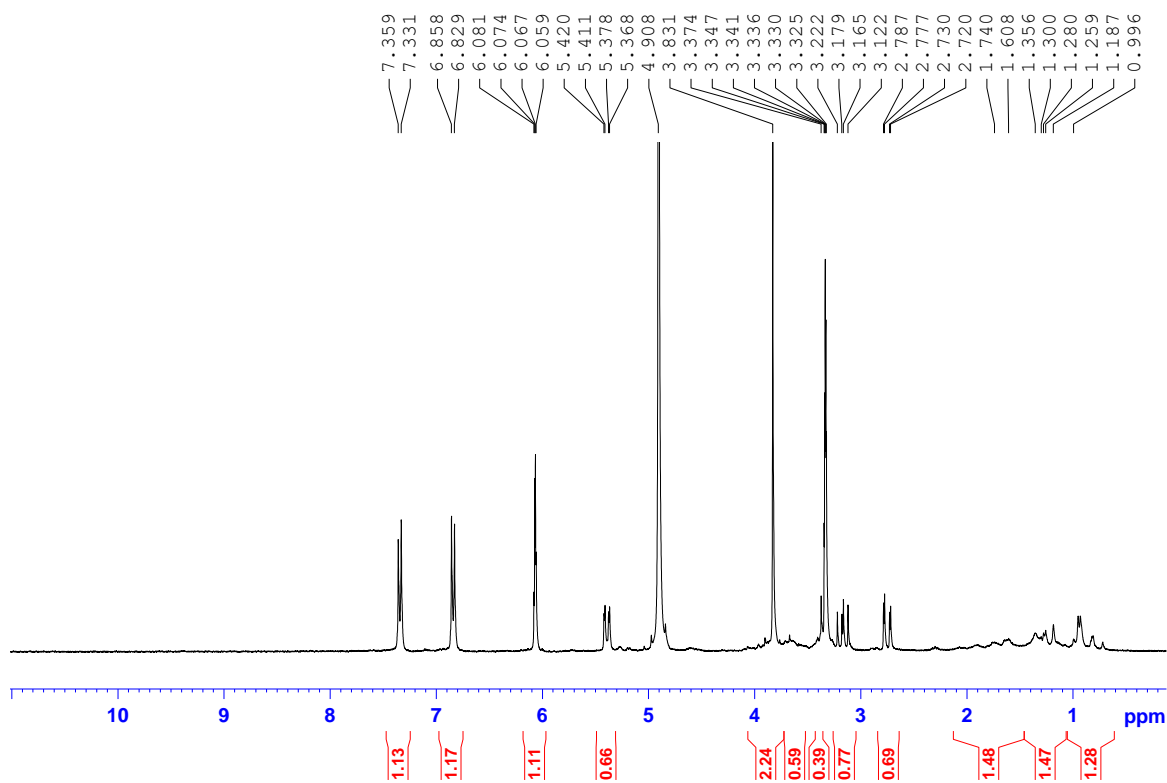


Figure 142 Proton NMR spectrum of F3GT-Me-P4/PA

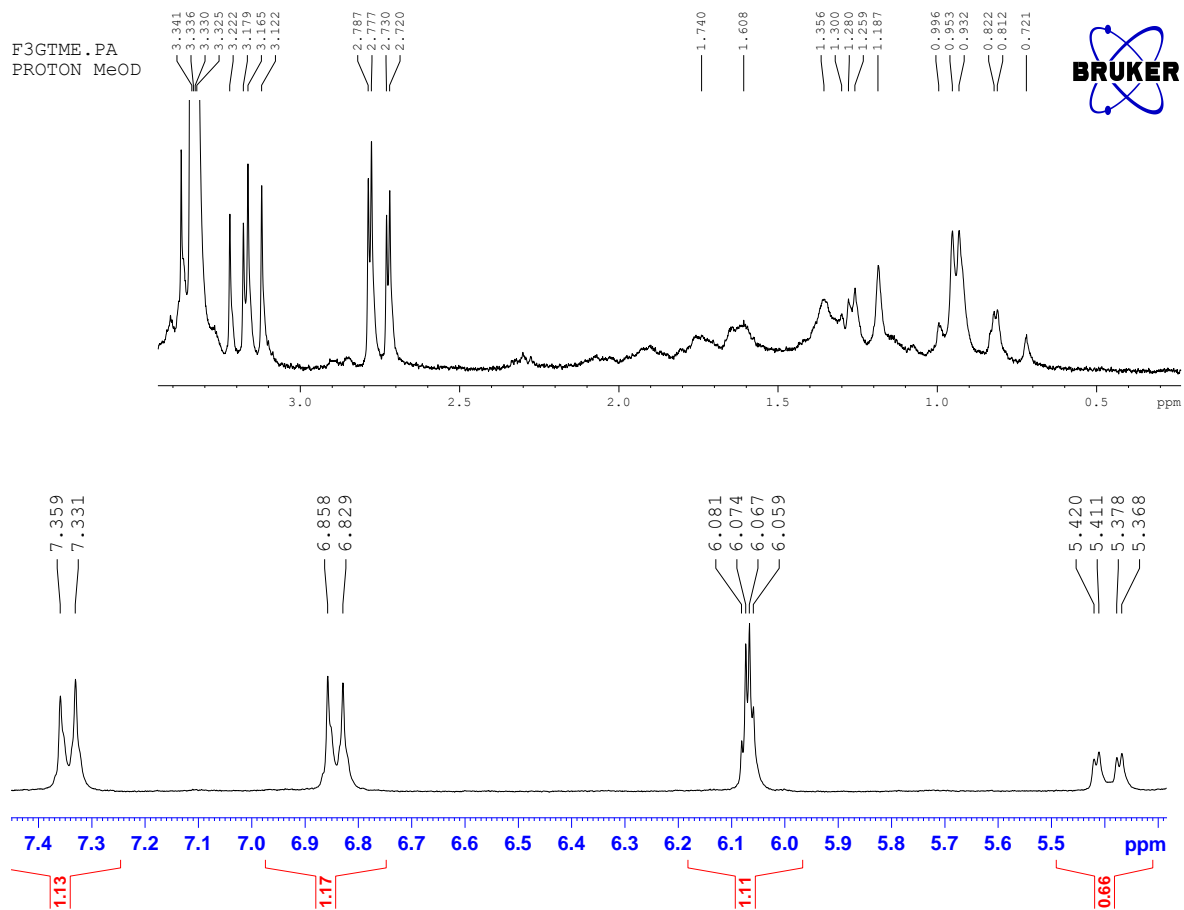


Figure 143 Proton NMR spectrum of F3GT-Me-P4/PA

F3GTME-P4* in MeOD-d4

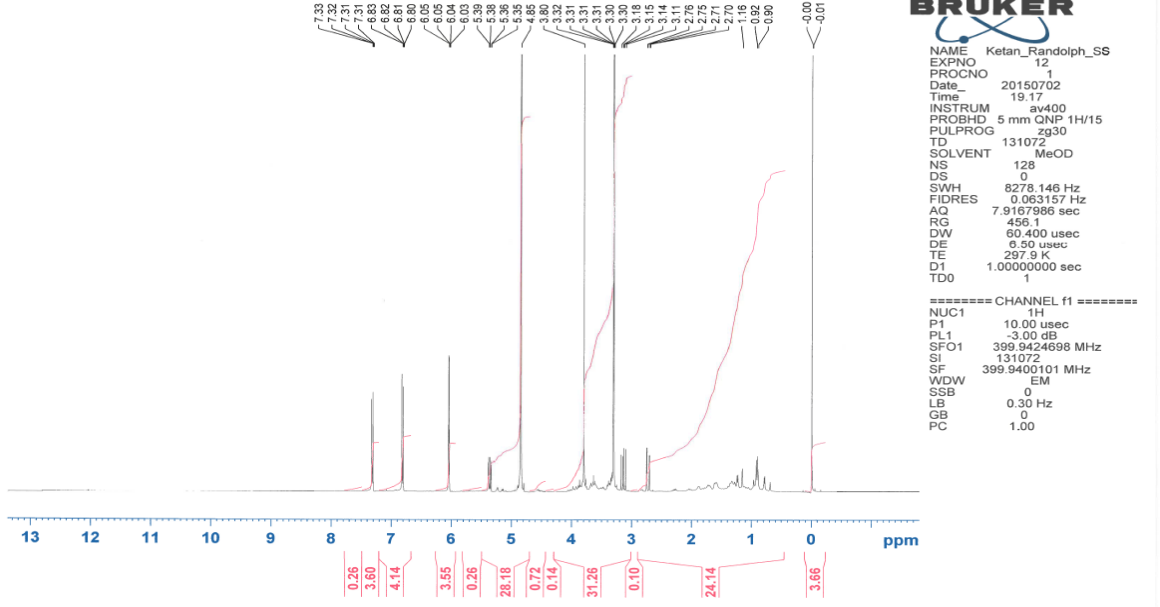


Figure 144 +H NMR spectrum of F3 GT-Me-P4

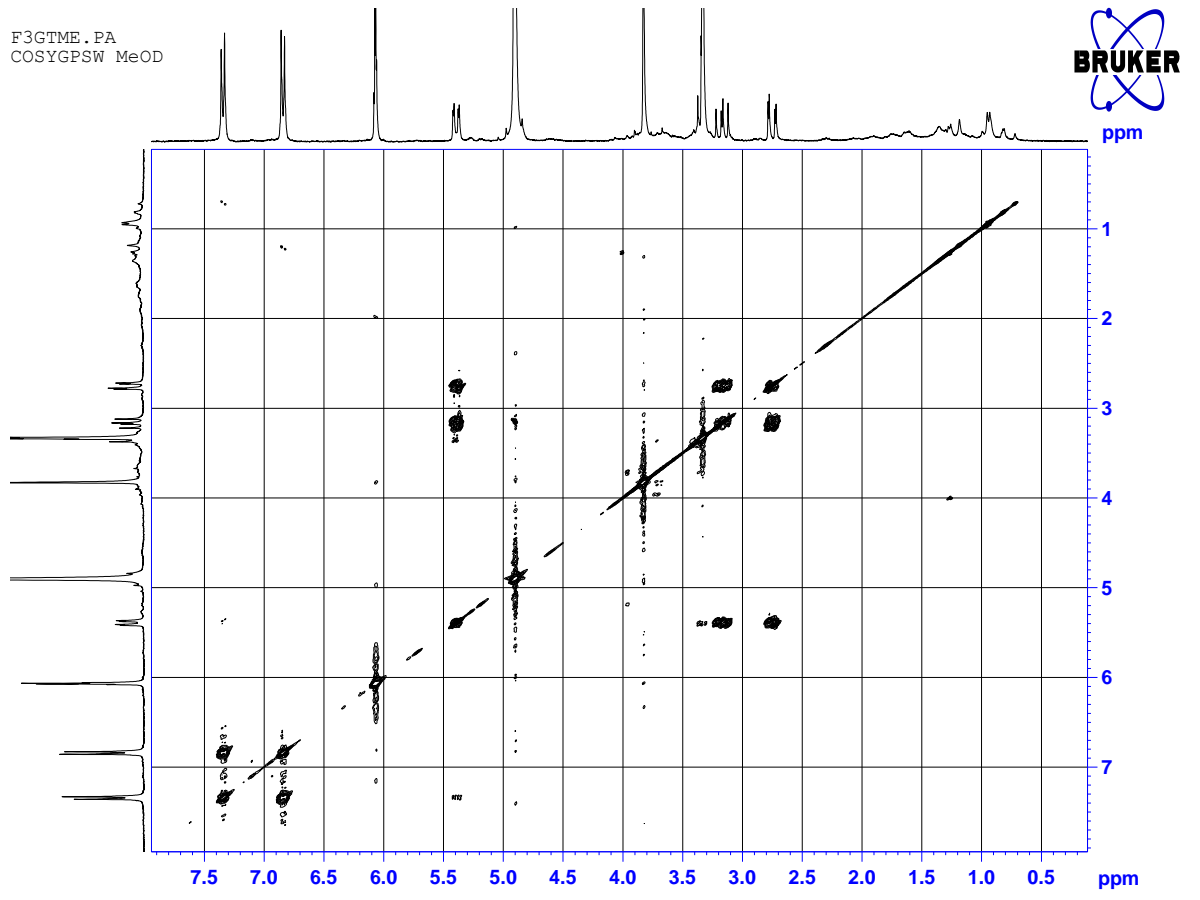
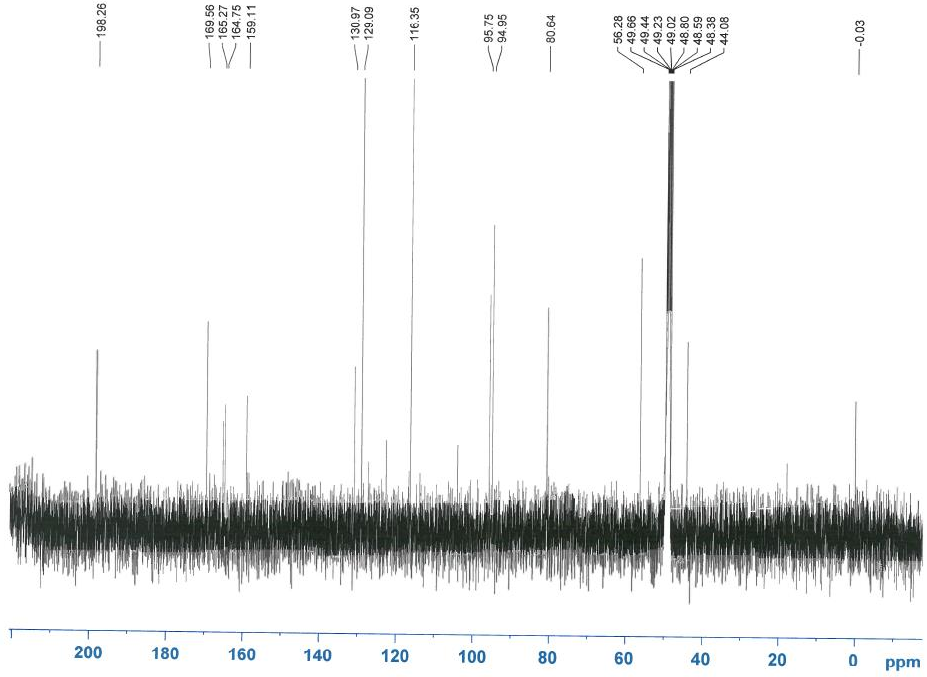


Figure 145 COSY experiment spectrum for F3GT-Me-P4/PA

F3GTME-P4* in MeOD-d4



```
NAME Ketan_Randolph_SS
EXPNO 13
PROCNO 1
Date_ 20150702
Time 20.17
INSTRUM av400
PROBHD 5 mm QNP 1H/15
PULPROG zgpg30
TD 65536
SOLVENT MeOD
NS 1024
DS 4
SWH 23980.814 Hz
FIDRES 0.365918 Hz
AQ 1.3964756 sec
RG 9195.2
DW 20.850 usec
DE 6.50 usec
TE 298.2 K
D1 2.00000000 sec
D11 0.03000000 sec
TDO 1

===== CHANNEL f1 =====
NUC1 13C
P1 9.00 usec
PL1 3.00 dB
SFO1 100.5750490 MHz

===== CHANNEL f2 =====
CPDPRG2 waltz16
NUC2 1H
PCPD2 85.00 usec
PL2 -4.00 dB
PL12 17.00 dB
PL13 17.50 dB
SFO2 399.9415898 MHz
SI 32768
SF 100.5648502 MHz
WDW EM
SSB 0
LB 1.00 Hz
GB 0
PC 1.40
```

Figure 146 ¹³C NMR spectrum of F3 GT-Me-P4/PA

F3GTME-P4* in MeOD-d4

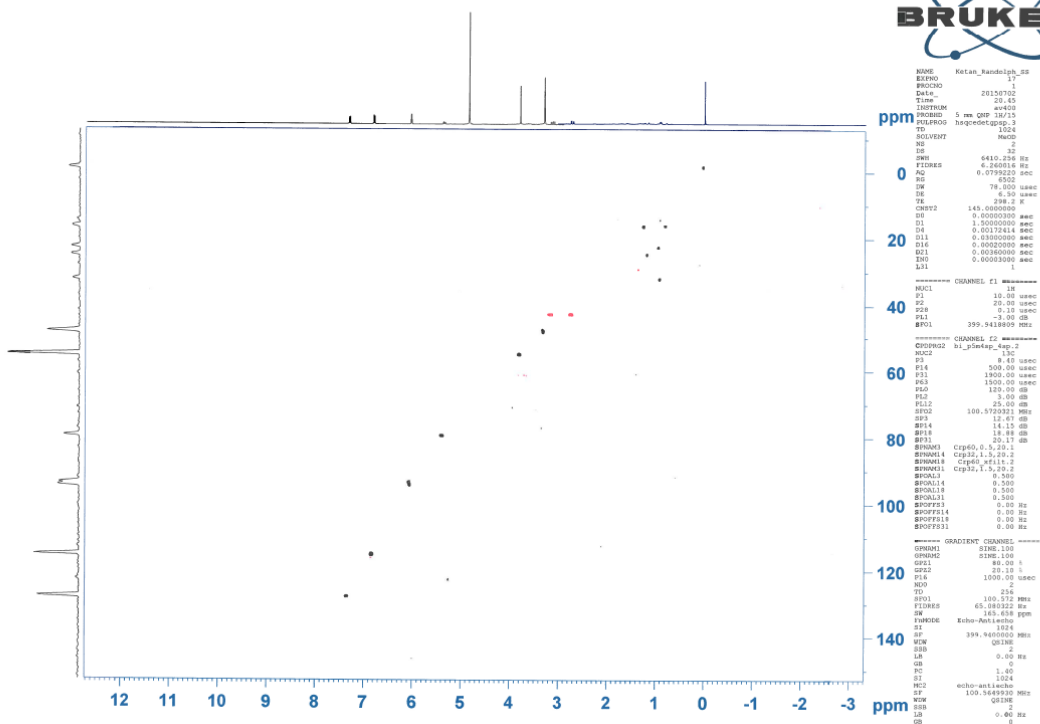


Figure 147 HSQC experiment spectrum of F3 GT-Me-P4/PA

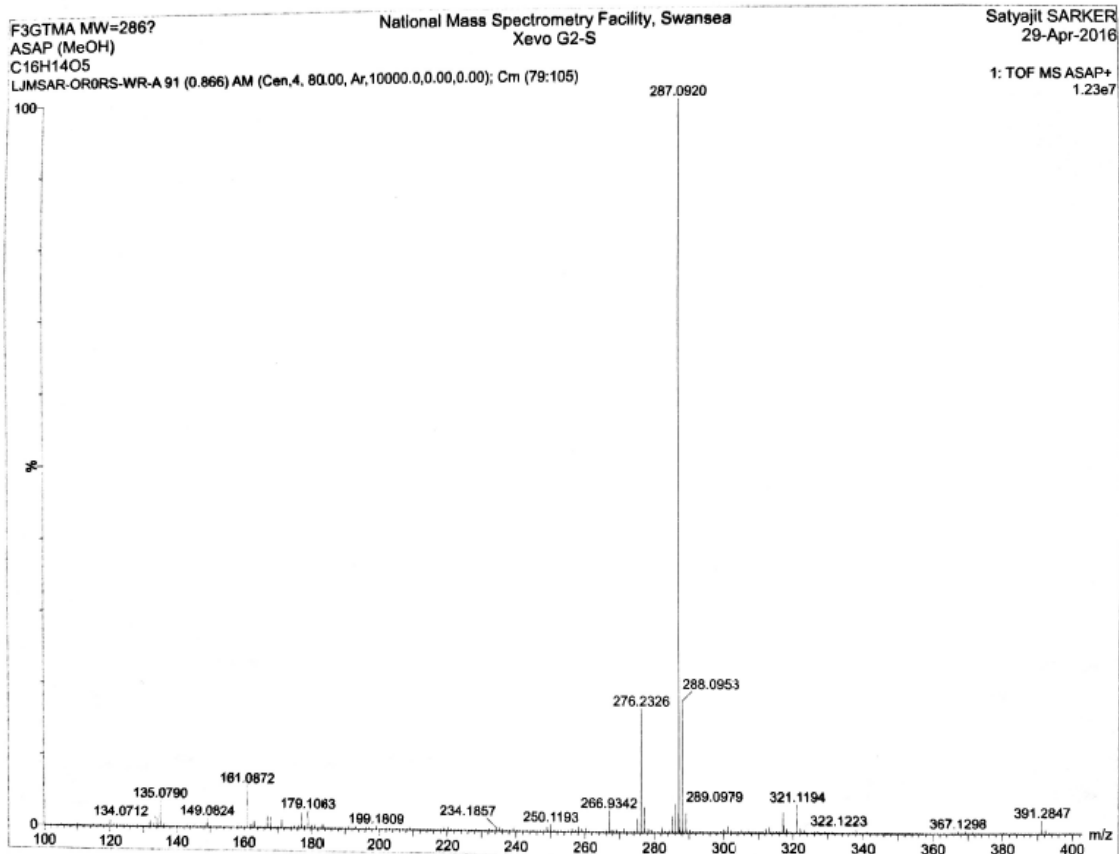


Figure 148 MS spectrum for F3 GT-Me-P4/PA (data entry error for sample name displayed at the top of spectrum)

LJMSAR037-OR-HNESN #44-79 RT: 0.73-0.92 AV: 8 SM: 7G NL: 2.41E7
T: FTMS - p NSI Full ms [120.00-615.00]

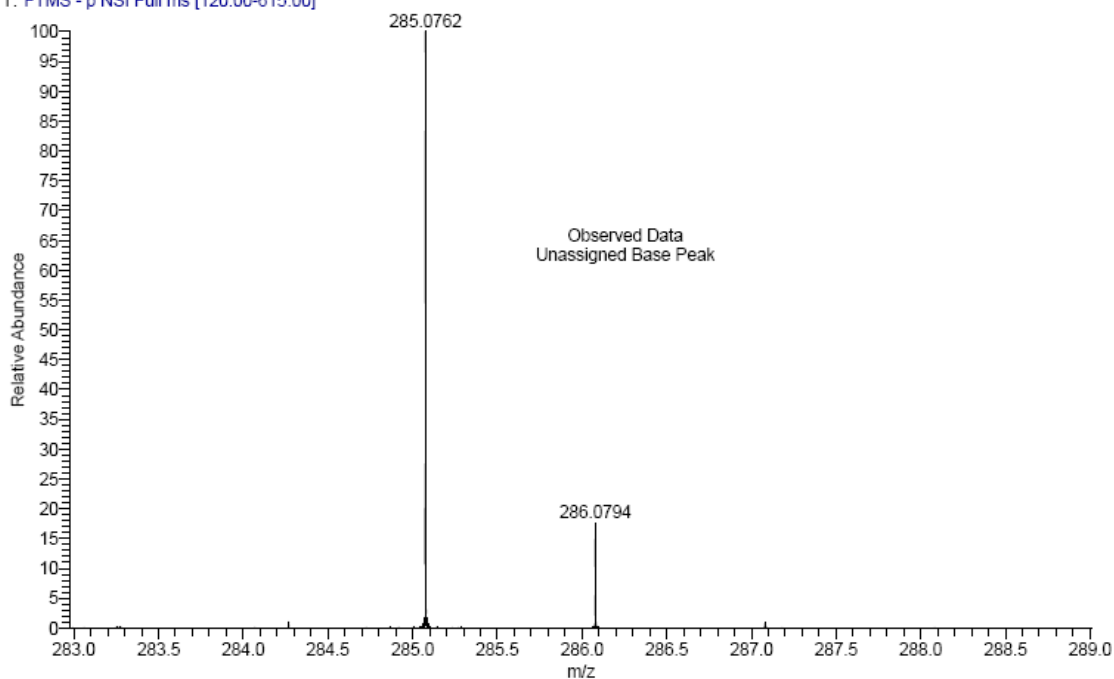


Figure 149 MS spectrum for F3 GT-Me-P4/PA (data entry error for sample name displayed at the top of spectrum)

LJMSAR037-OJ-HNESP-2 #41-44 RT: 0.98-1.04 AV: 3 SM: 7G NL: 1.37E6
T: FTMS + p NSI Full ms [140.00-1935.00]

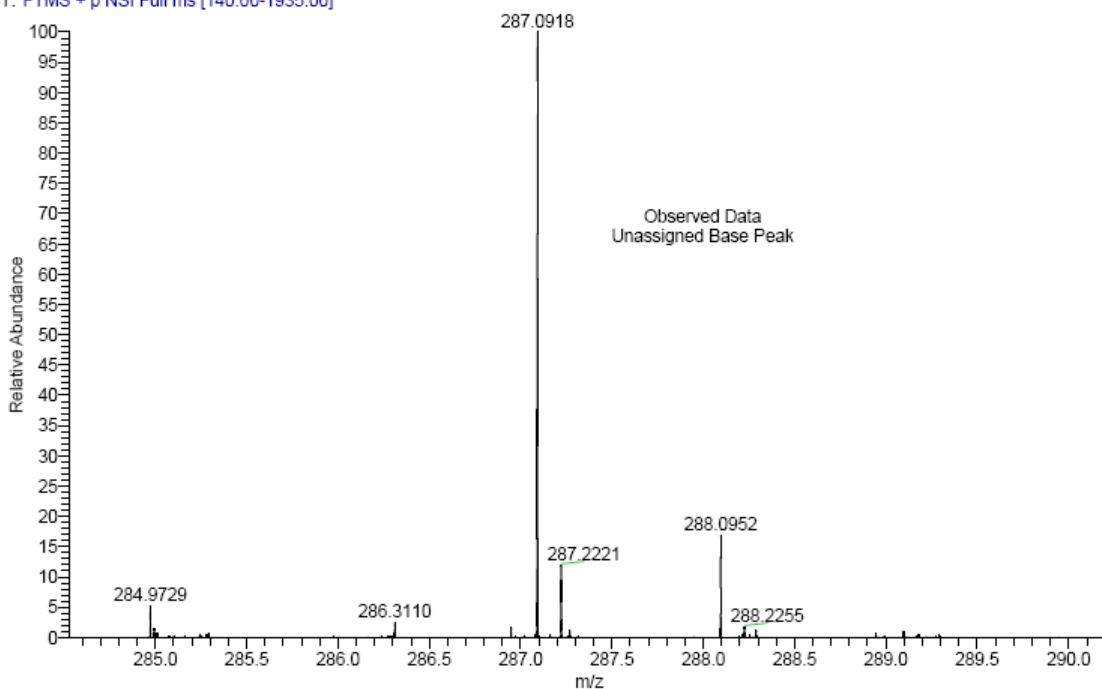


Figure 152 MS results for F3 GT-Me-P4/PA (data entry error for sample name displayed at the top of spectrum)